Redox Biology of Myeloid Leukaemias

A thesis submitted to the National University of Ireland, Cork,
in fulfilment of the requirement for the degree of

Doctor of Philosophy

by

Joanna Stanicka BSc.

School of Biochemistry and Cell Biology

University College Cork

January 2014

Supervisor: **Professor Thomas G. Cotter**

Head of Department: **Professor David Sheehan**

Declaration

This thesis has not been submitted in whole or in part to this or any other university for any degree and is, unless otherwise stated, the original work of the author.

Signed: _____

Joanna Stanicka

Acknowledgements

I am using this opportunity to express my gratitude to everyone who supported me throughout my PhD. Foremost I would like to thank my supervisor and lecturer Prof. Tom Cotter for seeding research enthusiasm during my bachelor degree and for giving me an opportunity undertake a PhD project in UCC. I have been very lucky to work in your laboratory for the past 3 years. I would like to thank you for your constant support and motivation that allowed me to complete the work in this thesis.

I also would like to thank Kate for constantly ensuring that everything runs smoothly in the lab and all possible equipment, computer, printer, order issues are resolved in the blink of an eye.

I would also like to thank all the members of TC's lab over the past 3 years (I hope I will not forget about anybody): John, Eileen, Alice, Sarah, Ashleigh, Will, Gillian, Fran, Maryanne, Lavinia, Dave, Peter, Jenny and Ani. It has been a great pleasure to know you all. Thank you for listening to my crazy research and non-research ideas and philosophies, and more ideas and philosophies over and over again. I hope you all know how much I appreciate your help and support throughout my PhD. Here I would like to especially thank Eileen and Alice who have been (and hopefully will always be) great, supportive friends who listened and nodded to all these ideas. Thank you for all the hours of laughs and minutes of tears. I would also like to thank Sarah and Ashleigh for the support when I was writing my thesis. I wish you were there all along!

I would also like to say a big ‘thank you’ to John (Dr. John Woolley) for teaching me absolutely everything in the lab! Answering all the possible questions! Battling and supporting my ideas over coffees, teas, muffins, scones and lunches. For teaching me how to think like a scientist and how to critically analyze data, a big ‘thank you’.

I also want to thank to my sweetest son Michal who supports me every day in everything that I do and always has something sweet and uplifting to say. Thank you for reminding me about what is most important in life.

I would also like to thank my best friends Iza, Klaudia, Ania and Monika for all the support and help in the world whenever (literally) I need it. I am very lucky to know you for all these years! Thank you for giving me strength and confidence to follow my dreams. With you girls everything just seems so much easier and brighter!

Last but not least, I would like to thank my family and Shane (who is like my family in Ireland) for all the love and support in whatever I do. Thank you for giving me courage and strength to pursue my dreams.

Table of Contents

Abstract

Internal tandem duplication of FMS-like receptor tyrosine kinase (FLT3-ITD) is present in 15-35% of acute myeloid leukaemia (AML) patients and it has been associated with an aggressive AML phenotype. FLT3-ITD expressing cell lines have been shown to generate increased levels of reactive oxygen species (ROS) and DNA double strand breaks (dsbs). However, the molecular basis of how FLT3-ITD-driven ROS leads to the aggressive form of AML is not clearly understood.

Herein, we show that in the FLT3-ITD expressing AML cell line, MV4-11, inhibition of FLT3 leads to a reduction in the levels of total ROS and H_2O_2, as measured by DCF and Peroxy Orange 1 (PO1) probes respectively. Interestingly, levels of both total ROS and H_2O_2 are attenuated by DPI and VAS-2870-achieved inhibition of NADPH oxidases (NOXs). In contrast, the aforementioned inhibitions do not affect amount of H_2O_2 in mitochondria, as analysed by MitoPY1 probe. We also observe that the majority of H_2O_2 in FLT3-ITD-expressing MV4-11 cells colocalises to the endoplasmic reticulum (ER). The inhibition of FLT3 or NOXs decreases the amount of H_2O_2 in the ER. Furthermore, ER localisation of ROS in MV4-11 cells corresponds to the localisation of $p22^{phox}$, a small membrane-bound subunit of NOX complex. This indicates that $p22^{phox}$ bound to NOX complex mediates generation of ROS in FLT3-ITD-expressing cells.

This work also presents a novel mechanism of FLT3-ITD-driven stimulation of NOX that occurs through a stabilisation of $p22^{phox}$. We show that 32D cells, a myeloblast-like cell line transfected with FLT3-ITD, possess higher steady protein levels of $p22^{phox}$ than their wild type FLT3 (FLT3-WT)-expressing counterparts.

Moreover, stimulation of FLT3-WT with FLT3 ligand (FL) results in an increase in $p22^{phox}$ protein levels, accompanied by an elevation in cellular H_2O_2. Similarly, the inhibition of FLT3-ITD signalling, using various FLT3 tyrosine kinase inhibitors (TKIs), uniformly results in a post-translational downregulation of $p22^{phox}$. Furthermore, siRNA knockdown of $p22^{phox}$ dramatically attenuates an accumulation of H_2O_2 in the ER. We also show that depletion of NOX2 and NOX4, but not NOX1 proteins causes a reduction in endogenous H_2O_2 levels, suggesting that these are the isoforms activated by elevated $p22^{phox}$ levels.

We show that genomic instability induced by FLT3-ITD, through stimulation of ROS production, leads to an increase in nuclear levels of H_2O_2, as measured by NucPE1 probe. The presence of H_2O_2 in the nucleus is largely reduced by inhibition of FLT3 or NOX. Furthermore, similar results are also observed following siRNA knockdowns of $p22^{phox}$ or NOX4.

We demonstrate that 32D cells, a myeloblast-like cell line transfected with FLT3-ITD have a higher level of both oxidised DNA and DNA dsbs than 32D cells transfected with the wild type FLT3 receptor (FLT3-WT). Furthermore, PKC412 treatment also causes reduction in oxidative DNA damage and DNA dsbs. Additionally, inhibition of FLT3-ITD, $p22^{phox}$ and NOX knockdowns decrease the number of DNA dsbs. We also show that NOX4 and $p22^{phox}$ partially localize to the nuclear membrane in MV4-11 cells expressing FLT3-ITD. Taken together these data indicate that NOX and $p22^{phox}$ mediate the ROS production downstream of FLT3-ITD and that, in turn, these ROS diffuse to the nucleus to cause genomic instability.

In summary, this study presents a novel mechanism of genomic instability generation in FLT3-ITD-expressing AML cells, whereby FLT3-ITD activates NOX complexes by stabilising p22phox. This in turn leads to elevated generation of ROS and DNA damage in these cells. Both of these phenomena contribute to the aggressiveness and chemoresistance of leukaemia. Therefore, NOXs are potentially attractive targets for novel treatments of AML.

Abbreviations

$^{\bullet}OH$	Hydroxyl
$^{1}O_2$	Singlet oxygen
3D	Three Dimensional
8-OHdG	8-Hydroxy-2' –Deoxyguanosine
A-EJ	Alternative End Joining
ABL	Abelson Murine Leukaemia Viral Oncogene
AC-220	Quizartinib
ADP	Adenosine Diphosphate
AKT	Protein Kinase B
ALL	Acute Lymphocytic Leukaemia
AML	Acute Myeloid Leukaemia
AP-1	Activator Protein 1
APF	2- [6-(4'-amino)phenoxy-3H-xanthen-3-on-9-yl]Benzoic Acid
AQP3/8	Aquaporin 3/8
ATP	Adenosine Triphosphate
Bad	Bcl-2-Associated Death Promoter
BCL-2	B-Cell Lymphoma 2
BCR	Breakpoint Cluster Region
BCR-ABL	Fusion Protein of BCR and ABL
BSA	Bovine Serum Albumin
Ca^{2+}	Intracellular Calcium
C/EBP	CCAAT-Enhancer-Binding Proteins

CEP-701	Lestaurtinib
c-KIT	Steel Factor Receptor
CML	Chronic Myeloid Leukaemia
c-MYC	Myelocytomatosis Viral Oncogene
Cys-SH	Cysteine
Cys-SOH	Cysteine Sulfenic Acid
Cys-S-S-Cys	Cysteine Disulfide
D835Y	Aspartic Acid (D) to a Tyrosine (Y) Substitution at 835
DCF	2’,7’-Dichlorodihydrofluorescein
DHE	Dihydroethidium
DMSO	Dimethyl Sulfoxide
DNA	Deoxyribonucleic Acid
DPI	Diphenyleneiodonium Chloride
Dsbs	Double Strand Breaks
DTT	Dithiothreitol
DUOX	Dual Oxidase
EBV	Epstein–Barr Virus
EBVNA-1	Epstein–Barr virus (EBV) Nuclear Antigen-1
EGF	Epidermal Growth Factor
ER	Endoplasmic Reticulum
ERK1/2	Extracellular Regulated Kinase 1/2
FACS	Fluorescence Activated Cell Sorting
FAD	Flavin Adenine Dinucleotide
FBS	Foetal Bovine Serum

FLK-2	Foetal Liver Kinase-2
FLT3	FMS-Like Tyrosine Kinase 3
FLT3-WT	Wild Type FLT3
FL	FLT3 Ligand
FMS	Macrophage Colony-Stimulating Factor Receptor
FOXO3a	Forkhead Transcription Factor 3a
GAPDH	Glyceraldehyde 3-Phosphate Dehydrogenase
GDP	Guanidine Diphosphate
GF	Growth Factor
γH2AX	Gamma H2AX (Phosphorylated H2AX)
GLUT-1	Glucose Transporter 1
GRB2	Growth Factor Receptor-Bound Protein 2
GSH	Reduced Glutathione
GSK3-β	Glycogen Synthase Kinase 3 Beta
GSSG	Oxidized glutathione
GTP	Guanosine Triphosphate
GDP	Guanosine Diphosphate
HDAC	Histone Deacetylase
H_2DCFDA	Dichlorodihydrofluorescein Diacetate
H_2O_2	Hydrogen Peroxide
HCl	Hydrochloric Acid
HOCl	Hypochlorus acid
HR	Homologous Recombination
HRAS	Harvey Rat Sarcoma Viral Oncogene

HSC	Haematopoietic Stem Cells
Ig-like	Immunoglobulin-Like
IGF-I	Insulin-like Growth Factor I
IL-3	Interleukin-3
IR	Ionising Radiation
IRDye	Infrared dye
ITD	Internal Tandem Duplication
JAK	Janus Kinase
JM	Juxtamembrane Domain
LSC	Leukaemic Stem Cell
MAPK	Mitogen-Activated Protein Kinase
MCP-1	Monocyte Chemoattractant Protein-1
MDS	Myelodysplasia
MEK	MAPK/ERK Kinase
MitoPY1	Mitochondrial Peroxy Yellow 1
MitoSOX	Red Mitochondrial Superoxide Indicator
mRNA	Messenger RNA
mTOR	Mammalian Target of Rapamycin
NAD	Nicotinamide Adenine Dinucleotide
NADP	Nicotinamide Adenine Dinucleotide Phosphate
NADPH	Reduced Nicotinamide Adenine Dinucleotide Phosphate
NEM	N-Ethylmaleimide
NF-κB	nuclear factor *kappa*-light-chain-enhancer of activated *B* cells
NHEJ	Non-Homologous End Joining

NOX	NADPH Oxidase
NOXA1	NOX Activator 1
NOXO1	NOX Organiser 1
NP-40	Nonyl Phenoxypolyethoxylethanol-40
NRAS	Neuroblastoma RAS Viral Oncogene Homologue
NucPE1	Nuclear Peroxy Emerald 1
NUP98	Nucleoporin 98 kDa
$O_2^{\bullet -}$	Superoxide
O_3	Ozone
$OH^{\bullet}$	Hydroxyl Radical
PBS	Phosphate-Buffered Saline
PDGF	Platelet-Derived Growth Factor
PDK1	3-Phosphoinositide-Dependent Protein Kinase-1
P-FLT3	Phospho-FLT3
PH	Plecstrin Homology
PIP2	Phosolipid Phosphatidylinositol Biphosphate
PIP3	Phosolipid Phosphatidylinositol 3,4,5-Triphosphate
PI3K	Phosphatidylinositol 3-Kinase
PIM1/2	Proviral Integration Site 1/2 Oncogene
PKC	Protein Kinase C
PKC412	Midostaurin
PM	Plasma Membrane
PMA	Phorbol 12-Myristate 13-Acetate
PO1	Peroxy Orange 1

Poldip2	Polymerase Delta-Interacting Protein
PP1	Protein Phophatase-1
PP1α	Protein Phophatase-1α
PP2A	Protein Phophatase-2A
P-STAT5	Phosphorylated Signal Transducers and Activators of Transcription 5
PtdIns	Phosphatidylinositol
PTEN	Phosphatase And Tensin Homolog
PTP1B	Protein Tyrosine Phospahatase 1 B
RAC1/2	RAS-Related C3 Botulinum Toxin Substrate 1/2
RAS	Rat Sarcoma Protein Kinase
RIPA	Radio Immunoprecipitation Assay
RNA	Ribonucleic Acid
RNS	Reacive Nitrogen Species
ROS	Reactive Oxygen Species
[ROS]	Concentration of ROS
RPMI	Roswell Park Memorial Institute
RT	Room Temperature
SD	Standard Deviation
SDS	Sodium Dodecyl Sulfate
SDS-PAGE	SDS-Polyacrylamide Gel Electrophoresis
SOCS1	Suppressor of Cytokine Signaling 1
SH	SRC-Homology Domain
SHP-1	SRC Homology Region 2 Domain-Containing Phosphatase-1

siRNA	Small Interfering RNA
siRNA(i)	$p22^{phox}$ siRNA ID-s3786 Transfected Cells
siRNA(ii)	$p22^{phox}$ siRNA ID-s194372 Transfected Cells
SOD	Superoxide Dismutase
SOS	Son of Sevenless
STAT5	Signal Transducers and Activators of Transcription 5
TBST	Tris-Buffered Saline/0.1% Tween-20
TGFβ	Transforming Growth Factor-β
TKD	Tyrosine Kinase Domain
TKI	Tyrosine Kinase inhibitor
TNF-α	Tumour Necrosis Factor-α
TPP^+	Triphenylphosphonium
VAS2870	3-enzyl-7-(2-benzoxazolyl)thio-1,2,3-triazolo[4,5-d]pyrimidine
VSMC	Vascular Smooth Muscle Cells
VEGF	Vascular Endothelial Growth Factor
WEHI-CM	WEHI-conditioned medium
w/v	Weight per Volume

Chapter 1

General Introduction

Leukaemia

Leukaemia is a myeloproliferative disease characterised by an abnormal growth of white blood cells. The word leukaemia comes from Ancient Greek leukos “white” and haima “blood”. The world incidence of leukaemia in 2012 was approximately 352,000 of new diagnosed cases, which accounts for 2.5% of all cancers (Ferlay et al., 2015).

Leukaemia is a broad term that describes a number of white blood disorders of different aetiology. It can be classified as myeloid or lymphocytic, depending on the lineage of the affected cells. Alternatively, leukaemia can be described as acute or chronic, depending on the aggressiveness of the disease. Combining the two criteria results in four main subtypes of leukaemia: chronic lymphocytic leukaemia (CLL), chronic myeloid leukaemia (CML), acute lymphocytic leukaemia (ALL) and acute myeloid leukaemia (AML) (LLS., 2011).

Epidemiology and Current Treatment of Acute Myeloid Leukaemia

AML is a heterogeneous clonal disorder of haemopoietic progenitor cells and the most common malignant myeloid disorder in adults. While the general prevalence is approximately 3.8 cases per 100,000, the figure dramatically rises to 17.9 cases in the population of adults over 65 year old (Estey and Döhner, 2006). The standard AML treatment has changed little in passed twenty years (Roboz, 2012). At the time of writing, the majority of AML patients, who are not participating in the clinical trials, receive an induction chemotherapy of cytarabine and an anthracycline

(idarubicin or daunorubicin), followed by consolidation therapy or stem cell transplantation. This standard chemotherapy maximally offers 60-70% complete remission rate and 30-40% 5-year overall survival (Emadi and Karp, 2014). The novel treatments have not been approved in the last few decades due to either high levels of toxicity or little levels of effectiveness in the clinical trials. This demonstrates the importance and the need for the development of new drugs.

Leukaemic Stem Cell

Survival, proliferation and differentiation are the three fundamental phenomena driving the process of haematopoiesis. In acute myeloid leukomogenesis, the haematopoietic progenitor acquire abnormalities that lead to imbalance between the three processes that lead to the expansion of the leukemic stem cell (LSC) clone (Bonnet and Dick, 1997). In order for these abnormalities to develop into fully malignant disease, multiple independent genetic and epigenetic alterations in proto-oncogenes and/or tumour suppressor genes are required to occur. LSCs are characterised by the limitless self-renewal, cytoprotection and attenuated telomerase activity (Lane and Gilliland, 2010). Furthermore, LSCs are rather not found in the blood circulation. They primarily reside in the bone marrow microenvironment that additionally enables them to avoid the cytotoxic effects of the chemotherapy and the re-emergence to result in relapse of the disease (Lane et al., 2009).

Molecular Basis of Pathogenesis of AML

AML is a biochemically complex heterogenous disease. Several chromosomal aberrations and genetic mutations are systematically being used to prognostically classify AML based on its cytogenetics. The European Leukaemia Net Prognostic System categorises patients into four risk groups: favourable, intermediate-1, intermediate-2 and adverse (Roboz, 2012). The groups are classified depending on the subsets of cytogenetic and molecular markers. This classification allows to prediction of the response to the chemotherapy or allogeneic stem cell transplantation. For example, internal tandem duplications of FML-like tyrosine kinase 3 (FLT3-ITD) are associated with poor outcomes due to an aggressive disease phenotype. There are also two other types of classification of AML cases. The French-American-British (FAB) classification that divides AML into 8 types, M0-M7, based on the type of cell which the leukaemia developed and its degree of maturity. The World Health Organisation classification divides AML into: AML with recurrent genetic abnormalities, AML with multilineage dysplasia, and AML and MDS, therapy related (Vardimann et al., 2012).

Chromosomal aberrations, for example deletions and translocations are detected in 55 % of AML patients (Döhner and Döhner, 2008). The evidence suggest that leukemogenesis is a multi-step process. For example, RUNX-RUNX1T1 fusion protein causes impairment in myeloid differentiation, however the protein does not result in fully leukaemic phenotype in a murine model (Döhner and Döhner, 2008). These initiating fusion oncogenes have to be followed by the complementing mutations that activate signal transduction pathways resulting in increased

proliferation/survival or block in apoptosis/differentiation. Often these mutations lead to activation of receptor tyrosine kinase signalling pathways, as it is in the case of FLT3, Neuroblastoma RAS Viral Oncogene Homologue (NRAS) or steel factor receptor (KIT) (Döhner and Döhner, 2008). Therefore AML mutations has classified into 2 major groups. Class I comprises mutations activating signal transduction pathways that lead to increased proliferation and survival of cells, for instance FLT3 or RAS. Class II contains mutations that affect differentiation or self-renewal properties of cells, for example CEBPA, MLL and NPM1. In order for the disease to develop class I mutation must be accompanied by class II mutation, which is the basis of the two-hit model of the development of AML.

FLT3 signalling

In total, 25-45% of patients with AML will have some form of mutation in FLT3, making it the most common genetic aberration in AML (Stirewalt and Radich, 2003). FLT3 also known as a FLK-2, is a class III receptor tyrosine kinase with a strong sequence similarities to other members of this class, macrophage colony-stimulating factor receptor (FMS), platelet-derived growth factor receptor (PDGF) and (KIT). All of the class III members play important roles in proliferation, differentiation and survival of the haematopoietic cells (Rosnet and Birnbaum, 1993). Mice with disruption of FLT3 and KIT possess deficiency in hematopoietic cell numbers and early lethality of the animals. This suggests that FLT3 acts in conjunction with other cytokines to stimulate proliferation and differentiation of the hematopoietic progenitors (Mackarehtschian et al., 1995).

FLT3 gene encodes 993-amino acid protein in human that is expressed in early myeloid and lymphoid haematopoietic cells (Rosnet et al., 1996). The protein is composed of the 5 extracellular immunoglobulin-like (Ig-like) domains, a transmembrane domain, a juxtamembrane domain and 2 cytoplasmic domains with a tyrosine kinase motif (Levis and Small, 2003) (Figure 1). Two forms of FLT3 have

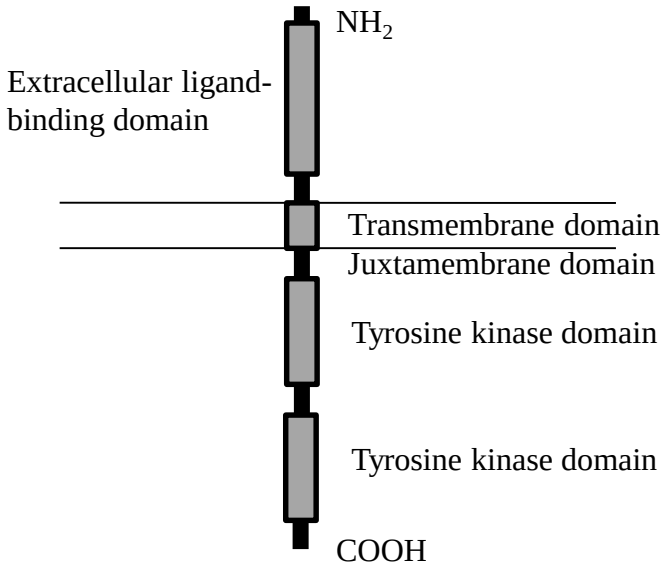

Figure 1. FLT3 structure.
The protein is composed of extracellular ligand-binding domain, a transmembrane domain, a juxtamembrane domain and 2 cytoplasmic domains with a tyrosine kinase motifs.

been described, a mature 160 kDa – glycosylated protein and an immature 130 kDa – unglycosylated protein (Stirewalt & Radich, 2003). In normal cells expression of FLT3 is restricted to early myeloid and lymphoid progenitors, whereas leukaemic cells express FLT3 in 70-90% of patients with AML and ALL (Stirewalt and Radich, 2003).

Unstimulated FLT3 resides as a monomer in the plasma membrane (PM) (Masson and Ronnstrand, 2009). The receptor remains in the inactive conformation due to the steric inhibition mediated by the juxtamembrane domain (Meshinchi and Appelbaum, 2009). Upon FLT3 ligand (FL) binding, it homodimerises, tyrosine kinases are activated. The receptor autophosphorylates at the tyrosine residues that become docking sites for receptor-binding signalling effectors (Masson and Ronnstrand, 2009) (Masson & Rönnstrand, 2009; Turner, Lin, Issarachai, Lyman, & Broudy, 1996). Phosphorylation of FLT3 can be detected as early as 5min post ligand stimulation (Fenski et al., 2000). FLT3 signalling is tightly regulated by the immediate internalisation of the FLT3-FL complex (Turner et al., 1996). This secure control of the FLT3-FL complex is a part of negative regulation of FLT3 signalling that monitors the proliferation/survival signals in these cells. The FLT3 signal is primarily transduced *via* phosphatidylinositol-3 kinase (PI3K) and rat sarcoma protein kinase (RAS) pathways leading to protein kinase B (AKT), signal transducers and activators of transcription 5 (STAT5) and extracellular regulated kinase 1/2 (ERK1/2) activation (Masson and Ronnstrand, 2009).

PI3K/AKT pathway is one of the most important cell growth and survival signalling pathways in cancer development. Growth factors activate PI3K lipid kinase that catalyses phosphorylation of the 3 position hydroxyl group of the inositol ring of phosphatidylinositol (PtdIns). This in turn recruits plecstrin homology (PH) possessing proteins e.g. AKT. AKT is a serine/threonine kinase and a positive modulator of survival through inhibition of the pro-apoptotic Bad and Foxo3a proteins. The latter also regulates cell cycle progression, rendering AKT an

important stimulant of cell proliferation. Indirectly, AKT also activates mammalian target of rapamycin (mTOR) serine/threonine kinase that by initiation of ribosomal translation of messenger RNA (mRNA) into proteins that play important role in cell growth, metabolism and cell cycle progression.

The RAS pathway commences with the activation of small GTPase, RAS that possesses an intrinsic ability to hydrolyze guanosine triphosphate (GTP) to guanosine diphosphate (GDP). Active RAS positively regulates a mitogen-activated protein kinase (MAPK) cascade that leads to activation of (extracellular regulated kinase) ERK1/2 which is involved in a block of differentiation, anti-apoptosis and proliferation.

Phosphorylated FLT3 kinase becomes a docking site for STAT5. Following the transduction of the phosphor-signal onto STAT5, the protein dimerises and translocates into the nucleus where it binds to STAT5 response elements. STAT5 acts as a potent activator of transcription for a variety of genes, e.g. proviral integration site 1/2 oncogene (PIM1/2) involved in anti-apoptosis and survival.

FLT3 mutations in haematological malignancies.

The most common FLT3 mutation is an internal tandem duplication (ITD) in exons 14 and 15, which occurs in 15-35% of AML cases, 1-3% of ALL cases and 5-10% of patients with myelodysplasia (MDS) (Stirewalt and Radich, 2003). The fragment of the juxtamembrane domain (JM) (3->400 base pairs) is duplicated and inserted in a direct head-to-tail orientation, resulting in an in-frame mutation

(Takahashi, 2011, Stirewalt and Radich, 2003). Regardless of the sequence or the length of the insert, the ITD in the JM domain drives a constitutive phosphorylation of tyrosines followed by the homodimerisation of the receptor (Kiyoi et al., 1998). Crystallisation studies have demonstrated that non-mutated JM region stabilises the auto-inhibited conformation of the kinase domain (Griffith et al., 2004). It seems that elongation of the JM domain attenuates the negative regulation of the phosphorylation of the receptor (Griffith et al., 2004, Kiyoi et al., 2002). Although ITD mutation can activate FLT3 independently of FL, the notion of FL not affecting ITD receptor may be incorrect. The majority of FLT3-ITD studies were performed in cell lines that express FL, thus it remained unclear, whether in addition to the independent route, FL-mediated activation of FLT3-ITD occurred. Consequently, Zheng *et al.* carried out a similar study in FL deficient cells, showing that stimulation of the cells with FL leads to further activation of ITD mutants, resulting in the increase in the receptor phosphorylation as well as the enhanced survival (Zheng et al., 2011).

FLT3-ITD mutations cause a constitutive activation of wild type-FLT3 (FLT3-WT) signalling, including PI3K and RAS pathways that are both crucial for the leukaemic transformation of AML cells (Gilliland and Griffin, 2002, Brandts et al., 2005a, Kothe et al., 2013). It has been demonstrated that constitutive activation of AKT is necessary for increased survival, proliferation and myeloid transformation (Brandts et al., 2005a). Furthermore, transfection of dominant negative RAS strongly inhibited the colony formation generated by mutated FLT3-ITD (Kothe et al., 2013).

Interestingly, the constitutive activation of FLT3-ITD results not only in the permanently dysregulated activation of FLT3-WT/FL pathway, but also in the additional FLT3-ITD unique signalling events. For example, cells stably transfected with FLT3-WT demonstrate little phosphorylation of STAT5 and show no STAT5 bound to DNA (Choudhary et al., 2007, Mizuki et al., 2000, Spiekermann et al., 2003). Conversely, cells stably transfected with FLT3-ITD manifest a strong STAT5 phosphorylation and STAT5 DNA binding. FLT3-ITD is thought to activate STAT5 in a different mechanism to IL-3-stimulated activation (Choudhary et al., 2007, Choudhary et al., 2009). It has been reported that STAT5 phosphorylation is independent of JAK and SRC kinases and it cannot be inhibited by overexpression of suppressor of cytokine signalling 1 (SOCS1), its negative regulator (Choudhary et al., 2007). STAT5 has also been shown to directly bind FLT3 *in vitro* (Choudhary et al., 2007). Additionally, FLT3-ITD represses the expression of crucial regulators of differentiation, Pu.1 and CCAAT-enhancer-binding protein (C/EBP), which FLT3-WT fails to accomplish, allowing the cells expressing FLT3-WT to differentiate (Choudhary et al., 2005b).

Mutations of the receptor tyrosine kinase may not only lead to their constitutive activation, but also to subcellular mislocalisation (Choudhary et al., 2009). FLT3-ITD mutation causes an impaired trafficking of the receptor and its prolonged residence, for example, in the endoplasmic reticulum (ER) (Choudhary et al., 2009). Thus, fully-glycosylated mature 160 kDa FLT3 is detected at the PM, while partially glycosylated, immature FLT3 form localises to the ER (Choudhary et al., 2009). Therefore, the signalling differences between activated FLT3-WT and FLT3-ITD

can be partially explained by their differential localisations. Kothe *et al.* have observed RAS activation mainly at the plasma membrane, suggesting that plasma-membrane FLT3 is responsible for the stimulation of RAS/ERK pathway in AML cells (Kothe et al., 2013). Conversely, the ER-present immature FLT3 aberrantly activates STAT5 and its downstream signalling (Choudhary et al., 2009) (Figure 2).

The second most common FLT3 mutation is a missense point mutation where aspartic acid is substituted for tyrosine (D835Y) in exon 20 of the tyrosine kinase domain (TKD). This mutation occurs in 5-10% of AML, 2-5% of MDS, and 1-3% of ALL patients (Yamamoto et al., 2001). Although the substitution renders FLT3 constitutively active and causes an interleukin-3 (IL-3) independent proliferation of 32Ds cells, the patients carrying the FLT3-ITD receptor have significantly poorer prognosis and shorter progression free-survival than the ones carrying FLT3-D835Y mutation (Choudhary et al., 2005a, Fenski et al., 2000, Meshinchi et al., 2006, Mizuki et al., 2000, Yamamoto et al., 2001). Interestingly, the two activating types of FLT3 mutations, yield substantial differences in the signalling downstream the phosphorylated receptor (Choudhary et al., 2005a) and transcription profiles (Lu et al., 2007).

Furthermore, the signalling downstream of constitutively phosphorylated FLT3-D835Y resembles more of the ligand stimulated FLT3-WT than of the FLT3-ITD (Choudhary et al., 2005a). The differences in the transforming potential of the two FLT3 activating mutations can be partially explained by the lack of support of colony formation by the FLT3-D835Y (Choudhary et al., 2005a). Additionally,

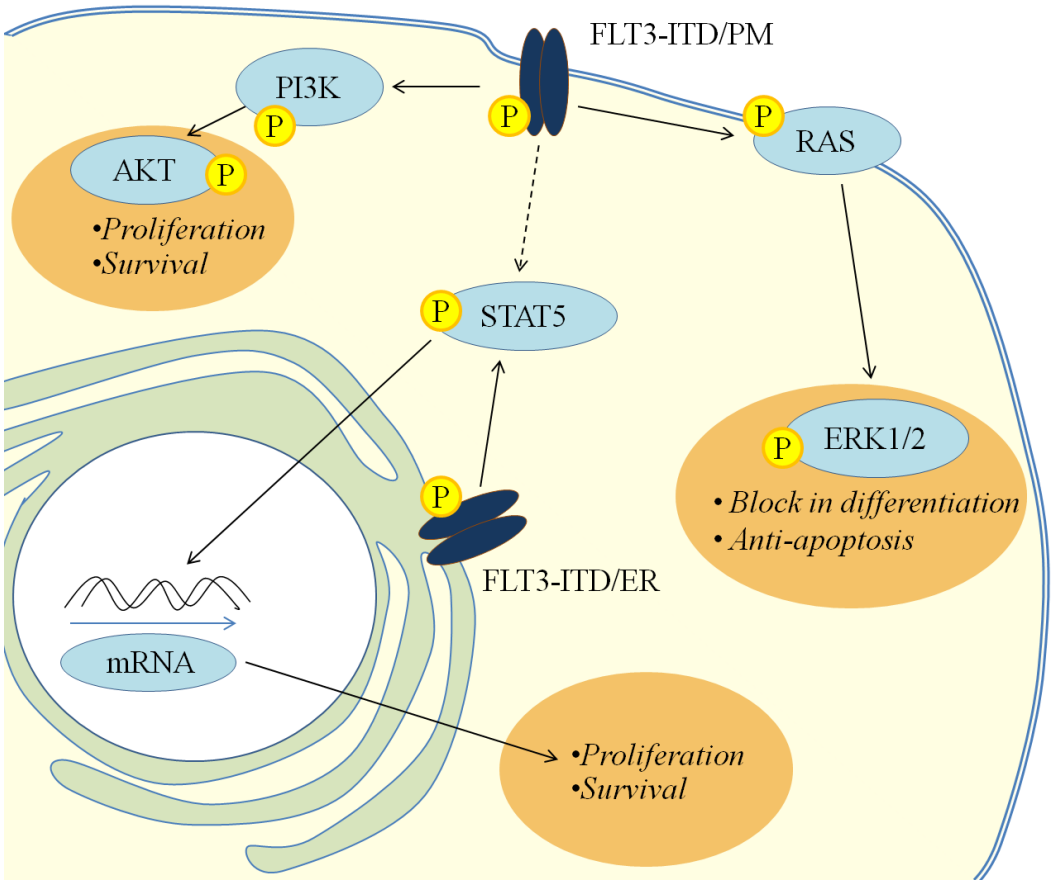

Figure 2. FLT3-ITD signalling at the endoplasmic reticulum and plasma membrane.

FLT3-D835Y fails to activate STAT5 and to repress the myeloid transcription factors c/EBPα and Pu.1 which are important signal transducers in the pathophysiology of AML (Choudhary et al., 2005a). Leischner *et al*. reported that SRC mediates the FLT3-ITD induced activation of STAT5 (Leischner et al., 2012). Tyrosines 598 and 591 are found to be essential for SRC binding and these are only weakly phosphorylated in FLT3-D835Y, preventing SRC to bind to FLT3 with mutation in TKD (Leischner et al., 2012).

Current management of patients with FLT3 mutations.

Newly diagnosed FLT3-ITD patients receive the standard induction therapy with similar results to other AML patients. However, patients that are hemizygous for FLT3/ITD mutations relapse more often and quicker than patients without the mutation (Grafone et al., 2012, Levis and Small, 2003). The survival in the relapse is also the poorest for these patients (Grafone et al., 2012). Allogeneic transplantation in first remission gives a better outcome than conventional consolidation chemotherapy in patients carrying the FLT3-ITD mutation (Levis, 2013). However, FLT3-ITD-harbouring cases still have a higher relapse risk than patients with other AML subtypes (Levis and Small, 2003). Moreover, there is a group of patients that cannot undergo allogeneic transplantation or intensive induction chemotherapy, e.g. the elderly, hence the treatment options for these patients are greatly limited.

Interestingly FLT3-ITD mutations are often accompanied by the abnormalities in the nucleophosmin (NPM1) gene that results in a mislocalisation of this protein to the cytoplasm. When present in the absence of FLT3, NPM1 mutations are regarded as favourable and allogeneic transplantation is usually unnecessary. Interestingly, it has been proposed that a favourable NPM1 mutation counter-balances the possession of the aggressive FLT3-ITD. However the evidence for this phenomenon is still under debate (Wander REF).

Small FLT3 tyrosine kinase inhibitors (TKIs), such as midostaurin (PKC412), have been developed and studied in the past few years (Grunwald and Levis, 2013, Wander et al., 2014). The main issue with medical efficacy of FLT3 inhibitors is the

inability to sustain the FLT3 inhibition *in vivo* at the dose that would not have serious off-target effects (Wander et al., 2014, Ostronoff and Estey, 2013). A breakthrough in the FLT3 pharmacology was a development of quizartinib (AC-220) that is significantly more potent than its precursors and is able to inhibit FLT3 *in vivo* at the tolerable doses (Grunwald and Levis, 2013, Wander et al., 2014). Although the results demonstrated the blast clearance and 51% remission rate in the group of patents >69 year old, it was observed that patients developed a resistance conferring point mutations in the FLT3 protein itself (Grunwald and Levis, 2013, Smith et al., 2012, Wander et al., 2014, Ostronoff and Estey, 2013). This suggests that possibly this potent inhibitor should be used in combination with other chemotherapeutics to prevent or delay the resistance (Wander et al., 2014).

Reactive Oxygen Species (ROS).

ROS are reactive, natural by-products of normal aerobic metabolism, formed by the partial reduction of the oxygen. The family includes: highly unstable oxygen radicals: superoxide ($O_2^{\bullet -}$), hydroxyl ($OH^{\bullet}$) and singlet ($^1O_2$) that can be quickly converted into more stable, freely diffusible non-radicals: hypochlorous acid, ozone (O_3), hydrogen peroxide (H_2O_2). Due to their chemical instability and reactivity, ROS have been known for years for their damaging effects to all types of macromolecules and hence cellular organelles and strictly associated with pathologies involving accumulation of damaged molecules (Murphy et al., 2011, Winterbourn, 2008, Cooke et al., 2003).

The balance between generation of ROS and ROS scavenging by cellular antioxidants provides the platform to redox homeostasis that can be easily tipped to an oxidative stress state when the ROS production exceeds its removal. Oxidative stress can be characterised by lipid peroxidation, protein carbonylation, damage to membranes and organelles and DNA. Antioxidants are molecules that by reacting with oxidants protect biomolecules from oxidative damage. They can be of enzymatic (e.g. catalase, superoxide dismutase) and non-enzymatic nature (e.g. glutathione, vitamin C, vitamin E).

In the past two decades, accumulative evidence in the literature has demonstrated that the oxidative properties of ROS exert a far larger role than the cellular injury and that their biological effects, in fact, can be beneficial. In the 1970, several groups reported that ROS are able to mimic signalling effects of insulin, followed by reports demonstrating that exogenous H_2O_2 can cause an increase in cell proliferation (Czech et al., 1974). These findings pioneered the field of redox signalling biology that focuses on the signalling effects of ROS. Since then, more than 10,000 papers have been published on the topic, manifesting the wide scope of ROS phenomenon as well as the enormous interest from the scientific community.

The pivotal property of the ROS to exerting the effects mentioned above is their ability to oxidatively modify molecules. In the case of nucleic acids, the oxidation involves damage to the genetic information (Cooke et al., 2003). This, in turn, can lead to mutagenic changes that could promote or initiate carcinogenic events. Regarding the effects of ROS on proteins, while high concentration of cellular ROS can lead to damaging effects, tightly regulated, local ROS generation can cause

reversible post-translational modification, at cysteine (Miki and Funato, 2012), selenocysteine (Hawkes and Alkan, 2010), methionine (Hoshi and Heinemann, 2001) and histidine (Lee and Helmann, 2006) residues of proteins. Cysteines (Cys-SH), for example, are readily oxidised by H_2O_2 to cysteine sulfenic acid (Cys-SOH) or disulphide (Cys-S-S-Cys). These oxidations belong to reversible modifications that can be reversed by cellular antioxidant enzymes. Thus, cysteines are often regarded as reversible redox switches, which through oxidative modification can change protein conformation, affect the active (or binding) site of the protein or change its surface properties (Wang et al., 2012).

A key to all signalling pathways is the transience and reversibility of the effect; although high concentrations of H_2O_2 (millimolar) cause irreversible oxidation of cysteines on target proteins, much lower nanomolar levels of H_2O_2 induce transient changes on these amino acids relevant to signal transduction (Day et al., 2012). All of the above characteristics allow H_2O_2 to act as the messaging substances in the redox signalling pathways on the various types of proteins e.g. transcription factors, phospholipases, protein kinases and phosphatases (Banno and Nozawa, 2003, Kojima et al., 2007, Marinho et al., 2014, Woolley et al., 2013a).

Due to high reactivity/instability of ROS signalling molecules like H_2O_2, the molecular target (e.g. protein, DNA) has to be localised relatively close to the site of ROS generation (Mishina et al., 2011). It is difficult to calculate the actual intracellular propagation distance of ROS molecules as it largely depends on the redox conditions of the compartment (Malinouski et al., 2011). The specific spatio-temporal character of the ROS signalling demonstrates the importance for

localisation, with redox signalling likely controlled to proximal targets (Ushio-fukai, 2009). For instance, it has been demonstrated in endothelial cells, that ER-residing NOX4 oxidises protein tyrosine phospahatase (PTP1B), modulating its activity (Chen et al., 2008). However, mutation in PTB1B changes the localisation of the protein from the ER-residing to diffused cytoplasmic distribution and NOX4 fail to oxidise and affect the function of mutant PTP1B (Chen et al., 2008).

As aptly noted by Murphy *et al.*, the term 'ROS' is often used in the literature to describe a functionally distinct molecule in cell signalling (Murphy et al., 2011). However, it should to be understood that various ROS have very different physical and chemical properties that allow them to behave in diverse ways modifying distinct target molecules e.g. different kinetics, degradation and chemical reactivity (Murphy et al., 2011). For instance, due to its extreme reactivity OH· is mainly considered as a damaging molecule that is not capable of signal transduction. OH· reacts virtually at the site of its production, as it has a very short half-life of 10^{-9} s. Contrastingly, H_2O_2 is not a radical and is sufficiently stable to diffuse in the cytoplasm (to a few microns) (Mishina et al., 2011), although the extent of diffusion of in the cell and across the biomembranes is still under debate. The small size of H_2O_2 allows it to diffuse, stability renders it able to convey the message and reactivity ensures the transience of the signal. On the other hand, it is possible that redox signalling utilises alternative mechanisms of H_2O_2 transport intra- and/or intercellularly. For example, it was shown that Aquaporin-3, a water channel, mediates the uptake of H_2O_2 from the extracellular space regulating signalling events inside the cells (Miller and Chang, 2010). It has also been reported that specific

aquaporins 3/8 (AQP3/8), transport NOX-derived H_2O_2 through PM from extracellular space in different cell types e.g. leukaemia. H_2O_2 shares numerous structural and chemical features with water, e.g. similar size, dipole moment and hydrogen bonding capabilities (Almasalmeh et al., 2014).

The dichotomy of ROS functioning renders them contributors to physiological and pathological conditions. Thus, while a low concentration of localised ROS is critical to downstream signalling of many growth factors, cytokines and hormones (Bae et al., 1997, Finkel, 1998, Martindale and Holbrook, 2002, Rhee et al., 2000, Sundaresan et al., 1995, Thannickal and Fanburg, 2000), an excessive ROS may cause cellular damage and death. ROS have been uniformly demonstrated to be elevated in many cancers e.g. prostate, colon cancer, and leukaemia (Szatrowski and Nathan, 1991, Zhou et al., 2003). Cancers are often caused by the mutations in the growth factor signalling pathways that render them constitutively active. This increased growth, in turn stimulates cellular metabolism that causes an abundant generation of ROS (Petros et al., 2005, Wallace, 2005). Alternatively, the growth factor-oncogenes stimulate NADPH oxidases that also generate ROS (Gough and Cotter, 2011, Reddy et al., 2011, Wu and Terada, 2009). However, the excess of ROS in cancer cells, generally does not lead to cell death. Cancer cells not only quickly adapt to the increased ROS levels, for instance, by activating additional DNA repair pathways, but even utilise them in stimulating cell proliferation or creating genomic instability (Mahalingaiah and Singh, 2014, Rassool et al., 2007, Sallmyr et al., 2008b). Thus, depending on the concentration of ROS and adaptation of cells to these, ROS can activate either pro-survival or pro-death pathways and in

the state of disease, these could lead to proliferative or degenerative disorders (Woolley et al., 2013a) (Figure 3).

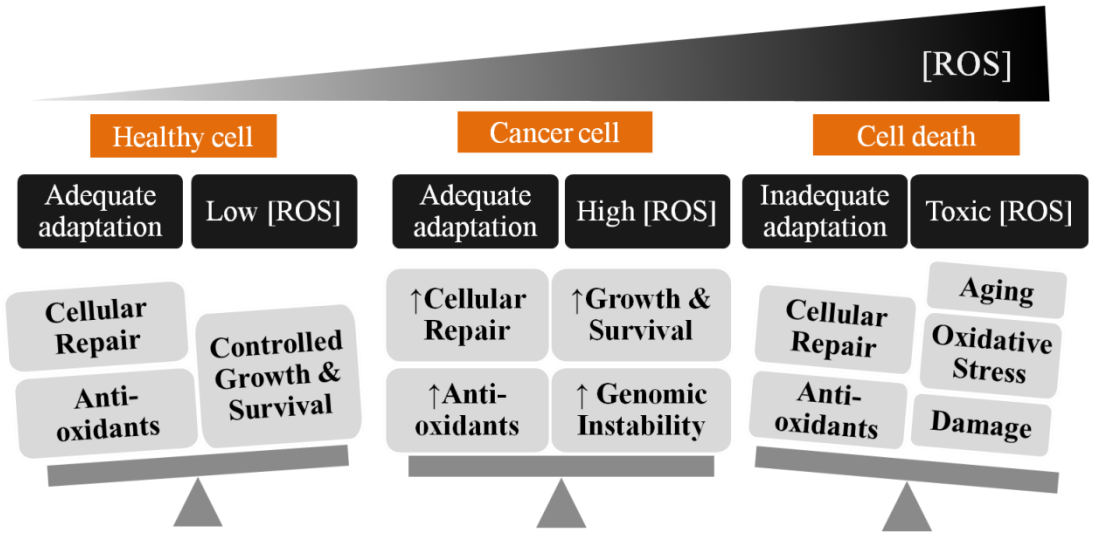

Figure 3. Paradigm of ROS effects in a cell. Healthy cells have developed adaptations to overcome damaging effects of ROS. Here, as a result of a balance of controlled generation of ROS, sufficient concentration of antioxidants and cellular repair, low concentration of ROS (low [ROS]) causes a limited proliferation and survival. Metabolism of cancer cells generates high concentration of ROS (high ([ROS]), this potentiates the growth and survival signalling and causes genomic instability. This could lead to significant cellular damage. However, cancer cells are equipped with an adequate adaptation to ROS. By stimulating both, supplementary repair pathways and expression of antioxidants, cancer cells utilize the benefits of ROS, without extensive damage. When the concentration of ROS in the normal cell rises dramatically, for instance, due to treatment with ROS-inducing agent, oxidative stress that damages biomolecules and organelles occurs. If the damage is irreparable, the cell undergoes cell death.

Endogenous ROS sources.

Mitochondria

There are many intracellular sources of ROS. In many cell types (Figure 4.) Mitochondria are thought to be one the largest contributors to the endogenous ROS pool. During the oxidative respiration, the electrons flow down the respiratory chain resulting in the reduction of molecular oxygen to water. Alternatively, some of the oxygen can also undergo a one-electron reduction to produce a superoxide anion. There are two main sites of last phenomenon occurring in the mitochondria, namely complex I and complex III of the electron transport chain. Similarly to other ROS, the mitochondria-originated ROS can have both damaging as well as signalling properties.

NADPH oxidase

NADPH oxidases (NOXs) are thought to be the first family of enzymes that generates ROS not as a by-product, but as their primary function (Bedard and Krause, 2007). Historically, NOXs have been identified as the sources of ROS in the phagocytes that contribute to the microbial killing (Babior, 1999, Henderson et al., 1987, Henderson and Chappel, 1996, Cross and Segal, 2004). When the expression

of NOX enzymes was reported, it was hypothesised that NOX-generated ROS may contribute to the pathological effects of oxidative stress, possibly linking NOX to

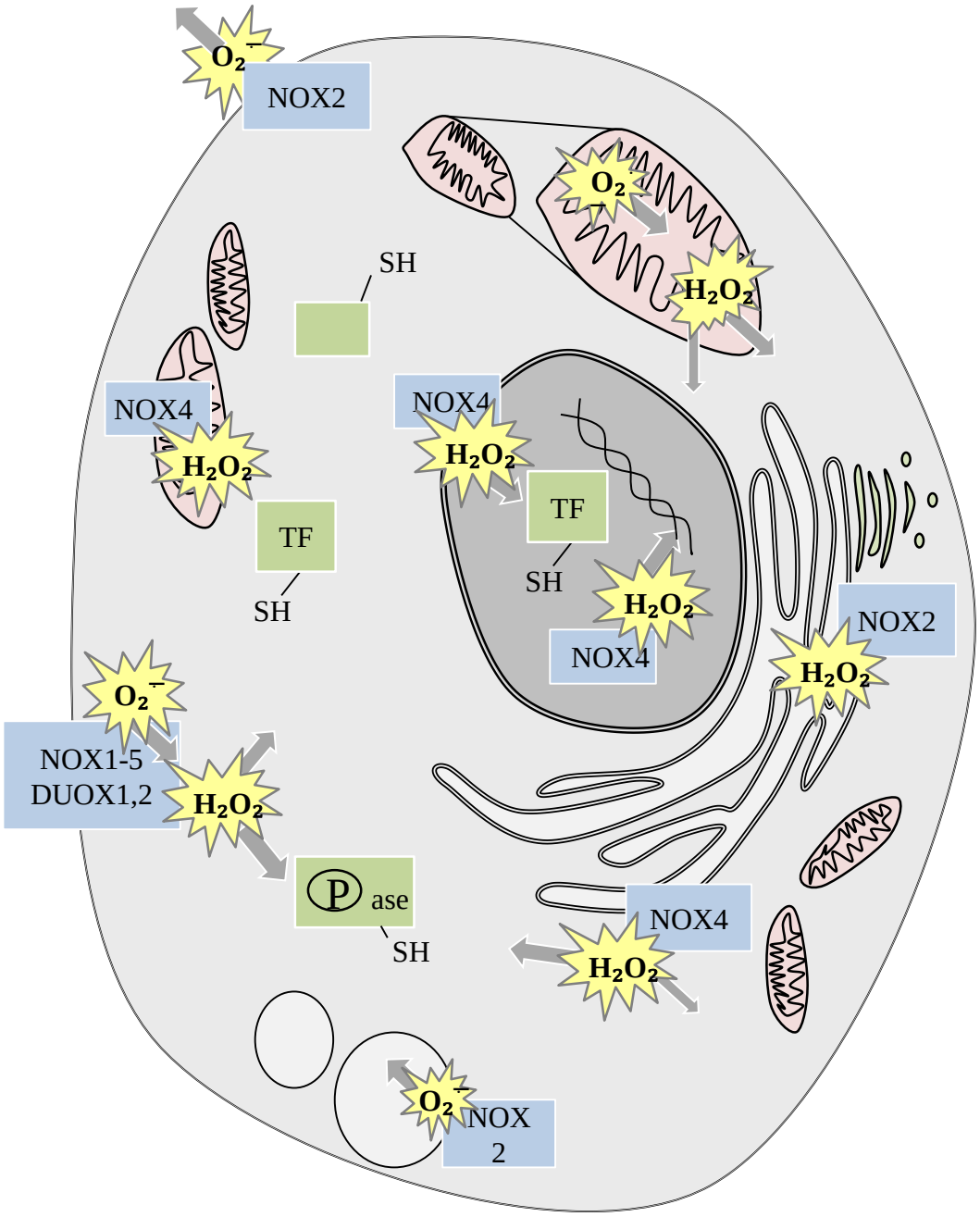

Figure 4. Localised intracellular ROS production. ROS are mainly produced by mitochondria and NOXs within the cell, and these are located in discrete cellular compartments. In order to understand redox reactions, knowledge of the spatial characteristics of ROS homeostasis is essential.

cellular transformation. The NOX family consists of 7 members: NOX1-5 and DUOX1, 2 that possess preserved functional and structural similarities (Bedard and Krause, 2007). They are all transmembrane proteins with a NADPH-binding site, a FAD-binding site, 6 transmembrane domains and four haeme-binding histidines (Bedard and Krause, 2007). Furthermore, they are able to transfer electrons from NADPH across biological membranes to molecular oxygen.

NOX2, also called $gp91^{phox}$ is a prototype of the NOX family. It was first described in phagocytes, however further expression studies have revealed that NOX2 is one of the most widely distributed NOX isoforms found in humans (Bedard and Krause, 2007). NOX2 is a highly glycosylated protein that migrates at 70-90 kDa. The active NOX2 is a complex of $gp91^{phox}$ and other subunits (Groemping and Rittinger, 2005). NOX2 is constitutively associated with $p22^{phox}$ membrane subunit that is essential for the complex stability (Dinauer et al., 1991). The activation of NOX2 requires the translocation of other cytosolic subunits (Groemping and Rittinger, 2005). Phosphorylated $p47^{phox}$ interacts with $p22^{phox}$ and organises the translocation of other activating subunits, i.e. $p67^{phox}$ and GTPase Rac1/2 (Bedard and Krause, 2007, Groemping et al., 2003). The fully assembled NOX2 complex allows the generation of superoxide by the transfer of electrons from NADPH in the cytosol to oxygen on the luminal or extracellular space (Figure 5) (Sumimoto et al., 1996).

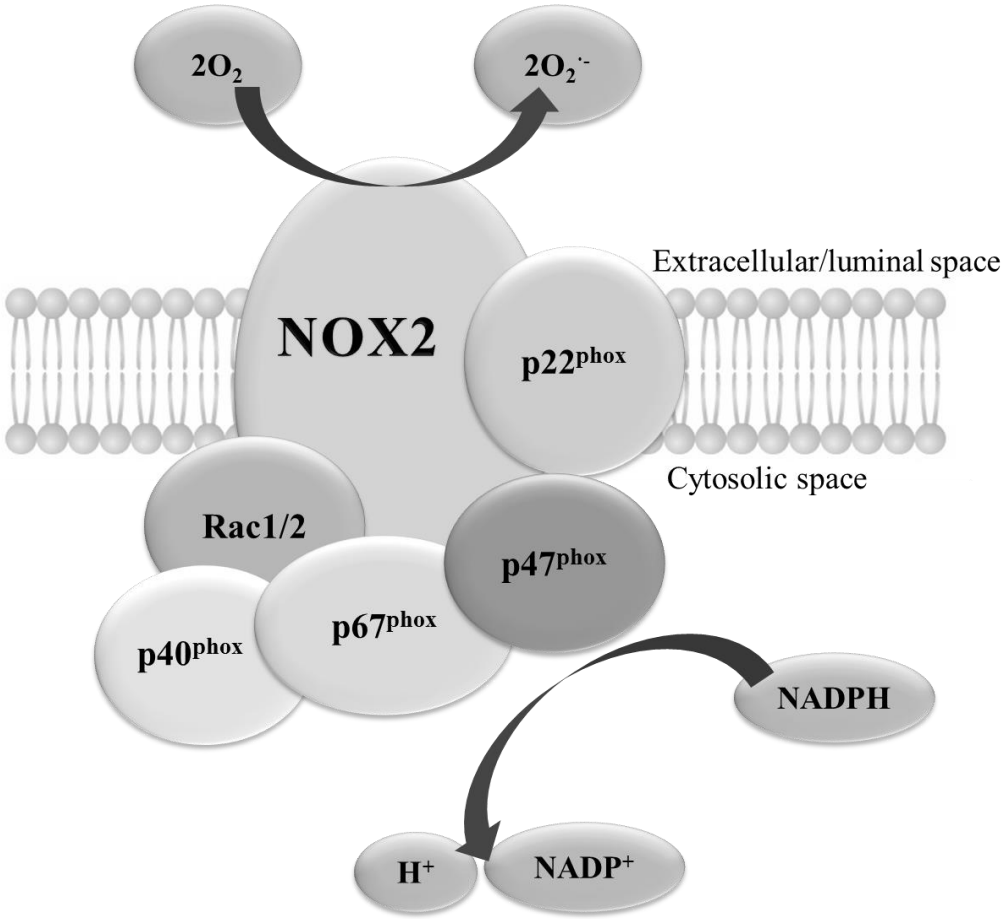

Figure 5. NOX2 complex structure and enzymatic activity. Gp91^{phox} is stabilized at the membrane by p22^{phox} subunit. Upon the activation, the phosphorylated p47^{phox} binds to the complex and organizes the translocation of p67^{phox}, p40^{phox} and Rac1/2 GTPase. The fully assembled complex uses cytosolic NADPH to produce superoxide on the luminal/extracellular side of the complex.

NOX1 has a molecular mass of 55-60 kDa (Cui et al., 2006). While NOX1 is most highly expressed in colon epithelium, it is also present in a variety of different tissues (Bedard and Krause, 2007, Juhasz et al., 2009). Similarly to NOX2, NOX1 is unstable in the absence of p22^{phox} subunit, and it requires an organiser subunit NOXO1 (p47^{phox} homolog), and activating subunit NOXA1 (p67^{phox} homolog) and

the Rac GTPase for the complex activation (Ambasta et al., 2004, Bedard and Krause, 2007).

NOX3 is primarily expressed in the inner ear, although low expression has also been detected in other tissues (Bánfi et al., 2004). NOX3 is activated in an analogous manner to NOX1 and NOX2 (Bánfi et al., 2004). However, the details of its activation are not as clear. NOX3 stimulation is dependent on $p22^{phox}$ and cytosolic subunits (Bánfi et al., 2004, Ueno et al., 2005). While NOX3 activity has been reported to increase in the presence of NOXO1, the effects of NOXA1, Rac GTPase vary (Bedard and Krause, 2007). Moreover, $p47^{phox}$ and $p67^{phox}$ were also demonstrated to induce NOX3 activation (Ueno et al., 2005).

NOX4 was initially shown to be highly expressed in kidney, but similarly to other NOX isoforms, it is expressed in a variety of tissues (Cheng et al., 2001, Bedard and Krause, 2007). It is evolutionary more distant to NOX2, 1 and 3 (Sumimoto, 2008). Subcellular localisation studies revealed that NOX4 resides mainly in the ER and the nucleus (Bedard and Krause, 2007, Chen et al., 2008, Anilkumar et al., 2013, Hilenski et al., 2004). NOX4 mRNA is induced in response to different stimuli e.g. ER stress and hypoxia (Bedard and Krause, 2007). While NOX4 requires $p22^{phox}$ for the complex stabilisation and ROS generation, the cytosolic regulatory subunits seem not required (Ambasta et al., 2004). The reports regarding the requirement of NOX4 for Rac1/2 are not entirely conclusive (Geiszt et al., 2000, Carmona-Cuenca et al., 2008, Kao et al., 2008, Martyn et al., 2006, Gorin et al., 2003, Inoguchi et al., 2003). However, in the heterologously NOX4-

expressing cell lines, Rac does not appear to be required for NOX4 activity (Kao et al., 2008, Bedard and Krause, 2007). What particularly distinguishes NOX4 from the previously described NOX isoforms is the fact that the ROS detected as a product of NOX4 activity is H_2O_2 and not $O_2^{\bullet -}$ (Takac et al., 2011, Nisimoto et al., 2014). Initially, it was thought that $O_2^{\bullet -}$ is such a reactive species that it immediately dismutates into H_2O_2. However, a recent study has proposed that NOX4 has an intrinsic ability to produce H_2O_2 and that the 3rd extracytosolic loop (E-loop) of NOX4 that possesses Cys-226, Cys-270 and His-222 are all essential for this property (Takac et al., 2011). Importantly, NOX4/ E-loop mutants have generated $O_2^{\bullet -}$ as the primary product that failed to increase the phosphorylation of ERK1/2, an important effect of NOX4-generated H_2O_2 (Takac et al., 2011). NOX4 is also the only constitutively active enzyme in the NOX family when exogenously expressed (Martyn et al., 2006). This characteristic lies in the B-loop and the penultimate C terminus of the protein (von Löhneysen et al., 2012).

In contrast to NOX1-4, NOX5 possesses Ca^{2+} -binding EF hand domain (Banfi et al., 2004). NOX5 migrates at 85kDa on the SDS-PAGE and it is suggested that the protein is not glycosylated (Brar et al., 2003, Bedard and Krause, 2007). NOX5 is widely expressed in a variety of tissues. NOX5 does not require p22^{phox} or the cytosolic subunits (Kawahara et al., 2005). However, an increase in the cytosolic Ca^{2+} is crucial for the protein-protein interaction inside the complex that is responsible for NOX5 activation (Banfi et al., 2004, Bedard et al., 2012). DUOX1 and DUOX2 were originally discovered at the plasma membrane in thyroid epithelial

cells (Ohye and Sugawara, 2010). They produce H_2O_2 in a Ca^{2+} dependant manner (Ohye and Sugawara, 2010). DUOXs possess Ca^{2+} EF hand domains and a peroxidase like domain of not clear function (Bedard and Krause, 2007).

The pathological mechanisms of variety of diseases have "utilised" the damaging products of NOX, ROS. While the spatially and temporarily controlled generation of ROS has been shown to play positive biological roles, the unconstrained production of these reactive molecules may lead to detrimental cellular pathologies. That is why, NOXs have been implicated in numerous diseases, e.g. diabetes, atherosclerosis, neurodegenerative disorders, cancers (Figure 6) (Lambeth and Neish, 2014, Lambeth, 2007, Altenhofer et al., 2012). The over-production of ROS from NOX in a disease-state may originate in the over-expression of NOX or their regulatory subunits or availability of their substrate, NADPH (Block and Gorin, 2012, Reddy et al., 2011).

NOX enzymes have been implicated in many cancers (Figure 6) of different origins (Block and Gorin, 2012, Weyemi et al., 2013). It seems that the elevated redox stimulation gives cancer cells some evolutionary advantage. As mentioned before, tumours adapt quickly to the oxidative origin (Irwin et al., 2013, Landriscina et al., 2009). Thus, increased levels of ROS could only benefit these cells by stimulation of cell survival as well as genomic instability, the two desired characteristics for cancer progression (Clerkin et al., 2008, Waris and Ahsan, 2006, Acharya et al., 2010, Landriscina et al., 2009, Trachootham et al., 2008). NOX-derived ROS, often act as secondary signalling molecules in growth factor signalling

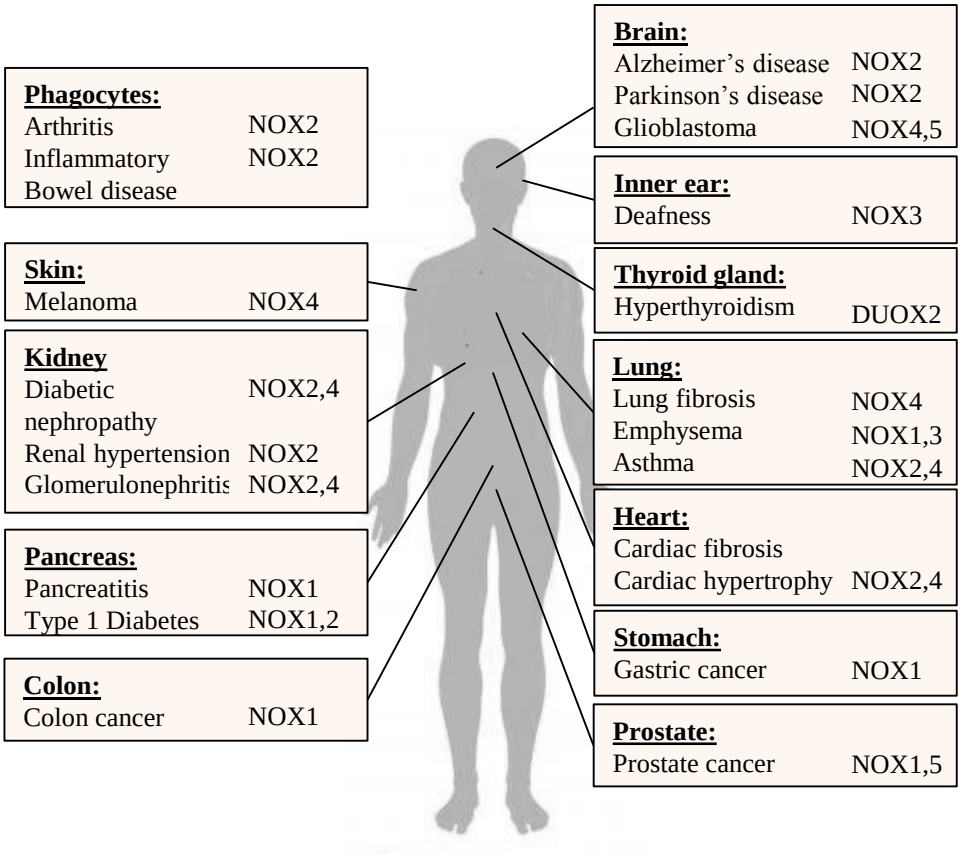

Figure 6. NOX isoforms in human diseases.

downstream of many growth factors e.g. epidermal growth factor (EGF) and platelet-derived growth factor (PDGF) (Chen et al., 2008, Mahadev et al., 2004, Sundaresan et al., 1995). Universally, NOX propagate the signal by hyperphosphorylation of kinases by oxidative inhibition of protein tyrosine phosphatases (PTPs) e.g. PTP1B, phosphatase and tensin homolog (PTEN) and SRC homology region 2 domain-containing phosphatase-1 (SHP-1) (Lou et al., 2008, Groen et al., 2005, Wright et al., 2009). PTPs possess redox sensitive cysteines, resulting in the deactivation of the catalytic function of the enzyme (Groen et al., 2005, Wang et al., 2012). This results in the loss of negative regulation of the kinases leading to increase in the uncontrollable proliferation and survival of cancer cells (Brandts et al., 2005a, Reddy

et al., 2011, Dickinson et al., 2011a, Mondol et al., 2014, Brar et al., 2003, Chen et al., 2008). Moreover, NOX signalling often leads to inactivation of tumour suppressors (Block and Gorin, 2012). For instance, NOX1 have been demonstrated to activate sirtuin 1, that inactivates p53, promoting an anti-apoptotic response (Puca et al., 2010). Interestingly, NOX2 and NOX4 have been involved in the glucose uptake, necessary for the increased metabolism of cancer cells (Prata et al., 2008). NOX1 and NOX4-originated ROS act also as stimulators to VEGF production that stimulates angiogenesis, necessary for the delivery of the nutrients and oxygen to the solid tumours (Block and Gorin, 2012). At the later stages of tumourigenesis, NOX play a role in the invasion and metastasis of cancer cells (Kim et al., 2010, Reddy et al., 2011, Block and Gorin, 2012). This is mainly achieved by the redox regulation of SRC and NF-κB at the invasive microdomains called invadopodia (Diaz and Courtneidge, 2012, Gianni et al., 2010a, Gianni et al., 2010b, Binker et al., 2009). At these sites, ROS control cell adhesion, migration and invasive matrix degradation.

To conclude, the dual nature of ROS - their ability to simultaneously promote growth and damage the biomolecules, has been extensively employed by the cancer machinery (Clerkin et al., 2008, Trachootham et al., 2008, Wu, 2006). In 2000, a review article was published titled “Hallmarks of cancer” (Hanahan and Weinberg, 2000). The authors summarised the critical features of cancer cells such as autonomous growth and evasion of apoptosis (Hanahan and Weinberg, 2000). The structural and functional diversity of NOX signalling substrates make them potent regulators in the majority of these cancer hallmarks and thus, excellent tools in the process of tumourigenesis (Figure 7) (Block and Gorin, 2012).

Fluorescent probes for ROS measurement

ROS signalling is controlled in a spatiotemporal manner and as such there is a need to study the dynamics at precise subcellular locations. There are many dyes commercially available that are used for ROS-detection, but most of them do not meet the ideal criteria that would allow for the localisation of the redox events (see Figure 8). Much recent work has been aimed and remedying this problem.

Most of the commercially available dyes for ROS are based on the oxidation-reduction processes between the ROS and reduced probe, which fluoresces upon oxidation. The most commonly utilised probe to detect ROS is 2',7'-dichlorodihydrofluorescein (DCF). The widespread usage of DCF has revealed a list of its shortcomings: 1) it is not selective for H_2O_2, 2) it is easily photo-oxidised and photo-bleached, 3) it does not react directly with H_2O_2, but it requires peroxidase or metal catalysts, 4) displays a non-linear relationship between concentration of ROS and fluorescent signal, and 5) it is easily membrane diffusible (Chen et al., 2010).

Many contradicting studies on the specificity of another commonly used ROS-probe, dihydroethidium (DHE). There have been some reports published that suggested a specificity towards superoxide anion (Bindokas et al., 1996, Carter Wo Fau - Narayanan et al., 1994), while other studies showed reactions between DHE

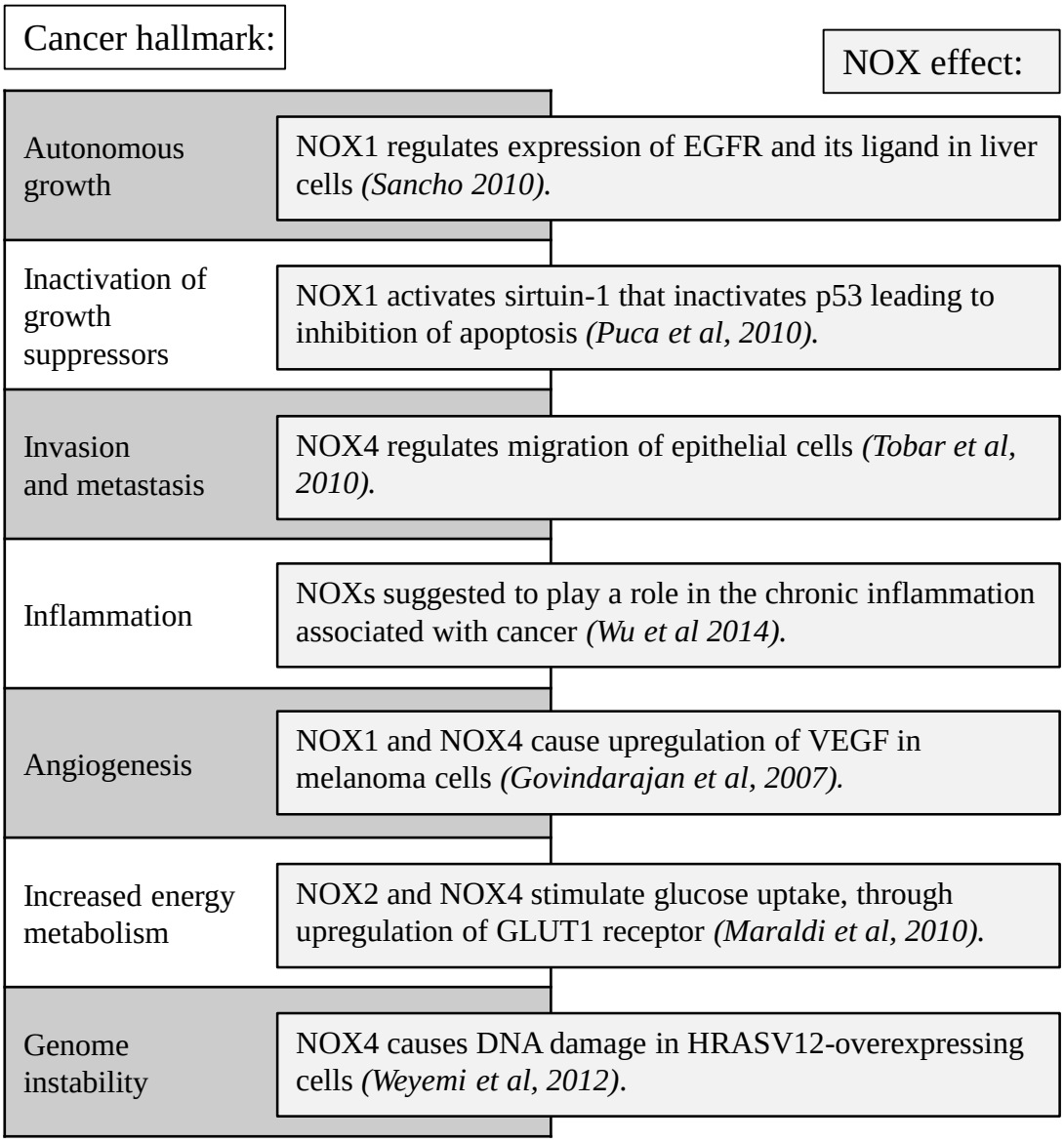

Figure 7. NOX isoforms and hallmarks of cancer.

and haeme proteins or ROS/ reactive nitrogen species (RNS) (Bilski et al., 2009, Palazzolo-Ballance et al., 2007). In 2010, Zielonka and Kalyanaraman extensively reviewed DHE as a ROS-detecting probe (Zielonka and Kalyanaraman, 2010). DHE fluorescent signals can be and DHE can be oxidised by various radicals to form

differentially oxidised products. However, only product reaction with superoxide giving the superoxide-specific product 2-OH-E(+) alters the signal so the probe can be excited by 396 nm wavelength. Thus, in order to reveal the superoxide-induced signal, a 396 nm wavelength should be used as an excitation source (Robinson et al., 2006, Robinson et al., 2008).

DHE has been conjugated to the triphenylphosphonium (TPP^+) moiety, resulting in the MitoSOX dye, in order to target the probe specifically to mitochondria. Cationic TPP+ allows the probe to move through the mitochondrial membrane and accumulate in the mitochondrial matrix. While MitoSOX possesses the inherent disadvantages associated with DHE, it is a promising tool to investigate mitochondrial superoxide/ROS production (Robinson et al., 2008).

Boronate-deprotection probes

The propensity of H_2O_2 to interact with boronate groups was employed in the synthesis a family of fluorescent probes allowing the precise investigation of this intracellular signalling ROS (see Figure 4) (Lippert et al., 2011). These monoboronate-based family of probes (Peroxyfluor-3, Peroxy Orange 1 and Peroxy

Ideal fluorescent ROS-detecting probe		
1.	Chemoselectivity	ROS-type chemoselectivity and no cross-reactivity with other ROS to avoid disambiguity of the type of ROS involved in the reaction; Based on the innate chemical nature of the ROS type;
2.	Membrane pearmibility	Good membrane permeability but little diffusion of the product to allow for localization of the reaction;
3.	Sensitivity	Good sensitivity (nano-micro range of ROS concentration) to detect signalling concentration of the ROS;
4.	Defined spectral peaks	Narrow peaks of excitation and emission spectra to allow simultaneous detection of more than one probe;
5.	Photostability	Little photo-oxidation and photo-bleaching to facilitate imaging on the microscope;
6.	Post-fixation retention	Retention after fixation to allow for simultaneous detection of the dye and the antibody for colocalization studies;
7.	Linear response	Linear relationship between the fluorescent signal to the ROS concentration to allow for quantitative studies of the ROS generation;
8.	Signal-to-noise ratio	Low fluorescence of the ROS-unbound form to avoid false signal from the accumulation of the probe in the cell;
9.	Bioorthogonality	Bioorthogonality and non-toxicity of the probe not to interfere with other biological processes;
10.	*In vivo* capability	Possibility of the probe usage in the in vivo studies to permit of the redox reaction studies in the animal models;
11.	Two-photon microscopy	Compatibility with two-photon microscopy to allow for deep tissue penetration imaging and prolonged observation without specimen damage;

Figure 8. Criteria of ideal fluorescent ROS-detecting probe.

Yellow 1) can detect physiological/signalling changes in H_2O_2 concentration upon phorbol 12-myristate 13-acetate (PMA), epidermal growth factor (EGF) stimulation (Dickinson et al., 2010a) The colour palette of these probes can be utilised to colocalise the H_2O_2 generation in the cell with an organelle-tracker or concurrent detection of H_2O_2 and other ROS probes e.g. 2- [6-(4'-amino)phenoxy-3H-xanthen-3-on-9-yl]benzoic acid (APF) (Dickinson et al., 2010a, Woolley et al., 2012).

Combination of boronate-phenol chemistries to organelle-targetable functioning groups, have proven particularly useful in the development of Mitochondrial Peroxy Yellow 1 probe (MitoPY1) that specifically detects H_2O_2 inside the mitochondria (Dickinson and Chang, 2010, Dickinson et al., 2013). Similar to MitoPY1, Nuclear Peroxy Emerald 1 (NucPE1) utilises boronate chemistry to measure H_2O_2 in the nucleus. This dye offers an opportunity to investigate H_2O_2 in the nucleus that potentially, could be a marker of genotoxic stress in cells.

Genomic Instability

Normal cells display very little of DNA damage that is usually immediately repaired by the extensive highly faithful cellular DNA repair system. However, DNA damage that escapes DNA repair or errors in the process of DNA repair results in genetic alterations that may lead to carcinogenesis (Burrell et al., 2013). Moreover, it has also been proposed that tumours require a certain level of genomic instability as the probability of cancer cells to transform into tumour cells is too low unless the cells are genomically unstable (Sieber et al., 2003).

One of the main origins of genomic instability is increased ROS production that causes excessive DNA damage (Sallmyr et al., 2008b, Sallmyr et al., 2008a). Both mitochondria and NOXs have been demonstrated to produce DNA damaging- ROS (Nieborowska-Skorska et al., 2012, Weyemi and Dupuy, 2012). Mitochondria of BCR-ABL expressing stem cells in chronic myeloid leukaemia produce increased amounts of H_2O_2 that leads to DNA damage (Nieborowska-Skorska et al., 2012).

Sallmyr *et al*. showed that FLT3-ITD-generated ROS are mediated by Rac1 GTPase, which is an essential component of NOX complex (Sallmyr et al., 2008a). Moreover, emerging work has suggested that NOX4-derived ROS may play a substantial role in genomic instability (Weyemi and Dupuy, 2012). Over-expression of Harvey rat sarcoma viral oncogene ($HRAS^{V12}$) induced NOX4-generated ROS and DNA damage that leads to cellular senescence (Weyemi and Dupuy, 2012). Furthermore, NOX4 has been localised to mitochondria where it could damage mitochondrial DNA resulting in mitochondrial dysfunction accompanied by increased production of ROS (Frazziano et al., 2014). Interestingly, NOX4 has also been localised to nuclear membrane and nucleus itself and although the physiological role of this phenomenon is unclear, it is possible that ROS generation in the nucleus could transduce redox signalling on nuclear protein targets e.g. transcription factors (Matsushima et al., 2013). Alternatively, a low level of genomic instability as a consequence of the presence of the ROS in the nucleus could provide some evolutionary advantage.

In addition to endogenous DNA damaging agents, cancer cells modify the DNA repair system e.g. by promoting the unfaithful mechanisms and silencing the error-

free mechanisms (Popp and Bohlander, 2010, Sallmyr et al., 2008b). FLT3-ITD and BCR-ABL oncogenes have been demonstrated to induce the alternative non-homologous end joining (NHEJ) pathways and to reduce the classical NHEJ (Fan et al., 2010). Alternative NHEJ is characterised by increased levels of translocations, increased size of DNA deletions that leads to accumulation of damaged DNA (Fan et al., 2010, Popp and Bohlander, 2010).

Overexpression of mutant NRAS and BCL2, often occurring in leukaemias, has been demonstrated to lead to disease progression through increased levels of NOX-generated ROS, DNA damage and error-prone repair pathways (Rassool et al., 2007). Authors suggest that as a mechanism of genomic instability acquisition that underlies leukemic progression. Another study has also investigated this hypothesis showing that NOX4 localises to the nucleus where it causes ROS production and DNA damage (Gordillo et al., 2010, Anilkumar et al., 2013, Spencer et al., 2011, Weyemi and Dupuy, 2012). NOX4 siRNA silencing resulted in the inhibition of ROS generation specifically in the nucleus as well as a decrease in the level of DNA double strand breaks (dsbs) (Guida et al., 2014).

Objectives

ROS-induced mediation of survival, proliferation, invasion and metastasis processes has already been well documented (Wu, 2006, Pelicano et al., 2004, D'Autreaux and Toledano, 2007, Trachootham et al., 2008, Waris and Ahsan, 2006, Clerkin et al., 2008). Therefore, identification of specific ROS sources, delineation

of mechanisms of their activation as well as their redox effects on tumourigenic processes are of great interest to cancer biologists. AML patients cells possess higher levels of ROS than their healthy counterparts (Hole et al., 2013). Interestingly, the presence of FLT3-ITD, an AML oncogene, has been previously associated with increased ROS levels. However the exact source and mechanism of stimulation of ROS-generation is still unclear. In light of this, the objective of this study was to identify the molecular source of ROS in FLT3-ITD-harbouring AML cells. Furthermore, due to the aforementioned dependency of the redox effects on ROS localisation, it was also of interest to localize ROS and their sources in these cells. Finally, considering the damaging nature of ROS, the final aim of this study was to investigate possible effects of the FLT3-ITD-stimulated ROS on genomic instability in AML cells.

Chapter 2

Materials and Methods

Reagents and Chemicals

The ROS probe DCF (2',7'-dichlorodihydrofluorescein diacetate; H_2DCFDA; #D-399) and MitoSOX (Red Mitochondrial Superoxide Indicator; #M36008), ER-Tracker™ Red dye (BODIPY® TR Glibenclamide; #E34250), ER-Tracker™ Green (BODIPY® FL Glibenclamide, # E34251) were all purchased from Molecular Probes (Life Technologies, Dublin, Ireland). Hoechst (bisBenzimide Hoechst 33342 trihydrochloride; #B2261) was purchased from Sigma-Aldrich (Dublin, Ireland).

The mitochondrial Peroxy Yellow 1 (MitoPY1), Peroxy Orange 1 (PO1) and Nuclear Peroxy Emerald 1 (NucPE1) were a kind gift from Dr. Christopher Chang, University of Berkley in CA, USA. Detailed protocols of their syntheses are available (Dickinson et al., 2011b, Dickinson et al., 2010a, Dickinson and Chang, 2010).

FLT3-ITD was inhibited using PKC412 (Midostaurin; [9S-(9α,10β,11β,13α)]-N-(2,3,10,11,12,13-Hexahydro-10-methoxy-9-methyl-1-oxo-9,13-epoxy-1H,9H-diindolo[1,2,3-gh:3',2',1'-lm]pyrrolo[3,4-j][1,7]benzodiazonin-11-yl)-N-methylbenzamide; Tocris Biosciences in Bristol, UK), AC-220 (Quizartinib; Urea, N-[5-(1,1-dimethylethyl)-3-isoxazolyl]-N'-[4-[7-[2-(4-morpholinyl)ethoxy]imidazo[2,1-b]benzothiazol-2-yl]phenyl]-; # S1526-SELL from Selleck Chem from Stratech in Suffolk, UK) or CEP-701 (Lestaurtinib; (9S,10S,12R)-2,3,9,10,11,12-Hexahydro-10-hydroxy-10-(hydroxymethyl)-9-methyl-9,12-epoxy-1H-diindolo[1,2,3-fg:3',2',1'-kl]pyrrolo[3,4-i][1,6]benzodiazocin-; #3395 from Tocris Biosciences in Bristol, UK) at the indicated times and concentrations.

NOX inhibition was achieved using diphenyleneiodonium (DPI; Sigma-Aldrich in Dublin, Ireland) or VAS-2870 (3-benzyl-7-(2-benzoxazolyl)thio-1,2,3-triazolo[4,5-d]pyrimidine) from Enzo Life Sciences (Lausen, Switzerland), at the indicated times and concentrations.

Once purchased, inhibitors were resuspended in dimethylsulfoxide (DMSO), aliquoted and stored at -20°C, as recommended by the producer.

Stimulation of wild type FLT3 (FLT3-WT) was achieved using a recombinant human FLT3 ligand FLT3 ligand (FL; 100 ng/ml) purchased from Peprotech in United States (#300-19). Bovine serum albumin (BSA; Sigma-Aldrich, Dublin, Ireland) was used as a vehicle.

In all cases, if not shown, inhibitor concentrations were chosen based on their greatest effect with a negligible decrease in cellular viability. Unless otherwise stated all other chemicals and reagents were purchased from Sigma-Aldrich in Dublin, Ireland.

Cell culture and treatments

Human patient-derived leukemic cell lines MV4-11 (homozygous for the FLT3-ITD mutation), MOLM-13 (heterozygous for the FLT3-ITD mutation) and HL-60 (homozygous for the FLT3-WT), were all purchased from DSMZ (Braunschweig, Germany). 32D, a murine immortalised myeloblast-like cell line cell line, stably transfected with FLT3-WT and FLT3-ITD, respectively, were a kind gift from Prof. Hubert Serve from Goethe University Frankfurt and Prof. Frank D. Bohmer from the

Universitatsklinkium Jena in Germany. The cell lines were maintained in Roswell Park Memorial Institute (RPMI) 1640 (Sigma-Aldrich in Dublin, Ireland) medium, supplemented with 10% Foetal Bovine Serum (FBS; Sigma-Aldrich in Dublin, Ireland), 1% penicillin/streptomycin (Sigma-Aldrich in Dublin, Ireland) and 2 mM L-glutamine (Gibco, Invitrogen Corporation, Paisley, UK) in a humidified incubator at 37°C with 5% CO_2. For 32D cell lines, 10% WEHI-conditioned medium was added as a source of interleukin-3 (IL-3). The WEHI conditioned medium was harvested from a 48 h culture of WEHI, a macrophage-like, derived from a BALB/c mouse treated for tumor induction cell line, which produce and secrete IL-3. Before carrying out experiments that involved a comparison of 32D/FLT3-WT and 32D/FLT3-ITD, the cells were washed twice with PBS and IL-3- starved overnight in 5% FBS medium, as recommended previously (Choudhary et al., 2009, Sallmyr et al., 2008a)

Except for 32D cells, all cell lines were maintained between 0.1-1.5x10^6 cells/ml and were subcultured every 2-3 days. 32D cells were maintained between 0.2-1.0x10^6 cells/ml and subcultured every 2 days. Cell counts were obtained using a haemocytometer under a light microscope. Cell viability was determined by trypan blue exclusion (Sigma-Aldrich in Dublin, Ireland).

Antibodies

Primary antibodies used for immunoblotting: anti-$p22^{phox}$ (Rabbit #sc-20781; Santa Cruz Biotechnology, CA, USA), anti-$p67^{phox}$ (Rabbit #sc-15342 ; Santa Cruz

Biotechnology, CA, USA), anti-NOX4 used in MV4-11 cell lysates: (Rabbit #NB110-58851; Novus Biologicals in CO, USA), anti-NOX4 used in 32D cell lysates (Goat #sc-21860; Santa Cruz Biotechnology, CA, USA), anti-NOX1 (Rabbit #ab55831, Abcam in Cambridge, UK), anti-GAPDH (Mouse #RGM2-500, Advanced Immunochemicals in Long Beach, CA, USA) anti-β-Actin (Mouse #A5441; Sigma-Aldrich in Dublin, Ireland) and anti-NOX5 (Rabbit #HPA019362; Sigma-Aldrich in Dublin, Ireland) anti-NOX2 (Rabbit #07-024; from Millipore/Upstate Biotechnology in MA, USA), anti-P-STAT5 (Rabbit Tyr694/699; #04-886; from Millipore/Upstate Biotechnology in MA, USA), anti-tubulin (Mouse #T5168 from Sigma-Aldrich in Dublin, Ireland), anti-FLT3 (Rabbit; 8F2 #3462S) and anti-P-FLT3 (Rabbit Tyr591, 33G6 Rabbit mAb #3474) were purchased from Cell Signaling Technology (Boston, MA, USA). Secondary antibodies for Western blotting were Li-Cor IRDye secondary antibodies: IRDye® 680RD Donkey anti-Rabbit IgG (H + L) (#926-68071), IRDye® 680RD Goat anti-Mouse IgG (H + L) (#926-68070) and IRDye® 800CW Donkey anti-Rabbit IgG (H + L) (#926-32213) were purchased from Li-Cor Biosciences, Nebraska, USA) used for detection with the Odyssey System.

Primary antibodies used for immunofluorescence: anti-8-OHdG (Mouse #ab26842; Abcam in Cambridge, UK), anti-γH2AX (Phospho-Histone H2A.X (Ser139) (20E3) Rabbit mAb (Alexa Fluor® 488 Conjugate; Rabbit #9719, from Cell Signaling Technology (Boston, MA, USA)), anti-NOX4 (Rabbit #NB110-58851; Novus Biologicals from Littleton in US), NUP98 (Mouse #SC-74578; Santa Cruz Biotechnology, CA, USA), anti-$p22^{phox}$ (Rabbit #SC20781; Santa Cruz

Biotechnology, CA, USA), anti-KDEL (Mouse 10C3 # ab12223; from Abcam in Cambridge, UK).

Measurement of intracellular H_2O_2

Total intracellular H_2O_2 was measured by incubating cells with 10 μM of cell-permeable H_2O_2–probe PO1 added to the medium for 1 h at 37°C in the dark. Cells were then briefly washed with phosphate buffered saline (PBS) and immediately read by flow cytometry using FACSCalibur (BD Biosciences, Europe) and Cellquest Pro software (Beckton Dickinson). The probe was excited using FL2-H (red) flow cytometry laser. The fluorescent intensity of cells of 10,000 events was recorder. The viability/healthiness of the cells, based on their size and granularity, was estimated using FSC-H and SSC-H lasers. The geometric mean of 3 technical replicates of fluorescence of viable cells was calculated. The fluorescence of control cells was expressed as 100% and the fluorescence of treated cells was expressed as a percentage of the control. The measurement of nuclear H_2O_2 was achieved using NucPE1. The cells were incubated for 45 min at 10 μM of NucPE1 added to the medium in the dark at 37°C. The incubation was followed by PBS washing and analysis by flow cytometry as explained above. The probe was excited using a FL1-H (green) flow cytometry laser. Mitochondrial ROS were measured using MitoSOX probe. The cells were incubated with 5 μM of freshly prepared MitoSOX for 15 min in the dark at 37°C. The incubation was followed by PBS washing and analysis by flow cytometry as explained above. The probe was excited using a FL2-H (red) flow cytometry laser.

Confocal live microscopy

Confocal fluorescence live imaging studies were performed with a Zeiss LSM510 META confocal microscope fitted with a 6361.4 plan apochromat lens. Excitation of PO1 at 543 nm was carried out with Ar laser and emission was collected between 560–615 nm. Excitation of MitoPY1 at 514 nm was carried out using Ar laser and collected between 505–550 nm. Excitation of ER tracker green at 488 nm was carried out using Ar laser and emission was collected between 505–530 nm. The live imaging of NucPE1 probe was carried out using excitation at 488 nm with Ar laser and emission was collected using a META detector at about 520 nm. The Hoechst dye was incubated together with NucPE1 where indicated. The multi-tracking mode of scanning was applied for acquisition of the images. Image analysis was performed in MetaMorph Offline and Carl Zeiss Zen 2009 Light Edition. Aprroximately 4–5 h (for PKC412 and VAS-2870 treatments) or 24 h (after siRNA transfection) before imaging MV4-11 cells were plated on poly-D-lysine (#P4707; Sigma-Aldrich in Dublin, Ireland) coated glass bottomed dishes (#P35G-1.5-14-C; MatTek Corporation, Ashland, US). An hour before imaging, cells were stained with green or red ER tracker dye (1 µM), as recommended by protocol provided by the producer. PO1 (5 µM), MitoPY1 (5 µM) or NucPE1 (10 µM) probes were added, as recommended by Dickinson *et al.* (Dickinson et al., 2011b, Dickinson et al., 2010a, Dickinson and Chang, 2010). Where indicated, cells were treated with DPI (5 µM or 1 µM) PKC412 (50 nM or 200 nM) or VAS-2870 (10 µM) for 1 h before imaging. After treatment, cells were washed twice with PBS buffer and incubated in fresh medium during imaging.

Immunofluorescence

MV4-11 cells were cultured for 16 h on Poly-D-lysine covered coverslips. Coverslips were then washed in PBS twice (all washes were 5min each) and fixed for 1 h in 3% PFA/ PBS, followed by a 5 min PBS wash. Cells were treated with 50mM NH_4Cl for 10 min which was followed by three PBS washes. The cells were subsequently permeabilised using 0.05% saponin/ 0.2% BSA/PBS for 5 min and washed with PBS. The antigens were blocked for 15 min with 5% FBS/PBS. The coverslips were incubated with 50 µl of KDEL, $p22^{phox}$, NOX4 or NUP98 primary antibody solutions (1/100 in 5% FBS/PBS) and incubated at room temperature for 1 h in humidification chambers. The primary antibody incubation was again followed by two 5 min-washings with PBS. 50 µl of Alexa fluor 594 or Alexa fluor 488 secondary antibody solutions (1/100 in 5% FBS/PBS) were added onto coverslips and incubated for 1 h at room temperature. The Hoechst stain (1:1000) was also added to the appropriate secondary antibody in FBS/PBS solution. The coverslips were subsequently washed thoroughly with PBS, followed by water and finally mounted on the slides using 5 µl of mowiol (Sigma-Aldrich, Dublin, Ireland). The slides were dried overnight at room temperature. Images were acquired using multiphoton laser scanning microscope Flouview1000 MPE (Mason Technology Dublin, Ireland) with 100x oil immersion objective.

γH2AX immunofluorescence

Approximately 200,000 cells were washed for 5 min in PBS and cytopsun for 5 min at 500 g onto the slides. The slides were allowed to dry for 1 h. Following drying, cells were fixed for 1 h in 3% PFA/ PBS. The fixing step was followed by a 5 min PBS wash. The slides with cells cytospun onto them were incubated in 70% ethanol overnight at -20°C. On the next day, the cells were washed twice with PBS for 5 min each time. The antigens were blocked for 15 min using 5% FBS/PBS and incubated with 50 µl of γH2AX primary antibody (1/100 in 5% FBS/PBS) and Hoechst solutions (1:1000 in 5% FBS/PBS) at room temperature for 1 h in the humidification chambers. The primary antibody incubation was followed by washing with PBS. Cells were visualised on a Leica DM LB2 fluorescence microscope (Leica, Nussloch, Germany) using a TRITC filter. Images of the cells were acquired by Nikon Digital Sight DS-Fi1C camera (Nikon, Japan) using NIS-Elements software (version 3.0, Nikon, Japan).

8-OHdG assay

Oxidative damage was assessed using 8-hydroxy-2`-deoxyguanosine (8-OHdG) as a marker, as described in Moiseeva *et al.* (Moiseeva et al., 2009). Approximately 2×10^6cells were washed with PBS and fixed for 1 h in 3% PFS/PBS. After washing off the fixative, the cells were treated with 2 M HCl for 20 min at room temperature. HCl was removed and the cells were treated with 0.1 M sodium borate, pH 8.5 for 2 min. Cells were then washed and permeabilised with 0.2% BSA, 0.05%

saponin/PBS. The permeabilisation buffer was washed off three times with 3% BSA/PBS and incubated with primary anti-8-OHdG antibody overnight at 4°C in a humidification chamber. On the next day, the cells were washed three times with 3% BSA/PBS solution, and incubated with the secondary antibody conjugated to Alexa fluor 594 for 1 h at room temperature. After removing the secondary antibody, the cells were washed three times in PBS and analysed using flow cytometry. 10,000 events were acquired for each of the technical replicates. The geometric mean was calculated based on gated healthy population of cells.

γH2AX quantification using flow cytometry

The levels of DNA double strand breaks (dsbs) were measured using γH2AX as a marker (Valdiglesias et al., 2013). Approximately 2×10^6cells were washed with PBS and fixed for 1 h in 3% PFA/PBS. The cells were then incubated in 70% ethanol at -20°C overnight. The next day, the cells were washed and blocked for 15 min with 1% BSA/PBS. Following washing, the cells were incubated in γH2AX antibody conjugated to Alexa Fluor 488 (Cell Signaling Technology, #9719) in 1% BSA/PBS solution at 4°C overnight. The cells were then washed and analysed by flow cytometry. 10,000 events were acquired for each of the technical replicates. The geometric mean was calculated based on gated healthy population of cells.

Western Blotting

Following the treatments of indicated durations or siRNA transfections, cells were washed with ice-cold PBS and centrifuged at 300g for 5 min at 4°C. Following careful removal of PBS, cells were incubated in Radio Immunoprecipitation Assay (RIPA) lysing buffer [Tris–HCl (50 mM; pH 7.4), 1% NP-40, 0.25% sodium deoxycholate, NaCl (150 mM), EGTA (1mM), sodium orthovanadate (1 mM), sodium fluoride (1 mM), cocktail protease inhibitors (Roche, Welwyn, Hertforshire, UK) and 4-(2-Aminoethyl) benzenesulfonyl fluoride hydrochloride (200 mM)] for 1 h on ice. Every 15 min cells in RIPA solution were vortexed to ensure the thorough cell lysis. This was followed by centrifugation at 14 000 g for 15 min to remove cell debris. The protein concentration in the supernatant was determined by the Bio-Rad Protein Assay (Bio-Rad, Hemel Hempstead, UK) using bovine serum albumin (BSA) as a protein standard. Based on the Bio-Rad Protein Assay, equivalent amounts of proteins (30-70 μg per lane) were diluted in 2X loading buffer (10% sodium dodecyl sulfate (SDS), 100mM dithiothreitol (DTT), glycerol, bromophenol blue, Tris-HCl) and loaded into the 10-15% SDS–polyacrylamide gel. The proteins were stacked at 90 V for 20 min and resolved at 120 V using SDS–polyacrylamide gel electrophoresis (SDS-PAGE). The proteins were then transferred from the SDS-polyacrylamide gel to the nitrocellulose membrane for 1 h (Schleicher and Schuell, Dassel, Germany). Following the transfer, membranes were washed with Tris-buffered saline/0.1% Tween-20 (TBST) for 5 min. Protein antigens on the membranes were blocked for 1 h with 5% (w/v) non-fat dry milk or 5% (w/v) BSA solutions, based on the producer's recommendations. The membranes were then

incubated overnight with the appropriate primary antibodies diluted in the blocking solution. The primary antibodies against the loading control proteins: GAPDH, tubulin and β-actin were incubated for 1 h. On the next day, the membranes were washed with two times with TBST and once with TBS for 5 min each time. The membrane was incubated in the secondary antibody coupled with Alexa Fluor 680 or 800 diluted in the blocking solution for 1 h, followed by the same TBST/TBS washing. The signal was detected with the Odyssey infrared imaging system (LI-COR Biosciences).

Small Interfering RNA (siRNA) transfection

The siRNA transfection of MV4-11 cells was performed using the Nucleofector Kit L (Amaxa, Cologne, Germany) and AmaxaNucleofector Technology according to the protocol provided by the company. The predesigned siRNAs used for silencing were: $p22^{phox}$ (ID: S3786 (A), S194371 (B), S194372 (C)), NOX4 (ID: S27015 (A), S27014 (B), S27013 (C)). For the negative control, the siRNA used was Silencer Select Negative Control #1 siRNA (Control). All were purchased from Ambion, Warrington, UK. Cells were seeded at 0.5×10^6/ml 16 h before the transfection. Before the procedure siRNA solutions were prepared in 50 µl of the nucleofection buffer provided. Approximately 2×10^6 cells were cytospun at 300g for 5 min at room temperature and resuspended in 50 µl of the same nucleofection buffer. The solutions of cells and siRNA were combined and the mixture of the two solutions was immediately transferred into the certified nucleofection cuvette. The cuvette was inserted into the nucleofection cuvette holder and the correct

nucleofection program was applied (Q-001). The contents of the cuvette were immediately diluted in the fresh medium (0.5 ml) and added dropwise onto the 6-well plate with more of fresh medium in it (1.5 ml). The final density of cells in the well following the transfection was 1×10^6/ml. The plate was transferred to a humidified incubator (37°C with 5% CO_2) and left there for 24 h.

The siRNA transfection of 32D cells was performed using the Nucleofector Kit V (Amaxa, Cologne, Germany) and Amaxa Nucleofector Technology (E-032 program) according to the protocol provided by the company. The predesigned siRNA were used for silencing: $p22^{phox}$ (ID: s201230 (A), s64648 (B), s201231 (C)), NOX4 (ID: s211726 (A), s211725 (B), s78320 (C)). All were purchased from Ambion, Warrington, UK. The nucleofection procedure applied for 32D cells was exactly the same as with MV4-11, except for the number of cells that was there was transfected in one sample was 1×10^6 rather than 2×10^6 cells. This also resulted in the final density of cells in the well following the transfection to be 0.5×10^6/ml.

Statistical Analysis

The results are expressed as a percentage of control, defined to 100%. Values are mean ± standard deviation (SD). Data were statistically analysed using Student's t-test with $p<0.05$.

Chapter 3

Localisation and cellular sources of ROS in FLT3-ITD-expressing AML cells.

Introduction

Cancer cells and cell lines have been shown to possess higher levels of ROS than their healthy counterparts (Kumar et al., 2008, Farquhar and Bowen, 2003, Fried and Arbiser, 2008). ROS are thought to promote cell survival (Woolley et al., 2013a), migration (Wu, 2006), metastasis (Ishikawa et al., 2008), proliferation (Reddy et al., 2011, Block and Gorin, 2012) and drug resistance (Trachootham et al., 2009). Therefore, ROS are increasingly recognised as powerful stimulants of tumourigenesis (Block and Gorin, 2012) and are thus attractive targets for molecular cancer chemotherapy.

ROS induce intracellular signalling through covalent modifications of their protein substrates. H_2O_2 exerts its signalling effects primarily through oxidation of key cysteine residues on target proteins (Miki and Funato, 2012). This, in turn, can modulate the activity of H_2O_2 signalling partners. For example, many protein tyrosine phosphatases possess redox-susceptible cysteines. These cysteines can be easily and reversibly oxidised by H_2O_2, which inhibits the enzymatic activity of the phosphatases (Ostman et al., 2011). Subsequent inactivation of phosphatases attenuates the negative regulation of kinases, leading to an increased phosphorylation state in the cell. Such a state facilitates phosphorylation-dependant growth factor signalling. An alternative mechanism of ROS signal transduction is by oxidation of kinases (Nakashima et al., 2002). For instance, oxidation of cysteines of SRC kinase leads to its activation, which is required for cell attachment to the extracellular matrix and tumourigenesis (Giannoni et al., 2005).

Many oncogenes have been found to induce generation of ROS in various cancers of different tissue origin (Vafa et al., 2002, Hole et al., 2013). Oncogenes have the molecular ability to stimulate mitochondria or NOX enzymes to generate these increased amounts of ROS. For example, c-MYC has been shown to induce ROS production that localises to mitochondria and damages mitochondrial DNA in human fibroblasts (Vafa et al., 2002). In the case of NOXs, the most common mechanism of achieving higher levels of ROS is through activation of the NOX complex by phosphorylation of NOX regulatory subunits such as $p47^{phox}$ or $p22^{phox}$ (Brandes et al., 2014). It has also been proposed that increased concentration of the NOX substrate, NADPH can lead to elevation in ROS production (Brandes et al., 2014).

Several oncogenes commonly mutated in different types of leukaemia have been shown to alter cellular levels of ROS (Reddy et al., 2011). Presence of BCR-ABL, prevalent in CML; and FLT3-ITD, RAS and c-KIT, common in AML; result in an increased concentration of ROS which in turn can affect growth and proliferation of leukaemic cells (Reddy et al., 2011, Sallmyr et al., 2008a). Moreover, elevation in ROS usually results in DNA damage that can lead to genomic instability and further increases in tumour aggressiveness of the disease (Jackson and Loeb, 2001). However, the molecular sources of ROS in these cells have not yet been elucidated.

FLT3-ITD is a frequent activating mutation which results in a constitutively active receptor tyrosine kinase (RTK). Mutated FLT3-ITD is a potent regulator of survival, proliferative and differentiation pathways, all of which are important in the

development of leukaemia (Gilliland and Griffin, 2002). The presence of FLT3-ITD mutation has been proposed to elevate ROS levels through NOX activation (Sallmyr et al., 2008a). In this study, FLT3-ITD-regulated phosphorylated STAT5 (P-STAT5) was shown to interact with Rac1, a GTPase involved in activation of NOX complex (Sallmyr et al., 2008a). Conversely, Reddy *et al*. have found that pharmacological inhibition of FLT3-ITD (and other leukaemic oncogenes) resulted in a reduction in mitochondrial superoxide levels. This suggests that mitochondria may be the source of the oncogene-induced ROS in leukaemia (Reddy et al., 2011). More importantly, the same study has demonstrated that NOX-generated ROS, as opposed to mitochondrial ROS, were involved in the regulation of cell growth and migration processes in AML cells (Reddy et al., 2011).

As H_2O_2-induced signal transduction is based on the oxidation of its target, it could be concluded that H_2O_2 oxidising reactivity would induce a number of non-specific signalling events. However, redox signalling processes are tightly regulated by the localisation of H_2O_2 production to the molecular target. This guarantees its chemical reactivity and signalling specificity (Mishina et al., 2011). Therefore, it is essential that studies of redox signalling biology should be accompanied by the localisation studies of ROS generating systems and their signalling partners.

The aims of our work were to localise ROS generated by the FLT3-ITD oncogene and to examine different sources of ROS, particularly H_2O_2, in FLT3-ITD expressing cells. This would allow us to investigate possible redox signalling downstream of FLT3-ITD in AML.

Results

FLT3 expression and phosphorylation in MV4-11 and HL-60 cell lines.

In order to study FLT3-ITD redox signalling, we chose the MV4-11 cell line model that was derived from an AML patient with the FLT3-ITD mutation. Western blotting analysis of MV4-11 lysates confirmed the expression of FLT3 in these cells (Figure 1.1.a). The upper band represents the glycosylated mature FLT3, which runs at 160 kDa and the lower band corresponds to the unglycosylated FLT3 that runs at 130 kDa. In order to compare FLT3-ITD and FLT3-WT signalling, we also selected HL-60, a patient-derived cell line that expresses wild type FLT3. Expression of FLT3 by Western blotting was also confirmed in these cells (Figure 1.1.a).

To study the molecular events downstream of FLT3, we employed a small tyrosine kinase inhibitor (TKI) of FLT3, PKC412. Attenuation of FLT3 phosphorylation in MV4-11 cells following the PKC412 treatment validated the inhibitory activity of PKC412 (Figure 1.1.b).

ROS levels following the inhibition of FLT3 using PKC412 in MV4-11 cells.

It has been previously published that inhibition of the FLT3-ITD oncogene, using CEP-701 inhibitor, resulted in a significant decrease in the levels of ROS in patient samples (Sallmyr et al., 2008a). To investigate if this is similarly occurring when using PKC412; and to establish how this changes over a range of concentrations of PKC412 at 1 h and 24 h incubations, MV4-11 cells were stained

a)

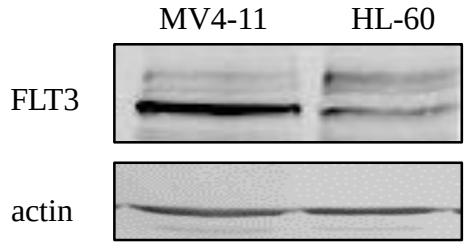

b)

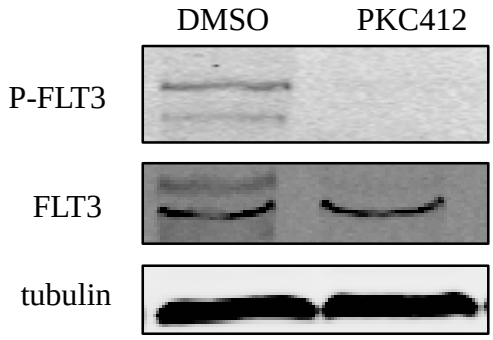

Figure 1.1. FLT3 expression/phosphorylation in MV4-11 and HL-60 cell lines. a) Western blotting analysis of FLT3 expression in MV4-11 and HL-60 cells. Actin was used as a loading control. b) Western blotting analysis of phosphorylated-FLT3 (P-FLT3), FLT3 in MV4-11 cells treated with the vehicle (DMSO) or 50 nM PKC412 for 24 h. Tubulin was used as a loading control.

with a fluorescent ROS probe, DCF. The fluorescence intensity of DCF was compared between control and treated cells (Figure 1.2.a). The results have shown that inhibition of FLT3 is followed by the inhibition of generation of ROS and that these ROS remain at the lower level over 24 h FLT3 inhibition (Figure 1.2.b).

Levels of ROS following NOX inhibition using DPI in MV4-11 cells.

NOX enzymes have been recently identified as one of the most important ROS sources in cancer cells (Block and Gorin, 2012). In order to investigate their effects in the MV4-11 cell line, we employed a common flavin protein inhibitor, DPI. To investigate the changes in ROS levels, the cells were treated with a range of DPI concentrations for 1 h (Figure 1.3.a) and 24 h (Figure 1.3.b). At 1 h, a 5 μM concentration was the smallest dose that resulted in the largest decrease in ROS, whereas at 24 h a concentration of 0.5 μM was the smallest DPI dose that led to the largest decline in ROS.

Comparison of ROS levels following FLT3 inhibition or NOX inhibition in MV4-11 cells

NOX-produced ROS have been reported to regulate cell growth and migration in cell lines expressing FLT3-ITD, such as MOLM-13 (Reddy et al., 2011). NOX-activating GTPase, Rac1 has also been shown to interact with STAT5, to induce ROS-generation downstream of FLT3-ITD. This has suggested that Rac1 could activate NOX enzymes in these cells (Reddy et al., 2011, Sallmyr et al., 2008a).

a)

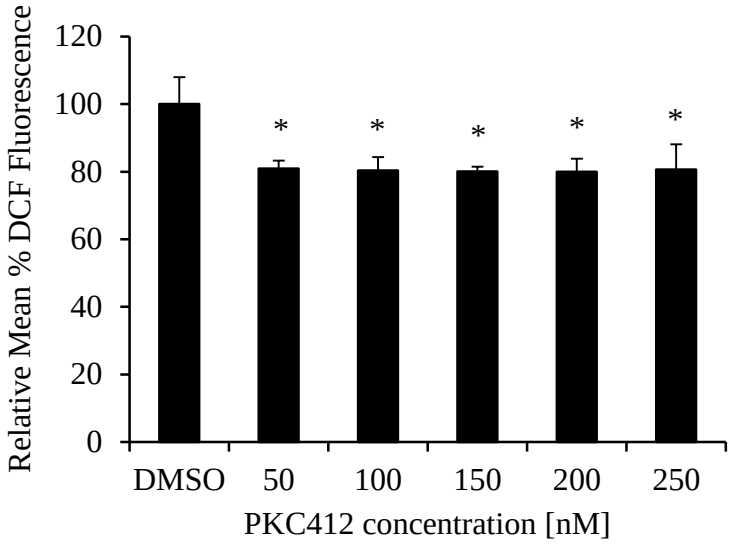

b)

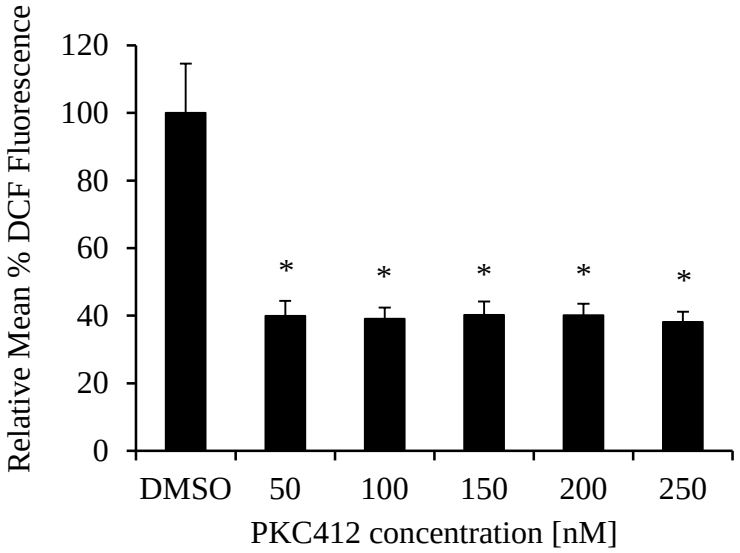

Figure 1.2. ROS levels following the inhibition of FLT3 using 50-250 nM range of PKC412 concentrations in MV4-11 cells. FACS analysis of DCF fluorescence as a measure of the levels of ROS following the PKC412 treatment at a) 1 h and b) 24 h. Results are shown as relative geometric mean ± SD. Statistical analysis was carried out using the Student's t-test ($p<0.005$ is marked with *).

a)

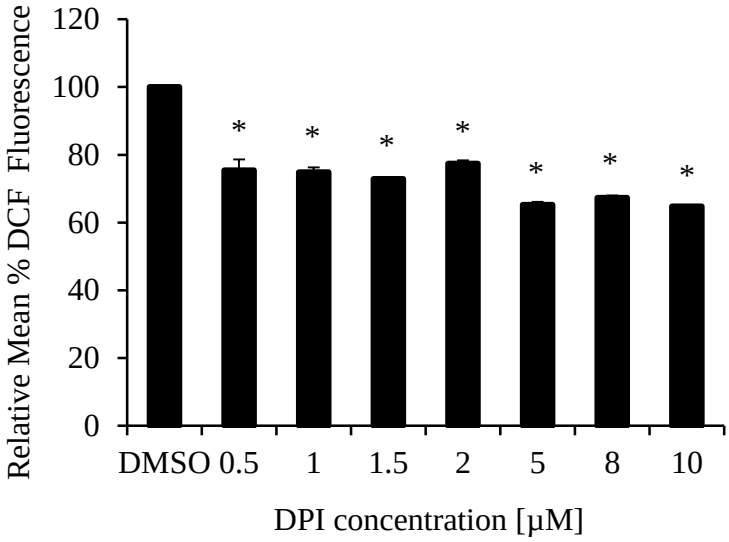

b)

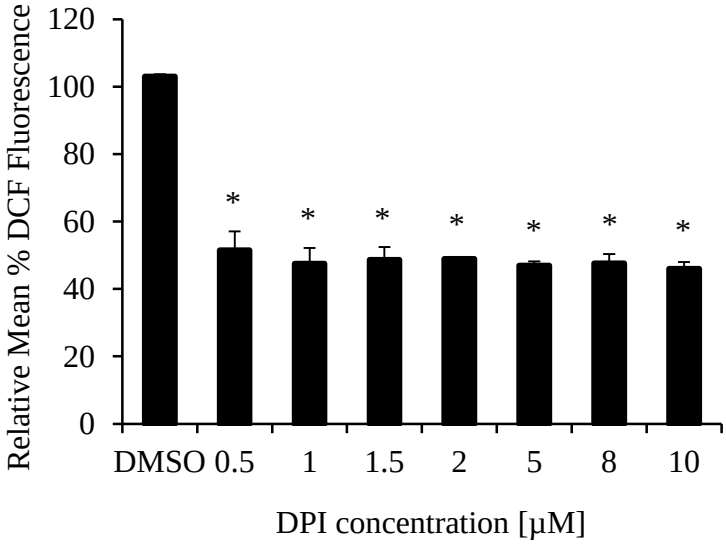

Figure 1.3. Levels of ROS following the inhibition of NOX using different 0.5-10 µm DPI concentrations in MV4-11 cells. FACS analysis of DCF fluorescence as a measure of the levels of ROS following the DPI treatment at a) 1 h and b) 24 h. Results are shown as relative geometric mean ± SD. Statistical analysis was carried out using the Student's t-test ($p<0.005$ is marked with *).

Based on the FLT3-ITD-NOX association, we decided to inhibit FLT3 or NOX in MV4-11 cells and compare the levels of ROS thereafter. Inhibition of NOX,achieved using DPI inhibitor resulted in approximately 30% reduction in the relative DCF fluorescence, whereas inhibition of FLT3 resulted in approximately 20% reduction (Figure 1.4).

Confocal microscopy of ROS production in MV4-11 treated cells.

Although the difference in redox state of healthy and AML cells is already established, the localisation and the cellular source of these ROS remain elusive. In the beginning of the localisation studies, with the aid of confocal microscopy, we attempted to image DCF fluorescent staining of ROS in MV4-11 cells. However, the pseudocoloured imaging of DCF– stained MV4-11 cells demonstrated an extensive diffusion of the probe inside cells (Figure 1.5.a). Nonetheless, DPI-treated cells possessed lower levels of ROS than the vehicle-treated control cells (Figure 1.5.b). Furthermore, we have also observed that regions of the highest DCF intensity localised substantially with the red endoplasmic reticulum (ER) tracker (Figure 1.5.b).

Confocal microscopy images of specific H_2O_2 levels in live MV4-11 cells following FLT3 inhibition or NOX inhibition

The extent of total levels of ROS induced by FLT3-ITD were previously reported (Sallmyr et al., 2008a). However, the levels of specific ROS have not been

a)

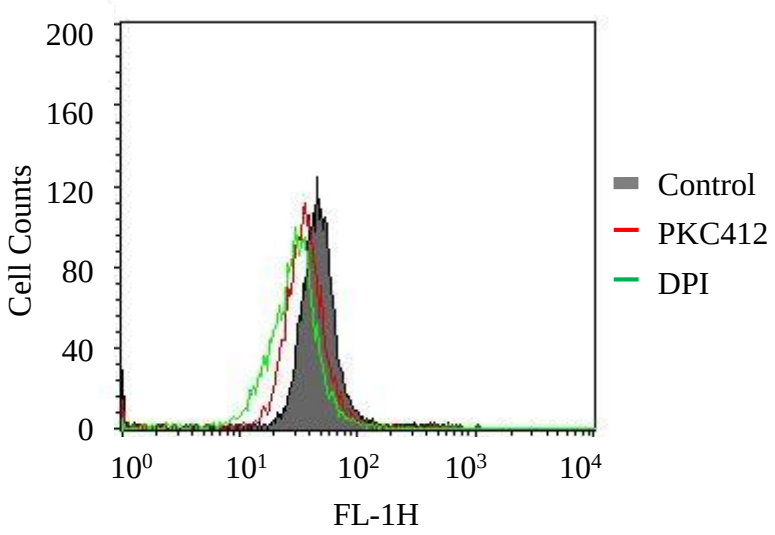

b)

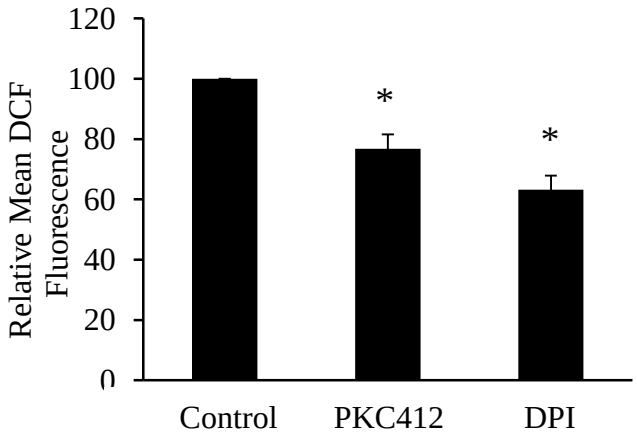

Figure 1.4. Levels of ROS in MV4-11 cells following treatment with FLT3 receptor inhibitor PKC412 and NOX protein inhibitor DPI. a) FACS analysis of relative DCF fluorescence of control (grey), PKC412 1 h 50 nM treated (red), DPI 1 h 5 µM treated (green). b) Bar chart representation of FACS results in a). Results are shown as relative geometric mean± SD. Statistical analysis was carried out using the Student's t-test ($p<0.005$ is marked with *).

a)

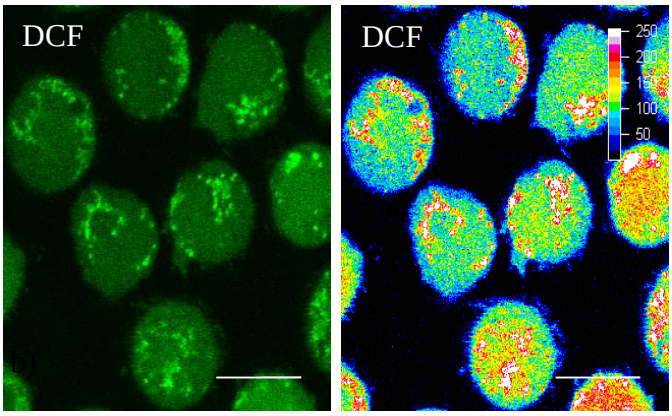

b)

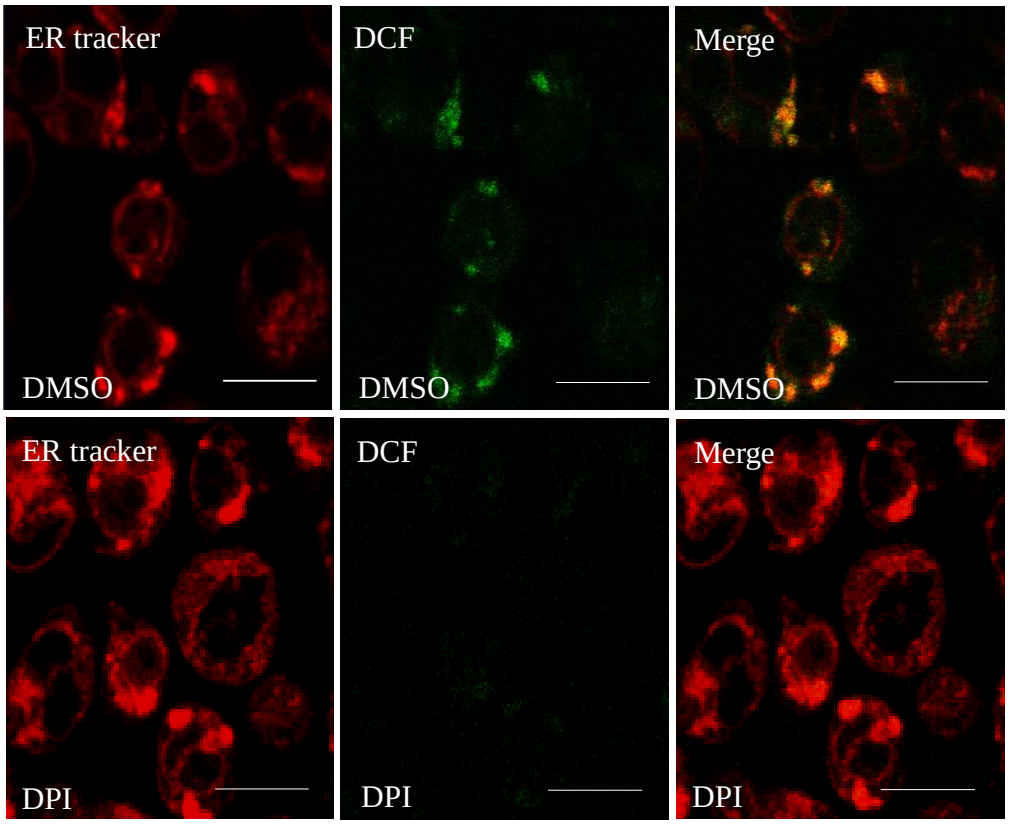

Figure 1.5. Confocal microscopy representing the localisation of ROS in live MV4-11 treated cells, using DCF. Level of ROS following NOX inhibition with DPI. a) Pseudo-coloured image of DCF on the right represents intensity distribution (from highest intensity indicated by white to the lowest designated by black). b) DCF staining (green) of ROS in DMSO treated and DPI 5 µM 1 h treated cells colocalising with ER tracker (red), followed by the merge panel. The scale bar corresponds to 10 µm.

yet examined. It is important to investigate the type of ROS involved, as each ROS induces specific oxidations, which can lead to different signalling events (D'Autréaux and Toledano, 2007). H_2O_2 is the main signalling ROS, yet probably due to technical limitations, FLT3-ITD driven formation of it was not yet investigated. In recent years a new family of boronate-based ROS probes has been developed that brightly fluoresce upon specific reaction with H_2O_2 (Miller et al., 2005). This provided us with the opportunity to specifically investigate FLT3-ITD generated H_2O_2, which has not been previously examined. Both inhibitions of FLT3 and NOX resulted in significant decreases in endogenous H_2O_2, as measured with Peroxy Orange 1 (PO1) (Figure 1.6.a and b). Similarly to DCF measurements, DPI treatment resulted in a larger decline in PO1 fluorescence (30%) than PKC412 treatment (20%).

This result encouraged us to pursue confocal imaging of live MV4-11 cells stained with PO1. As with DCF, we first examined distribution of the oxidised PO1 probe. The pseudocolouring of the PO1 staining revealed specific accumulation of PO1 in certain intracellular structures resembling the ER (Figure 1.7.a). Double staining of PO1 and green ER tracker revealed a high level of colocalisation between the two dyes (Figure 1.7.b). Moreover DPI treatment of MV4-11 cells prior to the staining caused a marked decrease in PO1 fluorescence (Figure 1.7.b). Due to the lack of specificity of DPI for NOXs, we employed a newly developed NOX specific inhibitor VAS-2870 (Freyhaus et al., 2006, Sancho and Fabregat, 2011). Similarly to the previous experiment, vehicle treated (DMSO) control MV4-11 cells showed

a)

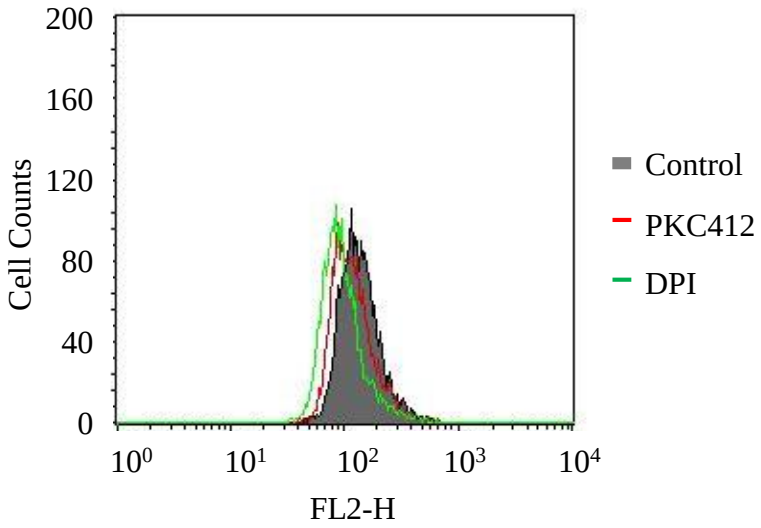

b)

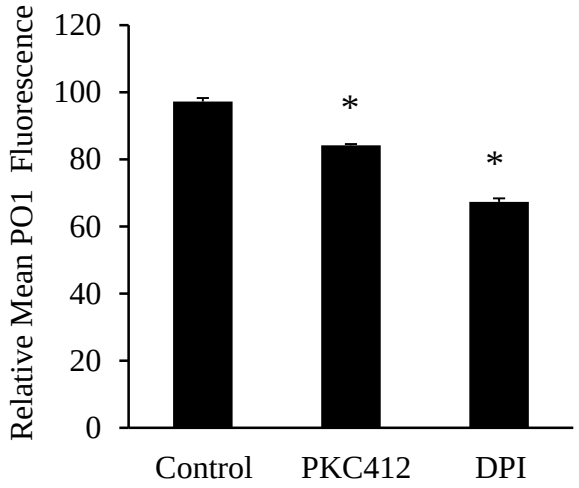

Figure 1.6. Levels of H_2O_2 in MV4-11 cells following treatment with FLT3 receptor inhibitor PKC412 and NOX protein inhibitor DPI. a) FACS analysis of relative PO1 fluorescence of control (grey), PKC412 1 h 50 nM treated (red), DPI 1 h treated (green). b) Bar chart representation of FACS results in a), results are shown as relative geometric mean± SD. Statistical analysis was carried out using the Student's t-test ($p<0.05$ is marked with *).

a)

b)

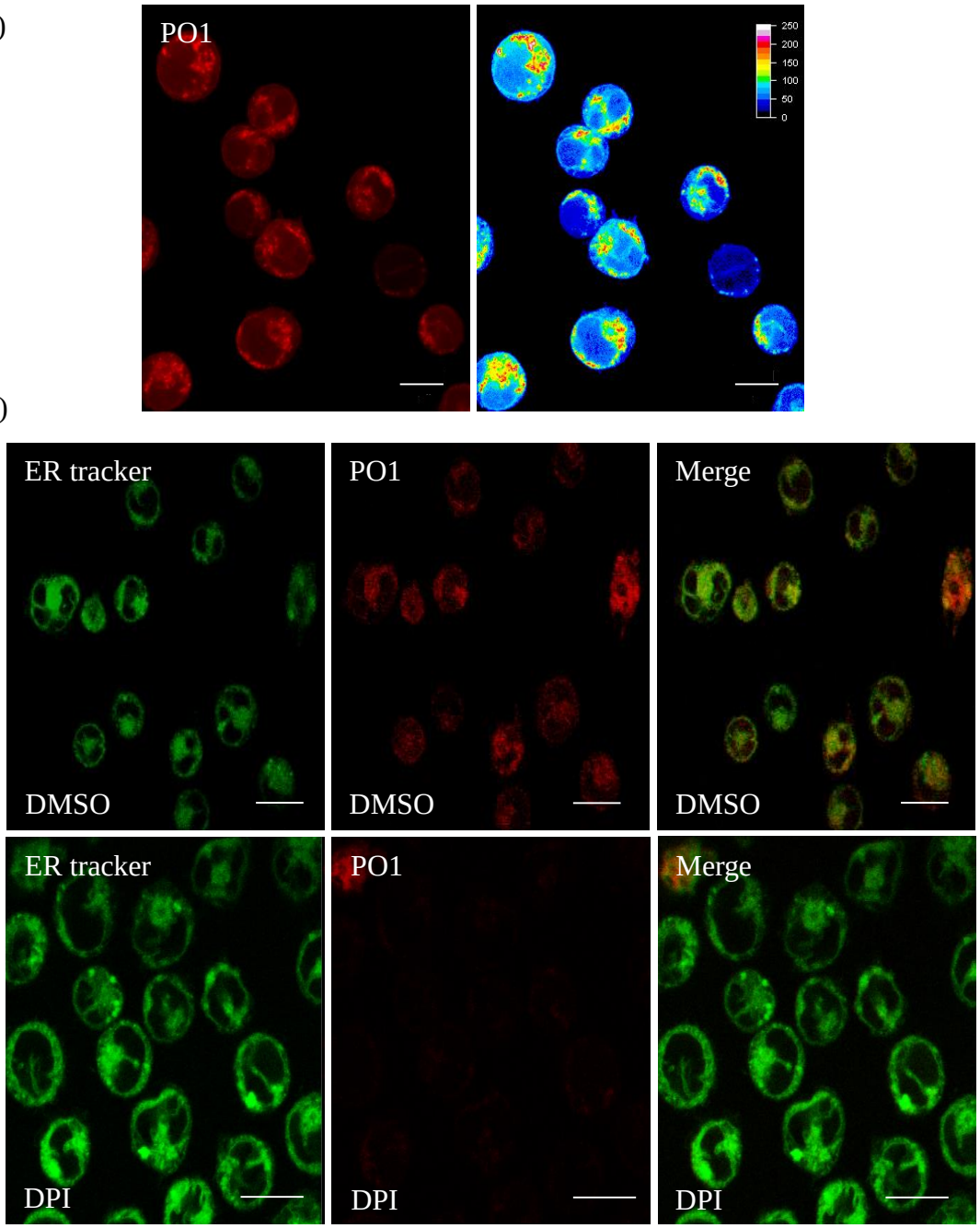

Figure 1.7. Confocal microscopy of live cells showing the localisation of H_2O_2, using PO1. Levels of H_2O_2 in MV4-11 cells following treatment with NOX protein inhibitor DPI. a) Pseudocolouring of the PO1 staining of MV4-11 cells. b) Colocalisation of ER tracker (left panel) and PO1 (middle panel) of MV4-11 cells, with merged stains (right panel). The scale bar corresponds to 10 µm.

colocalised staining of PO1with the green ER tracker stain. Analogously to DPI, treatment with VAS-2870 substantially abolished the PO1 fluorescence (Figure 1.8).

In order to examine the effects of FLT3-ITD on H_2O_2 formation, we analysed the co-staining of PO1 and ER tracker in PKC412-treated and control treated cells. The merged image of the ER tracker and PO1 probe confirmed the localisation of H_2O_2 in the ER of MV4-11 cells (Figure 1.9). Furthermore, PKC412-achieved FLT3 inhibition led to the attenuation of PO1 fluorescence, as analysed by confocal microscopy.

Confocal live microscopy images of H_2O_2 levels in mitochondria following FLT3 and NOX inhibition in MV4-11 cells.

Mitochondrial superoxide was previously shown to be altered following the inhibition of FLT3-ITD (Reddy et al., 2011). To investigate if FLT3-ITD inhibition could affect the mitochondrial H_2O_2, we imaged MitoPY1 probe subsequent to the inhibition of FLT3-ITD. MitoPY1 is a H_2O_2-specific probe that stains mitochondria (Dickinson and Chang, 2010). Surprisingly, H_2O_2 levels in mitochondria were not altered by the PKC412 treatment (Figure 1.10).

VAS-2870 is a newly developed NOX-inhibitor that has not been yet characterised (Freyhaus et al., 2006, Stielow et al., 2006, Sancho and Fabregat, 2011). The most common NOX inhibitor, DPI has been previously shown to inhibit electron transport of mitochondria (Li and Trush, 1998). In order to investigate non-specific off-target effects of VAS-2870 on mitochondrial ROS (Figure 1.11), we

have stained control cells and VAS-2870-treated cells with MitoPY1. The possibility of VAS-2870 inhibiting mitochondrial ROS formation.

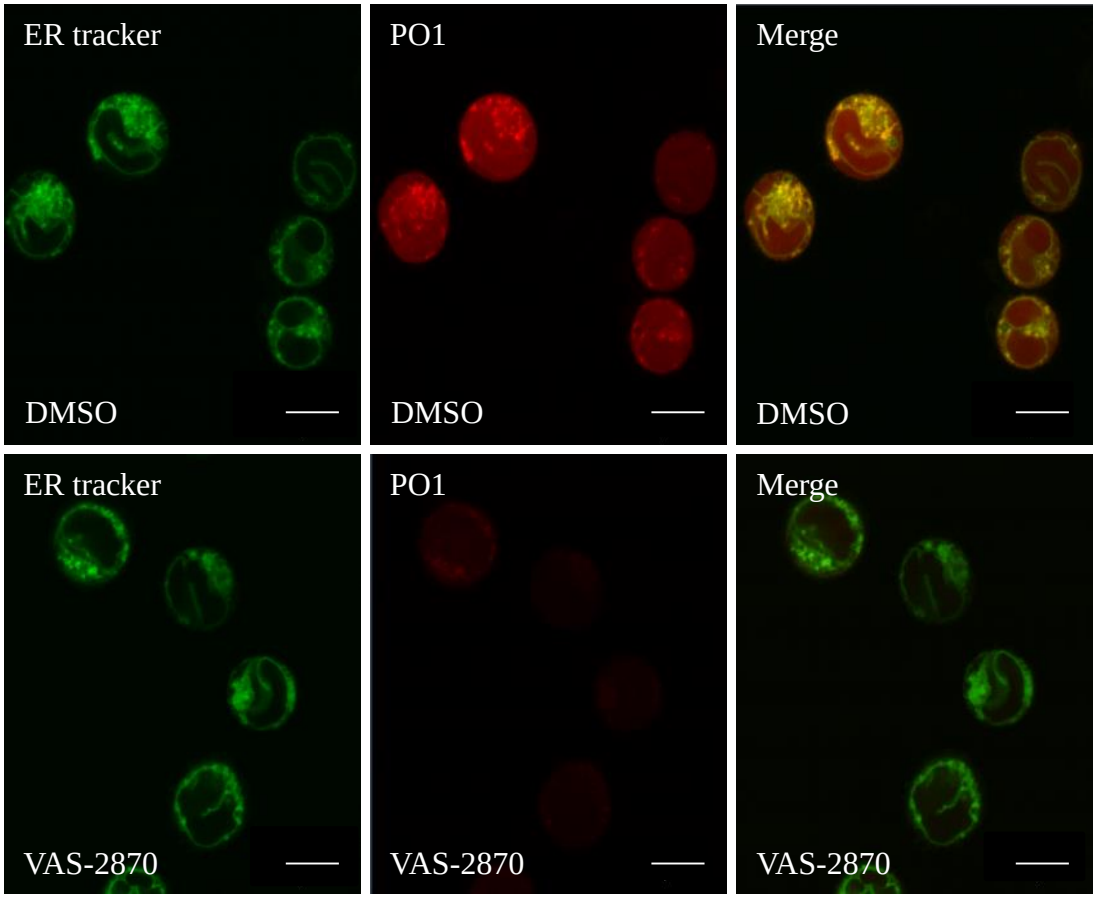

Figure 1.8. Confocal microscopy images of H_2O_2 levels following NOX inhibitor, VAS-2870 in live MV4-11 cells. PO1 staining (red; middle panel) of H_2O_2 in DMSO treated (upper image) and VAS-2870 10 µM 1 h treated cells (bottom image). ER tracker staining (green; left panel). The merged image of ER tracker and PO1 (right panel). The scale bar corresponds to 10 µm.

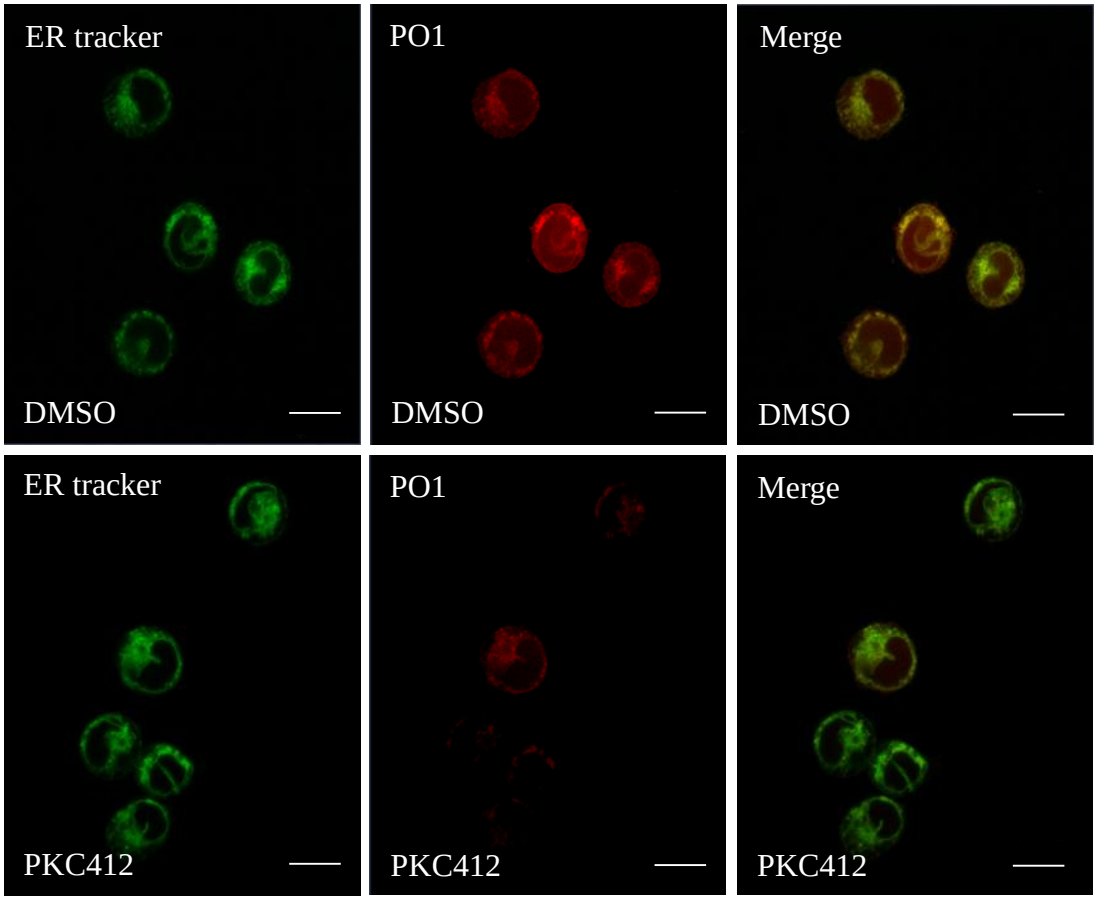

Figure 1.9. Confocal microscopy representing the localisation of H_2O_2 in MV4-11 treated cells, using PO1. Levels of H_2O_2 in MV4-11 cells following treatment with FLT3 inhibitor, PKC412. Colocalisation of H_2O_2-specific probe, PO1 staining and ER tracker to localise ROS production in untreated and PKC412 50 nM 1 h treated cells. The scale bar corresponds to 10 µm.

a)

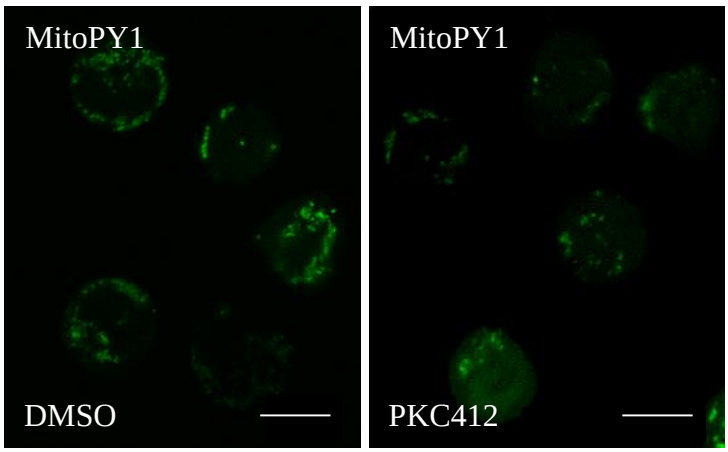

b)

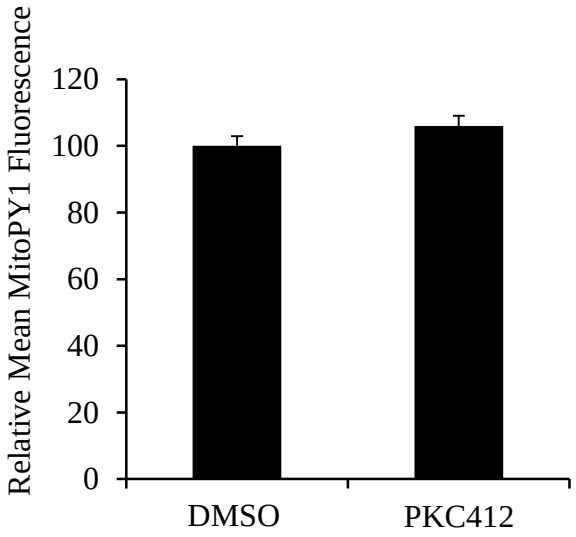

Figure 1.10. Confocal microscopy images of H_2O_2 levels in mitochondria following PKC412 treatment in live MV4-11 cells. a) MitoPY1, mitochondrial H_2O_2-specific probe staining comparing the DMSO and PKC412 (50 nM for 1 h) treated cells. b) Quantification of relative mean MitoPY1 fluorescence of DMSO and PKC412 (50 nM for 1 h) treated cells. The scale bar corresponds to 10 µm.

a)

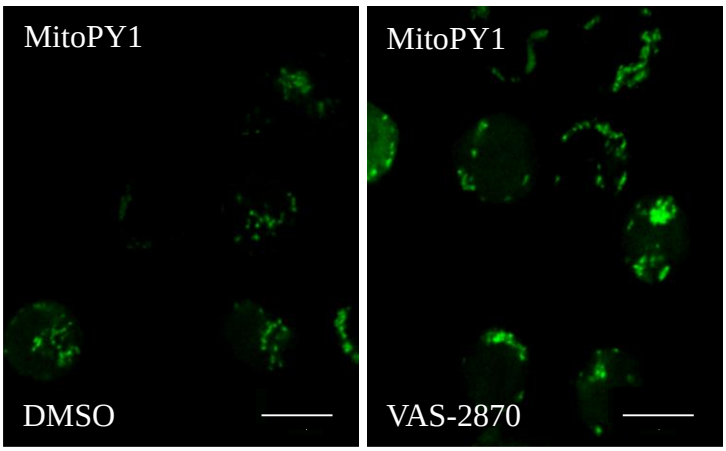

b)

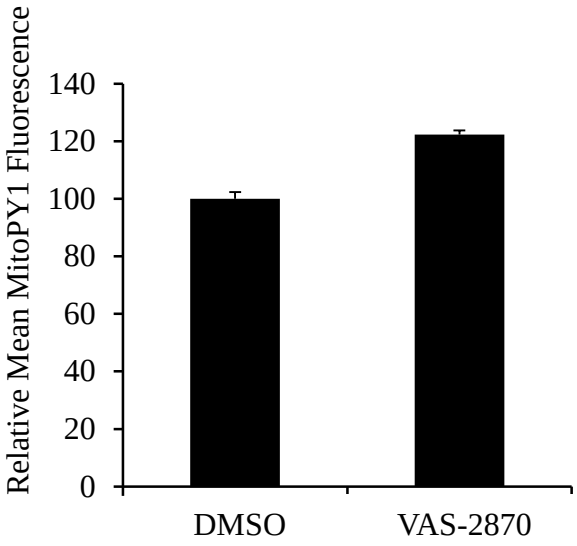

Figure 1.11. Confocal microscopy images of H_2O_2 levels in mitochondria following VAS-2870 treatment in live MV4-11 cells. a) MitoPY1, mitochondrial H_2O_2-specific probe staining comparing the DMSO and VAS-2870 (10 µM for 1 h) treated cells. b) Quantification of relative mean MitoPY1 fluorescence of DMSO and VAS-2870 (10 µM for 1 h) treated cells. The scale bar corresponds to 10 µm.

Discussion

A number of studies have demonstrated that cancer cells use ROS as secondary messengers to activate redox signalling, which affects cell proliferation, growth and genomic instability (Waris and Ahsan, 2006). However mechanisms that stimulate ROS production, as well as their molecular sources remain unclear. Leukaemic oncogenes have been previously shown to regulate ROS production (Reddy et al., 2011). In this chapter, we showed that cells expressing the mutated FLT3-ITD receptor generate H_2O_2 in the ER, primarily *via* NOXs.

We observed that primary AML blasts produce 5-fold more of ROS than their healthy counterparts (data not shown). This change is similar to what has already been reported by Hole *et al.* (Hole et al., 2013). Oxidative stress has been implicated as a factor in the relapse of AML patients (Zhou et al., 2010). Furthermore, the N-RAS and BCL-2 expressing murine model of AML has also manifested increased ROS and DNA damage (Rassool et al., 2007). Similarly, markers of increased oxidative stress were detected in the blood of chronic myeloid leukaemia (CML) and MDS patients (Farquhar and Bowen, 2003, Sallmyr et al., 2008b, Naughton et al., 2009). Moreover, the elevated ROS were demonstrated to be associated with increased DNA damage in MDS samples (Peddie et al., 1997).

ROS can induce damaging or signalling effects (Gough and Cotter, 2011). The dichotomous nature of ROS function allows them to stimulate proliferation and growth pathways, with simultaneous damage to DNA. This provides tumour cells with an evolutionary mechanism for AML progression (Hole et al., 2013).

Leukaemic oncogenes (for example FLT3, BCR-ABL and C-KIT) are known to generate increased levels of ROS (Hole et al., 2011). Mutated FLT3-ITD is one of the most prevalent genetic alterations in AML patients (Gilliland and Griffin, 2002). Stable transfection of 32D cell line with mutated FLT3-ITD was shown to elevate ROS in comparison to transfection of the same cells with FLT3-WT (Sallmyr et al., 2008a). We decided to examine the extent of ROS induced by FLT3-ITD in a non-over-expression system. We used the MV4-11 cell line as our model, as these are homozygous for FLT3-ITD. To examine FLT3-ITD signalling we also employed PKC412, a tyrosine kinase inhibitor against activated FLT3. PKC412 has been shown to inhibit FLT3 and reduce the number of leukaemic blasts in the patients' circulation (Stone et al., 2005). Following confirmation of FLT3 expression and its phosphorylation in MV4-11 cells, we established that inhibition of FLT3 using PKC412 results in a reduction in endogenous levels of ROS.

ROS are a family of heterogenous molecules that possess distinct oxidative properties, kinetics rates and diffusion characteristics (Murphy et al., 2011). Therefore, it is important to specify the type of ROS when studying redox- regulated processes. This is especially true for redox signalling as some ROS (e.g. H_2O_2) are capable of causing reversible oxidation of target proteins, which allows for reversible regulation of the signal. In contrast to this, hydroxyl radical ($OH^{\cdot}$) has been exclusively shown to have damaging properties accompanied by lack of any target specificity (Garcia-Santamarina et al., 2014).

Considering these differences, we investigated if FLT3 specifically induces H_2O_2 production, using newly developed H_2O_2-specific fluorescent probes (Woolley

et al., 2012). H_2O_2 specificity of the probes, developed by Dickinson *et al*., is based on the chemical reaction of H_2O_2 with boronate group upon which the probe emits a fluorescent signal (Dickinson et al., 2010a). We selected PO1 probe to specifically study H_2O_2 generation stimulated by FLT3-ITD. Following FLT3-ITD inhibition with PKC412, we demonstrated that H_2O_2 levels in MV4-11 cells were significantly decreased.

NOXs have been formerly shown to play an essential role in the growth, proliferation and migration of leukaemic cells (Reddy et al., 2011, Hole et al., 2013). Based on this knowledge, we investigated how much of the H_2O_2 generated in FLT3-expressing cell line originated from NOXs. In order to examine this, we treated FLT3-ITD expressing MV4-11 cells with DPI, a common NOX inhibitor. The use of DPI as a NOX inhibitor has been quite controversial due to the general inhibitory characteristics of DPI against flavin proteins (O'Donnell et al., 1993). Several reports have shown that an increased DPI concentration can also inhibit electron transport in mitochondria or cytochrome P-450 reductase (Li and Trush, 1998, Prabhakar, 2000). On the other hand, it has also been shown that lower concentrations of DPI are selective for NOX enzymes (Serrander et al., 2007). We demonstrated that changes in H_2O_2 levels following FLT3 inhibition largely reflect changes following DPI-achieved NOX inhibition. To date there have been mixed conclusions drawn regarding the molecular sources of ROS in FLT3-positive cells, oscillating between mitochondria and NOX proteins (Reddy et al., 2011, Sallmyr et al., 2008a). Although both of these reports have shown that NOX proteins regulated growth and migration of FLT3-ITD expressing cells (Sallmyr et al., 2008a, Reddy et

al., 2011), Reddy *et al*. did not report any significant changes in total levels of ROS following NOX siRNA knockdowns, as measured by DCF. However, we discovered, using the PO1 probe, that inhibition of NOXs result in the attenuation of ROS generation in FLT3-ITD AML cells. Similarly to AML, DPI treatment has been recently shown to reduce endogenous ROS levels in chronic myeloid leukaemia (CML) patient samples, Moreover, the study reported that DPI treatment has induced apoptosis in BCR-ABL expressing CML cells (Sanchez-Sanchez et al., 2014). Importantly to this project, when used in combination with PKC412, NOX inhibition has synergistically attenuated proliferation of MV4-11 cells (Sanchez-Sanchez et al., 2014). This has indicated a therapeutic potential of DPI against AML leukaemic cells.

Although DPI is a commonly used inhibitor of NOX, due to its possible off-target effects, we employed a novel NOX inhibitor, VAS-2870. VAS-2870 has been previously shown as a specific inhibitor of NOX activity (Freyhaus et al., 2006, Stielow et al., 2006, Sancho and Fabregat, 2011). Importantly, inhibition of NOX using VAS-2870 in MV4-11 cells also resulted in a dramatic reduction in the endogenous H_2O_2. This eliminated the specificity issues of DPI inhibition, confirming the role of NOX in the production of H_2O_2 in FLT3-ITD expressing MV4-11 cells.

Due to the high reactivity of H_2O_2 and hence limitations of its diffusion, the target of H_2O_2 oxidation has to be localised in close proximity to H_2O_2 generation. Cells protect their structures from the damaging oxidative effects by accumulating antioxidant molecules (Mishina et al., 2011, Irwin et al., 2013). Therefore, certain

distance between the source and the target of H_2O_2 could lead to neutralisation of H_2O_2 by an antioxidant enzyme. This emphasises the importance of localisation studies in redox biology. Up to few years ago, localisation of ROS at the subcellular level was almost impossible due to technical shortcomings related to ROS measurements. However recently, along with some developments in new fluorescent probes and genetically encoded ROS sensors, some localisation methods have become available. The family of boronate-based specific H_2O_2 sensors rely on the specific boronate-to-phenol switch upon reaction with H_2O_2 (Dickinson et al., 2010a, Miller et al., 2005, Dickinson et al., 2010b, Dickinson et al., 2011a, Dickinson et al., 2011b, Dickinson et al., 2013, Dickinson and Chang, 2010). They also have improved stability, increased sensitivity to signalling concentrations of H_2O_2 and limited diffusibility of the molecule (Dickinson et al., 2010a, Lippert et al., 2011). For instance, PO1 was used to localise H_2O_2 in the phagosomes of PMA-stimulated RAW264.7 macrophages (Dickinson et al., 2010a). They appeared to be suitable candidates for H_2O_2 localisation studies in AML cells. We demonstrated, using PO1 that the brightest regions of PO1 staining, which corresponds to the highest concentration of H_2O_2, localises to the ER in MV4-11 cells. It has been shown recently that NOX4 and $p22^{phox}$ reside in the ER of monocyte-derived macrophages (Lee et al., 2010). This could explain the ER-localisation of ROS in monocyte-like MV4-11 cells.

The ER-derived redox signalling is particularly interesting in FLT3-ITD expressing cells as it has been demonstrated that the partially glycosylated, immature form of FLT3-ITD is located on the ER membrane. The ER-bound FLT3-ITD

aberrantly activates STAT5, a potent regulator of growth and proliferation of leukaemic cells (Choudhary et al., 2009). We demonstrated that siRNA down-regulation of ER-residing $p22^{phox}$ led to a reduction in the phosphorylation of STAT5 (Woolley et al., 2012). In support of this finding, NOX knockdown resulted in a decrease in the phosphorylation of STAT5 and BCR-ABL in CML cell lines (Sanchez-Sanchez et al., 2014). H_2O_2 has been previously shown to specifically oxidise cysteine residues of phosphatases. ER-localised H_2O_2 in leukaemia could therefore potentially inhibit ER-resident redox-sensitive phosphatases, responsible for de-phosphorylation of STAT5 transcription factor. In fact, NOX4 has been demonstrated to regulate PTP1B phosphatase located in the ER of endothelial cells (Chen et al., 2008). Further highlighting the importance of NOX proximity to their target, a mutation in PTP1B, which de-localised it from the ER, abolished NOX4 ability to regulate this phosphatase.

In summary this work has shown that FLT3-ITD signalling leads to an increase in the level of ROS in AML cell lines. We found that H_2O_2, a common signalling molecule, is produced by FLT3-ITD. The highest concentration of H_2O_2 is located in the ER in MV4-11 cells, suggesting that the possible source of H_2O_2 is also localised there. This H_2O_2 generation was almost completely inhibitable by both PKC412 and DPI, indicating that it is both FLT3- and NOX- dependent.

Chapter 4

FLT3-ITD-activated NOX affects redox status of the nucleus in AML cells.

Introduction

Altered redox status is an important characteristic of cancers and the evidence for this has been found in many solid tumours and leukaemias. Myeloid leukaemia cells appear to have a dysfunctional redox metabolism (Wang et al., 2010, Hole, 2011, Hole et al., 2013, Irwin et al., 2013). In the context of AML, patients' samples are characterised by chronic oxidative stress that could induce aggressive features of AML, such as chemoresistance and relapse.

Along with mitochondria, NOX enzymes have been recently identified as one of the main sources of ROS in cancers (Sabharwal and Schumacker, 2014, Block and Gorin, 2012). NOX isoforms are composed of different subunits. The formation of the NOX1-3 complexes is dependent on recruitment of the membrane subunit $p22^{phox}$, cytosolic subunits, $p47^{phox}$, $p67^{phox}$, $p40^{phox}$ and the GTPase Rac1 (Bedard and Krause, 2007). NOX4 does not require cytosolic subunits and its activity is therefore only dependent on the presence of $p22^{phox}$ (Brandes et al., 2014). Specific down-regulation of any of the membrane or cytosolic subunits reduces ROS-production (Block and Gorin, 2012). NOX5 and DUOX1/2 do not bind other regulatory subunits and are activated by calcium (Bedard and Krause, 2007). Many cancer cell lines and cancer patient samples have been associated with higher levels of NOX catalytic or regulatory subunits at the mRNA and/or protein level (Block and Gorin, 2012). NOX-generated ROS have been demonstrated to regulate several features of tumour phenotypes such as activation of oncogenes, deregulation of cell growth, reduction in apoptosis, inactivation of tumour suppressors, induction of angiogenesis, as well as invasion and metastasis (Block and Gorin, 2012). Moreover,

ROS-mediated DNA damage could facilitate cancer evolution and the development of chemoresistance (Landriscina et al., 2009). NOXs are thus attractive therapeutic targets in many cancers (Block and Gorin, 2012).

Several oncogenes and growth factors have been shown to induce NOX expression or activation (Weyemi et al., 2012, Naughton et al., 2009, Reddy et al., 2011). For example, over-expression of H-RAS has been shown to increase expression of NOX4 and $p22^{phox}$ in the thyroid cell line, HThy-ori cells (Weyemi et al., 2012). Transforming growth factor-β1 (TGF-β1) has been demonstrated to induce NOX4 expression, which in turn mediated the differentiation of cardiac fibroblasts into myofibroblasts (Cucoranu et al., 2005).

In comparison to other intracellular signalling molecules, ROS have extremely short half-lives, lack target specificity. They achieve signal transduction through oxidation of target macromolecules. Therefore, the ability of NOX-generated ROS to act as signalling molecules is largely dependent on the proximity of the NOX to its molecular target (Winterbourn, 2008). It is thus not surprising that the location of NOX within the cell and consequently the location of ROS generation is critical. Indeed, kinetic studies of H_2O_2 reactions have demonstrated that redox signalling is highly compartmentalised, with H_2O_2 having limited diffusion from its site of generation (Mishina et al., 2011). For instance, live cell imaging of H_2O_2 has shown that PDGF-induced NOX generation of H_2O_2 was localised to specific locations in the cytoplasm (Mishina et al., 2011). Chen *et al*. demonstrated that NOX4 oxidises ER-localised PTP1B, while a mutant PTP1B, which does not to localise to the ER, does not undergo oxidation by NOX4 (Chen et al., 2008). Taken

together, these studies demonstrate the importance of subcellular colocalisation of the ROS generating system and their molecular targets.

NOX isoforms have been localised to nearly all organelles (Bedard and Krause, 2007). Moreover, localisation of a particular NOX isoform can vary between tissue and cell types (Bedard and Krause, 2007). NOX isoforms have been colocalised to the plasma membrane, mitochondrion, nucleus, nuclear membrane, ER and secondary and tertiary granules (Bedard and Krause, 2007). A number of studies have demonstrated that differential subcellular localisation of NOX isoforms can result in distinct molecular events. For example, in vascular smooth muscle cells (VSMC), the mitogenic activity of NOX1 and senescence-induction by NOX4 have led scientists to study the localisation of these two NOX isoforms. Interestingly, immunofluorescent staining revealed distinct localisation patterns of NOX1 and NOX4, with NOX1 localised on the cell surface, and NOX4 to focal adhesion points (Hilenski et al., 2004).

We previously demonstrated in chapter 3, that FLT3-ITD-stimulated ROS localise to the ER, and have suggested that NOXs are the main source of ROS in FLT3-ITD mutated leukaemia. The aim of this work is to determine the mechanism by which NOX is activated by oncogenic signals from FLT3-ITD; investigate the localisation of the ROS source in the AML cells as well as to examine the redox status of the nucleus. The knowledge resulting from such investigations will allow us to determine if NOX-produced ROS could play a role in the genomic instability seen in AML.

Results

NOX expression following FLT3-ITD inhibition.

Having established in the previous chapter that FLT3-ITD-induced ROS are generated by NOX enzymes, we examined the effects of FLT3-ITD signalling on expression of NOX proteins. It has been previously published that cells possessing a mutated FLT3 express NOX2, NOX4 and NOX5 as well as their regulatory subunits (Reddy et al., 2011). The inhibition of FLT3 with PKC412 for 8 and 24 h did not reveal any changes in NOX2, NOX4, NOX5 or $p47^{phox}$ expression (Figure 2.1). However, when we examined the protein level of $p22^{phox}$, a membrane subunit of NOX complexes, we discovered that FLT3 inhibition causes a significant reduction in the steady protein level of $p22^{phox}$ (Figure 2.2.a).

$p22^{phox}$ expression following the inhibition of FLT3-ITD.

Selective tyrosine kinase inhibitors (TKIs), including FLT3 inhibitors can also have effects on other kinases (Bain et al., 2007, Zarrinkar et al., 2009). In order to confirm that the $p22^{phox}$-reduction was solely due to FLT3 inhibition, we employed two other FLT3 kinase inhibitors: CEP-701 and AC-220. AC-220 was recently reported to potently inhibit FLT3 kinase at nanomolar concentrations without many off-target effects (Zarrinkar et al., 2009).

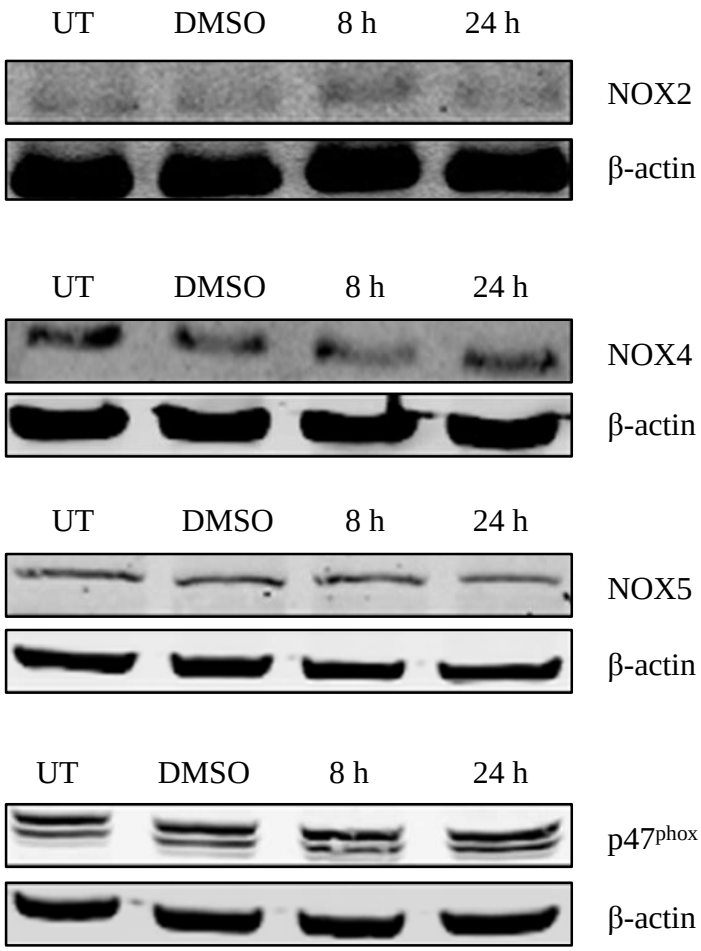

Figure 2.1. NOX expression following FLT3-ITD inhibition. Western blotting analysis of NOX isoforms 2, 4 and 5, as well as $p47^{phox}$ subunit expression following PKC412 treatment over 8 h and 24 h in MV4-11 cells. β-actin is shown as a loading control.

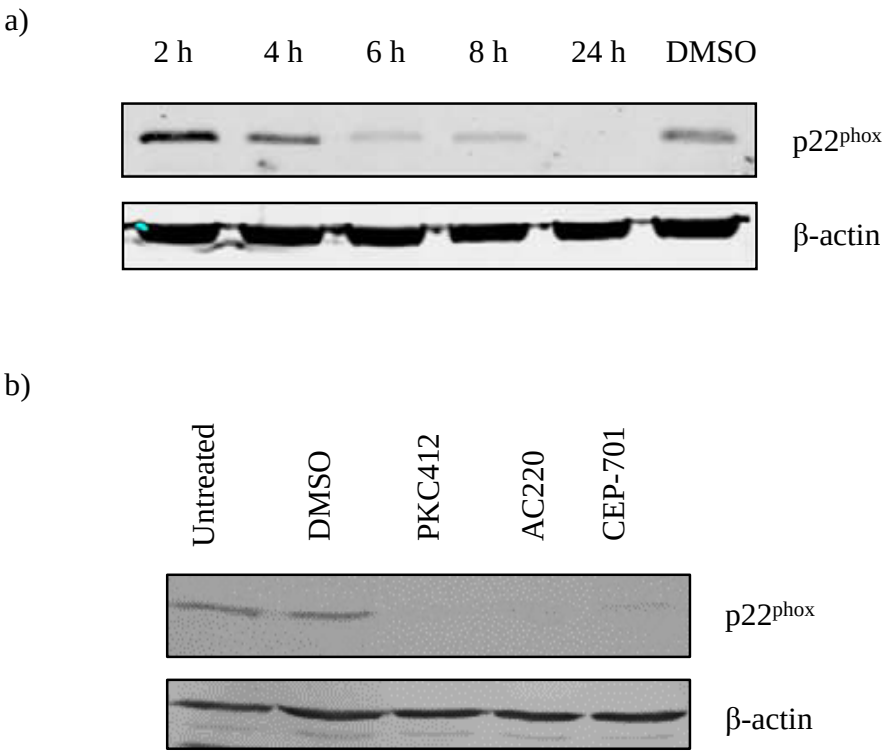

Figure 2.2. $p22^{phox}$ expression following the inhibition of FLT3-ITD in MV4-11 cells. a) The level of protein expression of $p22^{phox}$ following PKC412 treatment in MV4-11 cells for 2-24 h. b) The level of protein expression of $p22^{phox}$ following 24 h treatments with different FLT3 inhibitors, i.e. PKC412, AC220 and CEP-701. β-actin is shown as a loading control.

Inhibition of FLT3 with either of these drugs resulted in a reduction in $p22^{phox}$ protein levels (Figure 2.2.b) in MV4-11 cells.

In order to further examine the effects of FLT3 inhibition on $p22^{phox}$ levels, we have explored this result in MOLM-13 cells which are heterozygous for FLT3-ITD and HL-60 cells which are homozygous for FLT3-WT. PKC412 treatment of MOLM-13 cells for 8 and 24 h resulted in a partial reduction in $p22^{phox}$ protein level (Figure 2.3.a). On the other hand, the protein levels of $p22^{phox}$ in HL-60 cells were not affected by FLT3 inhibition (Figure 2.3.b).

Immunofluorescence staining of $p22^{phox}$ and KDEL (ER marker) in MV4-11 cells.

We have demonstrated that the H_2O_2-selective PO1 probe localises to the ER in MV4-11 cells. Therefore, we carried out a localisation study of $p22^{phox}$ in these cells. To confirm the specificity and suitability for immunofluorescence of the anti-$p22^{phox}$ antibody, we knocked down the $p22^{phox}$ protein using siRNA transfection (Figure 2.4.a). Secondly, we colocalised the anti-$p22^{phox}$ antibody with the anti-KDEL antibody, which is a standard ER marker (Figure 2.4.b). The colocalisation analysis revealed that approximately 70% of anti-$p22^{phox}$ colocalised with anti-KDEL, which demonstrated that $p22^{phox}$ is localised to the ER.

a)

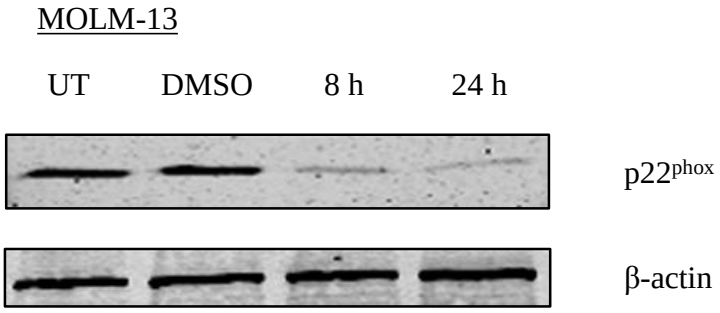

b)

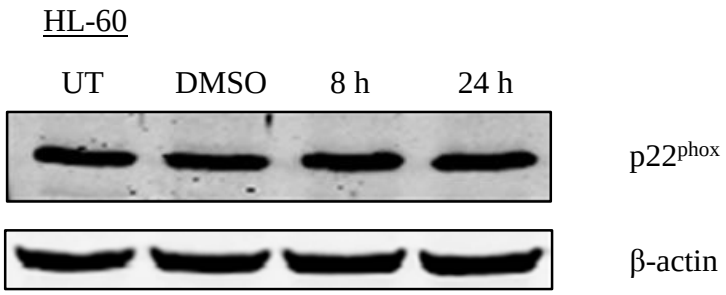

Figure 2.3. $p22^{phox}$ expression following the inhibition of FLT3-ITD and FLT3-WT expressing cells. a) Western blotting analysis of $p22^{phox}$ expression following 8-24 h PKC412 treatment in MOLM-13 cells. DMSO was used as a vehicle control. b) Western blotting analysis of $p22^{phox}$ expression following PKC412 8-24 h treatment in HL-60 cells. DMSO was used as a vehicle control. β-actin is shown as a loading control.

a)

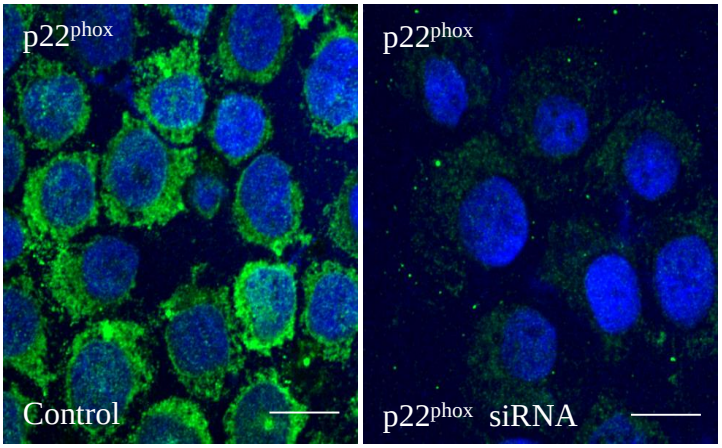

b)

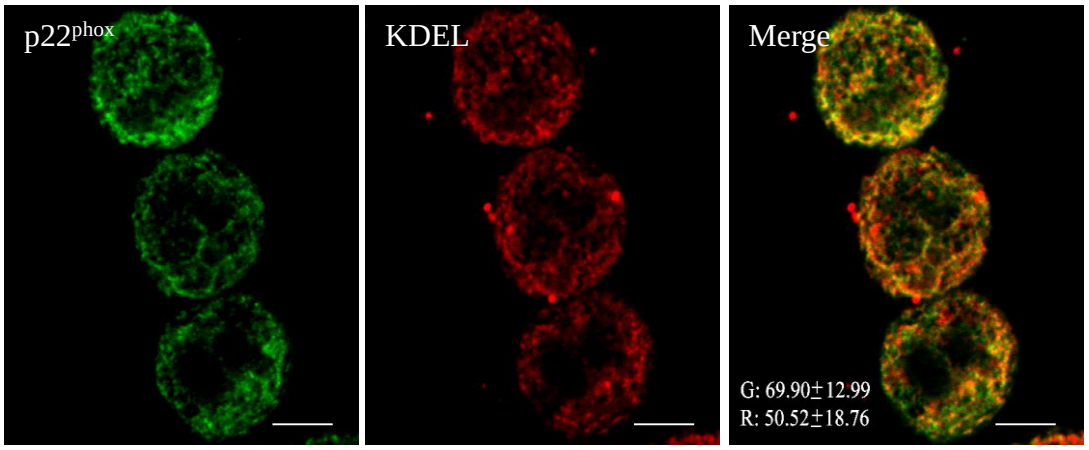

Figure 2.4. Colocalisation of p22^{phox} with KDEL (ER marker) in MV4-11 cells. a) Immunofluorescence staining of anti- p22^{phox} (green) with the nuclear Hoechst counterstain (blue) at 24 h post- p22^{phox} siRNA transfection. The left image represents cells treated with scrambled siRNA and the right image represents p22^{phox} siRNA treated cells. The scale bar is 10 μm. b) Immunofluorescence staining of colocalisation of p22^{phox} (green, left) protein with ER marker KDEL (red, middle) in MV4-11 cells. The merged image of KDEL and p22^{phox} is displayed in the right panel. The statistical analysis of the percentage of colocalisation of green overlapping with red (G) and red overlapping with green (R) is displayed in the bottom left corner of the merged image. The scale bar is 5 μm.

ROS levels following $p22^{phox}$ siRNA knockdown.

Considering that both H_2O_2 and $p22^{phox}$ colocalised to the ER, we investigated ROS levels in MV4-11 cells, following $p22^{phox}$ siRNA knockdown. The 3D histogram of DCF fluorescence of cells treated with scrambled siRNA (control) showed a substantial reduction in the fluorescent signal compared to the $p22^{phox}$ siRNA-treated cells (Figure 2.5).

We also employed PO1 as a H_2O_2 selective probe to study the colocalisation of H_2O_2 and the ER tracker. Similarly to what has been observed with DCF, we discovered that $p22^{phox}$ siRNA transfection has led to a decrease in the colocalisation of PO1 with the ER tracker (Figure 2.6).

Colocalisation of NucPE1 probe with Hoechst in MV4-11 cells.

Leukaemic oncogenes have been shown to affect genomic instability, which contributes to cancer aggressiveness and tumour progression (Reddy et al., 2011). In order to study the effect of ROS on genomic instability, we used the Nuclear Peroxy Emerald 1 (NucPE1) probe that specifically measures H_2O_2 in the nucleus (Dickinson et al., 2011b). NucPE1, just like its precursor PO1, possesses a boronate functional group to selectively respond to H_2O_2 and specifically accumulates in the nucleus (Dickinson et al., 2011b). The staining pattern of NucPE1 indicated a strong nuclear localisation, which was confirmed by co-staining with the Hoechst nuclear stain in MV4-11 cells (Figure 2.7).

a)

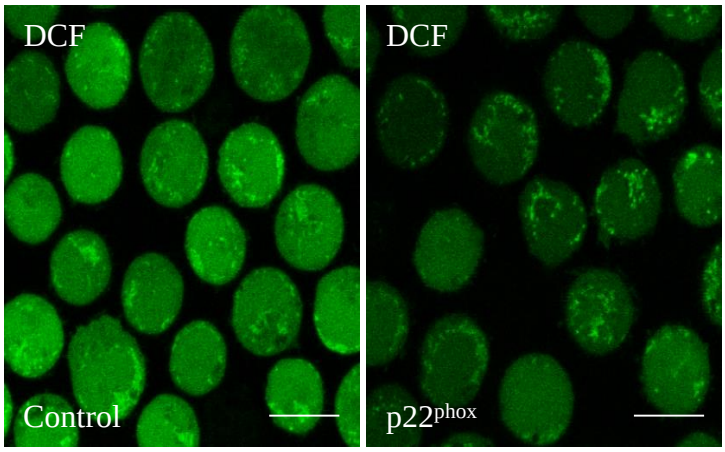

b)

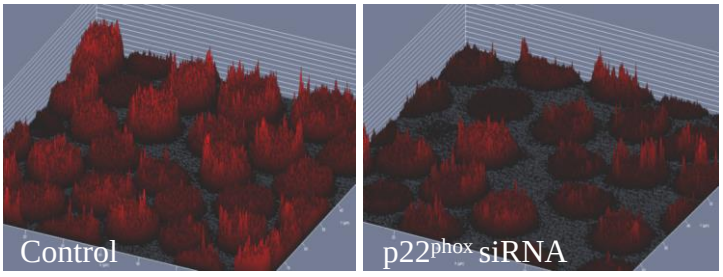

Figure 2.5. Level of ROS following $p22^{phox}$ siRNA knockdown, measured with DCF. a) Confocal microscopy of DCF staining of live MV4-11 cells following the treatement with $p22^{phox}$ siRNA (right image), compared with the scrambled siRNA treated control (left image). The scale bar is 10 μm. b) Histogram 3D representation of the DCF fluorescence in a), with the left image showing the control and the right image presenting the $p22^{phox}$ siRNA treated cells.

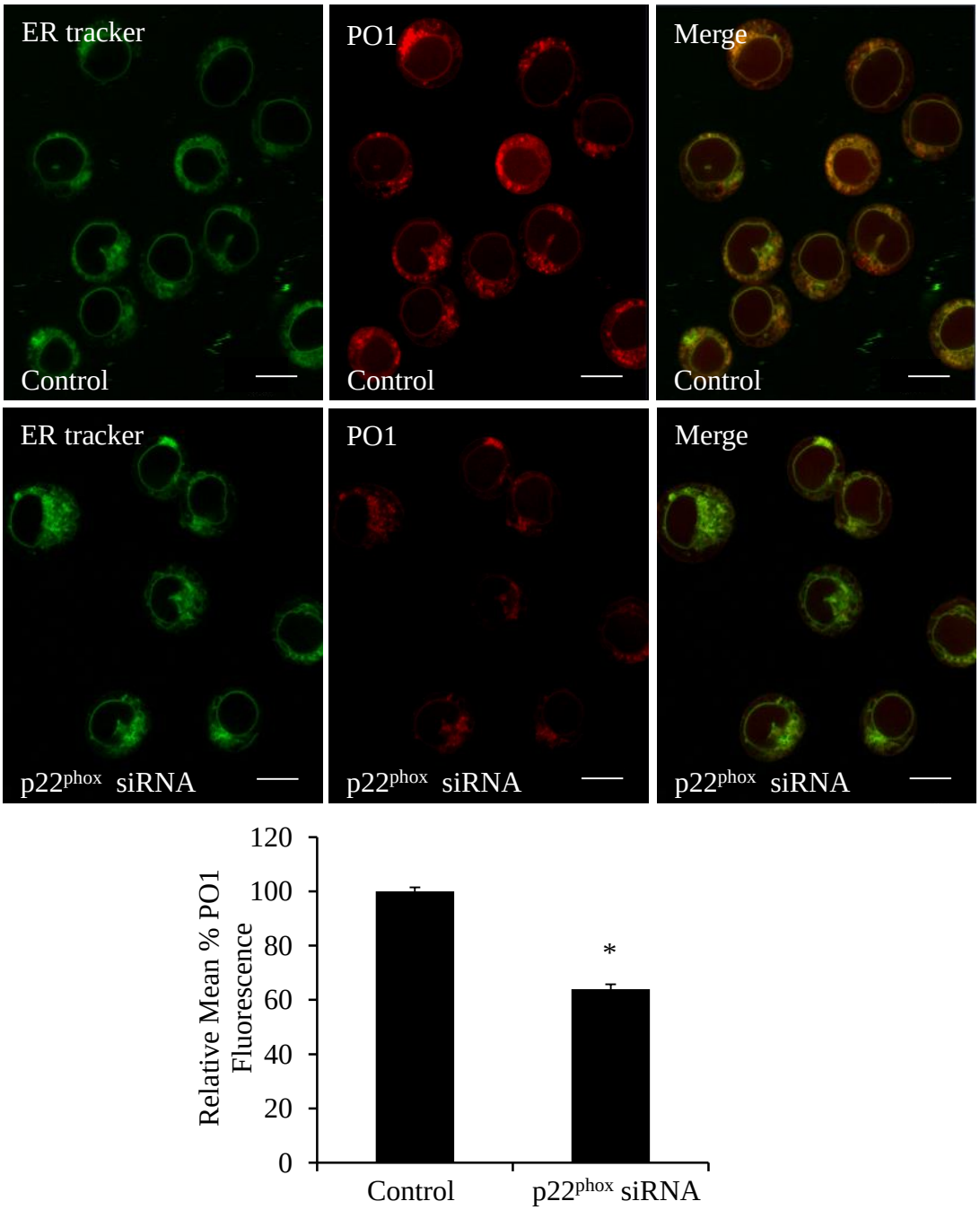

Figure 2.6. p22^{phox} siRNA knockdown reduced H_2O_2 levels in MV4-11 cells. a) MV4-11 cells were electroporated with either control siRNA (top panel) or p22^{phox} siRNA (bottom panel), stained with PO1 (middle panel) and ER tracker (left panel) and then imaged using confocal microscopy. Merged images of control and p22^{phox} siRNA treated cells are shown in the right panel. The scale bar represents 10 μm. b) Quantification of PO1 fluorescence based on the confocal microscopy images from (a). Results are shown as a relative mean % PO1 fluorescence ± SD. Statistical analysis was carried out using the student t-test ($p<0.005$ is marked with *).

a)

b)

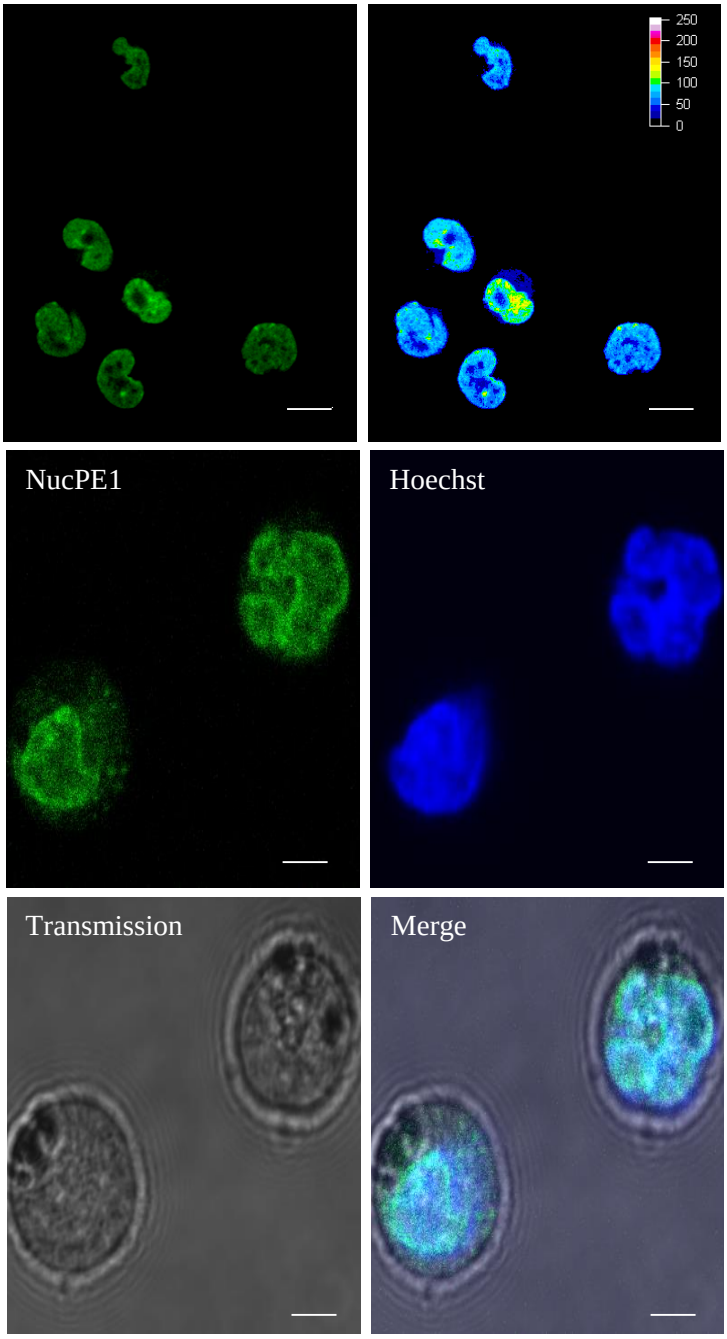

Figure 2.7. Colocalisation of NucPE1 probe with Hoechst in live MV4-11 cells. a) The pseudo-coloured image of NucPE1 on the left represents intensity distribution (from highest intensity indicated by white to the lowest designated by black). The scale bar represents 10 μm. b) MV4-11 cells were stained with NucPE1 and Hoechst, then imaged with a confocal laser scanning microscope. The scale bar represents 5 μm.

Levels of cellular and nuclear H_2O_2 following the FLT3-ITD inhibition.

In order to study the levels nuclear H_2O_2 generated by FLT3-ITD signalling, we inhibited FLT3 to investigate alterations in NucPE1 fluorescence. Analysis of NucPE1 and PO1 staining by confocal microscopy revealed that attenuation of FLT3-signalling reduced the level of H_2O_2 in both the cytosol and the nucleus (Figure 2.8).

Quantification of fluorescence of NucPE1 in a sample of 10,000 cells by flow cytometry demonstrated that cells treated with PKC412 have approximately 20% less H_2O_2 than their control equivalents (Figure 2.9).

Confocal microscopy of cellular and nuclear H_2O_2 following NOX inhibition.

We carried out a series of experiments to investigate whether NOXs are a source of the nuclear ROS observed. MV4-11 cells were treated with DPI inhibitor or vehicle control. The confocal images of NucPE1/PO1 showed that inhibition of NOX with DPI causes a reduction of cytosolic and nuclear H_2O_2 (Figure 2.10). Flow cytometry analysis of the staining showed that DPI decreased approximately 40% of NucPE1 fluorescence (Figure 2.11).

In order to confirm that the effects of DPI on nuclear H_2O_2 are due to NOX inhibition, rather than off target inhibitions, we used an additional NOX selective inhibitor, VAS-2870. The treatment of MV4-11 cells with VAS-2870 for 1 h resulted in a decrease in cellular and nuclear H_2O_2, as measured with PO1 and NucPE1 respectively (Figure 2.12).

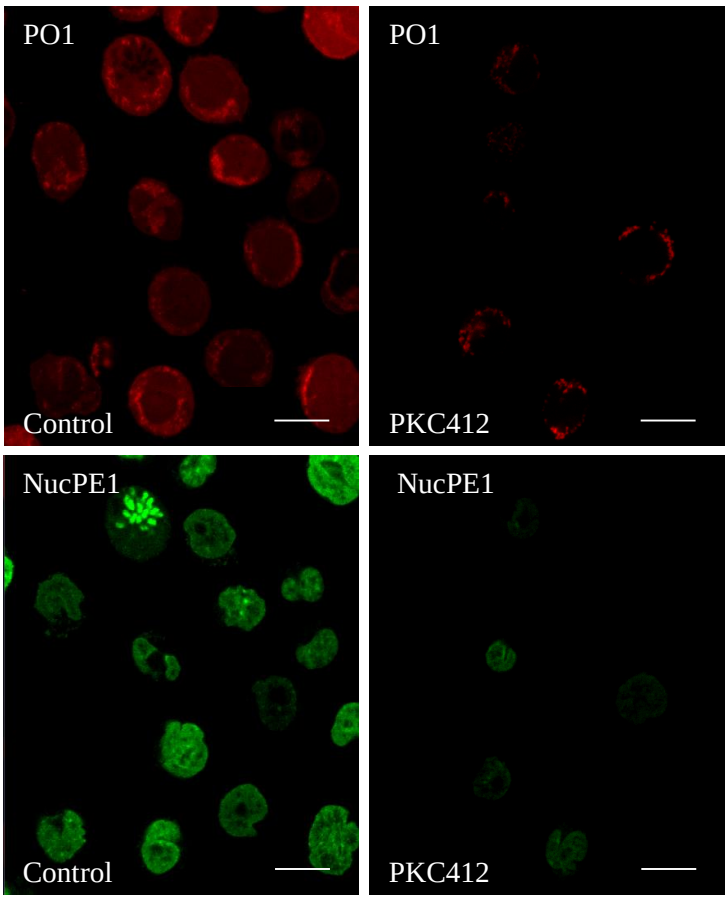

Figure 2.8. Cellular and nuclear H_2O_2 levels following the FLT3-ITD inhibition. PKC412-treated (right panel) and DMSO-treated (Control; left panel) live MV4-11 cells were stained with NucPE1 (bottom images) and PO1 (top images), then imaged with a confocal laser scanning microscope. The scale bar represents 10 μm.

a)

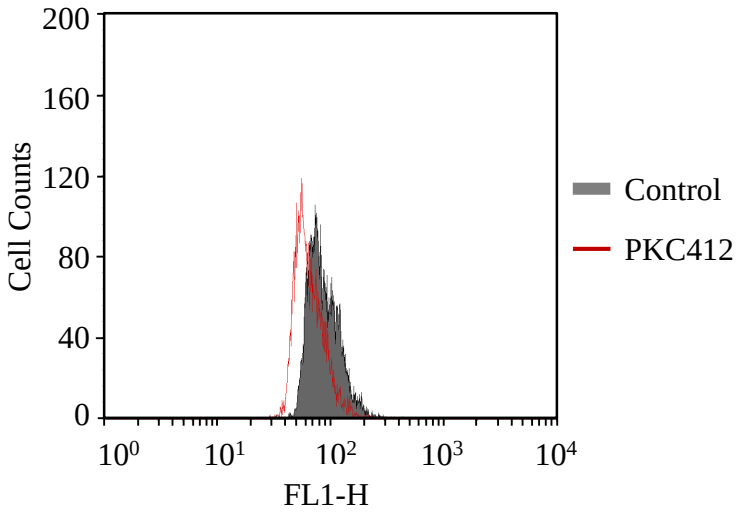

b)

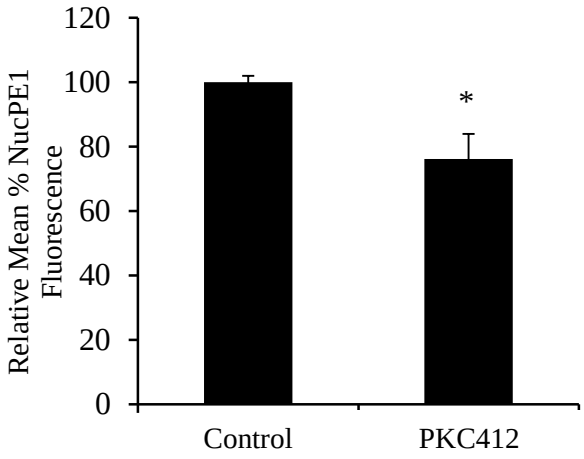

Figure 2.9. Levels of nuclear H_2O_2 following the FLT3-ITD inhibition. a) FACS analysis of relative mean NucPE1 fluorescence of control (DMSO; grey) and PKC412 treated MV4-11 cells (red). b) Bar chart represents flow cytometry analysis of mean relative % NucPE1 fluorescence of DMSO treated (Control) and PKC412 treated (50 nM; 1 h) MV4-11 cells. Results are shown as relative geometric mean± SD. Results are representative of at least 3 biological replicates. Statistical analysis was carried out using the student t-test ($p<0.005$ is marked with *).

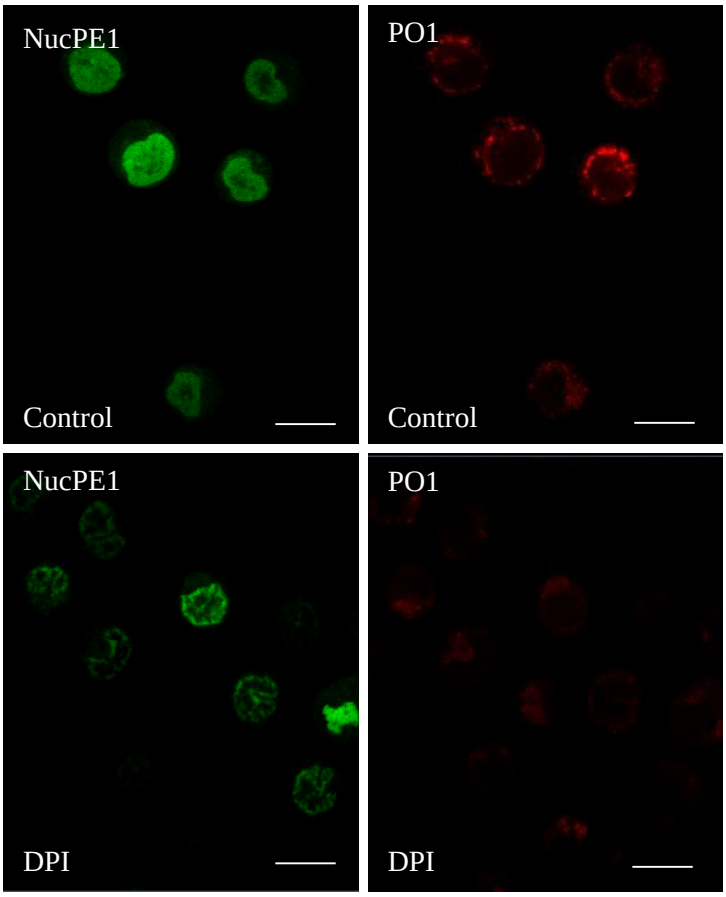

Figure 2.10. Confocal microscopy of cellular and nuclear H_2O_2 following NOX inhibition in live MV4-11 cells. DPI-treated (bottom panel) and DMSO-treated (Control; top panel) MV4-11 cells were stained with NucPE1 (green; left images) and PO1 (red; right images), then imaged with a confocal laser scanning microscope. The scale bar represents 10 μm.

a)

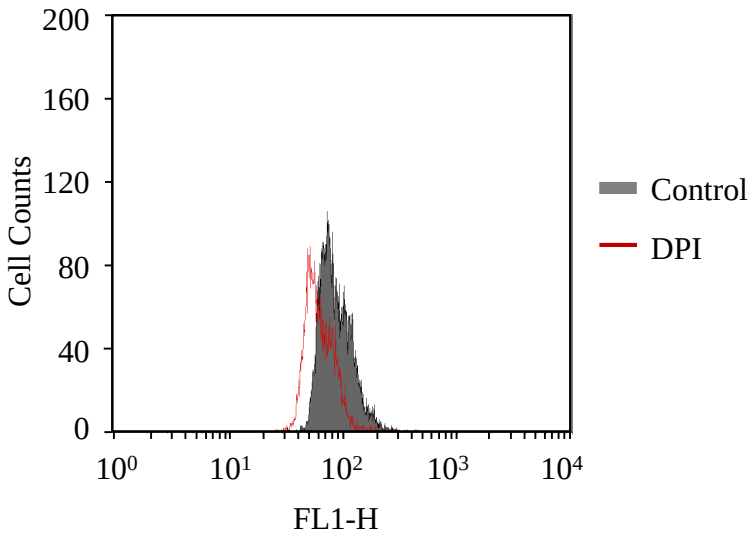

b)

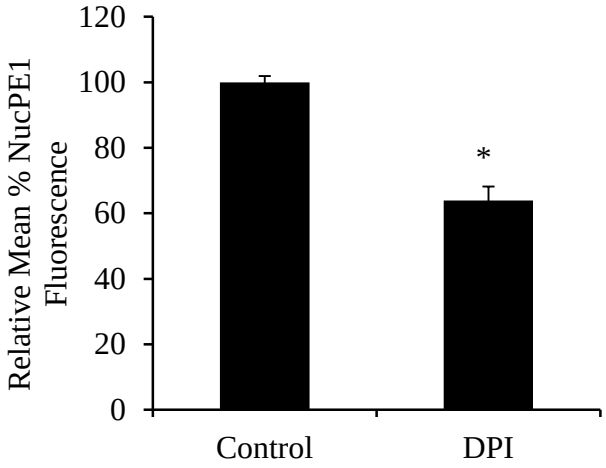

Figure 2.11. Quantification of nuclear H_2O_2 following NOX inhibition in MV4-11 cells. a) FACS analysis of relative mean NucPE1 fluorescence of control (DMSO; grey) and DPI-treated (1 µM; 1 h) MV4-11 cells (red). b) Bar chart represents flow cytometry analysis of relative mean % NucPE1 fluorescence of DMSO (Control) treated and DPI treated MV4-11 cells. Results are shown as relative geometric mean± SD. Results are representative of at least 3 biological replicates. Statistical analysis was carried out using the student t-test ($p<0.005$ is marked with *).

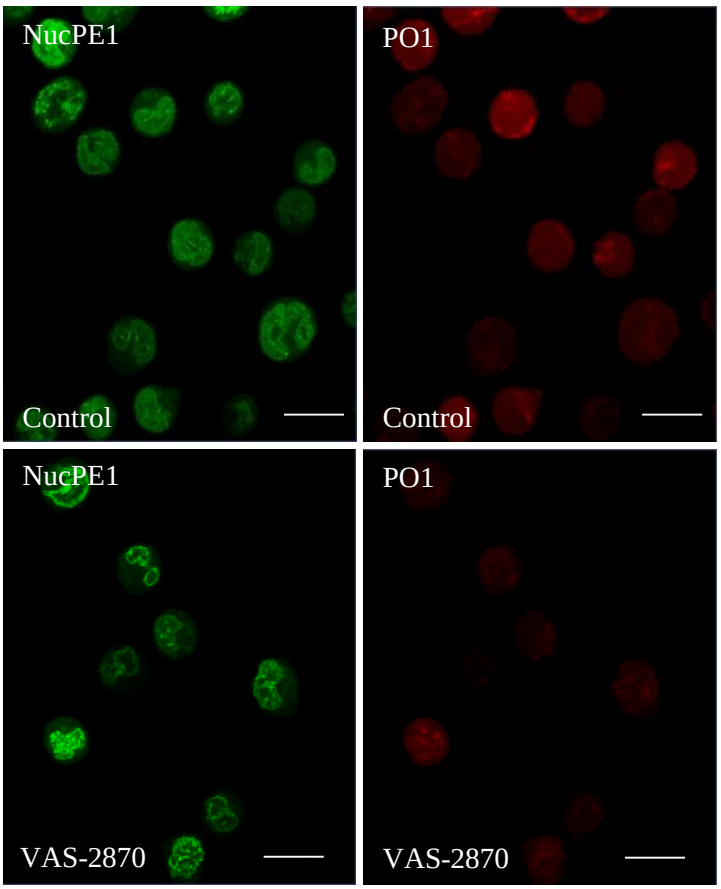

Figure 2. 12. Confocal microscopy of levels of cellular and nuclear H_2O_2 following NOX inhibition with VAS-2870 in live MV4-11 cells. VAS-2870-treated (bottom panel) and DMSO-treated (Control; top panel) MV4-11 cells were stained with NucPE1 (green; left images) and PO1 (red; right images), then imaged with a confocal laser scanning microscope. The scale bar represents 10 μm.

Confocal microscopy of cellular and nuclear H_2O_2 levels following $p22^{phox}$ siRNA knockdown in MV4-11 cells.

Considering that FLT3-ITD regulated NOX complex through stabilisation of $p22^{phox}$, we transfected MV4-11 with $p22^{phox}$ siRNA and investigated H_2O_2 levels in cytosol and the nucleus. Western blotting analysis of $p22^{phox}$ expression in MV4-11 cells following siRNA transfection revealed knockdown of the target protein (Figure 2.13.a). Comparing confocal images of siRNA and control treated cells showed that $p22^{phox}$ knockdown leads to reductions of H_2O_2, not only in the cytosol, but also in the nucleus (Figure 2.13.b). Flow cytometry analysis of the same experiment, demonstrated approximately 20% decrease in PO1/NucPE1 fluorescence following $p22^{phox}$ knockdown in MV4-11 cells, based on 10, 000 cells (Figure 2.14).

Colocalisation of NOX4/$p22^{phox}$ to the nuclear membrane in MV4-11.

Several reports suggested that NOX4 is localised to the nucleus and/or nuclear membrane (Lee et al., 2010, Weyemi and Dupuy, 2012, Weyemi et al., 2012). Based on the change in NucPE1 fluorescence following $p22^{phox}$ knockdown, we investigated NOX4 localisation in MV4-11 cells. At first, we co-stained the NOX4 antibody with Hoechst. However, we did not observe any colocalisation between these two stains (Figure 2.15). When analysing immunostaining of NOX4 and NUP98, which targets nuclear pores, we noticed a substantial colocalisation which indicated localisation of NOX4 in the nuclear membrane (Figure 2.15). Moreover, we have also colocalised anti-$p22^{phox}$ to

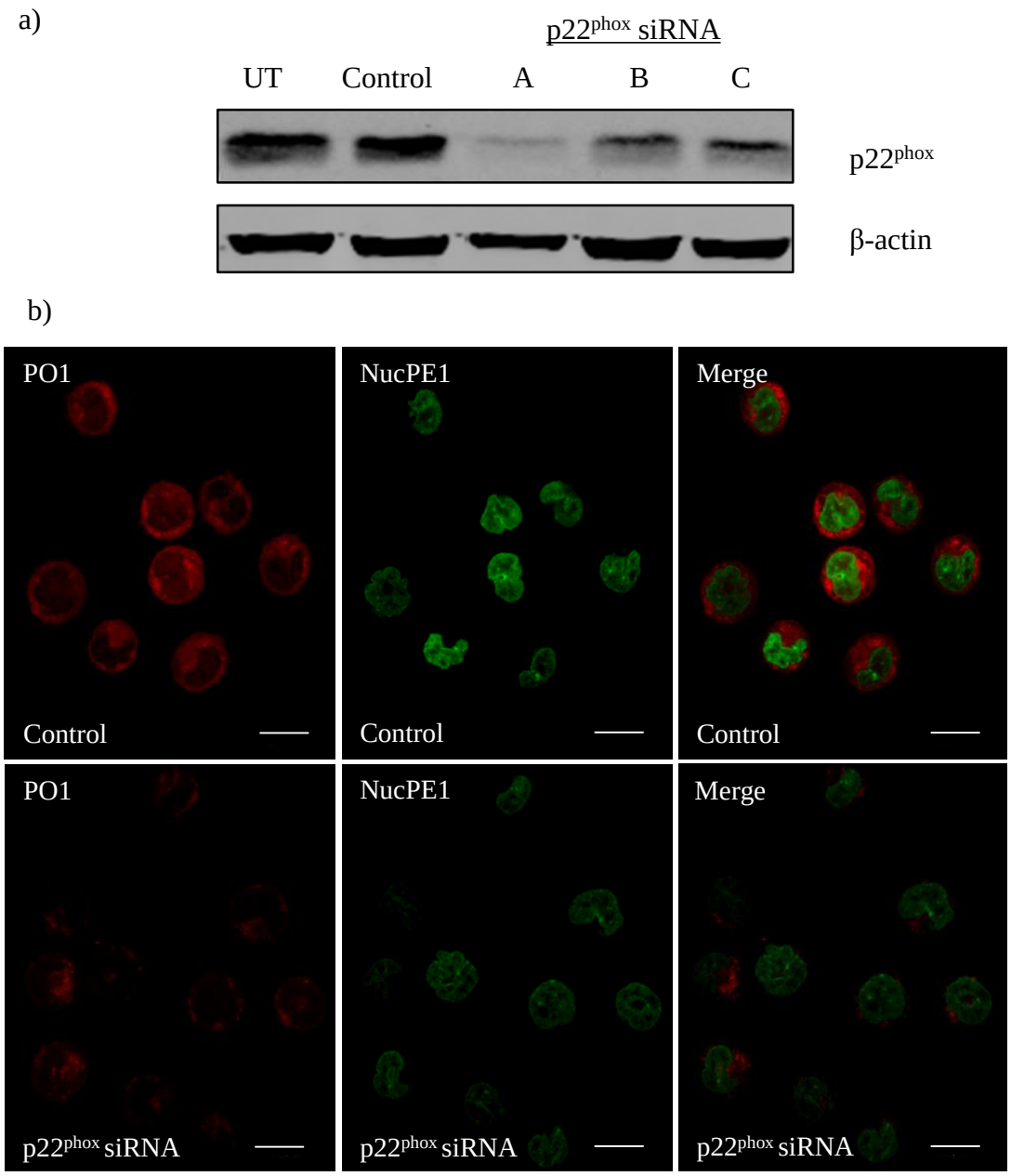

Figure 2. 13. Confocal microscopy of level of cellular and nuclear H_2O_2 following $p22^{phox}$ siRNA knockdown in live MV4-11 cells. a) Western blotting analysis of $p22^{phox}$ protein expression 24 h post-transfection. MV4-11 cells were transfected with scrambled siRNA or $p22^{phox}$ siRNA (A, B and C) and lysed 24 h later. β-actin was used as a loading control. b) MV4-11 cells were stained with PO1 (red; left panel) and NucPE1 (green; middle) for 1 h, 24 h post the transfection. Merges of the two probes are shown in the right images. Top panel shows scrambled siRNA treated cells (control) and bottom panel shows $p22^{phox}$ siRNA treated cells. The scale bar represents 10 μm.

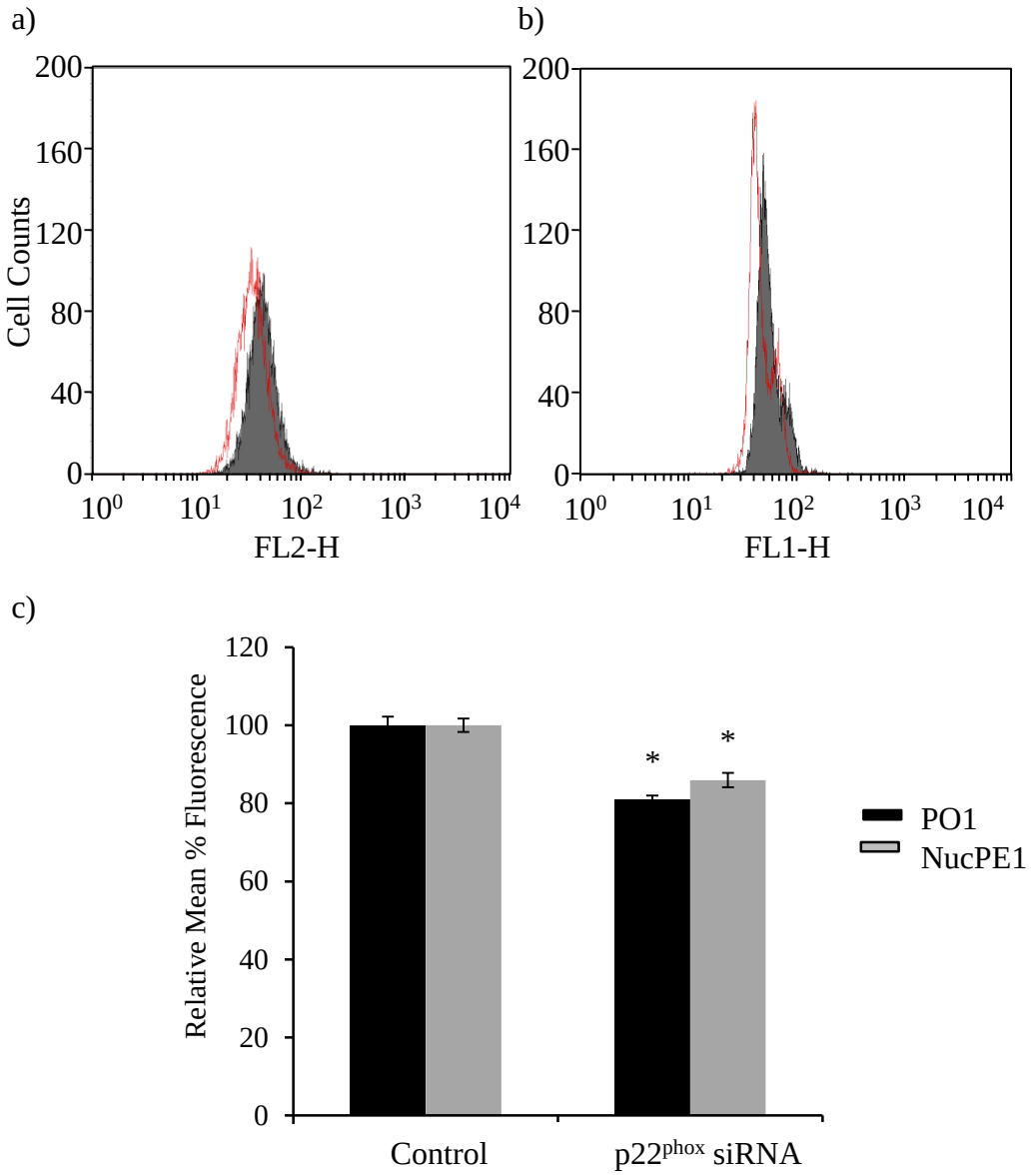

Figure 2. 14. Quantification of cellular and nuclear H_2O_2 following the $p22^{phox}$ siRNA knockdown. MV4-11 cells were stained with either PO1 (a) or NucPE1 (b) for 1 h, 24 h after the siRNA transfection. a) FACS analysis of relative mean PO1 fluorescence of control (scrambled siRNA; grey) and $p22^{phox}$ siRNA treated (Control; red) MV4-11 cells. b) FACS analysis of relative mean NucPE1 fluorescence of control (scrambled siRNA; grey) and $p22^{phox}$ siRNA treated (Control; red) MV4-11 cells. c) Bar chart represents flow cytometry analysis of mean relative %PO1 and % NucPE1 fluorescence of control treated and $p22^{phox}$ siRNA treated MV4-11 cells. Results are shown as relative geometric mean± SD. Results are representative of at least 3 biological replicates. The asterisk indicates statistically significant difference ($p<0.05$) as analysed by Student t-test. The error bars represent ±SD.

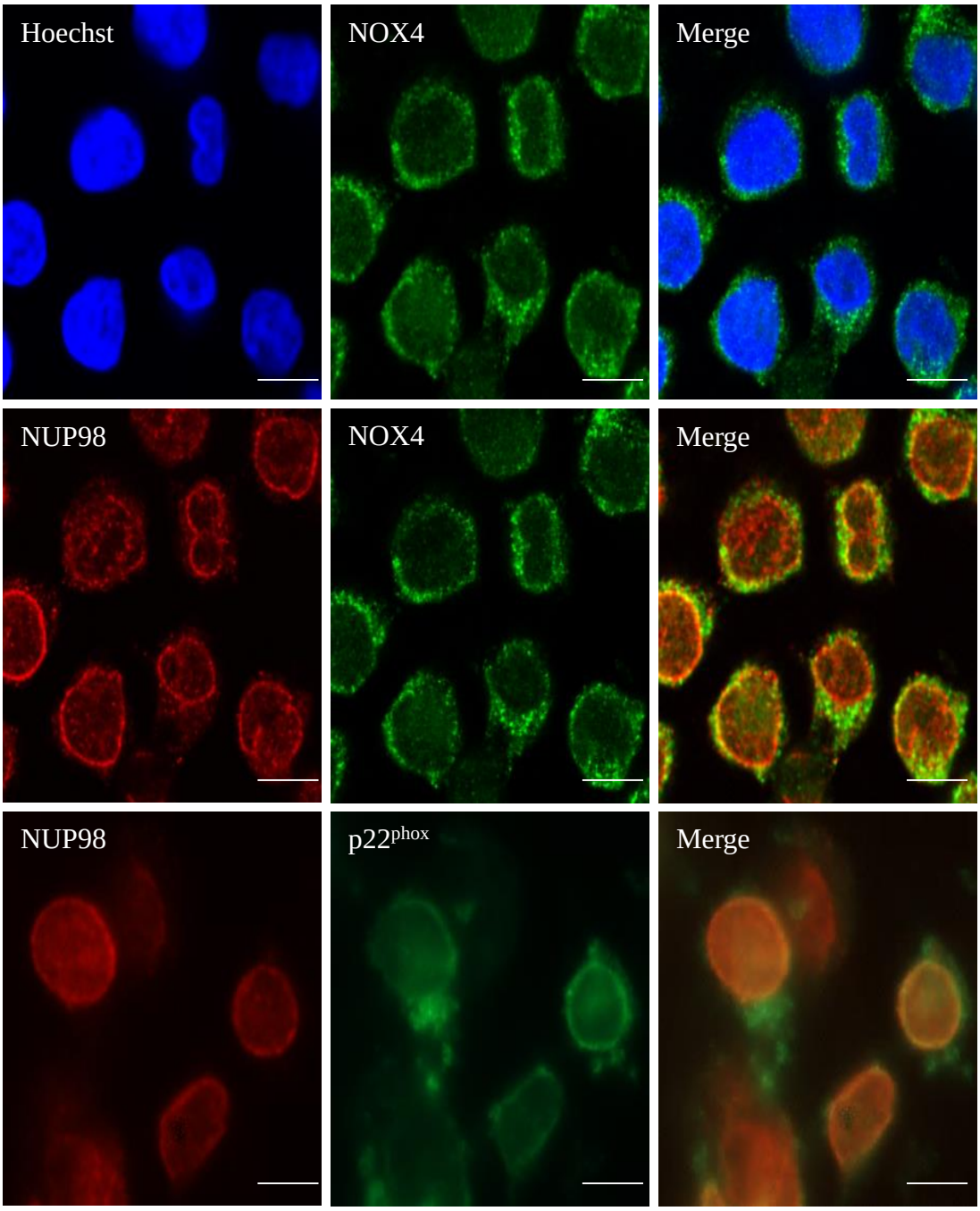

Figure 2. 15. Colocalisation of NOX4/$p22^{phox}$ and nuclear membrane in MV4-11. Confocal images represent NOX4, $p22^{phox}$ and NUP98 immunofluorescence as indicated on the images. The merged images are shown in the right panels. Cells were incubated on poly-D-lysine coated coverslips for 16 h, then fixed in 3% PFA/PBS and followed by NOX4, NUP98, $p22^{phox}$ and Hoechst staining. Images were acquired using confocal microscopy. The scale bar represents 10 μm.

anti-NUP98, suggesting that NOX4 and $p22^{phox}$ operate together in a complex at the nuclear membrane (Figure 2.15).

Discussion

The aim of this chapter was to investigate the mechanism of NOX activation by FLT3-ITD in AML. In the previous chapter, we showed that in the MV4-11 cell line NOXs were involved in the generation of H_2O_2 in the ER, stimulated by FLT3-ITD signalling. Inhibition of NOXs with DPI, a selective NOX inhibitor has resulted in a reduction in endogenous concentration of H_2O_2.

Tumour cells have elevated NOX-generated ROS that in turn stimulate proliferation, survival and genomic instability (Block and Gorin, 2012). Alterations in the redox environment and genomic instability of cancer cells have been recently reviewed as an enabling hallmark of cancer (Hanahan and Weinberg, 2011). Leukaemic oncogenes have been previously shown to affect redox homeostasis of cells; either by increasing the generation of ROS or by modulating the expression of antioxidants (Irwin et al., 2013). To date, two reports have associated FLT3-ITD to increased production of ROS. Sallmyr *et al.* proposed that FLT3-ITD leads to phosphorylation of STAT5 that in turn interacts with Rac1, a NOX GTPase (Sallmyr et al., 2008a). On the other hand, Reddy *et al*. has shown that the presence of FLT3-ITD mutation alters the concentration of NADPH, a substrate of NOX (Reddy et al., 2011).

Several oncogenes have been shown to increase the expression of NOX catalytic subunits. (Weyemi et al., 2012). However, we did not observe any changes in levels of NOX catalytic subunits following FLT3 inhibition (NOX1, 2, 4 and 5). Therefore, we investigated the expression of regulatory subunits. We showed that

FLT3-ITD drives the stabilisation of $p22^{phox}$, which is a novel mechanism of NOX regulation by mutated FLT3. $p22^{phox}$ is a small membrane subunit that is required for the formation of a functionally active NOX 1-4 complex (Bedard and Krause, 2007). By regulating steady levels of $p22^{phox}$, FLT3-ITD can control the activity of NOX isoforms (NOX1, 2 and 4) expressed in myeloid cells (Naughton et al., 2009). Studies have shown that due to the stabilisation function of $p22^{phox}$ in the NOX complex, $p22^{phox}$ knockdown leads to decreased NOX activity (Ambasta et al., 2004). Similarly to FLT3-ITD, Insulin-like growth factor (IGF-1) and foetal bovine serum (FBS) have been shown to activate NOX through $p22^{phox}$ in pancreatic cancer cells (Edderkaoui et al., 2011). However, in the latter case, $p22^{phox}$ was up-regulated transcriptionally (Edderkaoui et al., 2011). We demonstrated that FLT3-ITD up-regulates $p22^{phox}$ at the post-translational level by inhibition of its degradation (Woolley et al., 2012). In both AML and pancreatic cancer, $p22^{phox}$ has been shown to possess strong anti-apoptotic and pro-survival functions (Edderkaoui et al., 2011, Reddy et al., 2011). In support of these findings, similar regulation of NOX by oncogenes was seen in the BCR-ABL expressing CML cell line, K562 (Landry et al., 2013). Inhibition of BCR-ABL with Imatinib led to post-translational down-regulation of $p22^{phox}$ which resulted in the reduction of ROS production in these cells. These reports suggest that oncogenic up-regulation of the small regulatory subunit $p22^{phox}$ may be a common mechanism for regulating ROS generation in cancers.

Importantly, $p22^{phox}$ degradation was also observed when two additional FLT3 inhibitors, AC-220 and CEP-701, were used in MV4-11 cells. This strongly

supports the notion that FLT3 inhibition leads to $p22^{phox}$ degradation. Moreover, when the study was extended to MOLM-13 cells, which are heterozygous for FLT3-ITD, $p22^{phox}$-degradation was also seen. In contrast to this, PKC412-mediated FLT3 inhibition in HL-60 cells, which express inactive FLT3-WT, did not result in a change in $p22^{phox}$ protein level. This demonstrated that only active FLT3-ITD regulates protein level of $p22^{phox}$.

$p22^{phox}$ was previously reported to localise to the ER in many cell lines of different origin (Weyemi et al., 2012) However, its subcellular localisation was not investigated in leukaemic cells. Having established that H_2O_2 accumulated in the ER, we demonstrated colocalisation of $p22^{phox}$ and the ER marker antibody, KDEL. Analysis of $p22^{phox}$ and ER colocalisation revealed that 70% of $p22^{phox}$ immunostaining overlaps with KDEL. In support of this finding, this was also observed before in monocytes, cells of similar origin to AML cells (Lee et al., 2010).

Although pharmacological inhibition of NOX with DPI reduced FLT3-ITD-induced H_2O_2, the specific function of $p22^{phox}$ in generation of ROS was not shown (chapter 3). Using two different ROS probes, we demonstrated that $p22^{phox}$-targetted siRNA transfection caused a significant reduction in both total ROS and specifically H_2O_2. These results vary from previously published data by Reddy *et al.* which showed that $p22^{phox}$ knockdown does not affect the redox status of AML cells (Reddy et al., 2011). However, that study was carried out in MOLM-13 cells, that are heterozygous for FLT3-ITD, and solely used DCF as the ROS indicator which was then measured with flow cytometry (Reddy et al., 2011). Based on our confocal microscopy, analysis of DCF staining shows an equally dispersed pattern, difficult to

localise subcellularly. In contrast, PO1 has demonstrated not only to be H_2O_2 specific, but also more reliable in localisation studies. Disadvantages of DCF have also been extensively reviewed in several recent papers, hence our focus on the H_2O_2 specific, PO1 probe (Chen et al., 2010).

Importantly, $p22^{phox}$ siRNA knockdown has caused a significant reduction in cellular H_2O_2 in the ER, which confirms the hypothesis that FLT3-ITD induced stabilisation of ER-resident $p22^{phox}$ leads to the increase of H_2O_2. To our knowledge, it is one of the first studies that show a highly localised generation/accumulation of H_2O_2 in the ER.

ROS generation has also been known for years to have detrimental and damaging effects on all cellular structures. One of the consequences of the increased ROS generation, especially in cancer is genomic instability, defined by a high frequency of mutations in the genome. Genomic instability has also been considered recently as an enabling hallmark of cancer as it allows premalignant cells to evolve into fully cancerous cells. We have shown that accumulation of $p22^{phox}$ leads to H_2O_2 generation at the ER. Could this H_2O_2 diffuse from the ER to the nucleus to cause DNA damage? In order to answer this question, we used a newly-developed H_2O_2-specific probe, NucPE1, which specifically localises to the nucleus (Dickinson et al., 2011b). NucPE1 has been shown to fluoresce brightly upon reaction with H_2O_2 (Dickinson et al., 2011b).

The strong nuclear localisation of NucPE1 in leukaemic cells was confirmed by NucPE1 and Hoechst co-staining. In order to investigate the levels of nuclear and

cellular H_2O_2 in MV4-11 cells, we stained them with NucPE1 and PO1 respectively. The ability to monitor cellular and nuclear H_2O_2 gave us the opportunity to examine how redox changes in the cytosol affect nuclear H_2O_2. FLT3-ITD-induced nuclear ROS has never been studied before. In this thesis, we demonstrated using confocal microscopy and flow cytometry that inhibition of FLT3 leads to a reduction of both cytosolic and nuclear ROS in MV4-11 cells. This suggests that by stabilising $p22^{phox}$, FLT3-ITD induces H_2O_2 generation in the ER that diffuses to the nucleus. The involvement of NOX in generating nuclear H_2O_2 was examined by DPI and VAS-2870-mediated inhibition of NOX. Interestingly, NOX inhibition yielded a larger reduction in NucPE1 fluorescence than FLT3 inhibition. This is likely explained by NOX acting independently of FLT3 as well as through FLT3-stimulation. Moreover, the general activity of NOX in AML patient samples suggests that FLT3-ITD-regulated stabilisation of $p22^{phox}$ only potentiates NOX activity (Hole et al., 2013). Interestingly, a study was published subsequently to our work reporting that MOLM-13 and THP-1 cells produce a reduced amount of nuclear H_2O_2 following NOX inhibition, as measured with NucPE1(Guida et al., 2014).

Specific knockdown of $p22^{phox}$ reduced H_2O_2 in the ER. Interestingly, the same knockdown also reduced nuclear H_2O_2. Since $p22^{phox}$ is an essential subunit of NOX1-4 isoforms, we suspect that these are the isoforms that are involved in endogenous ROS production. NOX 1, 2 and 4 are the isoforms that have been previously reported to be expressed in myeloid cells (Reddy et al., 2011, Lee et al., 2010). Furthermore, specific NOX4 knockdown has been demonstrated to reduce

nuclear ROS production in myelodysplastic syndromes (MDS), a disease closely related to AML (Guida et al., 2014).

In addition to confocal microscopy, we quantified PO1 and NucPE1 staining by flow cytometry that allowed us to analyse a larger population of cells. This analysis revealed about 20% reduction in cytosolic and nuclear H_2O_2 following $p22^{phox}$ siRNA knockdown. This change corresponds strongly to the decrease previously seen with PKC412-mediated FLT3 inhibition. This suggests that the H_2O_2 production by FLT3-ITD involves $p22^{phox}$-dependent stabilisation of NOX. Initially, this result seems to contrast the data published by Reddy *et al.*, where it was suggested that even though $p22^{phox}$ is a potent regulator of growth and migration in MOLM-13 cells, mitochondria were the main ROS source stimulated by FLT3-ITD (Reddy et al., 2011). However, the levels of ROS following the $p22^{phox}$ knockdown were assessed using DCF, which corresponds to the total ROS level. On the other hand, we have shown that $p22^{phox}$ knockdown specifically down-regulates H_2O_2 in the ER when measured with PO1. Moreover, we used MV4-11 cells that are homozygous for FLT3-ITD mutation, rather than MOLM-13 that are heterozygous for FLT3-ITD. NOX enzymes were previously suggested to regulate ROS generation downstream of FLT3-ITD by interaction of Rac1 with phosphorylated STAT5 (Sallmyr et al., 2008a). The knockdown of either proteins resulted in a significant reduction of endogenous ROS (Sallmyr et al., 2008a). The involvement of Rac1 suggests that the NOX1 and 2 are activated by this interaction, but not NOX3 as this isoform is not expressed in myeloid cells (Bedard and Krause, 2007). In addition to this, it has recently been demonstrated that Rac1 could additionally activate NOX4

(Hajas et al., 2013). This suggests that NOX1, 2 and 4 could be regulated by Rac1-STAT5 interaction.

Reactive chemistry of ROS forces their generation to be localised close to their target (Mishina et al., 2011). We have shown that $p22^{phox}$ siRNA knockdown affects the redox environment of the nucleus as the concentration of nuclear H_2O_2 was reduced following the siRNA transfection. This suggested that NOX/$p22^{phox}$-generated H_2O_2 should be produced near to or even in the nucleus. Out of 7 NOX isoforms, NOX4 has been previously shown to be localised to the nucleus (Hajas et al., 2013, Kuroda et al., 2005, Matsushima et al., 2013, Spencer et al., 2011). H-RAS-induced NOX4/$p22^{phox}$ complex has been localised to the nuclear fraction of the lysed HThy-ori3 cells (Weyemi et al., 2012). Furthermore, NOX4 was shown to localise to the nucleus in cells similar to ours, including MOLM-13, THP-1 and MDS patient samples (Guida et al., 2014). Surprisingly, in the AML model, staining of NOX4 with Hoechst did not reveal any NOX4 foci present in the nucleus. Although plausible for our hypothesis, the high content of hydrophobic residues in the transmembrane region of NOX4 may not allow NOX4 to form a functional protein in the nucleus. However, it has been published recently that the 28 kDa splice variant of NOX4, which lacks the putative transmembrane domains, localised to the nucleus where it produces H_2O_2 in vascular cells (Anilkumar et al., 2013).

DNA within the cell is enclosed by the nuclear membrane, where membrane-bound NOX4 could possibly generate H_2O_2. Thus, we have co-stained MV4-11 cells with nuclear pore marker (NUP98) and antibodies against the NOX4/$p22^{phox}$ complex. The colocalisation study revealed that a significant portion of

NOX4/$p22^{phox}$ overlapped with nuclear membrane. Interestingly, this result was later confirmed in a study showing that NOX4 localised to the nuclear membrane with GTP-bound Rac1 in the alveolar epithelial cells (Hajas et al., 2013). This would suggest that possibly NOX4 could interact with Rac1, a GTPase previously implicated in AML at the nuclear membrane.

In summary, this work has shown that FLT-ITD stimulates ROS-generation from NOX by stabilising $p22^{phox}$, a small membrane component of the NOX complex. We have demonstrated that this $p22^{phox}$ localises to the ER, where H_2O_2 was accumulating. The H_2O_2 generation at the ER is reduced following the pharmacological inhibition of FLT3, NOX or the siRNA knockdown of $p22^{phox}$. Moreover, NOX-generated H_2O_2 downstream of FLT3-ITD changes the levels of H_2O_2 in the nucleus in MV4-11 cells. The localisation experiment has shown that NOX4 and $p22^{phox}$ localises to the nuclear membrane in these cells, suggesting that H_2O_2 generated at NOX diffuses into the nucleus.

Chapter 5

NOX-generated ROS damage DNA in FLT3-ITD positive AML cells.

Introduction

Genomic instability has been suggested to be the main cause of genetic diversity of cancer that ultimately leads to tumour cell evolution. It was proposed that tumour cells must acquire some form of genomic instability, because the normal rate of mutation is insufficient to provide the number of mutations required for the oncogenic transformation (Sieber et al., 2003, Loeb et al., 2003, Sallmyr et al., 2008b). In AML the evolution of a leukaemic clone is accompanied by the acquisition of increased number of genetic defects, which lead to increased cell survival, proliferation and a halt in differentiation towards functional white blood cells.

There are several mechanisms implicated in genomic instability (Burrell et al., 2013). For example, ROS production has been associated with genomic instability due to the damaging DNA oxidation. Cancer cells often possess increased levels of DNA damage along with increased ROS production (Waris and Ahsan, 2006, Cooke et al., 2003), suggesting that mutagenesis by ROS can contribute to the initiation of cancer as well as its promotion and progression.

Oxidative DNA damage can cause a wide range of DNA alterations such as base pair mutations, deletions and insertions (Cooke et al., 2003). Although all ROS possess oxidative characteristics, only few of them, for instance hydroxyl radical ($OH^{\cdot}$), have a capacity to damage DNA (Cooke et al., 2003). While superoxide anion and H_2O_2 have not been shown to damage DNA directly, they can undergo a series of reactions that will lead to generation of mutating $OH^{\cdot}$ (Henle and Linn, 1997). For

example H_2O_2 can be converted into $OH^{\cdot}$ in the presence of iron in the Fenton reaction (Henle and Linn, 1997). The extremely reactive chemistry of $OH^{\cdot}$ suggests that in order to damage DNA, it must be generated in the nucleus. Therefore, ROS should be produced in or in the proximity of the nucleus to form $OH^{\cdot}$ close to DNA, that can in turn cause DNA damage (Mishina et al., 2011). Moreover, the presence of endogenous ROS in the nucleus can modify how cells respond to stress and regulate the genes' expression of proteins that are responsible for cell proliferation, survival and differentiation (Wu, 2006).

ROS-induced genotoxic stress could be an important source of resistance to drugs (Karihtala and Soini, 2007). Although a significant progress has been made in the success of chemotherapies against cancer over the last few decades, ultimately many patients stop responding to the therapy due to acquisition of chemoresistance. Adaptation to higher concentration of ROS by stimulation of survival mechanisms and antioxidant systems could give cells a mechanism for the induction of resistance to drugs (Trachootham et al., 2008).

An alternative mechanism for the generation of genomic instability is associated with unfaithful or insufficient repair of DNA damage, for instance, dsb repair or replicative stress (Sieber et al., 2003, Pelicano et al., 2004). Cells possess a complex network of DNA repair mechanisms to prevent accumulation of genetic mutations that could arise from the oxidative stress. DNA dsbs are one of the most dangerous lesions that can results in deletions, insertions and translocations of DNA. There are two DNA repair mechanisms responsible for DNA dsb repair: a precise homologous recombination (HR) and a less-precise non-homologous end-joining

(NHEJ) (Sallmyr et al., 2008b). The accuracy of the DNA dsb repair depends highly on the requirement of the homologous DNA duplex. Furthermore, recent studies suggest that a novel, alternative end-joining (A-EJ) plays a significant role in cancer cells (Sallmyr et al., 2008b). The alternative NHEJ often subjects DNA to severe errors, such as deletions and translocations.

In AML, the presence of mutated FLT3-ITD in patients leads to an increased relapse risk after chemotherapy. In leukaemia, oncogenic signalling from FLT3-ITD and BCR-ABL has been demonstrated to increase expression of unfaithful A-EJ DNA repair proteins with a simultaneous down-regulation of DNA repair members of the faithful NHEJ (Fan et al., 2010). Interestingly, it was also shown that increased efficiency of FLT3-ITD-stimulated DNA repair contributes to drug-resistance (Seedhouse et al., 2006). These findings suggest that oxidative stress and alterations in DNA repair could lie in the basis of relapse concerns in FLT3-ITD-positive AML.

We have previously shown that FLT3-ITD oncogene stimulates NOX-enzymes to generate H_2O_2 at the ER and nuclear membrane in AML cell lines. The aim of this chapter is to investigate if mutated FLT3-ITD is able to induce oxidative DNA damage by activation of NOX enzymes. This knowledge could reveal the role of NOX-generated ROS in genomic instability in FLT3-ITD-positive AML.

Results

In previous chapters, we established that FLT3-ITD stimulates H_2O_2 generation in the ER. This formation of H_2O_2 is attenuated when FLT3 is inhibited with the tyrosine kinase inhibitor, PKC412. Moreover, level of H_2O_2 is also reduced when FLT3-ITD possessing MV4-11 cells are treated with a NOX inhibitor, DPI. We also demonstrated that mutated FLT3-ITD regulates NOX enzymes by inhibiting degradation of $p22^{phox}$. Confocal microscopy following a specific $p22^{phox}$-targeted siRNA knockdown revealed a reduction of H_2O_2 in the ER in the anti-$p22^{phox}$ siRNA treated cells. In order to investigate possible effects of NOX-generated ROS on genomic instability in AML, levels of nuclear H_2O_2 were investigated. Attenuation of FLT3 signalling, NOX activity or $p22^{phox}$ siRNA knockdown all led to significant reduction in the oxidative state in the nucleus. Furthermore, the localisation study of NOX4 and $p22^{phox}$ demonstrated that they both localised to the nuclear membrane in MV4-11 cells. This suggests that the stimulation of NOX activity by the FLT3-ITD oncogene contributes to the genomic instability in AML cell lines.

In this chapter, in addition to FLT3-ITD expressing MV4-11 AML cell line, we also employed an over-expression FLT3 system. FLT3-WT or mutated FLT3-ITD plasmids were stably transfected into 32D cells. 32D is a murine immortalised myeloblast-like cell line that is grown in IL-3 supplemented medium. Following transfection, due to a strong cytokine-like FLT3-ITD signalling, 32D/FLT-ITD expressing cells became IL-3 independent (Mizuki et al., 2000, Fenski et al., 2000). In order to confirm the expression and phosphorylation status of the FLT3 receptor in the 32D-transfected cells, Western blotting of anti-FLT3 and anti-phosphorylated

FLT3 (P-FLT3) was carried out. The analysis revealed expression of FLT3-ITD in 32D/FLT3-ITD cells and expression of FLT3-WT in 32D/FLT3-WT (Figure 3.1.a). Phosphorylation of STAT5 was also investigated to confirm the signalling differences between 32D/FLT3-WT and 32D//FLT3-ITD. As expected, FLT3/WT did not lead to phosphorylation of STAT5 (P-STAT5), whereas FLT3/ITD manifested a strong P-STAT5 signal (Figure 3.1.b). Moreover, treatment of 32D/FLT3-ITD cells with PKC412, a FLT3-selective tyrosine kinase inhibitor, led to dephosphorylation of FLT3-ITD (Figure 3.1.c).

Levels of H_2O_2 in 32D cells transfected with FLT3-WT or FLT3-ITD.

In previous chapters we showed that inhibition of FLT3-ITD results in the depletion in H_2O_2. In order to analyse how FLT3/ITD compares to FLT3/WT signalling regarding H_2O_2 formation in 32D cells, we utilised the PO1 probe. To remove IL-3 signalling, we starved 32D cells for 4 h before the experiment. IL-3 is a potent cytokine that affects similar pathways to FLT3-ITD, thus its presence in the medium could mask potential FLT3-ITD-signalling effects. Quantification of PO1 fluorescence demonstrated that 32D cells transfected with FLT3-ITD possess approximately 100% more H_2O_2 than 32D cells expressing FLT3-WT (Figure 3.2).

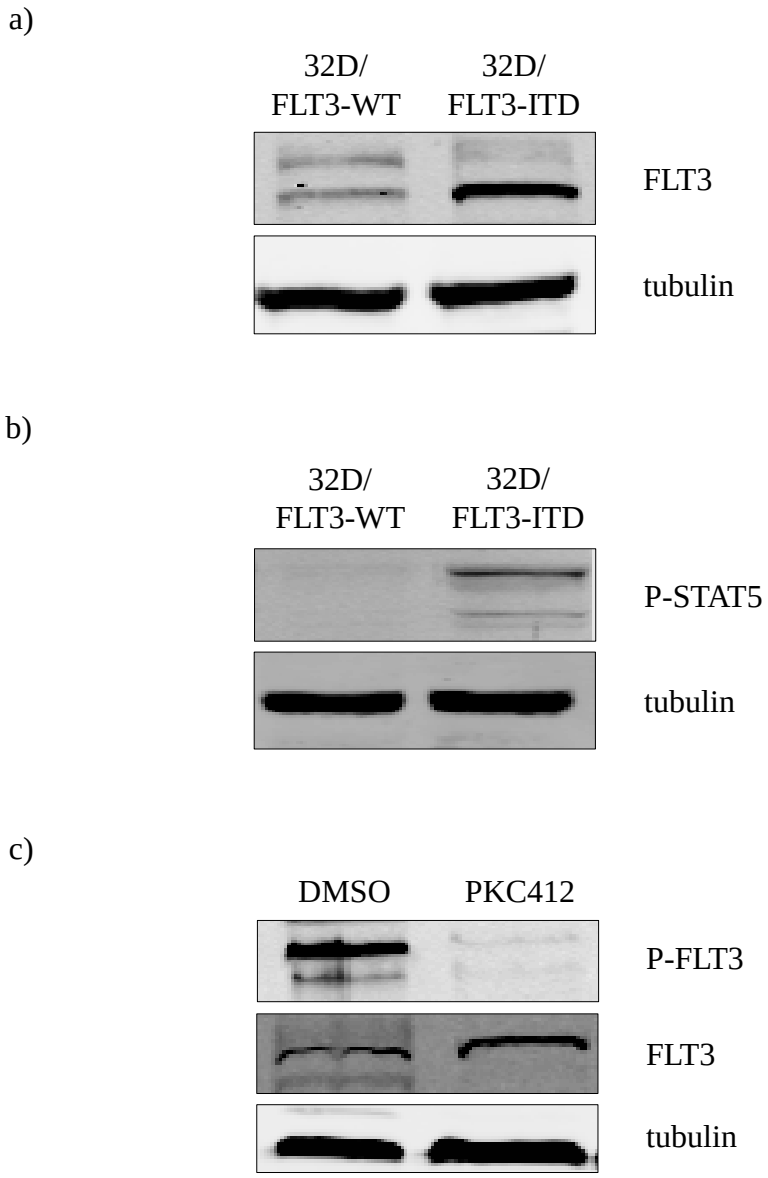

Figure 3.1. Expression and phosphorylation of FLT3 and FLT3/ITD and its effects on signalling in 32D cells transfected with FLT3-WT or FLT3-ITD. a) Western blotting analysis of FLT3 expression in 32D/FLT3-WT or 32D/FLT3-ITD lysed cells. The top band represents the mature glycosylated FLT3 (160 kDa). The lower band represents the immature unglycosylated FLT3 (130 kDa). b) Western blotting of phosphorylated STAT5 (P-STAT5) in 32D/FLT3-WT or 32D/FLT3/ITD lysed cells. c) Western blotting of phosphorylated FLT3 (P-FLT3) and total FLT3 in vehicle treated (DMSO) or PKC412 treated 32D/FLT3-ITD cells. Tubulin was used as a loading control in both immunoblots.

a)

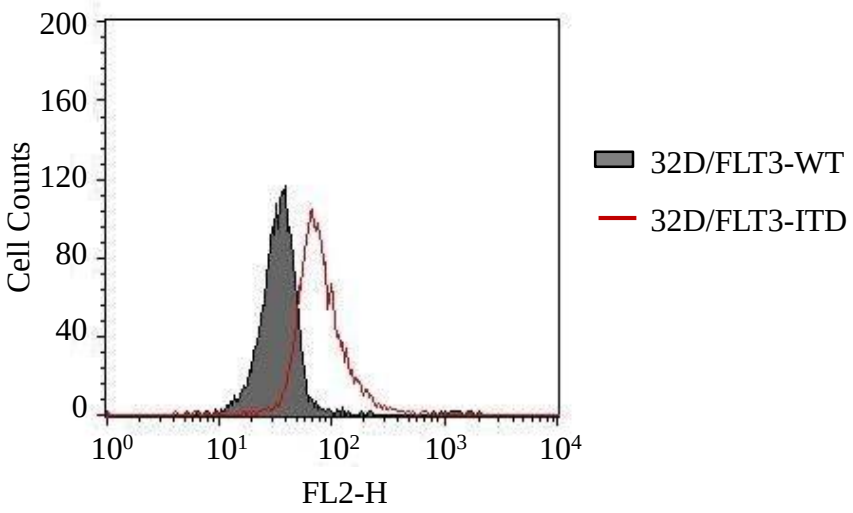

b)

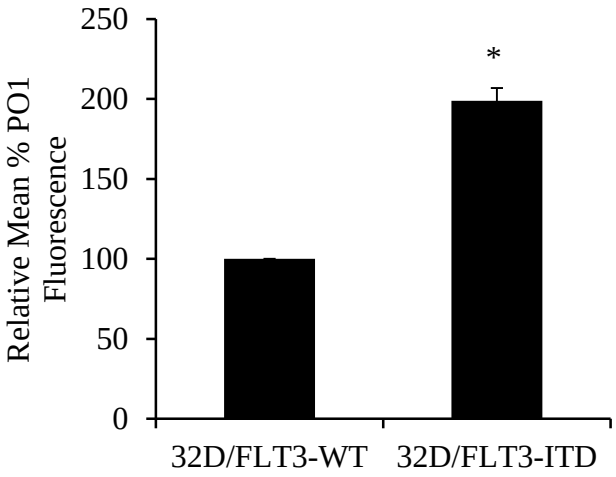

Figure 3.2. Level of H_2O_2 in 32D cell line transfected with FLT3-WT or FLT3-ITD receptor. a) FACS analysis of relative PO1 fluorescence of 32D cells transfected with FLT3-WT (grey) or FLT3-ITD (red). b) Bar chart representation of FACS results in a). Results are shown as relative geometric mean± SD. Results are representative of at least 3 independent experiments. Statistical analysis was carried out using the student t-test ($p<0.05$ is marked with *).

Levels of H_2O_2 in 32D cells transfected with FLT3-WT or FLT3-ITD following NOX or FLT3-ITD inhibition.

In order to investigate the extent of ROS induction by FLT3-expression we used PKC412 to inhibit FLT3 in 32D cells. PKC412 treatment of 32D/FLT3-ITD resulted in a 30% decrease in the level of H_2O_2, based on the PO1 probe analysed by flow cytometry (Figure 3.3). In contrast, 100 nM PKC412 did not affect the level of H_2O_2 in 32D cells transfected with FLT3-WT. To further examine the role of NOX in H_2O_2 production in 32D cells, we employed DPI, a previously used NOX inhibitor. Using PO1 probe, we demonstrated that DPI treatment depleted the H_2O_2 pool by 30% in the 32D cells expressing FLT3-ITD, the effect that mimicked FLT3 inhibition. Interestingly, inhibition of NOX with DPI in 32D/FLT3-WT cells did not reduce endogenous H_2O_2 levels (Figure 3.3).

Nuclear H_2O_2 levels in 32D cells transfected with FLT3-WT or FLT3-ITD.

Having confirmed the changes in the redox state when either FLT3-ITD or FLT3-WT was expressed in 32D cells, we decided to investigate if the endogenously produced H_2O_2 was affecting levels of H_2O_2 in the nucleus. This was necessary to ensure that the FLT3 over-expression cell lines could be used to investigate genomic instability in these cells. We demonstrated using NucPE1 that FLT3-ITD expression in 32D cells resulted in an approximately 25% increase in the nuclear ROS in comparison to cells expressing FLT3-WT (Figure 3.4).

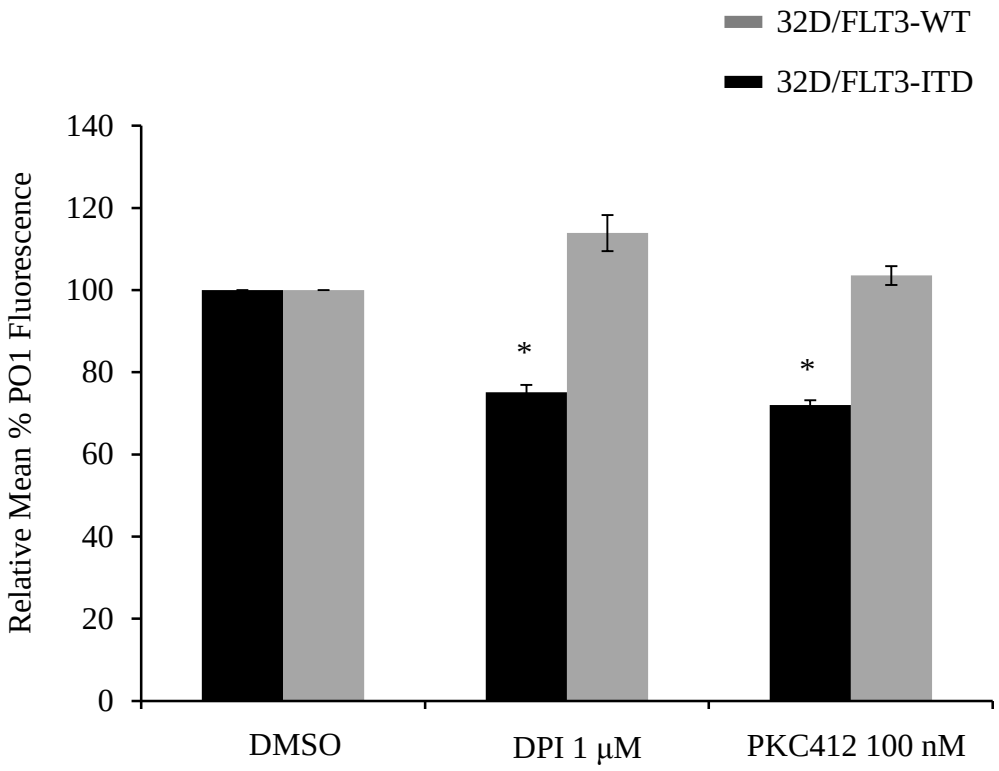

Figure 3.3. Level of H_2O_2 in 32D cell line transfected with FLT3-WT or FLT3-ITD receptor, following NOX or FLT3-ITD inhibition. Bar chart representation of a FACS analysis of relative PO1 fluorescence of 32D cells transfected with FLT3-WT or FLT3-ITD following treatment with DPI 1 μM or PKC412 100 nM. Results are shown as relative geometric mean± SD. Results are representative of at least 3 independent experiments. Statistical analysis was carried out using the student t-test ($p<0.05$ is marked with *).

a)

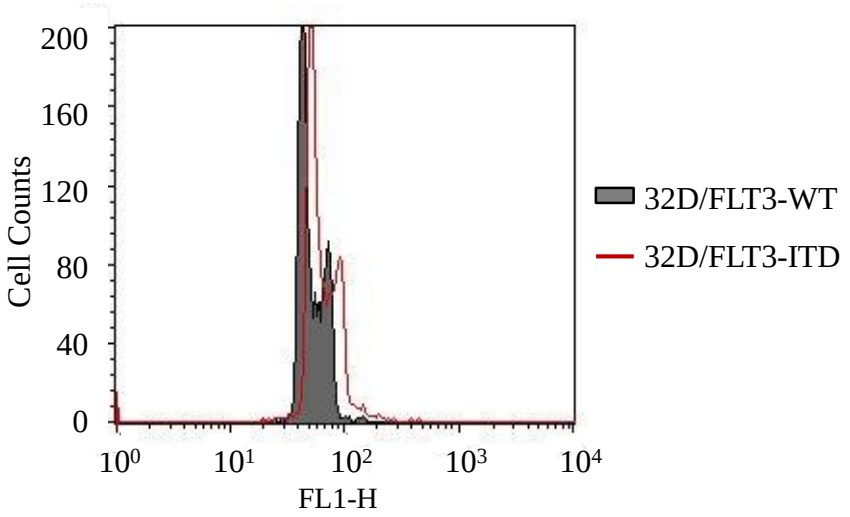

b)

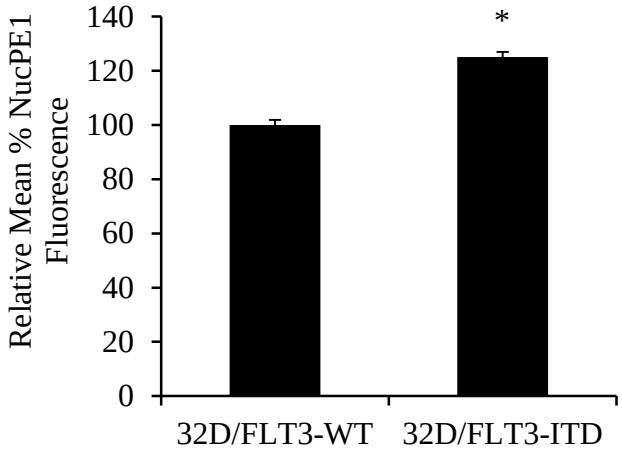

Figure 3.4. Level of nuclear H_2O_2 in 32D cell line transfected with FLT3-WT or FLT3-ITD receptor, as measured with NucPE1. a) FACS analysis of relative NucPE1 fluorescence of 32D cells transfected with FLT3-WT (grey) or FLT3-ITD (red). b) Bar chart representation of FACS results in a). Results are shown as relative geometric mean± SD. Results are representative of at least 3 independent experiments. Statistical analysis was carried out using the student t-test ($p<0.05$ is marked with *).

Mitochondrial ROS in 32D cells transfected with FLT3-WT or FLT3-ITD.

Since mitochondria were previously suggested to be implicated in the redox status of FLT3-expressing cell line, we decided to measure mitochondrial ROS in both FLT3-WT and FLT3-ITD expressing 32D cells (Reddy et al., 2011). Interestingly, there was no significant difference noted in mitochondrial ROS, as measured with MitoSOX fluorescence analysis, using flow cytometry (Figure 3.5).

Level of DNA dsbs in FLT3-WT and FLT3-ITD expressing cells.

In order to study genotoxic stress in FLT3-ITD leukaemia, we employed gamma H2AX (γH2AX) immunofluorescence. H2AX is a nucleosome core histone and induction of DNA dsbs triggers its phosphorylation in cells. The phosphorylated H2AX is referred to as γH2AX and it has become one of the most commonly used measure of DNA dsbs (Valdiglesias et al., 2013). At first, we followed the previously used immunofluorescence protocol with paraformaldehyde (PFA) based fixation step. However, this protocol did not reveal an expected punctuate staining of γH2AX foci (Figure 3.6.a). Therefore, we applied a protocol previously published by Sallmyr *et al*. (Sallmyr et al., 2008a). The latter procedure requires fixation by 70% cold ethanol treatment. This protocol greatly improved the staining, revealing a clear γH2AX foci (Figure 3.6.b).

a)

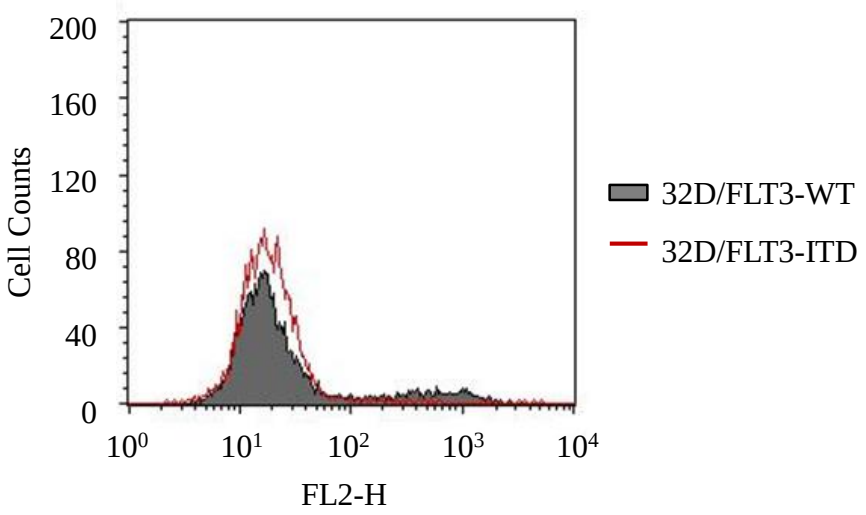

b)

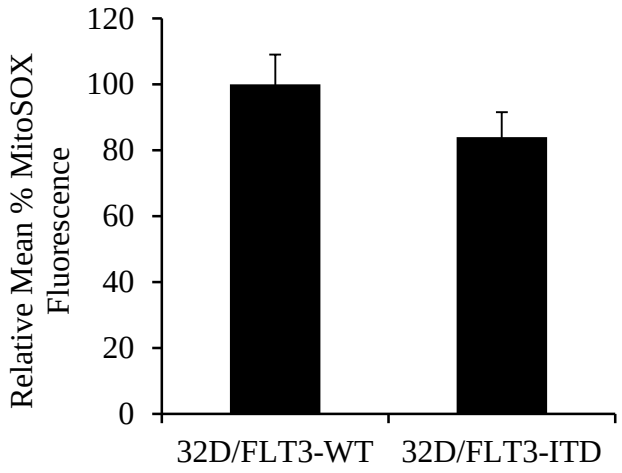

Figure 3.5. Level of mitochondrial ROS in 32D cell line transfected with FLT3-WT or FLT3-ITD, as measured with MitoSOX. a) FACS analysis of relative MitoSOX fluorescence of 32D cells transfected with FLT3-WT (grey) or FLT3-ITD (red). b) Bar chart representation of FACS results in a). Results are shown as relative geometric mean± SD. Results are representative of at least 3 independent experiments. Statistical analysis was carried out using the student t-test ($p<0.05$ is marked with *).

a)

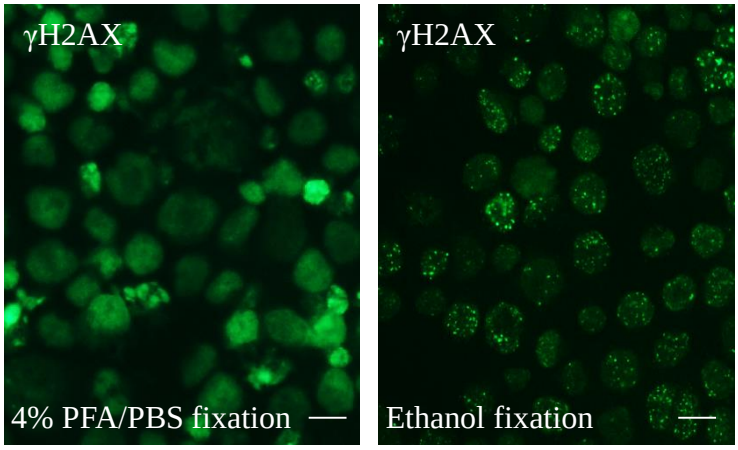

b)

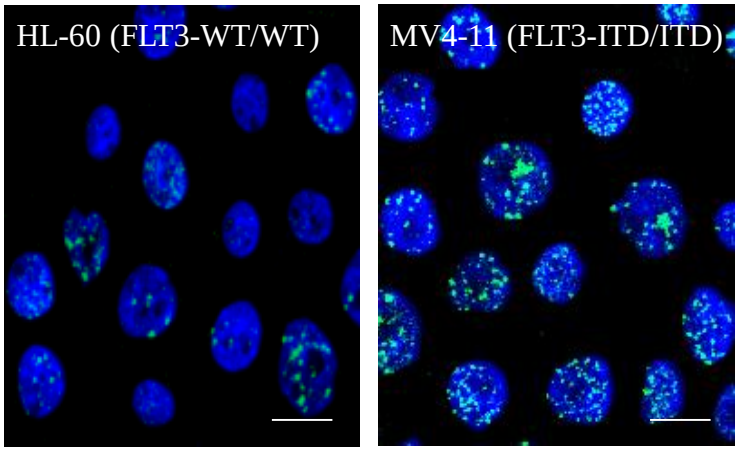

Figure 3.6. Comparison of the number of DNA dsbs in HL-60 cells and MV4-11 cells, using γH2AX immunofluorescence. a) Optimisation of γH2AX staining using different antibody concentrations in MV4-11 cells. Left image presents γH2AX immunofluorescence using 4% PFA/PBS as a fixation agent. Right image shows γH2AX immunofluorescence using ethanol as a fixation agent. b) Cells were incubated on the poly-D-lysine coated coverslips for 16 h. Cell were then fixed in ethanol and followed by γH2AX and Hoechst staining. The scale bar represents 10 μm.

Before pursuing genomic instability studies in the 32D over-expression system, we investigated DNA damage levels in cell lines expressing FLT3-WT (HL-60) and FLT3-ITD (MV4-11). Confocal microscopy of γH2AX immunofluorescence revealed its nuclear localisation and punctuate pattern of staining. Based on analysis of γH2AX immunostaining, FLT3-WT expressing HL-60 cells showed fewer DNA dsbs that FLT3-ITD-expressing MV4-11 (Figure 3.6).

In order to accelerate the quantification of γH2AX staining per cell, flow cytometry was used as an analytical tool rather than confocal microscopy (Figure 3.7). MV4-11 cells that are homozygous for FLT3-ITD mutation possessed the highest number of DNA dsbs. Also MOLM-13 cells, which are heterozygous for FLT3-ITD, displayed approximately 20% less DNA dsbs. Finally, FLT3-WT expressing only HL-60 showed 30% less DNA dsbs than MV4-11 cells.

The same dsb-marker, γH2AX was used to investigate DNA damage in cells transfected with FLT3-WT or FLT3-ITD. 32D/FLT3-ITD cells showed approximately 75% more DNA dsbs than 32D/FLT3-WT cells (Figure 3.8).

Oxidised DNA levels in 32D cells transfected with FLT3-WT or FLT3-ITD

FLT3-ITD has been demonstrated to alter the repair of DNA dsbs which could lead to changes in the levels of dsbs independent of ROS. In order to compare oxidative damage of DNA in FLT3-ITD versus FLT3-WT expressing 32D cells, we employed a second DNA damage marker, 8-hydroxy-2'-deoxyguanosine (8-

a)

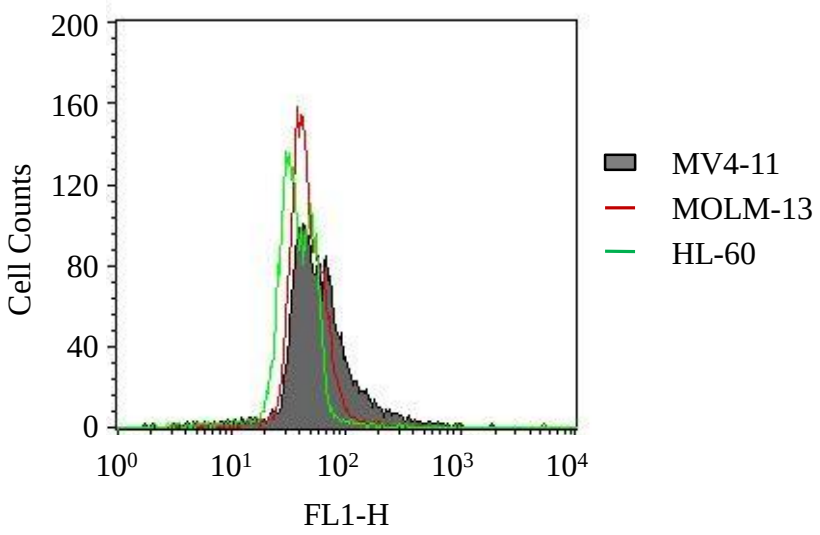

b)

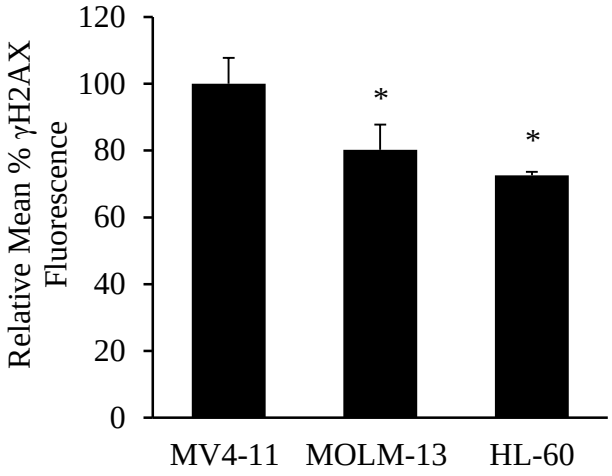

Figure 3.7. Levels of DNA dsbs in HL-60, MOLM-13 and MV4-11, using γH2AX immunofluorescence. a) FACS analysis of relative anti-γH2AX fluorescence of MV4-11 cells (grey), MOLM-13 cells (red) and HL-60 cells (green). b) Bar chart representation of FACS results in a). Results are shown as relative geometric mean± SD. Results are representative of at least 3 independent experiments. Statistical analysis was carried out using the student t-test ($p<0.05$ is marked with *).

a)

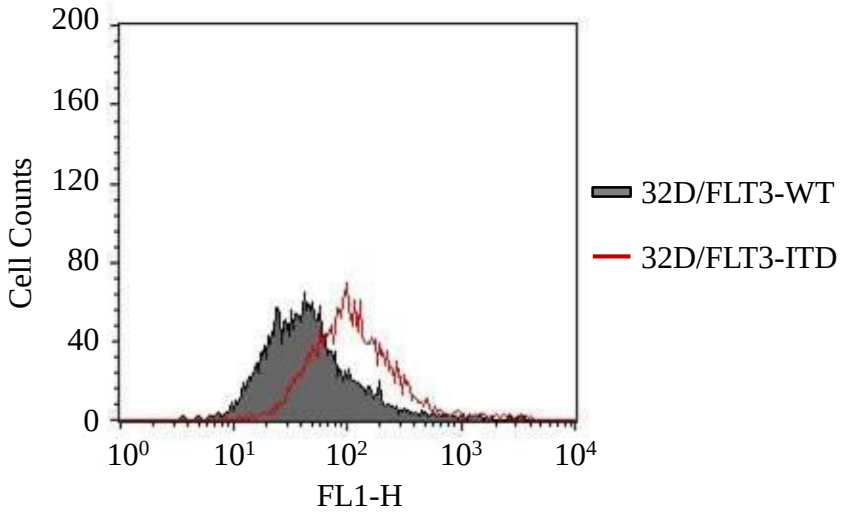

b)

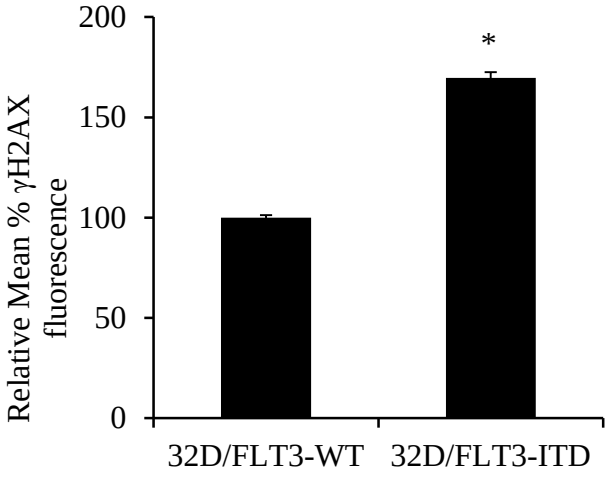

Figure 3.8. Level of DNA dsbs in 32D cell line transfected with FLT3-WT or FLT3-ITD receptor, as measured with γH2AX immunofluorescence. a) FACS analysis of relative anti-γH2AX fluorescence of 32D cells transfected with FLT3-WT (grey) or FLT3-ITD (red). b) Bar chart representation of FACS results in a). Results are shown as relative geometric mean± SD. Results are representative of at least 3 independent experiments. Statistical analysis was carried out using the student t-test ($p<0.05$ is marked with *).

OHdG). 8-OHdG is a predominant form of ROS-induced DNA lesion and therefore is widely used as a biomarker of oxidative stress (Valko et al., 2004). The immunofluorescence of anti-8-OHdG, quantified using flow cytometry revealed that 32D/FLT3-ITD cells possess over 100% more 8-OHdG than their wild type counterparts (Figure 3.9).

DNA dsbs levels in 32D cells expressing FLT3-WT or FLT3-ITD, following the inhibition of NOX or FLT3-ITD.

In previous chapters we showed that NOX enzymes generate ROS in the FLT3-ITD expressing MV4-11 cells. We also demonstrated that there is a significant difference between level of oxidative DNA damage in 32D/FLT3-WT and 32D/FLT3-ITD. In order to investigate the source of DNA damage in 32D cells transfected with FLT3-ITD, we used DPI, a NOX-selective inhibitor. When 32D cells expressing either FLT3-WT or FLT3-ITD were treated with DPI, a 30% decrease in γH2AX was noted in 32D/FLT3-ITD. In contrast, a 20% increase in γH2AX was observed in 32D/FLT-WT (Figure 3.10).

PKC412 treatment of 32D/FLT3-ITD cells led to a reduction in the endogenous levels of H_2O_2. We investigated if the PKC412-mediated FLT3 inhibition in 32D cells would lead to a reduction in DNA dsbs levels. PKC412 treatment, over a 24 h period resulted in a 40% decrease in γH2AX fluorescence. To confirm specificity of the PKC412-induced effects, the same treatment was applied to 32D/FLT3-WT cells. This did not decrease the number of DNA dsbs (Figure 3.10).

a)

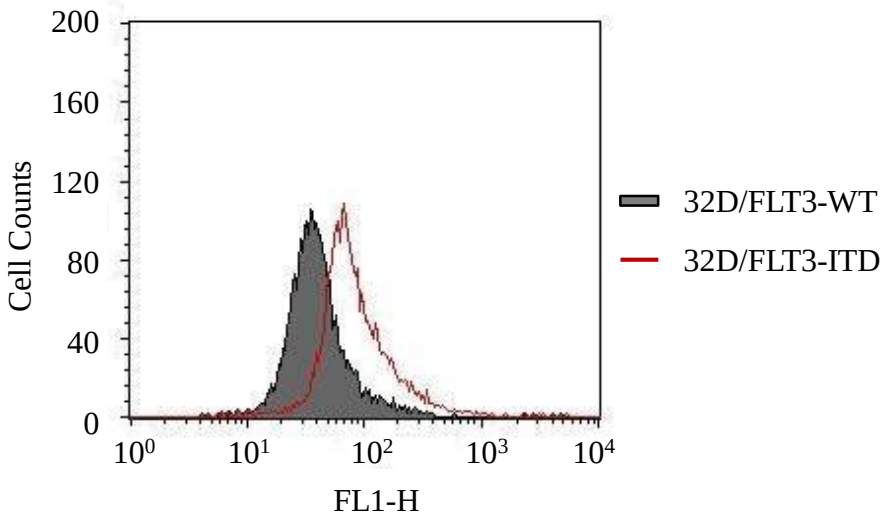

b)

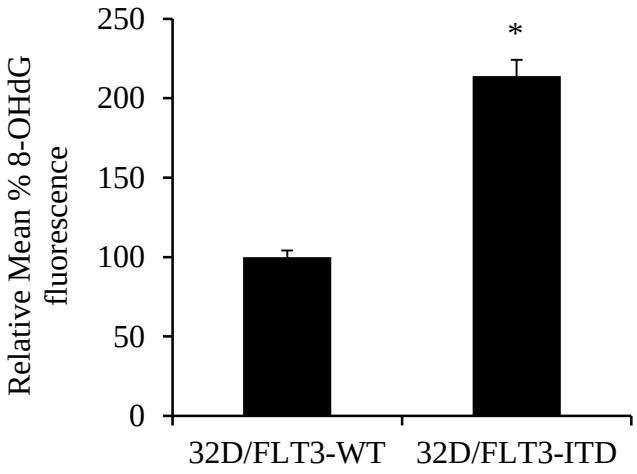

Figure 3.9. Level of oxidised DNA in 32D cell line transfected with FLT3-WT or FLT3-ITD receptor, as measured with 8-OHdG immunofluorescence. a) FACS analysis of relative anti-8-OHdG fluorescence of 32D cells transfected with FLT3-WT (grey) or FLT3-ITD (red). b) Bar chart representation of FACS results in a). Results are shown as relative geometric mean± SD. Results are representative of at least 3 independent experiments. Statistical analysis was carried out using the student t-test ($p<0.05$ is marked with *).

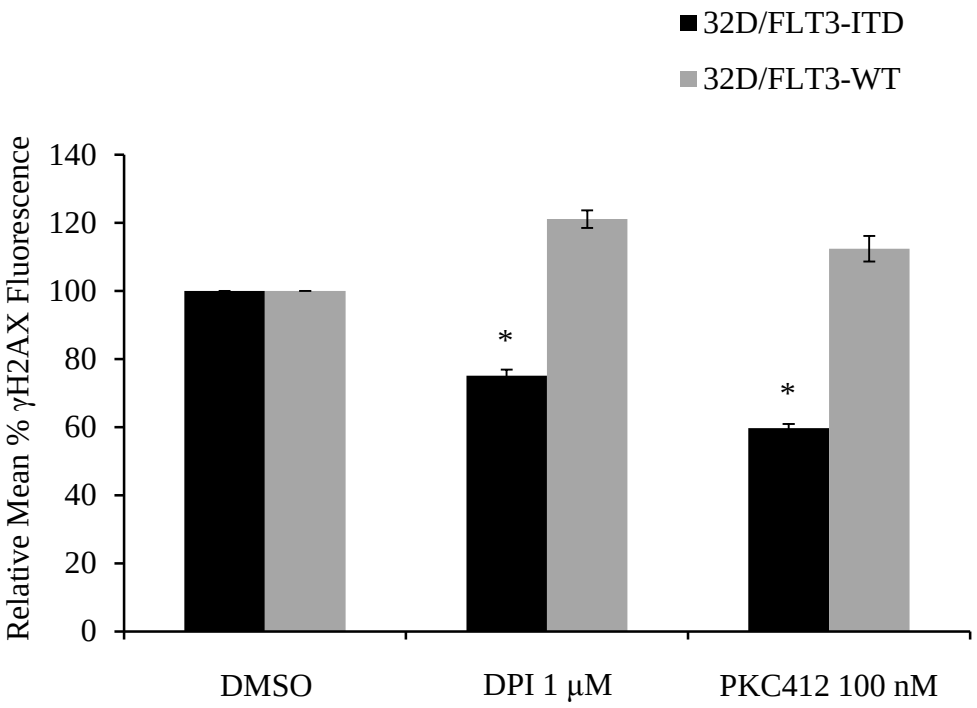

Figure 3.10. Level of DNA dsbs in 32D cell line transfected with FLT3-WT or FLT3-ITD receptor, following NOX or FLT3-ITD inhibition, as measured with γH2AX immunofluorescence. Bar chart of FACS analysis of anti-γH2AX fluorescence of 32D cells transfected with FLT3-WT (grey) or FLT3-ITD (black). The cells were treated for 24 h with the treatments of the indicated concentrations. Results are shown as relative geometric mean± SD. Statistical analysis was carried out using the student t-test ($p<0.05$ is marked with *).

Reversible FLT3-ITD inhibition effects on the levels of DNA damage in MV4-11 cells.

To investigate if the oxidised DNA damage could be readily reversed in MV4-11 cells, we used PKC412 and DPI inhibitors. At first we treated cells with PKC412 for 24 h, which resulted in a 35% reduction of 8-OHdG. Upon removing PKC412 and allowing the cells to recover for 16 h, the level of 8-OHdG almost returned to 100%. Importantly, when PKC412 removal was followed by the addition of DPI to the recovery conditions 8-OHdG only declined by 5-10% (Figure 3.11).

DNA dsbs are one of the most serious DNA lesions. The protocol used in the previous paragraph was also applied to measure the reversibility of DNA dsbs in FLT3-ITD expressing MV4-11 cells. PKC412 treatment reduced the level of DNA dsbs by 20%. The 24 h recovery period from the drug resulted in the regeneration of DNA dsbs in these cells (Figure 3.12). However, the increase in the level of DNA dsbs was slightly higher than that in the control. This may be due to the fact that the PKC412 inhibitor may distinctly affect 8-oxoguanine/γH2AX generating and repairing pathways. The removal of FLT3-inhibitor led to an immediate stimulation of the major oncogene signalling pathway in these cells. This may have led to a temporary up-regulation/down-regulation of certain pathways that would result in the increase in the γH2AX e.g. DNA dsb repair. Importantly, when the cells were treated with DPI during the recovery time, restoration of the initial number of DNA dsbs was partially prevented. These data suggested that FLT3 and NOX-generated DNA damage could be reversed by inhibiting either of these proteins.

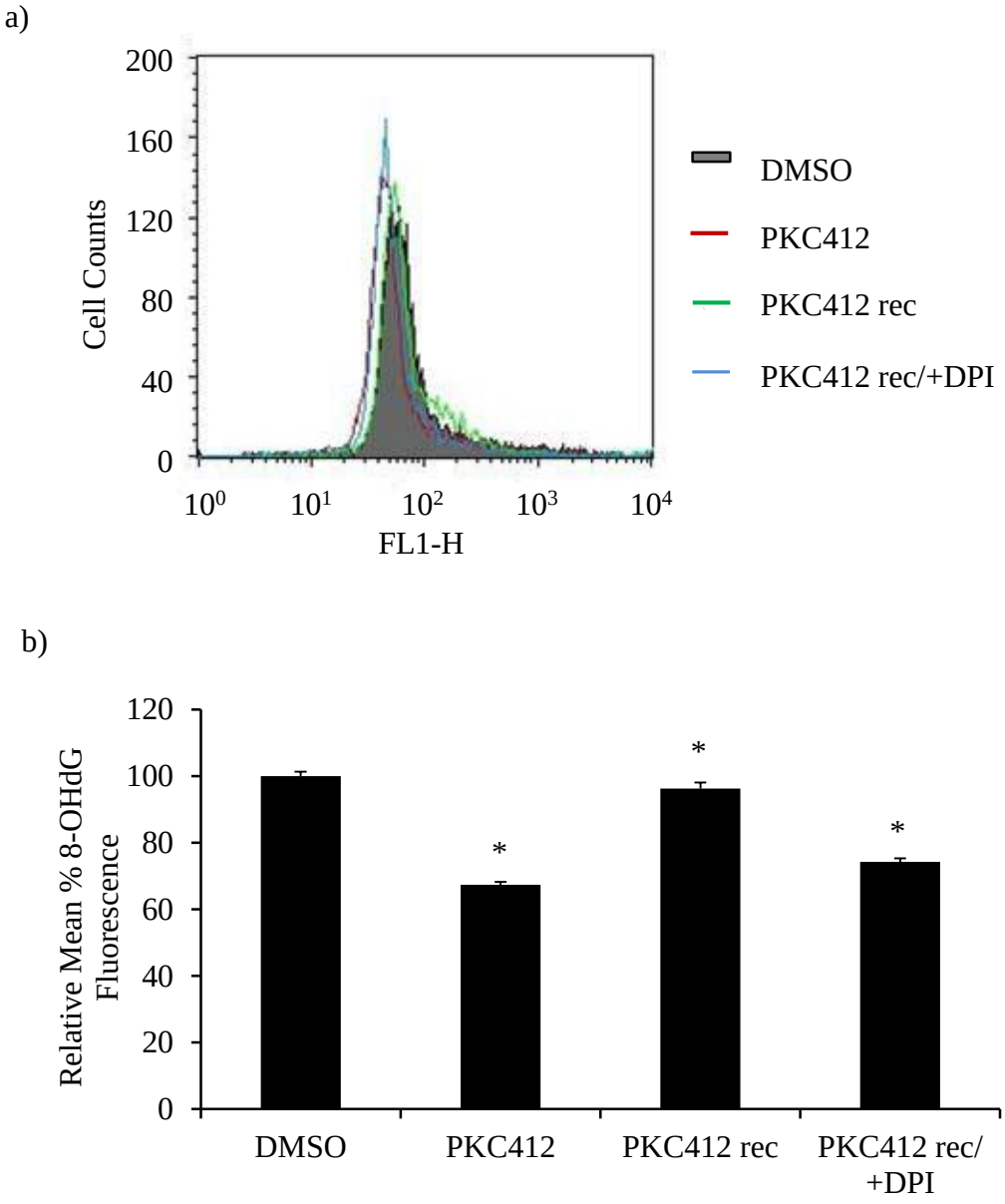

Figure 3.11. Reversible FLT3-ITD inhibition effects on the levels of oxidised DNA in MV4-11 cells. a) FACS analysis of relative anti-γH2AX fluorescence of MV4-11 cells treated with drug vehicle DMSO (grey), 50 nM PKC412 for 24 h (red), 50 nM PKC412 for 24 h followed by PBS wash and 16 h recovery time (green), 50 nM PKC412 for 24 h followed by PBS wash and 16 h recovery time in the presence of 1 μM DPI. b) Bar chart representation of FACS results in a). Results are shown as relative geometric mean± SD. Statistical analysis was carried out using the student t-test ($p<0.05$ is marked with *).

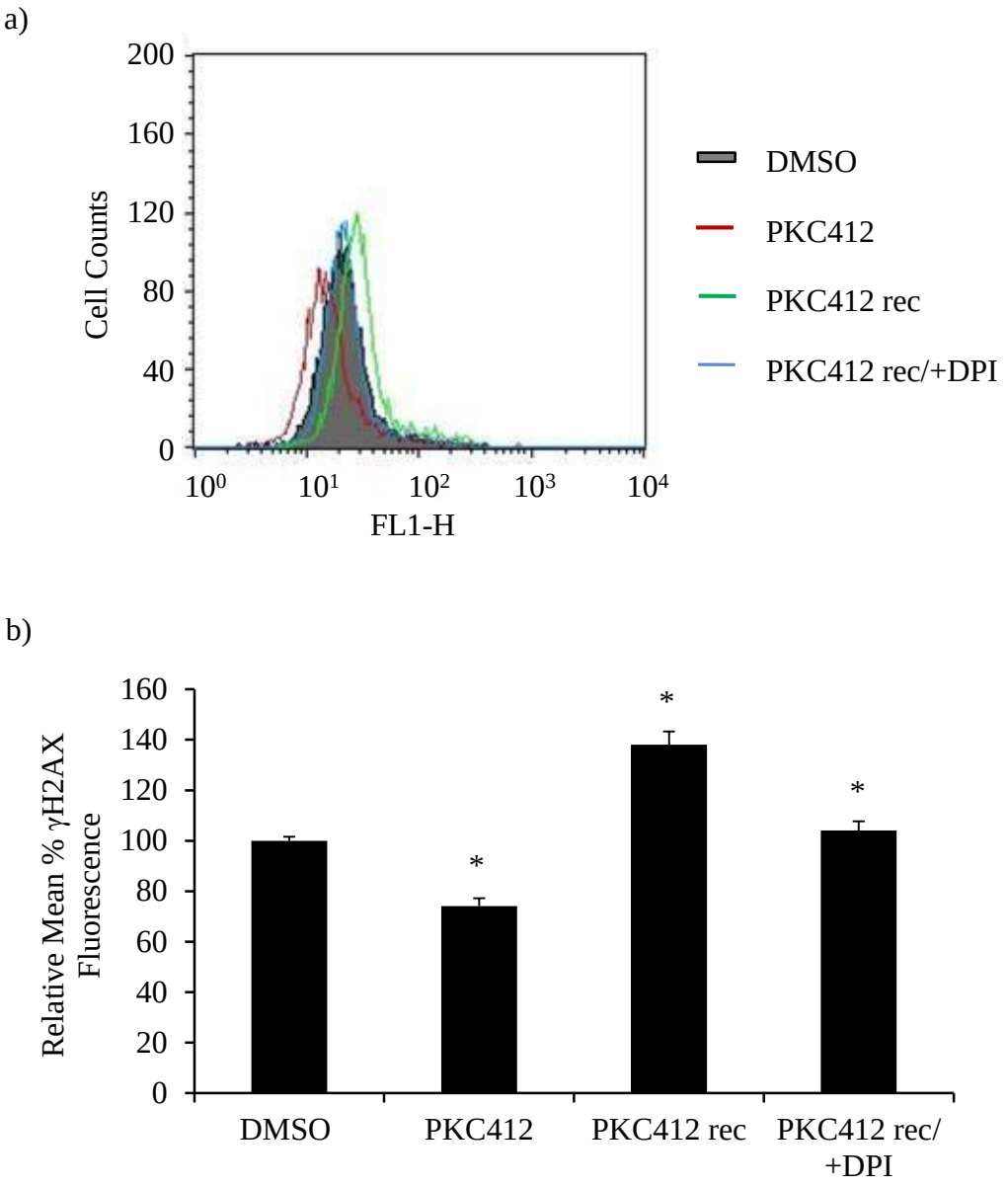

Figure 3.12. Reversible FLT3-ITD inhibition effects on the levels of DNA dsbs in MV4-11 cells. a) FACS analysis of relative anti-γH2AX fluorescence of MV4-11 cells treated with drug vehicle DMSO (grey), 50 nM PKC412 for 24 h (red), 50 nM PKC412 for 24 h followed by PBS wash and 16 h recovery time (green), 50 nM PKC412 for 24 h followed by PBS wash and 16 h recovery time in the presence of 1 μM DPI. b) Bar chart representation of FACS results in a). Results are shown as relative geometric mean± SD. Statistical analysis was carried out using the student t-test ($p<0.05$ is marked with *).

Effects of $p22^{phox}$ siRNA knockdown on oxidative DNA damage in MV4-11 cells.

We showed that FLT3-ITD regulated NOX proteins *via* the stabilisation of $p22^{phox}$ subunit. Moreover, we demonstrated that specific $p22^{phox}$ siRNA knockdown reduced the level of nuclear H_2O_2, implying that $p22^{phox}$ as a component of NOX could play a role in oxidative DNA damage in these cells. In order to examine this hypothesis, we analysed 8-OHdG immunofluorescence in cells transfected with control siRNA or anti-$p22^{phox}$ siRNA. Western blot analysis revealed that level of $p22^{phox}$ protein was reduced 24 h post siRNA transfection (Figure 3.13.a). The same cells were also stained for 8-OHdG and analysed by flow cytometry (Figure 3.13.b) c). Scrambled siRNA treated cells (control) showed 30% more 8-OHdG than the cells transfected with siRNA directed against $p22^{phox}$ (Figure 3.13.b and c).

Once we established that $p22^{phox}$ was necessary for NOX-generated ROS to oxidatively damage DNA, we examined if it could also cause DNA dsbs in MV4-11 cells. The γH2AX immunofluorescence was examined using flow cytometry at 24 h post-transfection. MV4-11 cells transfected with $p22^{phox}$ siRNA were observed to have 30% less DNA dsbs than control cells (Figure 3.14.a and b).

Effects of NOX4 siRNA knockdown on H_2O_2 in MV4-11 cells

In chapter 4, we localised NOX4 to the nuclear membrane. In order to examine if NOX4 plays a role in genomic instability in FLT3-ITD expressing cells,

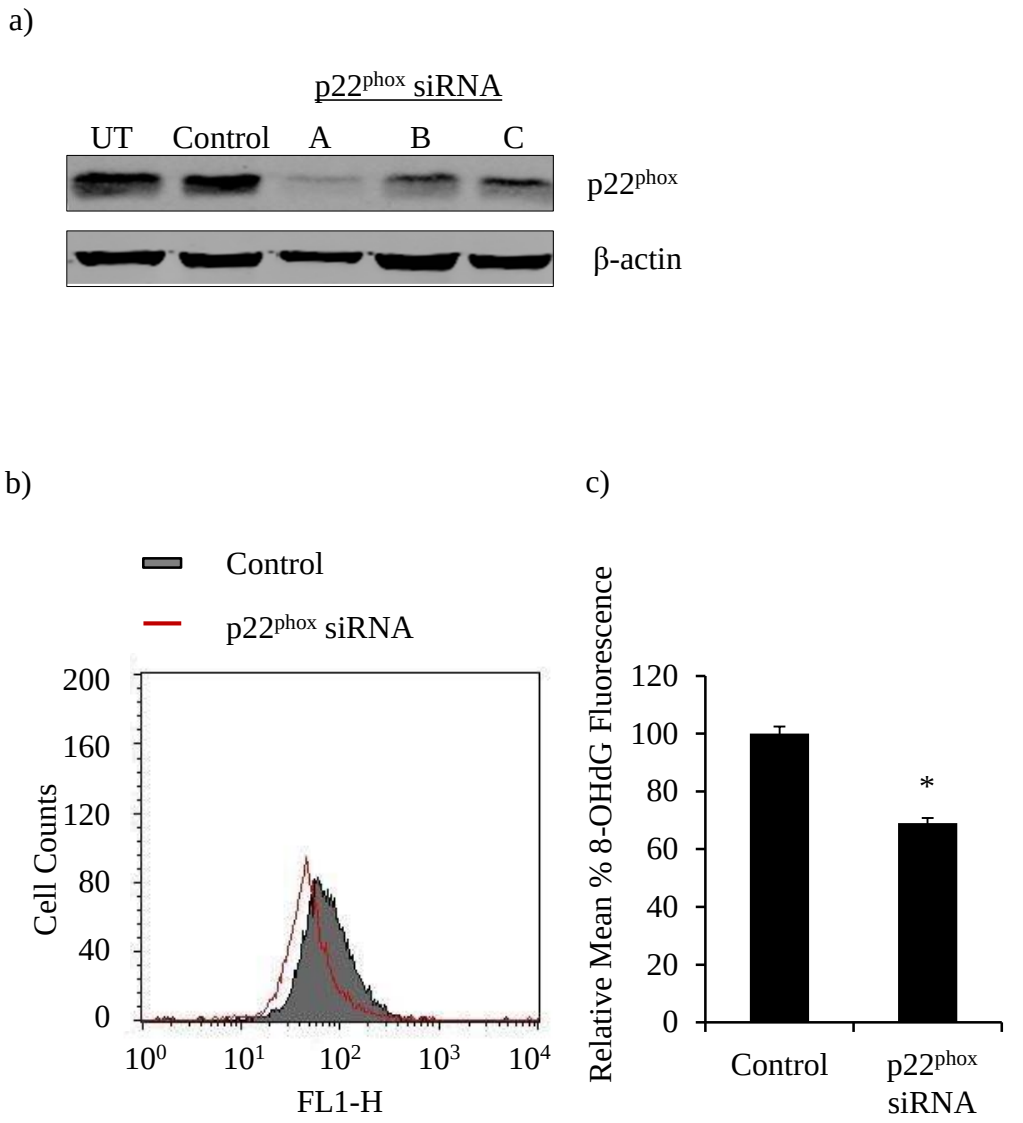

Figure 3.13. Effects of $p22^{phox}$ siRNA knockdown on oxidative DNA damage in MV4-11 cells, as measured with 8-OHdG marker. a) Western blotting analysis of $p22^{phox}$ knockdown 24 h following the nucleofection with either scrambled siRNA or $p22^{phox}$ siRNA of the indicated sequence. b) FACS analysis of relative anti-8-OHdG fluorescence of MV4-11 cells treated with scrambled siRNA (grey) or $p22^{phox}$ siRNA (red). c) Bar chart representation of FACS results in b). Results are shown as relative geometric mean± SD. Statistical analysis was carried out using the student t-test ($p<0.05$ is marked with *).

a)

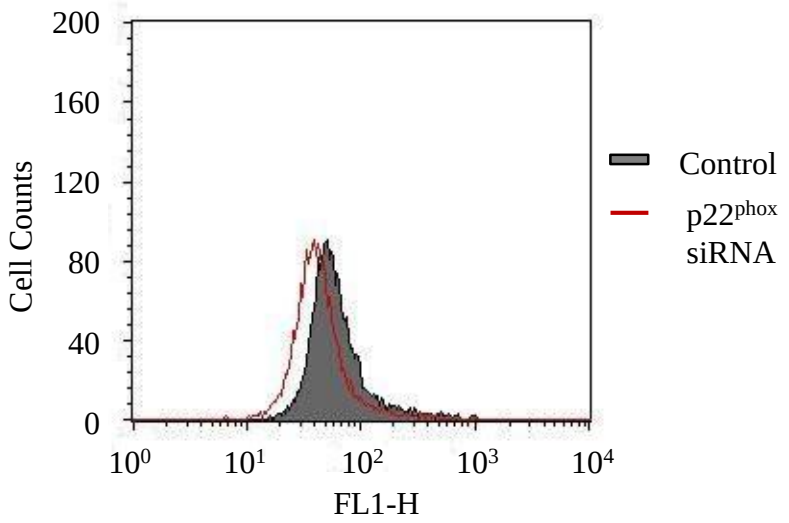

b)

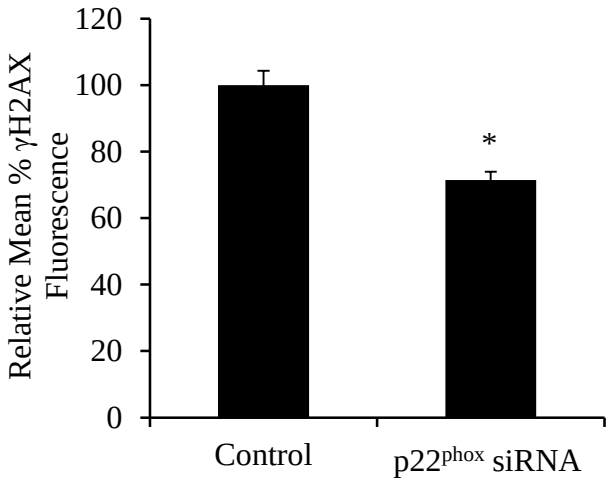

Figure 3.14. Effects of p22phox siRNA knockdown on DNA dsbs in MV4-11 cells. a) FACS analysis of relative anti-γH2AX fluorescence of MV4-11 cells treated with scrambled siRNA (grey) or p22phox siRNA (red). b) Bar chart representation of FACS results in a). Results are shown as relative geometric mean± SD. Results are representative of at least 3 independent experiments. Statistical analysis was carried out using the student t-test ($p<0.05$ is marked with *).

we utilised an siRNA knockdown approach. Firstly, using Western blotting we confirmed a successful NOX4 knockdown. While siRNA sequences A and C did not seem to change the NOX4 expression at the protein level, NOX4 siRNA B significantly reduced the amount of NOX4 protein in these cells (Figure 3.15.a).

Secondly, we examined if NOX4 was generating H_2O_2 in MV4-11 cells. MV4-11 cells transfected either with scrambled siRNA or NOX4-targeted siRNA were stained with the H_2O_2-probe, PO1. Flow cytometric analysis revealed that cells with NOX4 protein knocked down generated 30% less H_2O_2 than the control cells (Figure 3.15.b and c).

To demonstrate that NOX4 was the NOX isoform responsible of redox changes in the nucleus, we employed the NucPE1 probe on the siRNA treated cells. Following NOX4 protein down-regulation MV4-11 cells produced about 20% less of the nuclear H_2O_2 than the scrambled siRNA treated cells, as analysed using flow cytometry (Figure 3.16.a and b).

Effects of NOX4 siRNA knockdown on DNA dsbs in MV4-11 cells.

Once we established that NOX4 was localised to the nuclear membrane and was responsible for changes in the level of H_2O_2 in the nucleus, we examined if NOX4-generated H_2O_2 could cause DNA damage in MV4-11 cells. This could link NOX4 activity to genomic instability in AML cells. Using flow cytometry, we examined the number of DNA dsbs, 24 h post-transfection. We demonstrated that

NOX4 siRNA knockdown led to approximately 20% reduction in the number of DNA dsbs in FLT3-ITD expressing MV4-11 cells (Figure 3.17).

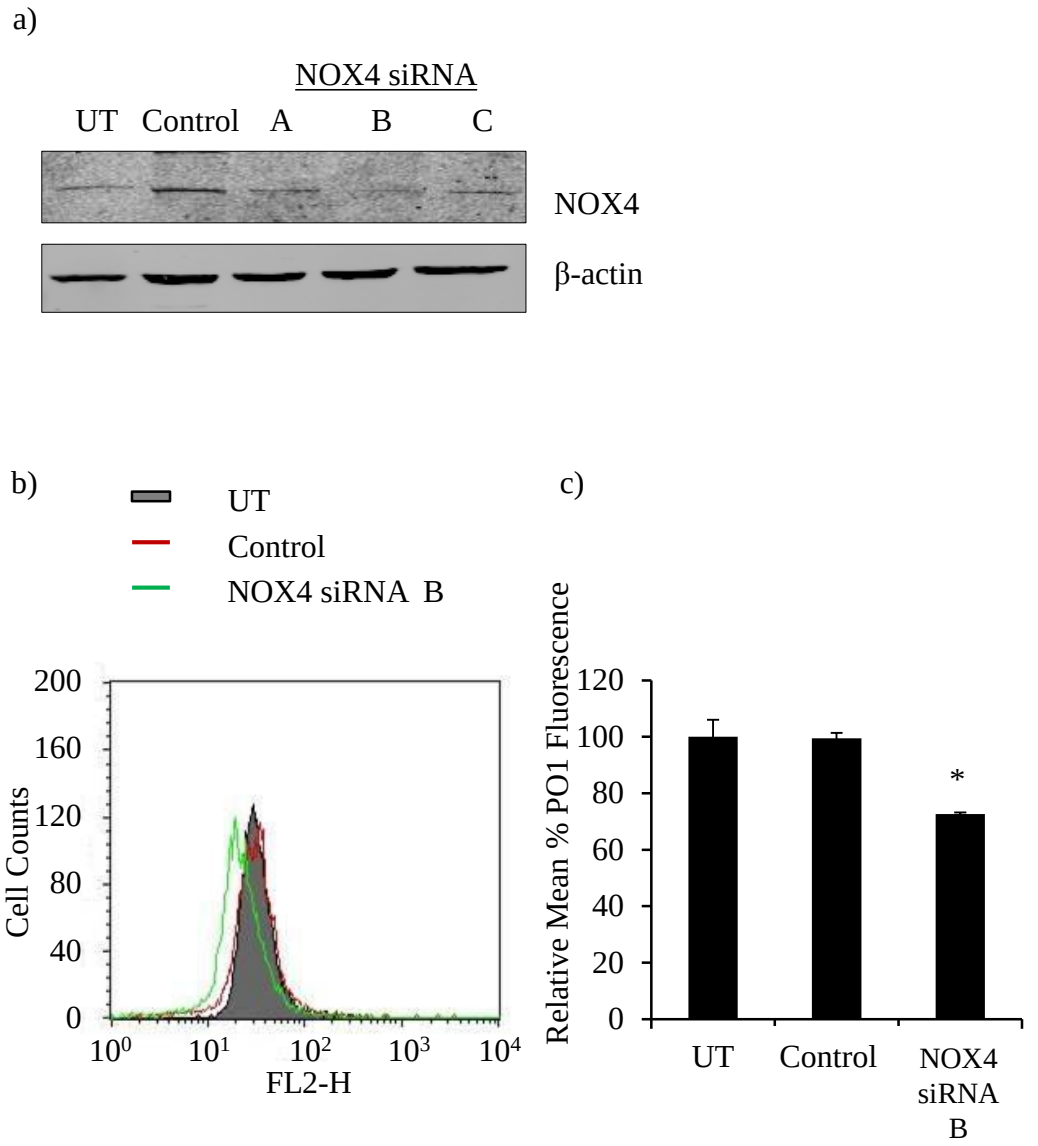

Figure 3.15. Effects of NOX4 siRNA knockdown on endogenous H_2O_2 in MV4-11 cells. a) Western blotting analysis of NOX4 knockdown 24 h following the nucleofection with either scrambled siRNA (Control) or NOX4 siRNA of the indicated sequence. b) FACS analysis of relative PO1 fluorescence of MV4-11 cells: untreated (grey) with scrambled siRNA (red) or NOX4 siRNA (green). c) Bar chart representation of FACS results in b). Results are shown as relative geometric mean± SD. Statistical analysis was carried out using the student t-test ($p<0.005$ is marked with *).

a)

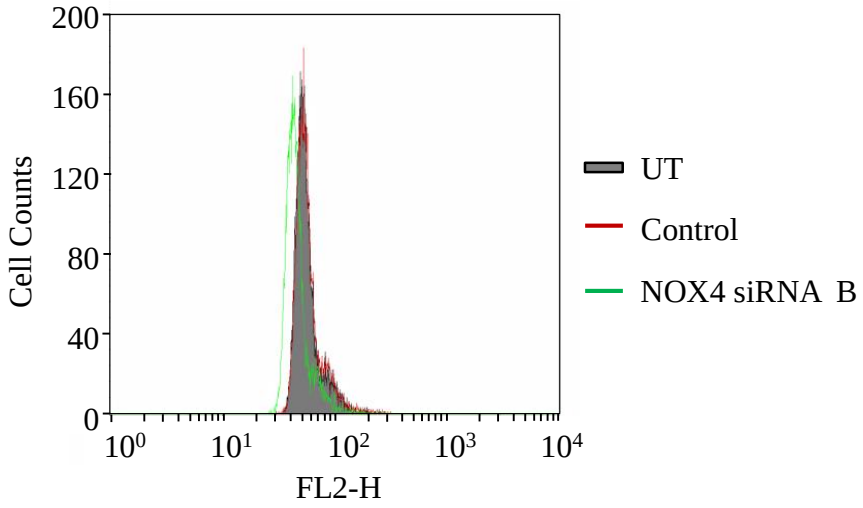

b)

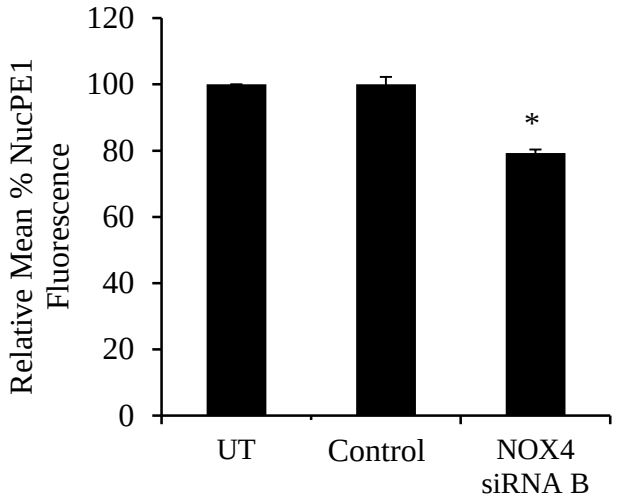

Figure 3.16. Effects of NOX4 siRNA knockdown on nuclear H_2O_2 in MV4-11 cells. a) FACS analysis of relative NucPE1 fluorescence of MV4-11 cells: untreated (grey), treated with scrambled siRNA (Control; red) or NOX4 siRNA (green). b) Bar chart representation of FACS results in a). Results are shown as relative geometric mean± SD. Statistical analysis was carried out using the student t-test ($p<0.005$ is marked with *).

a)

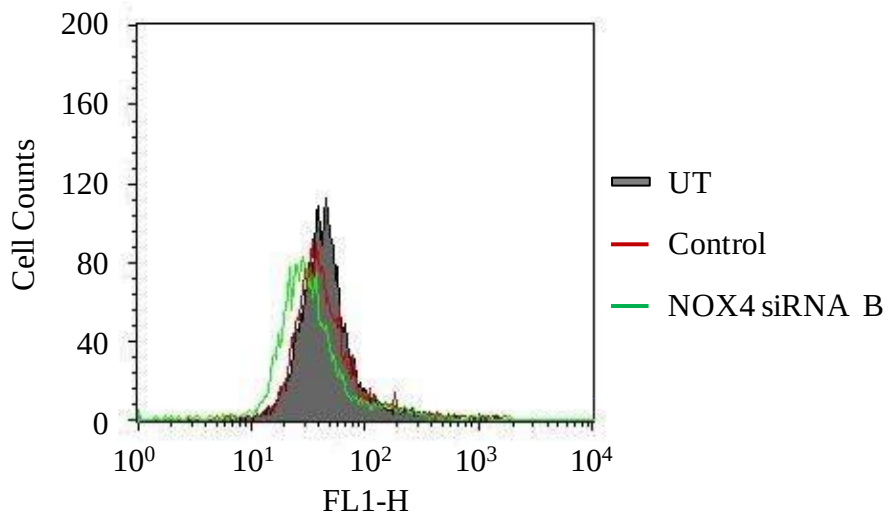

b)

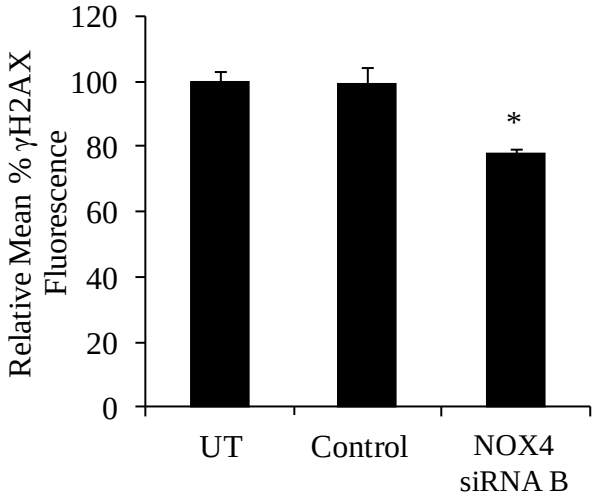

Figure 3.17. Effects of NOX4 siRNA knockdown on DNA dsbs in MV4-11 cells. a) FACS analysis of relative anti-γH2AX fluorescence of MV4-11 cells: untreated (grey), treated with scrambled siRNA (red) or NOX4 siRNA (green). b) Bar chart representation of FACS results in a). Results are shown as relative geometric mean± SD. Statistical analysis was carried out using the student t-test ($p<0.005$ is marked with *).

$p22^{phox}$ expression in 32D/FLT3-WT or 32/FLT3-ITD cells

Steady state levels of $p22^{phox}$ were dramatically reduced following FLT3 inhibition in MV4-11 cells and MOLM-13 cell lines (Figure 2.2/2.3). In order to demonstrate this in 32D cells, we compared $p22^{phox}$ protein levels in cells expressing FLT3-WT, FLT3-ITD and following PKC412 inhibition or IL-3 starvation. Western blotting analysis of $p22^{phox}$ revealed that the cells transfected with FLT3-ITD possessed a higher level of $p22^{phox}$ than their wild type counterparts (Figure 3.18), which expressed very low levels of the protein. Similarly to MV4-11 cells, the inhibition of FLT3 receptor with PKC412 over 24 h caused a partial decrease in $p22^{phox}$ expression. IL-3 starvation resulted in a slight down-regulation of $p22^{phox}$. This is not surprising as IL-3 has been shown to activate the AKT pathway, which in turn has been implicated in stimulating $p22^{phox}$ expression (Songyang et al., 1997, Edderkaoui et al., 2011).

Effects of $p22^{phox}$ knockdown on cellular H_2O_2 in 32D cells transfected with FLT3-WT or FLT3-ITD.

We concluded that NOX4/$p22^{phox}$ complex was producing DNA-damaging H_2O_2 in FLT3-ITD expressing MV4-11 cells. How much of this NOX-generated H_2O_2 was stimulated by FLT3-ITD signalling was still not clear. Specific $p22^{phox}$ siRNA knockdown in 32D cells, allowed us to investigate the effects of $p22^{phox}$-dependent NOX isoforms in cells expressing wild type or mutant FLT3.

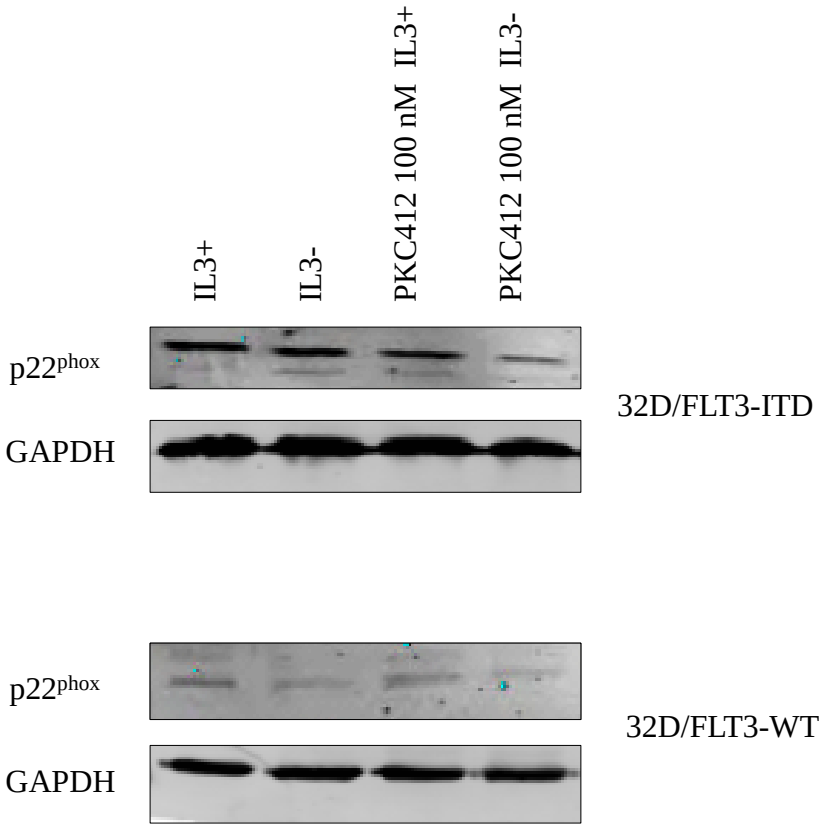

Figure 3.18. $p22^{phox}$ expression in 32D cells, transfected with FLT3-WT or FLT3-ITD following IL-3 starvation or FLT3 inhibition. Western blotting analysis of $p22^{phox}$ protein expression, followed by no treatment (IL-3+), 16 h IL-3 starvation (IL-3-), PKC412 100 nM without IL-3 starvation (PKC412 100 nM IL3+), or PKC412 100 nM with IL-3 starvation (PKC412 100 nM IL3-) in 32D cells transfected with FLT3-WT or FLT3-ITD. GAPDH was used as a loading control.

In order to confirm the siRNA knockdown, $p22^{phox}$ protein levels were analysed using Western Blotting 24 h post siRNA transfection (Figure 3.19.a). This analysis revealed that $p22^{phox}$ siRNA sequence B was successful at down-regulating $p22^{phox}$. In the next step, using PO1 we decided to measure endogenous H_2O_2 in 32D/FLT3-WT treated either with scrambled siRNA or $p22^{phox}$ siRNA. We did not observe any differences between control and $p22^{phox}$ depleted 32D cells transfected with FLT3-WT (Figure 3.19.b).

$p22^{phox}$ effects on production of H_2O_2 were then investigated in 32D cells expressing FLT3-ITD. Firstly, Western blotting confirmed protein depletion 24 h post transfection (Figure 3.20.a). Cellular H_2O_2 was reduced by over 20% in cells treated with $p22^{phox}$ siRNA in comparison to control treated cells (Figure 3.20.b). This result confirmed $p22^{phox}$-mediated effects occurring downstream of activated mutant FLT3.

Effects of $p22^{phox}$ knockdown on DNA dsbs in 32D/FLT3-ITD and 32D/FLT3-WT cells.

In the previous figures we showed that $p22^{phox}$ is a key partner driving ROS formation downstream of FLT3-ITD signalling. In order to examine if $p22^{phox}$-driven H_2O_2 contributes to the difference in the level of DNA damage between FLT3-WT or FLT3-ITD expressing 32D cells, we analysed γH2AX immunofluorescence of post-$p22^{phox}$-transfected cells. $p22^{phox}$-depleted FLT3-ITD-expressing 32D cells possessed 20% less DNA dsbs than their control counterparts (Figure 3.21.a). Moreover, analogous $p22^{phox}$ knockdown did not affect DNA dsbs in

a)

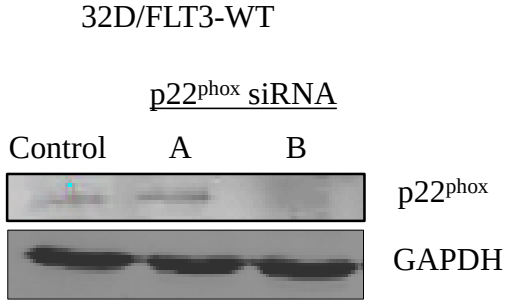

b)

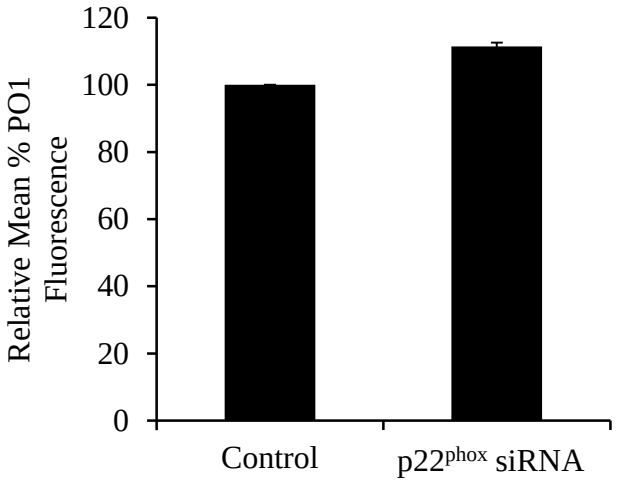

Figure 3.19. Effects of $p22^{phox}$ knockdown on cellular H_2O_2 in 32D cells transfected with FLT3-WT. a) Western blotting analysis of $p22^{phox}$ protein expression at 24 h followed the siRNA nucleofection of 32D cells. Control cells were treated with scrambled siRNA. GAPDH was used a loading control. b) Bar chart representation of flow cytometric analysis of relative mean % PO1 fluorescence, 24 h following the $p22^{phox}$ siRNA knockdown. Results are shown as relative geometric mean± SD.

a)

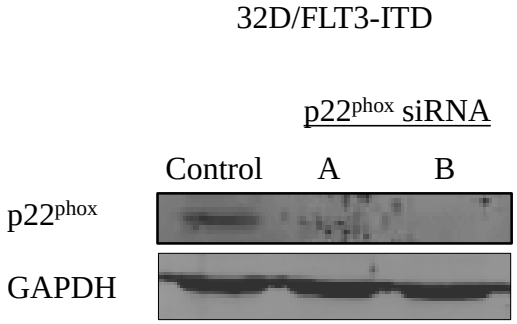

b)

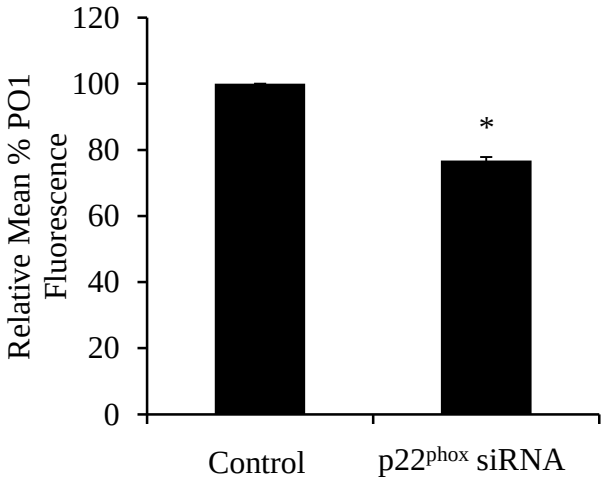

Figure 3.20. Effects of $p22^{phox}$ knockdown on cellular H_2O_2 in 32D cells transfected with FLT3-ITD. a) Western blotting analysis of $p22^{phox}$ protein expression 24 h followed the siRNA nucleofection of 32D cells. Control cells were treated with scrambled siRNA. GAPDH was used a loading control. b) Bar chart representation of flow cytometric analysis of relative mean % PO1 fluorescence, 24 h following the $p22^{phox}$ siRNA knockdown. Results are shown as relative geometric mean± SD. Statistical analysis was carried out using the student t-test ($p<0.005$ is marked with *).

a)

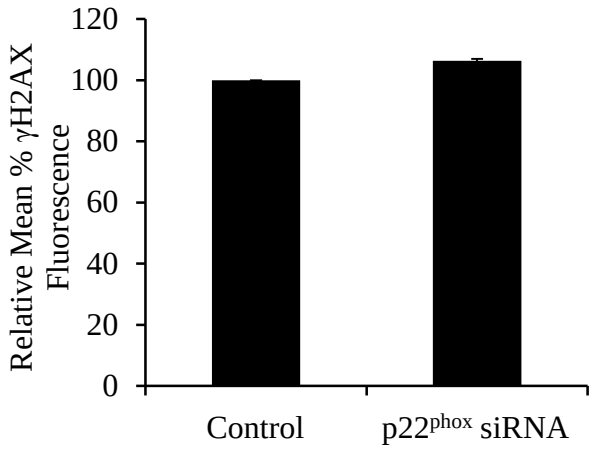

b)

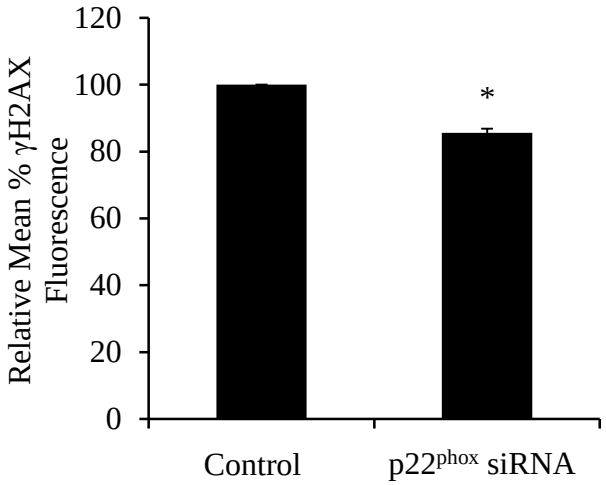

Figure 3.21. Effects of $p22^{phox}$ knockdown on DNA dsbs in 32D cells transfected with FLT3-ITD or with FLT3-WT. a) Bar chart representation of flow cytometric analysis of relative mean γH2AX fluorescence, 24 h following the $p22^{phox}$ siRNA knockdown in 32D/FLT3-WT. b) Bar chart representation of flow cytometric analysis of relative mean γH2AX fluorescence, 24 h following the $p22^{phox}$ siRNA knockdown in 32D/FLT3-ITD. Results are shown as relative geometric mean± SD. Statistical analysis was carried out using the student t-test ($p<0.005$ is marked with *).

32D cells expressing FLT3-WT (Figure 3.21.b).

Effects of NOX4 siRNA knockdown on cellular H_2O_2 in 32D cells, transfected with FLT3-ITD.

So far we have established that FLT3-ITD stabilised $p22^{phox}$, which through NOX activation mediated DNA damage formation. This could possibly lead to genomic instability in these cells. MV4-11 cells were shown to express NOX4 at their nuclear membrane. Knockdown of NOX4 in these cells led to a reduction in nuclear H_2O_2 and DNA dsbs. In order to examine NOX4 function in murine 32D/FLT3-ITD cells, we next decided to knock down NOX4 using siRNA transfection. Treatment with the siRNA sequence against murine NOX4 resulted in a decrease in a NOX4 steady protein level (Figure 3.22.a). 32D/FLT3-ITD cells depleted of NOX4 were shown to possess 30% less endogenous H_2O_2, as measured with PO1 (Figure 3.22.b). Moreover, γH2AX fluorescence of the NOX4 siRNA treated cells revealed that the number of DNA dsbs was decreased by over 30% in relation to the scrambled siRNA treated cells (Figure 3.22.c). Unexpectedly, NOX4 knockdown (30%) led to a larger effect than $p22^{phox}$ knockdown (20%).

Effects of NOX1 siRNA knockdown on cellular H_2O_2 in 32D cells, transfected with FLT3-ITD.

We established an association between FLT3-ITD, $p22^{phox}$ and NOX4 in contributing to genomic instability in FLT3-ITD-expressing cells. However, since FLT3-ITD regulates NOX activity through $p22^{phox}$ stabilisation, it should be

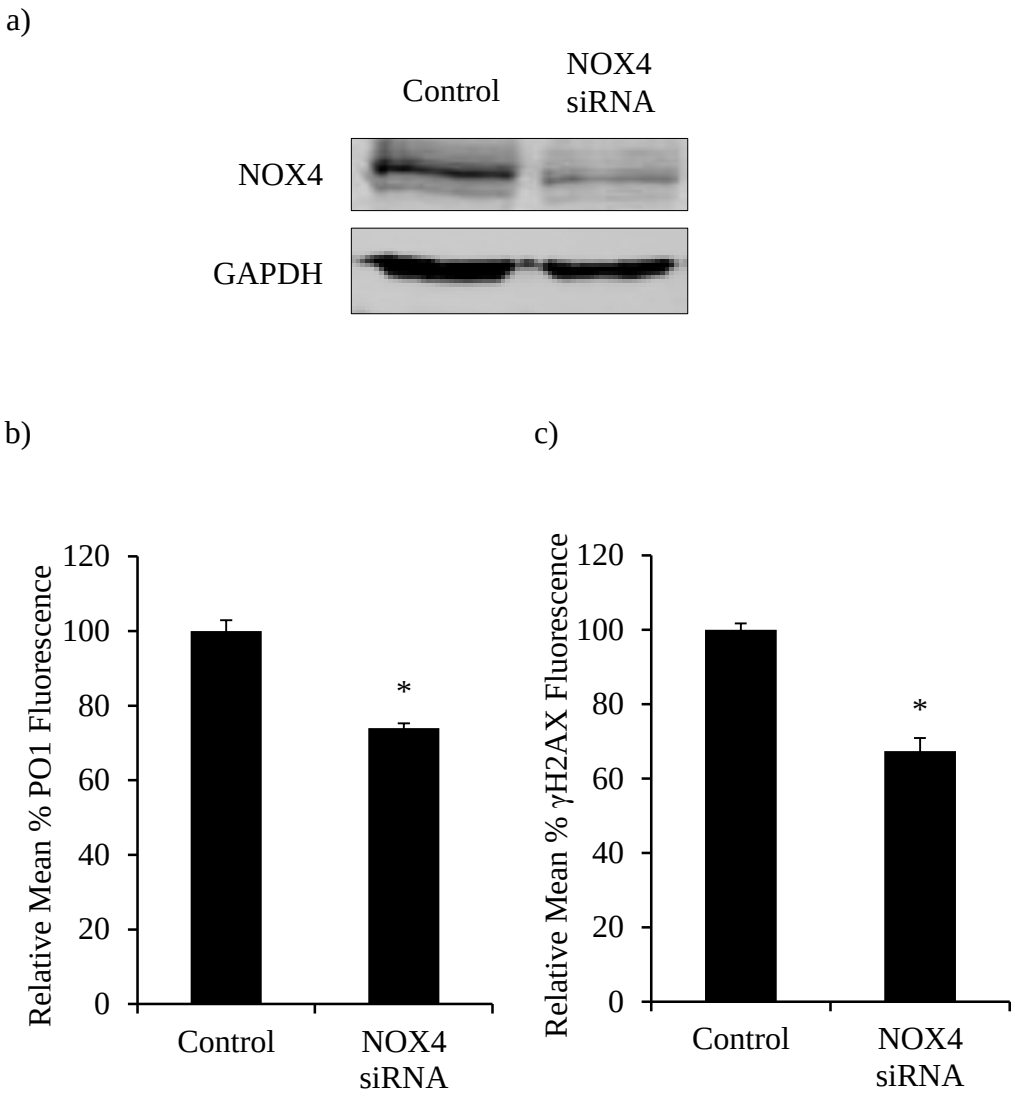

Figure 3.22. Effects of NOX4 siRNA knockdown on cellular H_2O_2 in 32D cells, transfected with FLT3-ITD. a) Western blotting analysis of NOX4 expression, 24 h following the siRNA nucleofection. GAPDH was used as a loading control. b) Bar chart representation of flow cytometric analysis of relative mean % PO1 fluorescence, 24 h following the NOX4 siRNA knockdown in 32D/FLT3-ITD. c) Bar chart representation of flow cytometric analysis of relative mean % γH2AX fluorescence, 24 h following the NOX4 siRNA knockdown in 32D/FLT3-ITD. Results are shown as relative geometric mean± SD. Statistical analysis was carried out using the student t-test ($p<0.005$ is marked with *).

investigated if other $p22^{phox}$-dependent NOX isoforms also coul play a role in genomic instability in these cells. Myeloid cells have previously been shown to express NOX1, NOX2, NOX4 and NOX5 (Naughton et al., 2009, Lee et al., 2010). However, murine 32D cells do not have the Nox5 gene. NOX1 and NOX2 are $p22^{phox}$-dependant as well as NOX4, thus it is possible that they could also play a role in FLT3-ITD-induced genomic instability. In order to study possible NOX1 effects in FLT3-ITD AML, we specifically knocked down NOX1 using anti-NOX1 siRNA (Figure 3.23.a). Endogenous level of H_2O_2 was measured using PO1, between control cells and NOX1 siRNA treated cells. The NOX1-depleted cells had the same level of H_2O_2 as the control treated cells (Figure 3.23.b). Furthermore, γH2AX fluorescence was not altered by NOX1 down-regulation (Figure 3.23.c).

Effects of NOX2 siRNA knockdown on cellular H_2O_2 in 32D cells, transfected with FLT3-ITD.

The last $p22^{phox}$-dependant NOX isoform expressed in 32D cells that we did not investigate was NOX2. This isoform has been previously implicated, along with NOX4, to regulate growth and migration of FLT3-ITD expressing cells (Reddy et al., 2011). The NOX2 siRNA knockdown was confirmed 24 h post transfection by Western blotting (Figure 3.24.a). Comparison of the endogenous H_2O_2 levels between control and NOX2 siRNA treated cells was carried out using PO1. The analysis of PO1 fluorescence revealed 20% difference between NOX2-depleted and untreated cells (Figure 3.24.b). In order to investigate the

a)

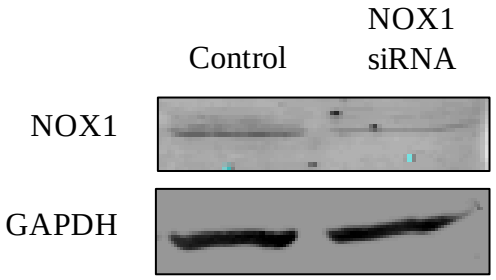

b)

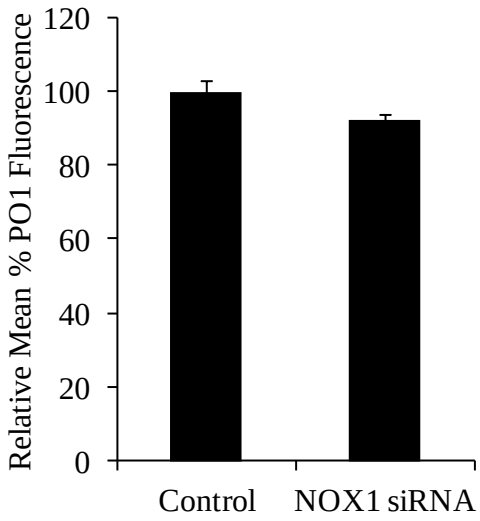

c)

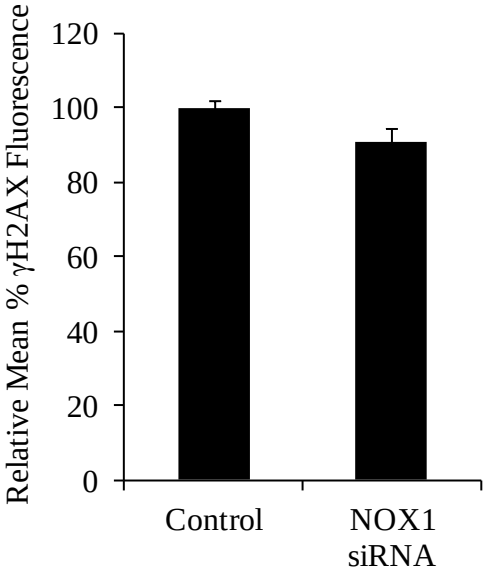

Figure 3.23. Effects of NOX1 siRNA knockdown on cellular H_2O_2 in 32D cells, transfected with FLT3-ITD. a) Western blotting analysis of NOX1 expression, 24 h following the siRNA nucleofection. GAPDH was used as a loading control. b) Bar chart representation of flow cytometric analysis of relative mean PO1 fluorescence, 24 h following the NOX1 siRNA knockdown in 32D/FLT3-ITD. c) Bar chart representation of flow cytometric analysis of relative mean γH2AX fluorescence, 24 h following the NOX1 siRNA knockdown in 32D/FLT3-ITD. Results are shown as relative geometric mean± SD. Statistical analysis was carried out using the student t-test ($p<0.005$ is marked with *).

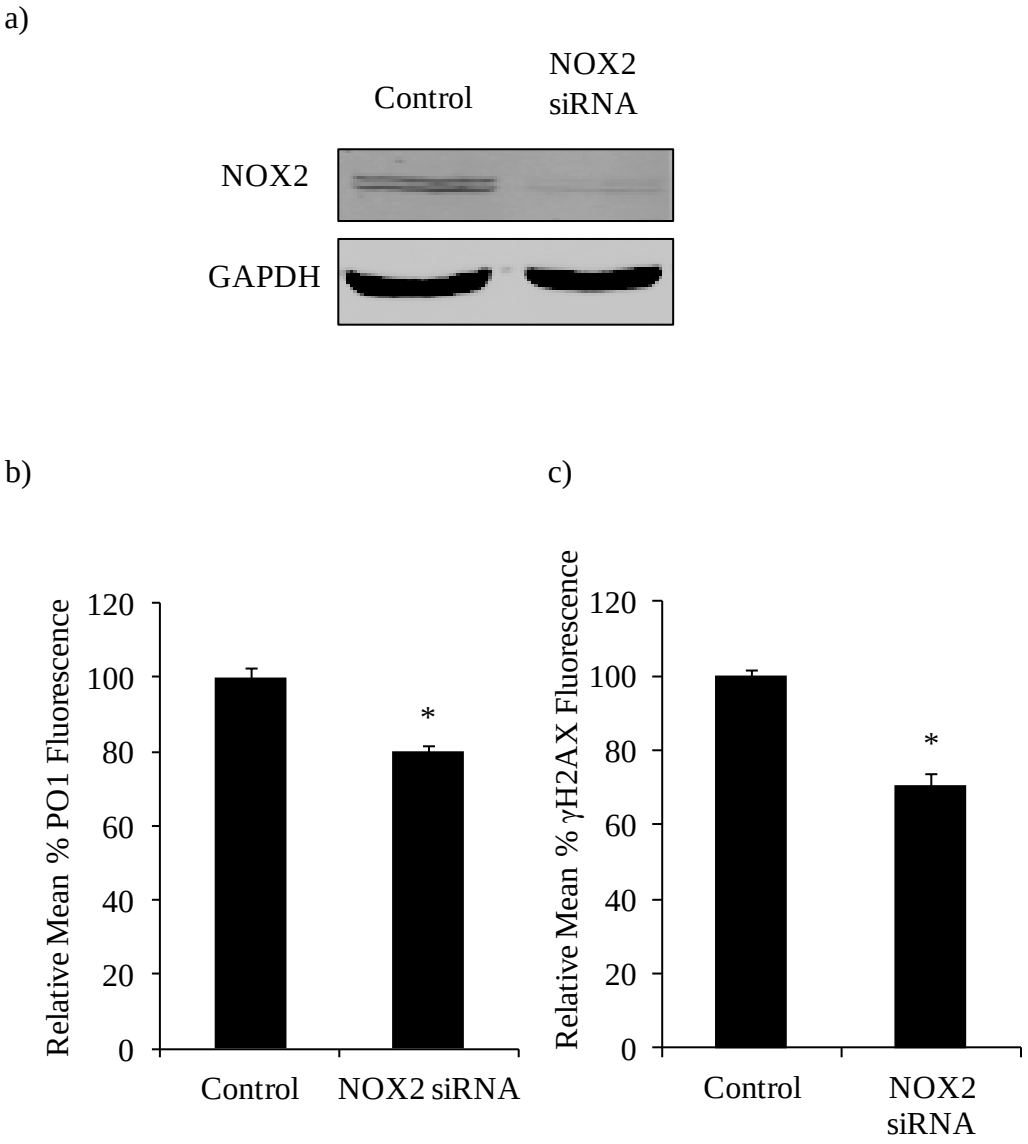

Figure 3.24. Effects of NOX2 siRNA knockdown on cellular H_2O_2 in 32D cells, transfected with FLT3-ITD. a) Western blotting analysis of NOX2 expression, 24 h following the siRNA nucleofection. GAPDH was used as a loading control. b) Bar chart representation of flow cytometric analysis of relative mean PO1 fluorescence, 24 h following the NOX2 siRNA knockdown in 32D/FLT3-ITD. c) Bar chart representation of flow cytometric analysis of relative mean γH2AX fluorescence, 24 h following the NOX2 siRNA knockdown in 32D/FLT3-ITD. Results are shown as relative geometric mean± SD. Statistical analysis was carried out using the student t-test ($p<0.005$ is marked with *).

association between NOX2 and genomic instability in FLT3-ITD mutated AML, we examined DNA dsbs following NOX2 knockdown. Corresponding to the number of DNA dsbs, γH2AX fluorescence was reduced by over 30% in the cells treated with NOX2 siRNA in relation to scrambled siRNA treated cells (Figure 3.24.c).

FLT3 ligand (FL) effects on cellular and nuclear H_2O_2, and DNA dsbs in 32D/FLT3-WT cells.

FLT3-ITD has been reported to induce differential signalling events compared to activated FLT3-WT. For example, in contrast to stimulated FLT3-WT, FLT3-ITD causes a strong activation of STAT5 (Choudhary et al., 2009). This may be a result of the distinct subcellular localisations of the two (Choudhary et al., 2009). Given that constitutively active FLT3-ITD stimulates generation of ROS and DNA damage, we investigated if the activated FLT3-WT had a similar effect. Following 16 h incubation of the FL with 32D cells transfected with FLT3-WT, we observed an increase in $p22^{phox}$ expression (Figure 3.25.a b). Moreover, this was followed by the 44% increase in the generation of H_2O_2, as measured by PO1. This suggested that activated FLT3-WT regulated ROS-generation in a similar manner to FLT3-ITD.

In order to investigate FL-driven damaging effects of H_2O_2 in 32D/FLT3-WT cells, we investigated if H_2O_2 affects the redox state of the nucleus in these cells. Nuclear H_2O_2 was shown to increase by 20% following 16 h of FL stimulation as measured by NucPE1 fluorescence (Figure 3.26.a). This was also followed by

a)

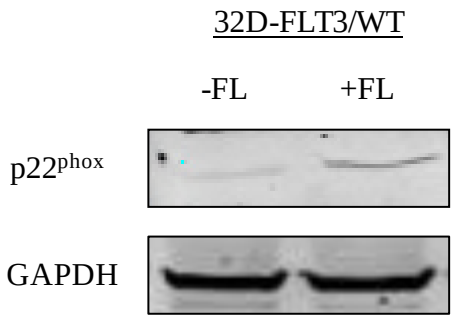

b)

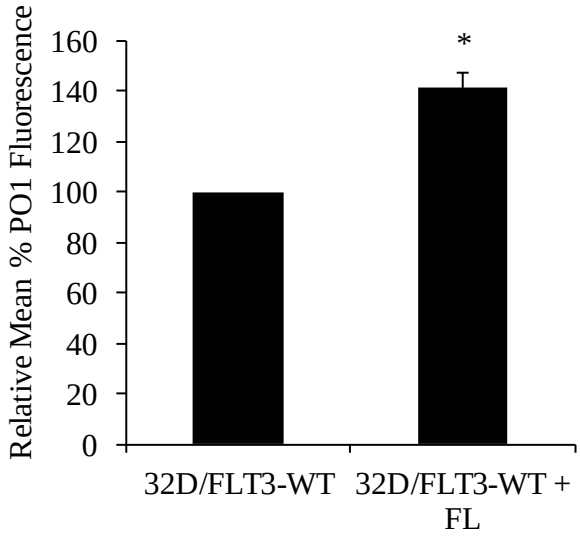

Figure 3.25. Stimulation of 32D cells expressing wild type FLT3 (FLT3-WT) with FLT3 ligand (FL) causes an increase in $p22^{phox}$ expression, increase in cellular H_2O_2. a) Western blotting of analysis of expression of $p22^{phox}$ following FLT3-WT stimulation with FL for 16 h. GAPDH was used as a loading control. b) Flow cytometric analysis of total cellular H_2O_2 as measured with PO1. The bar charts show relative mean fluorescence of cells treated expressed as a percentage of control. The mean is representative of three independent experiments. The asterisk indicates statistically significant difference ($p<0.05$) as analyzed by Student t-test. The error bars represent ±SD.

a)

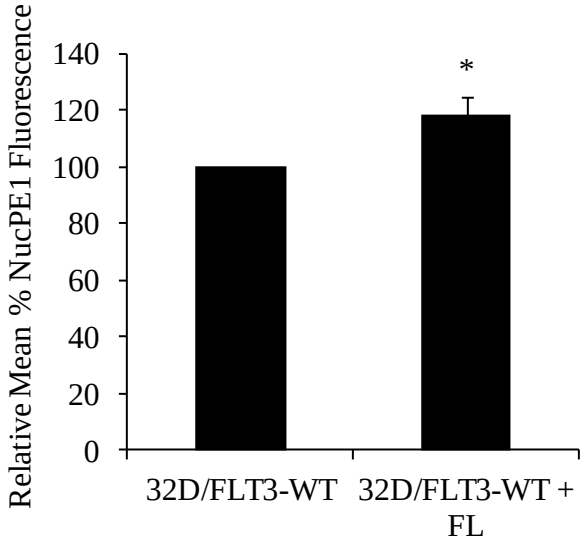

b)

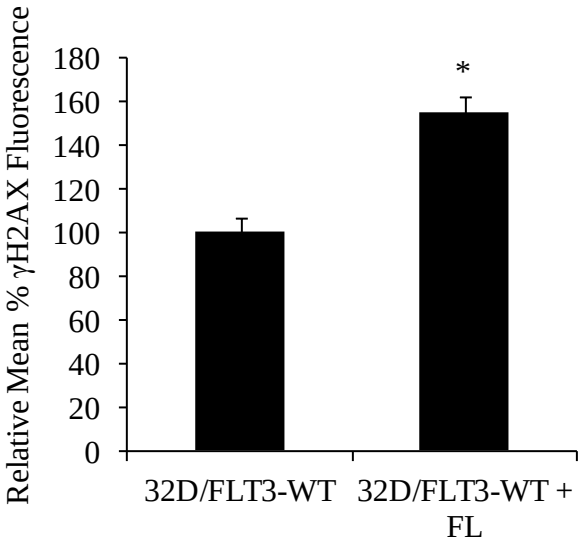

Figure 3.26. Stimulation of 32D cells expressing wild type FLT3 (FLT3-WT) with FLT3 ligand (FL) causes an increase in nuclear H_2O_2 and in turn an increase in DNA dsbs. a) Bar chart representing a flow cytometric analysis of nuclear H_2O_2 as measured with NucPE1. b) Flow cytometric analysis of DNA dsbs, measured with γH2AX following the 16 h treatment with FL. The bar charts show relative mean fluorescence of cells treated expressed as a percentage of control. The mean is representative of three independent experiments. The asterisk indicates statistically significant difference ($p<0.05$) as analyzed by Student t-test. The error bars represent ±SD.

over 50% increase in the number of dsbs, demonstrating the DNA damaging properties of FLT3-induced H_2O_2 (Figure 3.26.b).

Discussion

The aim of this work was to investigate the NOX-driven DNA damage in FLT3-ITD mutated AML cells. In previous chapters, we showed that FLT3-ITD stimulated H_2O_2 generation from NOX isoforms localised at the ER. It was also demonstrated that FLT3-ITD stimulated NOX by $p22^{phox}$ stabilisation. Specific $p22^{phox}$ siRNA knockdown resulted in the attenuation of ROS accumulation at the ER and in the nucleus.

AML is an aggressive disease that is the most common type of acute leukaemia in adults. Even though the number of patients responding to initial therapy is growing, unfortunately the disease relapses in almost all cases unless it is eliminated by the additional therapy (Roboz, 2012, Peloquin et al., 2013).

FLT3-ITD is the most common mutation in AML. Patients who are hemizygous for FLT3-ITD mutation are often refractory to induction chemotherapy (Whitman et al., 2001). Moreover FLT3-ITD carrying patients relapse more often and quicker than patients negative for this mutation (Stirewalt and Radich, 2003). This makes FLT3 an attractive target in the treatment of AML.

Genomic instability is an intrinsic feature of all cancers. It has been also proposed that genomic instability is a requirement for cancer progression (Sieber et al., 2003). Leukaemic oncogenes such as RAS, BCR-ABL and FLT3-ITD have been shown to stimulate genomic instability (Weyemi et al., 2012, Sallmyr et al., 2008b). However, the exact mechanism of this induction of genotoxic stress is not clear.

Sallmyr *et al.* has already shown that expression of FLT3-ITD leads to an increase in the ROS level (Sallmyr et al., 2008a). However, in this thesis, we demonstrated the specific effects of FLT3-ITD mutation on the generation of H_2O_2. It is important to distinguish between various types of ROS when studying their signalling/damaging effects. It is known that due to their specific oxidation chemistry, ROS molecules can induce different signalling events (D'Autréaux and Toledano, 2007). Moreover, using pharmacological inhibition of NOX or FLT3, H_2O_2 accumulation was attenuated in 32D/FLT3-ITD cells. This was not seen in 32D/FLT3-WT cells, implying that NOX enzymes are involved in H_2O_2 formation only downstream of mutated FLT3.

In order for ROS to damage DNA, they must diffuse from their site of generation to the nucleus. Here, we showed, using NucPE1 staining that FLT3-ITD mutation leads to a direct alteration in the redox status of the nucleus. The difference in the nuclear H_2O_2 was substantially smaller than the difference in the total H_2O_2. This could mean that only some of the H_2O_2 actually reaches the nucleus. Alternatively, the sensitivity of the PO1 probe that was used to investigate total H_2O_2 seems to be much greater than the sensitivity of NucPE1, a nuclear H_2O_2 probe (Dickinson et al., 2011b). In order to examine if mitochondria were responsible for the differences in H_2O_2 levels in transfected 32Ds, we investigated the mitochondrial ROS. When we compared the mitochondrial ROS levels in 32D/FLT3-ITD and 32D/FLT3-WT, we saw no significant difference between them.

Following the finding of FLT3-induced H_2O_2 affecting the nucleus, we investigated if this H_2O_2 could lead to DNA damage and thus to genomic instability

in these cells. We showed using an over-expression of FLT3-WT or FLT3-ITD in 32D cells and patient-derived HL-60 (FLT3-WT) and MV4-11 (FLT3-ITD), that cells carrying a mutated FLT3-ITD generate a higher level of H_2O_2 and DNA dsbs, as measured by γH2AX. The extent of FLT3-ITD induced DNA damage agrees with previously published work by Sallmyr *et al.* (Sallmyr et al., 2008a). DNA dsbs are the most toxic DNA damage lesions that can lead to a variety of mutations. Therefore, generation of DNA dsbs is a prominent mechanism of genomic instability. Interestingly, pharmacological inhibition of NOX with DPI or FLT3 with PKC412 led to reduction in the number of DNA dsbs, suggesting that DNA damage can be quickly repaired following withdrawal of the damaging element. This gives NOX and FLT3 inhibitors a therapeutic opportunity with respect to the inhibition of genomic instability which could possibly slow down progression of AML.

Although pharmacological inhibition of NOX is desirable from the therapeutic point of view, it carries an element of uncertainty regarding the specificity of the inhibitor. Even though DPI is the most commonly used NOX inhibitor, it has been shown to have many off-target effects (Aldieri et al., 2008). In order to investigate which NOX isoform is the actual molecular source of H_2O_2 stimulated by FLT3-ITD, we used siRNA knockdown approach. In the previous chapter, we validated that inhibition of FLT3-ITD with PKC412 led to down-regulation of $p22^{phox}$. Therefore, NOX enzymes that are expressed in myeloid cells and can be activated by $p22^{phox}$ are NOX1, 2 and 4. The siRNA knockdown of either $p22^{phox}$, NOX2 or NOX4 led to the reduction of cellular H_2O_2, nuclear H_2O_2 and DNA damage in FLT3-ITD expressing MV4-11 and 32D cells. Since activities of

NOX2 and NOX4 are dependent on $p22^{phox}$ it would be expected that the magnitude of the effect following $p22^{phox}$ knockdown would result in twice as much H_2O_2 as either of the NOX knockdowns. However this was not observed in 32D cells. In fact, NOX4 knockdown had actually larger effects suggesting that possibly NOX4 could be operating independently of $p22^{phox}$.

Nonetheless, to our knowledge, this is the first report of NOX enzymes functioning as stimulants of genomic instability in AML. Subsequently to our results, NOX4 has been implicated in the generation of nuclear H_2O_2 in genomically unstable MDS (Guida et al., 2014). Similarly, the mechanism of NOX4-generated release of H_2O_2 in/to the nucleus has been demonstrated in different cancers and other diseases (Hajas et al., 2013, Kuroda et al., 2005, Spencer et al., 2011, Weyemi et al., 2012). For instance, in cardiomyocytes, NOX4-produced H_2O_2 was also observed to specifically oxidise nuclear proteins e.g. HDAC (Matsushima et al., 2013). Also, NOX4, localised in the perinuclear space was also the source of nuclear superoxide generation in hepatocytes (Spencer et al., 2011). Interestingly, exposure of mice to ionising radiation (IR) increased the expression of NOX4 in the haematopoietic stem cells (Wang et al., 2010, Brandts et al., 2005b). The inhibition of NOX in the IR treated mice, attenuated the ROS and DNA damage, associated with the IR (Pazhanisamy et al., 2011). Alveolar epithelial cells have been reported to possess nuclear H_2O_2-generating NOX4 that was suggested to regulate 8-oxoguanine DNA-glycosylase-1, a key enzyme in the repair of oxidatively modified DNA (Hajas et al., 2013). Interestingly, both of these groups suggested Rac1GTPase interaction with NOX4 that has been previously shown not to affect NOX4 activity.

Although NOX2 has been shown to have a potent mitogenic activity in AML cell lines and patient samples, it was quite surprising that it plays a role in genomic instability (Reddy et al., 2011, Hole et al., 2013). To this date, there is no clear evidence of NOX2 initiating DNA damage.

We demonstrated in the previous chapter that inhibition of FLT3-ITD signalling by pharmacological inhibition leads to degradation of $p22^{phox}$ in MV4-11. Thus, we concluded that $p22^{phox}$ is a major component in the link between FLT3-ITD and NOX signalling. We also investigated these molecular interactions in 32D cells transfected with WT or ITD FLT3 oncogene. As expected, FLT3-ITD expressing 32D cells expressed more $p22^{phox}$ than FLT3-WT. Moreover, siRNA knockdown of $p22^{phox}$ led to a decrease in H_2O_2 or DNA damage only in 32D/FLT3-ITD cells. Also FLT3 inhibition in 32D/FLT3-ITD cells was followed by the degradation of $p22^{phox}$, confirming the importance of $p22^{phox}$ in FLT3 signalling in 32D cells.

Similarly, to what we see in FLT3-ITD expressing cells, H-RAS-induced increased NOX4 expression, is accompanied by the increase in nuclear H_2O_2 and DNA dsbs (Weyemi et al., 2012). Conversely, in the FLT3-ITD model, we suggest that the $p22^{phox}$ expression is essential for regulation of NOX4/2-derived ROS burst that causes DNA damage.

Constitutive activation of FLT3-ITD could suggest that FLT3-WT stimulated with FLT3 ligand (FL) should have analogous signalling to that of FLT3-ITD. This appears to be true for the majority of signalling events driven by phosphorylated FLT3. However, while FLT3-ITD stimulates phosphorylation of STAT5, activated

FLT3-WT does not have any effect on phosphorylation status of this potent transcription factor (Choudhary et al., 2009). Therefore, we examined if accumulation of $p22^{phox}$ also occurs in 32D/FLT3-WT cells treated with FL. FL-activated FLT3-WT signalling resulted in an increase in $p22^{phox}$ expression, an increase in total H_2O_2, followed by accumulation of DNA damage. From a clinical point of view, this result suggests that patients expressing FLT3-WT (70-100% AML cases) could also stimulate NOX-generated ROS, in the presence of FL. FL levels have been shown to rise rapidly following FLT3-targeted chemotherapy (Sato et al., 2011). This increase in FL could lead to FLT3-ITD-analogous redox signalling effects, where a prolonged increase in $p22^{phox}$, by activating NOX could damage DNA, leading to chemoresistance or relapse in FLT3-WT expressing patients.

While FLT3 seems an attractive target in AML, the resistance arising to FLT3 inhibitors remains a significant problem (Smith et al., 2012, Grunwald and Levis, 2013, Mizuki et al., 2000). Resistance to FLT3 inhibitors was demonstrated to be associated with mutations within the FLT3 gene (Mizuki et al., 2000, Piloto et al., 2007, Heidel et al., 2006). Therefore, it is of interest to study the mechanisms that lead to mutagenesis. 8-OHdG is one of the most persistent and mutagenic type of lesions that is another marker of oxidative damage. It was shown recently that patients in AML relapse possessed higher levels of 8-OHdG (Zhou et al., 2010). We show here, that FLT3-ITD is not only associated with increased levels of DNA dsbs, but also increased levels of 8-OHdG. Increased levels of 8-OHdG was shown to play a role in self-mutagenesis of BCR-ABL that led to imatinib resistance (Koptyra et al., 2006). We suggest that a similar mechanism can operate in FLT3-ITD. What is

more, DNA dsbs were documented to arise from oxidative DNA damage in S/G_2M phase in BCR-ABL cells (Nowicki et al., 2004). Repair of 8-OHdG results in a removal of the oxidised base that produces a single strand break (Kuzminov, 2001). When the latter one is encountered by the replication fork, it can result in a dsb (Lu et al., 2001). We suggest that similar phenomenon may be occurring in the FLT3-ITD AML.

Chapter 6

General Discussion

In the majority of AML patients, induction chemotherapy consisting of cytarabine and idarubicin/daunorubicin leads to a complete remission (Peloquin et al., 2013, Roboz, 2012). However, only 40% of patients younger than 60 years, and 10-20% of older patients, remain in remission at 5 years following the induction therapy (Roboz, 2012, Peloquin et al., 2013). Although the incidence of AML is moderately low in comparison to other cancers (3.8 cases per 100,000 in US and Europe) (Showel and Levis, 2014), relapse statistics and an overall survival rate (40-50%) are much worse for AML than for the vast majority of other tumours (Peloquin et al., 2013). This indicates the urgent need for the development of new treatments for AML. Furthermore, the high percentage of AML relapse highlights the requirement for investigations of the molecular sources and mechanisms of this phenomenon.

Imatinib mesylate was the first small-molecule tyrosine kinase inhibitors (TKIs) used as a standard cancer chemotherapy in the clinic that selectively targets BCR-ABL, the main oncoprotein in the leukaemogenesis of chronic myeloid leukaemia (CML). Imatinib treatment has improved the 5 year survival rate from 50% to around 90% of CML patients, proving the effectiveness of molecular-targeted chemotherapy in cancer (Druker, 2009). Following the success of imatinib, there has been great interest in discovering more effective chemotherapeutics against other cancer-driving oncoproteins.

The main genetic alterations that influence the prognosis of AML patients are NPM1, FLT3 and CEBPα, and these are routinely tested for following diagnosis

(Peloquin et al., 2013). Expression of FLT3 is normally restricted to CD34+, early progenitors in bone marrow (Levis and Small, 2003). However, 70-90% of AML cases express FLT3 without CD34-restriction (Grafone et al., 2012, Stirewalt and Radich, 2003). Moreover, 25-35% of adult AML patients and 10-17% of paediatric patients possess an activating FLT3-ITD mutation that confers a poor prognosis and a high incidence of relapse (Grafone et al., 2012).

Due to the high prevalence of FLT3-ITD mutation among AML patients and its adverse clinical effects, FLT3 is an attractive target for novel molecular AML chemotherapy (Wander et al., 2014, Grunwald and Levis, 2013). However, clinical trials of the first assortment of FLT3 inhibitors (CEP-701, SU5416, MLN518 and PKC412) did not yield impressive results (Stirewalt and Radich, 2003, Ostronoff and Estey, 2013). A new-generation FLT3-selective inhibitor, AC-220, has shown favourable pharmacokinetics, potency and tolerability in AML patients (Ostronoff and Estey, 2013). However, the clinical outcome of remission duration from the first clinical trials is still suboptimal (Ostronoff and Estey, 2013, Wander et al., 2014).

Although the clinical outcome of these trials has not matched the success of Imatinib treatment, one should consider that even though both AML and CML originate in myeloid precursors, they have diverse dynamics of the malignant progression. Indeed, AML is more genetically heterogeneous and far more aggressive than CML, which generally reduces the effectiveness of single chemotherapies (Stirewalt and Radich, 2003). In addition, the levels of genomic variability may be further exacerbated in patients harbouring FLT3-ITD (Sallmyr et al., 2008b). This heterogeneity of AML suggests that FLT3 inhibition as a

monotherapy may not be sufficiently efficacious. Leukaemic blasts and/or leukaemic stem cells (LSCs) may not be solely FLT3-ITD-addicted, and most likely possess additional malignant mutations such as NPM1 (Gilliland and Griffin, 2002). Therefore, FLT3 inhibitors could be more effective in combination with other chemotherapeutics. In fact, AC-220, a new generation FLT3 inhibitor, is currently being clinically tested in combination with induction and consolidation chemotherapies in newly diagnosed AML patients , which has been shown to be safe in a phase 1 clinical trial (Ostronoff and Estey, 2013, Wander et al., 2014).

Although FLT3 inhibition in combination with standard AML chemotherapy seems promising, this therapeutic strategy as a general AML treatment carries certain shortcomings. As learnt from clinical studies on imatinib, TKIs-based therapies often lead to chemoresistance (Branford et al., 2002, Jabbour and Kantarjian, 2014). For instance, additional secondary mutations in FLT3 kinase may occur that could reduce patients' responsiveness to the therapy (Grunwald and Levis, 2013). Indeed, these genetic alterations have already been demonstrated in relapsing AC-220-treated patients (Moore et al., 2012, Smith et al., 2012, Wander et al., 2014). Furthermore, FLT3 inhibitors were demonstrated to induce expression and release of FLT3 ligand (FL) (Sato et al., 2011). It has also been reported *in vitro* that FL interferes with the effectiveness of FLT3 inhibitors, reducing their inhibitory activity to 50% (Sato et al., 2011). This could lead to stimulation of relapse and/or chemoresistance (Sato et al., 2011). The limitations discussed above are important considerations in the search for new AML chemotherapies.

We and others have demonstrated that patient AML blasts generate increased levels of ROS (Hole et al., 2013), which are known to damage biomolecules and cellular structures (Schieber and Chandel, 2014). However, growing evidence in the literature indicates that these reactive molecules can also act as signalling molecules in a wide array of processes regulating proliferation, growth, survival and differentiation (Clerkin et al., 2008, Gough and Cotter, 2011, Schieber and Chandel, 2014, D'Autreaux and Toledano, 2007). Cancer cells appear to up-regulate and/or activate the sources of ROS, such as NOX enzymes, to stimulate these tumourigenic processes (Block and Gorin, 2012). The alteration in the redox state of cancer cells requires adaptation to the damaging effects of ROS. For example, to prevent an accumulation of excessive concentrations of ROS, cancer cells induce expression of antioxidant enzymes, which neutralise ROS (Pelicano et al., 2004). Furthermore, in order to cope with the oxidative cellular damage, tumour cells up-regulate repair systems, for instance DNA dsb repair (Popp and Bohlander, 2010, Pelicano et al., 2004). It is thought that through redox-driven adaptations, tumour cells maintain a high, stimulating level of ROS without extensive intracellular damage that could lead to cell death. From a clinical point of view, adaptations to increased concentrations of ROS can make cancer cells less responsive to cytotoxic chemotherapy, which often operates through severe oxidative stress (Schumacker, 2006, Pelicano et al., 2004, Trachootham et al., 2009). Therefore, delineation of sources and mechanisms of ROS production could disclose novel protein targets in cancer, which when combined with standard chemotherapy, could increase and prolong response to chemotherapeutics.

This work demonstrated that mutated FLT3 stimulated H_2O_2 formation in human patient-derived and mouse cell lines. This H_2O_2 production was readily reduced by the inhibition of FLT3. Furthermore, activation of FLT3-WT with FL led to a great increase in endogenous H_2O_2 levels. The phenomenon of FLT3-ITD driving total ROS has already been reported (Sallmyr et al., 2008b, Sallmyr et al., 2008a). However, ROS consist of a diverse family of reactive molecules of different kinetics and oxidative properties. Indeed, different types of ROS have previously been shown to exert distinct biochemical reactions (D'Autreaux and Toledano, 2007). Therefore, it is important to investigate the type of ROS implicated in the redox effect, particularly when studying signalling biology.

Dickinson *et al*. have recently developed H_2O_2-detecting fluorescent probes that have allowed us to specifically detect changes in intracellular H_2O_2 levels (Dickinson et al., 2010a, Dickinson et al., 2010b, Dickinson et al., 2011a, Dickinson et al., 2011b, Lippert et al., 2011, Woolley et al., 2013b). The H_2O_2-specificity of these sensors is achieved by chemically unique conversion of a boronate moiety into phenol group upon reaction with H_2O_2 (Dickinson et al., 2010a, Lippert et al., 2011). Furthermore, high sensitivity of the probes has previously allowed the detection of physiological changes in H_2O_2 (Dickinson et al., 2010a).

Another important aspect of ROS signalling is its intracellular localisation. The specificity of ROS signal transduction largely originates in the close localisation of ROS source and its target (D'Autreaux and Toledano, 2007). This is particularly evident in NOX-generated ROS, as distinct subcellular localisations of NOX isoforms in the same cells, induced different signalling phenomena (Hilenski et al.,

2004). This is not surprising considering their extreme reactivity and much shorter half-life than other signalling molecules. It also unclear how molecular targets of H_2O_2, which have a rate constant ranging from 10 to 10^3 M^{-1} s^{-1}, can compete with antioxidant enzymes with rate constants up to 2×10^7 M^{-1} s^{-1} (Mishina et al., 2011). These figures suggest that only highly co-localised ROS source and its target are capable of inducing an oxidation reaction, leading to signal transduction. In support of this theory, it was demonstrated, using live imaging, that diffusion of H_2O_2 across the cytoplasm of HeLa-Kyoto and NIH-3T3 cells is strongly limited (Mishina et al., 2011). Taken together, these findings highlight the importance of the intracellular localisation of redox processes.

Recent advances in the fluorescent probes and genetic ROS detection systems have provided novel tools to localise ROS accumulation/generation in cells, tissues and even live animals (Woolley et al., 2012). Due to varying emission wavelengths, the novel boronate-probes can be co-stained with either additional ROS probes to monitor changes in different types of ROS or with organelle trackers, to monitor the localisation of ROS within cells (Dickinson et al., 2010a, Woolley et al., 2012). FLT3-ITD has previously been associated with higher ROS levels (Sallmyr et al., 2008a). However, this work not only revealed the type of ROS formed, but also localised the accumulated ROS in FLT3-ITD expressing cells to the endoplasmic reticulum (ER). To our knowledge, this is the first report of ROS localisation in leukaemic cells. This H_2O_2 localisation could be explained by NOX4 and $p22^{phox}$ localisation in the ER of these cells, as demonstrated in this and other reports (Woolley et al., 2012, Lee et al., 2010). ER-localisation of ROS is particularly

important in FLT3-ITD-expressing cells, as the immature form of FLT3-ITD itself localises to the ER (Choudhary et al., 2009). ER-residing FLT3-ITD aberrantly activates STAT5, which is recognised as a key regulator of the myeloid transformation (Choudhary et al., 2009, Schmidt-Arras et al., 2009, Spiekermann et al., 2003, Choudhary et al., 2007). One of the phosphatases, which has been shown to regulate the mislocalised FLT3-ITD, is the ER-resident protein tyrosine phosphatase 1 B (PTP1B) (Stuible and Tremblay, 2010, Schmidt-Arras et al., 2005). PTP1B-deficient fibroblasts showed elevated levels of auto-phosphorylated FLT3-ITD (Schmidt-Arras et al., 2005). Interestingly, NOX4/$p22^{phox}$ complex has been previously demonstrated to specifically oxidise ER-localised PTP1B, leading to its inactivation (Mahadev et al., 2004, Mondol et al., 2014, Chen et al., 2008, Hiraga et al., 2013). This indicates that through activation of NOX4/$p22^{phox}$ in the ER, FLT3-ITD could provide an ROS source to inactivate PTP1B, resulting in a maintenance of the autophosphorylation status of FLT3-ITD. Moreover, active PTP1B was also found to promote FLT3-ITD maturation and surface localisation, suggesting that inactivation of PTP1B by oxidation could cause an ER-retention of FLT3-ITD in AML (Schmidt-Arras et al., 2005). If this was true, NOX-generated ROS, stimulated by FLT3-ITD, could potentially regulate the oncogene activity and localisation itself. In fact, NOX-generated ROS have also been shown to inactivate a density-enhanced phosphatase-1, DEP-1 in AML cells (Godfrey et al., 2012). DEP-1 is a tumour suppressor phosphatase, as it negatively regulates autophosphorylation and signalling of wild type FLT3 kinase (Arora et al., 2011). Overproduction of ROS

from NOXs led to the oxidation of redox-sensitive cysteines of DEP-1, which in turn sustained phosphorylation of FLT3-ITD.(Godfrey et al., 2012).

In this work, we demonstrated that FLT3-ITD regulates NOX activity by stabilisation of $p22^{phox}$, its small membrane component (Figure 6.1). Our group has shown that this stabilisation was achieved through phosphorylation of Glycogen Synthase Kinase 3 β (GSK3- β), which caused its inactivation (Woolley et al., 2012). GSK3-β is a serine/threonine kinase downstream of AKT, a crucial regulator of survival and proliferation in FLT3-ITD signalling (Altomare and Testa, 2005, Fresno Vara et al., 2004). It has been found that AKT is activated by the mature, glycosylated plasma membrane (PM)-bound FLT3-ITD. This suggests that $p22^{phox}$ stabilisation is accomplished by the activation of AKT through PM-operating FLT3-ITD. Therefore, it could be possible that PM-bound FLT3-ITD inactivates PTP1B at the ER, by the activation of the NOX4/$p22^{phox}$ complex. In addition, it has demonstrated that PTPs' inactivation, including PTP1B, leads to incorrect folding of FLT3-ITD, resulting in its ER retention (Schmidt-Arras et al., 2009). Therefore, through the maintenance of inactive PTP1B, FLT3-ITD could operate in a phosphorylated, misfolded state at the ER. This in turn could additionally stimulate aberrant P-STAT5 signalling, providing these AML cells with an evolutionary advantage. In this potential mechanism, NOX4-generated ROS may be *de facto* inducing FLT3-ITD retention and STAT5 signalling. In support of this theory, our group has reported that siRNA knockdown of $p22^{phox}$, led to the abolishment of STAT5 phosphorylation in FLT3-ITD expressing cells (Woolley et al., 2012).

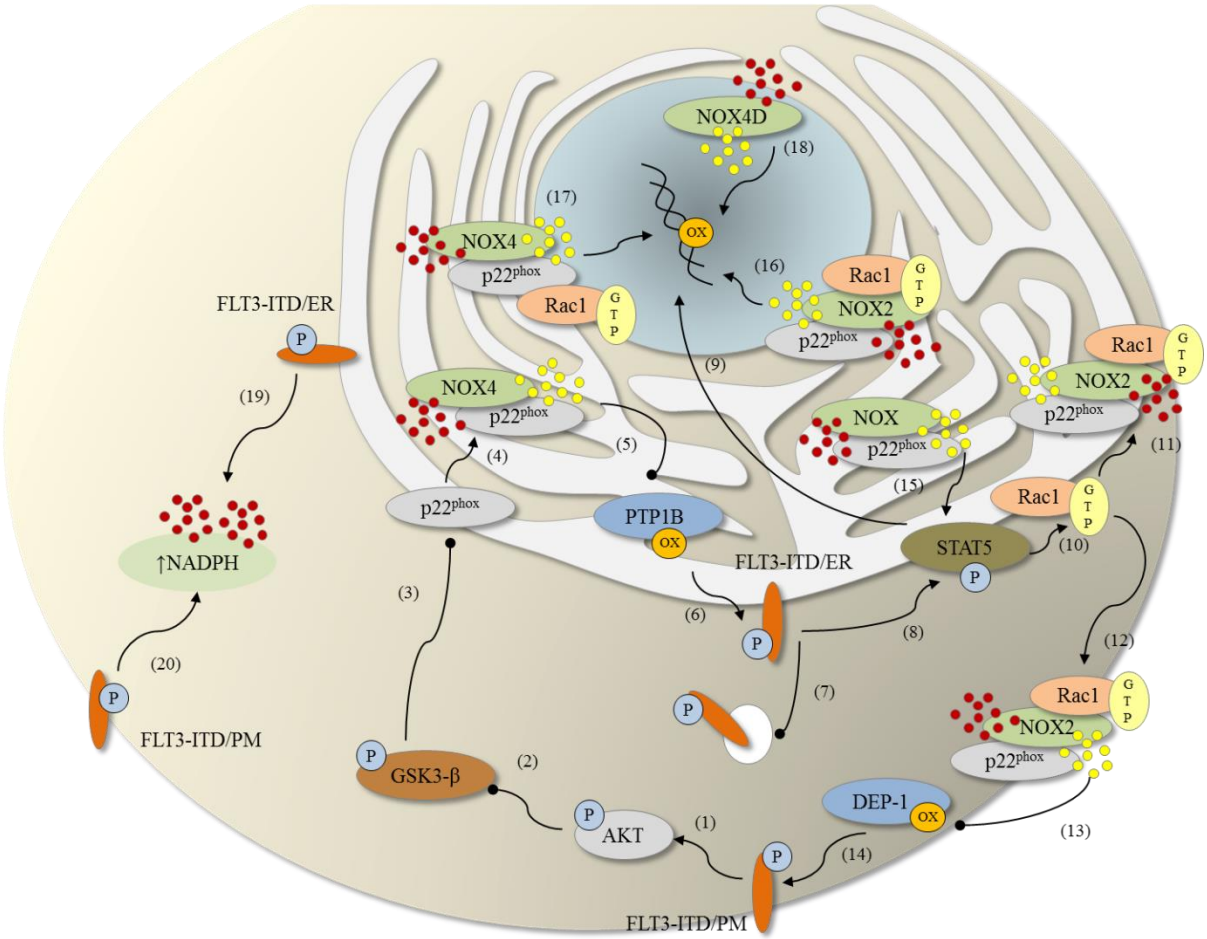

Figure 6.1. Proposed schematic of FLT3-ITD-induced activation of NOX enzymes and the intracellular consequences of NOX-generates ROS. (**1-2**) PM-bound FLT3-ITD stimulates phosphorylation of AKT, which in turn, phosphorylates GSK3-β that causes its inactivation. (**3-4**) This leads to $p22^{phox}$ stabilisation, which results in an activation of NOX4 complex at the ER. (**5-6**) NOX4/$p22^{phox}$ generated H_2O_2 oxidatively inactivates ER-residing PTP1B, leading to an increase in phospho-FLT3-ITD. (**7**) The hyper-phosphorylation of FLT3-ITD in the ER reduces the receptor's maturation and thus its translocation to PM. (**8-9**) ER-bound FLT3-ITD aberrantly activates STAT5, which moves to the nucleus to induce transcription of its target genes, including PIM-1/2. (**10-12**) P-STAT5 also binds and activates Rac1 GTPase, which stimulates NOX2 to produce ROS at the ER and the PM. (**13-14**) PM-bound NOX2 oxidises DEP-1, which results in the maintenance of the phosphorylation of FLT3-ITD/PM. (**15**) ER-localised NOX4/$p22^{phox}$ generates more ROS at the ER to inactivate other PTPs that negatively regulate P-STAT5. **(16-17**) NOX2 and NOX4/$p22^{phox}$ complex (bound to Rac1?) at the nuclear membrane produces oxidative DNA damage. (**18**) $p22^{phox}$-independent NOX4D generates H_2O_2 that also damages DNA. (**19-20**) FLT3-ITD (localised at the PM and/or the ER) causes an increase in the production of NADPH oxidase substrate, NADPH.

Along with few other reports, this work presents an insight into FLT3-ITD-achieved elevation of cellular ROS (Woolley et al., 2012, Sallmyr et al., 2008a). However, the levels of ROS following the FL activation of 32D/FLT3-WT cells have not been previously investigated. We showed here that FL stimulation led to an increase in the levels of endogenous ROS, which corresponded to an increase in steady protein levels of $p22^{phox}$. Based on the GSK3-β function in $p22^{phox}$ degradation, it can be expected that the increase in $p22^{phox}$ levels may also be induced by AKT activation downstream of PM-bound wild type FLT3 signalling.

In line with our results, stabilisation of $p22^{phox}$ as a mechanism of NOX activation was also found in BCR-ABL harbouring CML cell line (Landry et al., 2013). Similarly to PKC412, imatinib treatment resulted in the post-translational down-regulation of $p22^{phox}$. Upon oncogene inhibition, in both AML and CML cell line models, GSK3-β became activated, promoting $p22^{phox}$ ubiquitination and subsequently its proteasomal degradation (Landry et al., 2013, Woolley et al., 2012).

Although not through protein stabilisation, but as a consequence of transcriptional induction, $p22^{phox}$ has also been found to act as a mediator of NOX4 activation in pancreatic cancer cells (Edderkaoui et al., 2011). IGF-1 and FBS have been shown to induce $p22^{phox}$ mRNA through AKT kinase signalling, which in turn elevated the levels of active NOX4/ $p22^{phox}$ complex. An increase in $p22^{phox}$ mRNA has also led to an increase in NADPH NOX activity in aortas from hypertensive rats (Fukui et al., 1997). In agreement with this work, these findings demonstrated that the amount of active NOX4 may be modulated by an increase in $p22^{phox}$ expression, rather than through a rise in the expression of NOX4 catalytic subunit itself.

AKT kinase is a central node of signalling pathways stimulated by various oncogenes and growth factors (Altomare and Testa, 2005) . It is thus possible that AKT/GSK-3β-mediated $p22^{phox}$ stabilisation, which causes NOX-activation in FLT3-ITD cells, may potentially be a universal phenomenon, occurring downstream of many oncogenes and growth factors. It has been demonstrated previously that ROS regulate growth factor signalling through inactivation of phosphatases (Miki and Funato, 2012). Therefore, it could be hypothesised that growth factors and oncogenes switch off negative regulation of their signalling by activation of AKT which, through regulation of $p22^{phox}$ levels, activates NOX.

In addition to $p22^{phox}$ stabilisation, there are other mechanisms reported of NOX activation downstream of FLT3-ITD signalling (Sallmyr et al., 2008a, Reddy et al., 2011). Reddy *et al*. have demonstrated an increase in NOX substrate, NADPH, in FLT-ITD-expressing AML cells (Reddy et al., 2011). On the other hand, another study reported that FLT3-ITD activated NOXs through direct interaction of Rac1-GTP with P-STAT5 (Sallmyr et al., 2008a). As 32D cells without mutated FLT3 do not stimulate STAT5 phosphorylation, NOX activation only occurred in FLT3-ITD expressing cells (Sallmyr et al., 2008a). Rac-1-mediated NOX activation by FLT3-ITD suggests that NOX1 and/or NOX2 isoforms were activated. However, some reports have suggested that Rac1 could also potentially activate NOX4 (Guida et al., 2014, Hajas et al., 2013, Gorin et al., 2003). Interestingly, Rac1 has been shown to mediate an increase in nuclear ROS via NOX4, residing in the nuclear membrane (Hajas et al., 2013). In summary, these findings indicate that, due to the increasing

importance of ROS effects on growth, migration and genomic instability, FLT3-ITD employs various mechanisms to activate NOX complexes.

Based on our ROS localisation studies and siRNA knockdowns, we suspect that the aforementioned FLT3-ITD-stimulated stabilisation of $p22^{phox}$ leads to NOX2 and NOX4, but not NOX1 activation in the ER. NOX4-originated redox signalling in the ER was investigated in several reports (Hilenski et al., 2004, Petry et al., 2006, Lee et al., 2010, Bedard and Krause, 2007, Chen et al., 2008). However, the concept of NOX2 operating in the ER is still in its infancy. Both isoforms were observed in the ER from where, through generation of ROS under basal conditions, they stimulated endothelial cells' proliferation (Petry et al., 2006). Furthermore, in support of our findings, NOX1 depletion did not alter ROS levels and hence the proliferation of these cells.

In support of the importance of NOX2 and NOX4 in AML, depletion of NOX2, NOX4 or $p22^{phox}$ siRNA led to approximately 50% decrease in growth and migration in FLT3-ITD-expressing MOLM-13 cells (Reddy et al., 2011). Furthermore, it has also been demonstrated that either inhibition or knockdown of a RAC1 GTPase attenuated 50% of ROS formation in 32D cells transfected with FLT3-ITD (Sallmyr et al., 2008a). Similarly to our work, the reduction in ROS upon NOX inhibition was not observed in 32D expressing FLT3-WT.

NOX2 has also been implicated in the c-KIT activation and survival of AML M07e cells (Maraldi et al., 2009). Importantly, NOX2 was identified as a source of the overproduction of superoxide in AML patient samples, where patients expressing

higher levels of NOX2 possessed elevated amounts of endogenous ROS (Hole et al., 2013). The study also suggested that the proliferation-promoting ROS generation in AML originated from NOX2 and NOX4 complexes.

Taken together, we propose that NOX2 and NOX4 are the main source of the oncogene driven-ROS in the 32D cells expressing FLT3-ITD. However, both NOX enzymes and mitochondria have been implicated as an ROS source in AML studies (Sallmyr et al., 2008a, Sallmyr et al., 2008b, Reddy et al., 2011, Godfrey et al., 2012). In this work, we found that the analysis of mitochondrial ROS levels of cells expressing FLT3-WT and FLT3-ITD revealed no significant difference. Furthermore, inhibition of FLT3-ITD did not result in any changes in mitochondrial H_2O_2, as measured with MitoPY1, a mitochondrial H_2O_2-sensing probe. In light of this finding, Hole *et al*. have demonstrated that while patient AML blasts produced more superoxide than their healthy counterparts, they possessed less mitochondrial ROS (Reddy et al., 2011).

In addition to the ER-localisation of $p22^{phox}$-dependent NOX, we demonstrated that NOX4/$p22^{phox}$ complex is bound to the nuclear membrane. This is not surprising as the nuclear membrane is continuous with the ER membrane system. We propose that H_2O_2 generated on the nuclear membrane, diffuses to the nucleus, leading to genotoxic stress in FLT3-ITD-expressing cells. In line with this hypothesis, FL-ligand-activated FLT3-WT, which caused an increase in steady $p22^{phox}$ protein levels, also resulted in an increase in nuclear ROS. In analogy to this, we found that pharmacological inhibition of FLT3-ITD or NOX caused a decrease in H_2O_2 levels in the nucleus. Furthermore, specific NOX4 or $p22^{phox}$ knockdown

resulted in a depletion of nuclear H_2O_2. This result was recently confirmed in THP-1, an AML cell line, where NOX4 knockdown largely abolished levels of nuclear H_2O_2 (Guida et al., 2014). Furthermore, the same study showed that nuclear fractions of THP-1 and MOLM-13 cells possessed NOX4, $p22^{phox}$ and Rac1 proteins. This contradicts the immunofluorescence images of MV4-11 cells, which did not reveal any NOX4 foci in the nucleus. The high content of hydrophobic residues in 70-75 kDa NOX4 may not allow this splice variant to operate inside the nucleus. However, a 28 kDa NOX4 splice form (NOX4D), that lacks putative transmembrane domains, formed a functional soluble protein in vascular smooth muscle cells (VSMCs) (Anilkumar et al., 2013). In fact, NOX4D has been specifically localised to the inside of the nucleus in various cell lines, while NOX4D siRNA knockdown abolished its intranuclear staining. Interestingly, although largely truncated, over-expressed NOX4D has been shown to generate ROS and γH2AX, suggesting that this isoform could play a role in genomic instability.

In this work we demonstrated in MV4-11 cells that NOX4 knockdown, when compared to $p22^{phox}$ knockdown, resulted in a larger decrease in the nuclear H_2O_2 levels. Furthermore, in 32D cells, NOX4 siRNA treated cells possessed less DNA dsbs than the same cells treated with $p22^{phox}$ siRNA. This is surprising as in order for the full length NOX4 to form a functional ROS-producing enzyme, the protein needs to be stabilised at the membrane by binding to $p22^{phox}$ ((Ambasta et al., 2004)). The differences between NOX4 and $p22^{phox}$ knockdowns suggest that NOX4D may play a role in the nuclear H_2O_2 production, independently of $p22^{phox}$. This hypothesis is supported by the structural differences between 70-75 kDa and 28 kDa NOX4 splice

variants, with NOX4D is missing the D loop which is responsible for the $p22^{phox}$ interaction (Anilkumar et al., 2013).

The presence of NOX4-generated H_2O_2 in the nucleus was demonstrated to promote redox regulation of nuclear proteins. For example, nuclear membrane-bound NOX4 induced expression of monocyte chemoattractant protein-1 (MCP-1), a key regulator of haemangioendothelioma (Gordillo et al., 2010). It has been suggested that this occurred through oxidative activation of nuclear factor *kappa*-light-chain-enhancer of activated *B* cells (NF-κB) or Activator Protein 1 (AP-1) transcription factors. NOX4-derived H_2O_2 was also shown to oxidise cysteines of histone deacetylase 4 (HDAC4) that led to cardiac hypertrophy in cardiomyocytes (Matsushima et al., 2013). These examples demonstrate that, as observed in this work, NOX4 localisation in the nucleus/the nuclear membrane could expand the array of redox-controlled signalling on nuclear targets.

In addition to stimulation of the aforementioned signalling pathways, deregulated redox metabolism also results in oxidative DNA damage. 8-OHdG, a product of such DNA oxidation, is widely used as a biomarker of oxidative stress (Valavanidis et al., 2009, Wu et al., 2004). It has been demonstrated that AML patients at relapse possess higher levels of 8-OHdG (Zhou et al., 2010). This indicates that redox reactions could play a role in AML relapse, which remains a significant issue in the clinic. In this case, manipulation of ROS generation may have a therapeutic potential in preventing or postponing AML relapse. We demonstrated that the presence of FLT3-ITD mutation is associated with elevated 8-OHdG levels. Interestingly, this oxidative damage could easily be reversed by inhibition of FLT3

or NOX, or $p22^{phox}$ knockdown. In support of this finding, nuclear membrane-bound NOX4 was shown to directly deliver H_2O_2 to the nuclei of haemangioendothelioma cells, which led to an accumulation of 8-OHdG (Gordillo et al., 2010). We propose that oxidative DNA damage may accelerate the onset of AML relapse, which could be potentially prevented by chemotherapy involving FLT3 and/or NOX inhibition.

The endogenous oxidative DNA damage may provide a machinery for promotion of chemoresistance, as cells with advantageous new mutations could be selected for growth. Although, FLT3 and NOX inhibition prevented accumulation of damaged DNA, the removal of an inhibitory agent led to the return of DNA damage. This suggests that both 8-OHdG formation and its repair are dynamic processes, strictly dependent on the presence of FLT3-ITD redox signalling. Therefore, in order to prevent the reoccurrence of oxidative damage, when used as chemotherapeutics in the clinic, plasma concentrations of FLT3 inhibitors should be sufficiently high to provide a maximal FLT3 inhibition.

Genomic instability can be defined as the mechanisms of acquiring genetic alterations and it has been recently reviewed as an enabling hallmark of cancer, as it allows other hallmarks of cancer to occur (Burrell et al., 2013, Popp and Bohlander, 2010, Sallmyr et al., 2008b, Hanahan and Weinberg, 2011). Cells evolved extensive network of faithful DNA repair pathways which ensure the DNA stability (Fan et al., 2010, Popp and Bohlander, 2010).Therefore, it has been proposed that due to the requirement of several mutations, cancer cells must possess some form of inherent genomic instability. Genomic instability originates from processes resulting in the generation of mutations and their subsequent unfaithful repair. ROS-produced

oxidative DNA damage can lead to a variety of mutations (Schieber and Chandel, 2014, Cooke et al., 2003). These in turn could cause activation of oncogenes or deactivation of tumour suppressors. DNA dsbs are one of the most toxic genetic lesions because they can result in genome rearrangements (Khanna and Jackson, 2001). These alterations can cause enhancement of tumourigenic processes as well as chemoresistance. Through elevating endogenous ROS and altering DNA repair, FLT3-ITD mutation renders genome of AML cells highly unstable. This could be the cause of the earlier relapse onset in FLT3-ITD-expressing patients. This work demonstrated that inhibition or siRNA knockdown of NOX isoforms attenuated ROS production and, thus, DNA dsbs formation in FLT3-ITD expressing cell lines. Consequently, in addition to reducing survival and proliferation, an inhibition of ROS source may also potentially prevent accumulation of new genomic alterations in the clinic. Interestingly, these results may not be solely relevant for FLT3-ITD-expressing cases (20-30% of AML). FL-achieved activation of FLT3-WT, present in 70-100% of AML cases, also resulted in a significant increase in the number of DNA dsbs. As FL ligand levels rise during the course of chemotherapy treatment, this DNA damage may play a role in relapse and/or chemoresistance of both FLT3-WT and FLT3-ITD expressing patients (Sato et al., 2011).

In support of these results, an increasing number of studies have identified NOX4 as a source of ROS and DNA damage in various tumour cell lines (Weyemi and Dupuy, 2012, Anilkumar et al., 2013, Guida et al., 2014, Weyemi et al., 2012). In line with FLT3-ITD, H-RAS oncogene has been shown to activate NOX4 to produce ROS and DNA damage (Weyemi et al., 2012). Similarly to AML cells,

NOX4 was detected in the ER, nuclear membrane and the nuclear compartment of H-RAS-expressing thyrocytes (Weyemi et al., 2012). However, while FLT3-ITD activates NOX4 by stabilisation of $p22^{phox}$, H-RAS induces expression of NOX4 and $p22^{phox}$. Interestingly, this study has suggested that NOX4-generated ROS could stimulate the process of senescence in thyroid cells, potentially assigning NOX4 with a novel function in tumour suppression.

As discussed above, the role of NOX4 in causing DNA damage has been previously addressed (Anilkumar et al., 2013, Weyemi and Dupuy, 2012, Guida et al., 2014, Weyemi et al., 2012). However, the contribution of NOX2 to this process has not been yet greatly characterised. In support of this work, it has been demonstrated that the Epstein–Barr virus (EBV) nuclear antigen-1 (EBVNA-1) stimulated NOX2-generated ROS that caused genomic instability in EBV expressing cells (Gruhne et al., 2009).

All of the above findings present the extent of NOX-induced tumourigenic signalling in FLT3 expressing AML cells. Various mechanisms of NOX activation by FLT3-ITD demonstrate how important these enzymes are in the network of activated FLT3 signalling. As outlined in this report, other oncogenes implicated in various cancers have also been shown to induce redox-signalling *via* NOXs. It was recently hypothesised that the pleiotropic nature of NOX-generated ROS provides cancer cells with an evolutionary advantage in survival and growth (Block and Gorin, 2012). Therefore, NOXs are becoming recognised as attractive targets in cancer therapy. The differential expression of NOX between healthy and cancer patients could give NOX inhibitors some selectivity towards tumour cells, which

could minimise the possible side effects. However, due to the lack of specific inhibitors, the therapeutic potential of NOX inhibitors is still in its infancy. In this study, we achieved NOX inhibition using DPI and VAS-2870 treatments. DPI is a flavin protein inhibitor, and while its non-specific effects are well known, it is the most commonly used NOX inhibitor (Li and Trush, 1998, Wind et al., 2010). VAS-2870 and VAS-3947, novel pan-NOX inhibitors, belong to triazolo pyrimidines family of compounds. Although their mechanism of NOX inhibition is still unknown, they do not interfere with xanthine oxidase or nitric oxidase activities (Wind et al., 2010). We demonstrated that both VAS-2870 and DPI treatments resulted in a decline of both cellular and nuclear levels of H_2O_2 in AML cells. We also showed that VAS-2870 did not inhibit H_2O_2 formation in mitochondria, measured with MitoPY1, suggesting that this drug does not affect mitochondrial electron transport. These results indicate that pharmacological inhibition of NOX resembles siRNA knockdowns of $p22^{phox}$ or NOX2 or NOX4 proteins, highlighting the potential of NOX inhibitors for AML chemotherapy (Figure 2.).

Interestingly, following this work, DPI and VAS-2870 were recently proposed as chemotherapies in BCR-ABL- harbouring CML (Sanchez-Sanchez et al., 2014, Landry et al., 2013). When used in combination with Imatinib, DPI and VAS-2870 demonstrated highly synergistic apoptotic effects (Sanchez-Sanchez et al., 2014). The authors showed that NOX inhibition attenuated BCR-ABL signalling, resulting in a pronounced cell-cycle arrest. Imatinib/ DPI combination caused dephosphorylation of BCR-ABL, STAT5 and ERK1/2 that led to reduction in proliferation and cell viability of CML cells. Importantly, 2 mouse models and

CD34+ patient samples confirmed synergistic effects of this drug combination for targeting CML. Due to the similarities of BCR-ABL and FLT3-ITD signalling, we suspect that simultaneous inhibition of FLT3-ITD and NOX could lead to analogous results. In fact, according to the aforementioned study, a combination of PKC412 and DPI resulted in a synergistic increase in cell death of FLT3-ITD expressing MV4-11 cells.

In summary, this study has demonstrated a novel mechanism of NOX activation downstream of the activated FLT3 receptor tyrosine kinase. $p22^{phox}$-dependent NOX2 and NOX4 have been found to be an important ROS sources in FLT3-ITD signalling. This work has also presented an additional function of NOXs in AML, which is generation of genomic instability. All of these results were consistent in human and mouse cell lines models of AML. These findings confirm the importance of NOX-originated ROS in leukaemia, which may be considered as novel target in AML chemotherapy.

Future work

The work described in this thesis demonstrated the important function of ROS in the AML phenotype. The current model of the FLT3-ITD-induced activation of NOX enzymes and the subsequent signalling effects is presented in the Figure 1. |The model combines the published literature with the novel data presented in this thesis. While this work depicts the mechanism of the NOX-activation and its effects in leukaemia, the details of it are still unclear. For example, while it is plausible that NOX4 generates ROS in the ER, the phosphatases/proteins affected by this ROS

signalling are not known. Based on the literature, the important candidates to investigate are the aforementioned PTP1B and DEP-1. Furthermore, due to the differential ER and PM signalling downstream of mutated FLT3 it would also be beneficial to examine how FLT3 localisation affects the activation of NOX.

This work has demonstrated that NOX4 contributes to genomic instability in AML cell lines. In light of recent reports, the contribution of the aforementioned in general discussion, NOX4D to this process should be investigated.

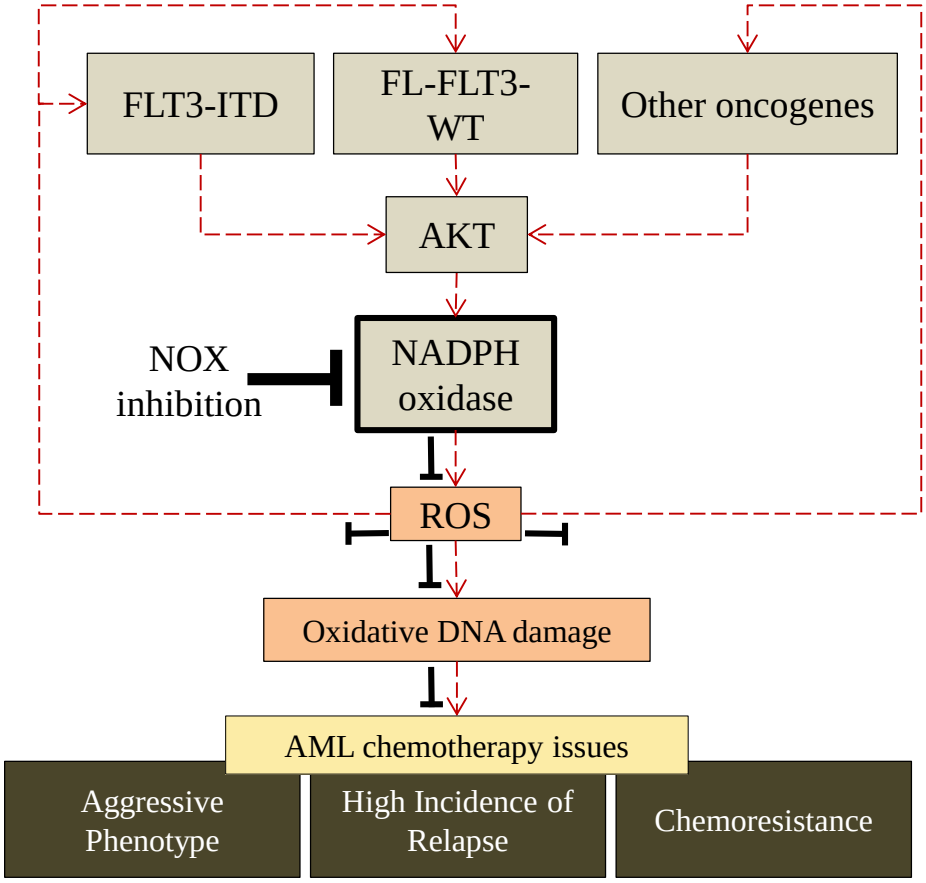

Figure 2. NOX inhibition as a potential AML chemotherapy

Bibliography

ACHARYA, A., DAS, I., CHANDHOK, D. & SAHA, T. 2010. Redox regulation in cancer: a double-edged sword with therapeutic potential. *Oxid Med Cell Longev,* 3**,** 23-34.

ALDIERI, E., RIGANTI, C., POLIMENI, M., GAZZANO, E., LUSSIANA, C., CAMPIA, I. & GHIGO, D. 2008. Classical inhibitors of NOX NAD(P)H oxidases are not specific. *Current Drug Metabolism,* 9**,** 686-96.

ALMASALMEH, A., KRENC, D., WU, B. & BEITZ, E. 2014. Structural determinants of the hydrogen peroxide permeability of aquaporins. *FEBS Journal,* 281**,** 647-56.

ALTENHOFER, S., KLEIKERS, P. W., RADERMACHER, K. A., SCHEURER, P., ROB HERMANS, J. J., SCHIFFERS, P., HO, H., WINGLER, K. & SCHMIDT, H. H. 2012. The NOX toolbox: validating the role of NADPH oxidases in physiology and disease. *Cellular and Molecular Life Sciences,* 69**,** 2327-43.

ALTOMARE, D. A. & TESTA, J. R. 2005. Perturbations of the AKT signaling pathway in human cancer. *Oncogene,* 24**,** 7455-64.

AMBASTA, R. K., KUMAR, P., GRIENDLING, K. K., SCHMIDT, H. H., BUSSE, R. & BRANDES, R. P. 2004. Direct interaction of the novel Nox proteins with p22phox is required for the formation of a functionally active NADPH oxidase. *Journal of Biological Chemistry,* 279**,** 45935-41.

ANILKUMAR, N., SAN JOSE, G., SAWYER, I., SANTOS, C. X., SAND, C., BREWER, A. C., WARREN, D. & SHAH, A. M. 2013. A 28-kDa splice variant of NADPH oxidase-4 is nuclear-localized and involved in redox signaling in vascular cells. *Arteriosclerosis Thrombosis and Vascular Biology,* 33**,** e104-12.

ARORA, D., STOPP, S., BOHMER, S. A., SCHONS, J., GODFREY, R., MASSON, K., RAZUMOVSKAYA, E., RONNSTRAND, L., TANZER, S., BAUER, R., BOHMER, F. D. & MULLER, J. P. 2011. Protein-tyrosine phosphatase DEP-1 controls receptor tyrosine kinase FLT3 signaling. *Journal of Biological Chemistry,* 286**,** 10918-29.

BABIOR, B. M. 1999. NADPH Oxidase: An Update. *Blood,* 93**,** 1464-1476.

BAE, Y. S., KANG, S. W., SEO, M. S., BAINES, I. C., TEKLE, E., CHOCK, P. B. & RHEE, S. G. 1997. Epidermal growth factor (EGF)-induced generation of hydrogen peroxide. Role in EGF receptor-mediated tyrosine phosphorylation. *Journal of Biological Chemistry,* 272**,** 217-21.

BAIN, J., PLATER, L., ELLIOTT, M., SHPIRO, N., HASTIE, C. J., MCLAUCHLAN, H., KLEVERNIC, I., ARTHUR, J. S. C., ALESSI, D. R. & COHEN, P. 2007. The selectivity of protein kinase inhibitors: a further update. *Biochemical Journal,* 408**,** 297-315.

BÁNFI, B., MALGRANGE, B., KNISZ, J., STEGER, K., DUBOIS-DAUPHIN, M. & KRAUSE, K.-H. 2004. NOX3, a Superoxide-generating NADPH Oxidase of the Inner Ear. *Journal of Biological Chemistry,* 279**,** 46065-46072.

BANFI, B., TIRONE, F., DURUSSEL, I., KNISZ, J., MOSKWA, P., MOLNAR, G. Z., KRAUSE, K. H. & COX, J. A. 2004. Mechanism of Ca2+ activation of the NADPH oxidase 5 (NOX5). *Journal of Biological Chemistry,* 279**,** 18583-91.

BANNO, Y. & NOZAWA, Y. 2003. Hydrogen peroxide-induced phospholipase D activation and its PKC dependence are modulated by pH changes in PC12 cells. *Biochemical and biophysical research communications,* 312**,** 1087-1093.

BEDARD, K., JAQUET, V. & KRAUSE, K. H. 2012. NOX5: from basic biology to signaling and disease. *Free Radical Biology & Medicine,* 52**,** 725-34.

BEDARD, K. & KRAUSE, K. H. 2007. The NOX family of ROS-generating NADPH oxidases: physiology and pathophysiology. *Physiological Reviews,* 87**,** 245-313.

BILSKI, P. J., KARRIKER, B. & CHIGNELL, C. F. 2009. Quenching and generation of singlet oxygen by hydroethidine and related chromophores. *Chemical Physics Letters,* 475**,** 116-119.

BINDOKAS, V. P., JORDAN, J., LEE, C. C. & MILLER, R. J. 1996. Superoxide production in rat hippocampal neurons: selective imaging with hydroethidine. *Journal of Neuroscience,* 16**,** 1324-36.

BINKER, M. G., BINKER-COSEN, A. A., RICHARDS, D., OLIVER, B. & COSEN-BINKER, L. I. 2009. EGF promotes invasion by PANC-1 cells through Rac1/ROS-dependent secretion and activation of MMP-2. *Biochemical and Biophysical Research Communications,* 379**,** 445-50.

BLOCK, K. & GORIN, Y. 2012. Aiding and abetting roles of NOX oxidases in cellular transformation. *Nature Reviews Cancer,* 12**,** 627-37.

BONNET, D. & DICK, J. E. 1997. Human acute myeloid leukemia is organized as a hierarchy that originates from a primitive hematopoietic cell. *Natural Medicines,* 3**,** 730-737.

BRANDES, R. P., WEISSMANN, N. & SCHRÖDER, K. 2014. Nox family NADPH oxidases: Molecular mechanisms of activation. *Free Radical Biology and Medicine,* 76**,** 208-226.

BRANDTS, C. H., SARGIN, B., RODE, M., BIERMANN, C., LINDTNER, B., SCHWABLE, J., BUERGER, H., MULLER-TIDOW, C., CHOUDHARY, C., MCMAHON, M., BERDEL, W. E. & SERVE, H. 2005a. Constitutive activation of Akt by Flt3 internal tandem duplications is necessary for increased survival, proliferation, and myeloid transformation. *Cancer Research,* 65**,** 9643-50.

BRANDTS, C. H., SARGIN, B., RODE, M., BIERMANN, C., LINDTNER, B., SCHWÄBLE, J., BUERGER, H., MÜLLER-TIDOW, C., CHOUDHARY, C., MCMAHON, M., BERDEL, W. E. & SERVE, H. 2005b. Constitutive activation of Akt by Flt3 internal tandem duplications is necessary for increased survival, proliferation, and myeloid transformation. *Cancer research,* 65**,** 9643-50.

BRANFORD, S., RUDZKI, Z., WALSH, S., GRIGG, A., ARTHUR, C., TAYLOR, K., HERRMANN, R., LYNCH, K. P. & HUGHES, T. P. 2002. High frequency of point mutations clustered within the adenosine triphosphate-binding region of BCR/ABL in patients with chronic myeloid leukemia or Ph-positive acute lymphoblastic leukemia who develop imatinib (STI571) resistance. *Blood,* 99**,** 3472-5.

BRAR, S. S., CORBIN, Z., KENNEDY, T. P., HEMENDINGER, R., THORNTON, L., BOMMARIUS, B., ARNOLD, R. S., WHORTON, A. R., STURROCK, A. B., HUECKSTEADT, T. P., QUINN, M. T., KRENITSKY, K., ARDIE, K. G., LAMBETH, J. D. & HOIDAL, J. R. 2003. NOX5 NAD(P)H oxidase regulates growth and apoptosis in DU 145 prostate cancer cells. *American journal of physiology. Cell physiology,* 285**,** C353-69.

BURRELL, R. A., MCGRANAHAN, N., BARTEK, J. & SWANTON, C. 2013. The causes and consequences of genetic heterogeneity in cancer evolution. *Nature,* 501**,** 338-345.

CARMONA-CUENCA, I., RONCERO, C., SANCHO, P., CAJA, L., FAUSTO, N., FERNANDEZ, M. & FABREGAT, I. 2008. Upregulation of the NADPH oxidase NOX4 by TGF-beta in hepatocytes is required for its pro-apoptotic activity. *Journal of Hepatology,* 49**,** 965-76.

CARTER WO FAU - NARAYANAN, P. K., NARAYANAN PK FAU - ROBINSON, J. P. & ROBINSON, J. P. 1994. Intracellular hydrogen peroxide and superoxide anion detection in endothelial cells. *Journal of Leukocyte Biology,* 55**,** 253-8.

CHEN, K., KIRBER, M. T., XIAO, H., YANG, Y. & KEANEY, J. F. 2008. Regulation of ROS signal transduction by NADPH oxidase 4 localization. *The Journal of cell biology,* 181**,** 1129-39.

CHEN, X., ZHONG, Z., XU, Z., CHEN, L. & WANG, Y. 2010. 2',7'-Dichlorodihydrofluorescein as a fluorescent probe for reactive oxygen species measurement: Forty years of application and controversy. *Free Radical Research,* 44**,** 587-604.

CHENG, G., CAO, Z., XU, X., VAN MEIR, E. G. & LAMBETH, J. D. 2001. Homologs of gp91phox: cloning and tissue expression of Nox3, Nox4, and Nox5. *Gene,* 269**,** 131-40.

CHOUDHARY, C., BRANDTS, C., SCHWABLE, J., TICKENBROCK, L., SARGIN, B., UEKER, A., BOHMER, F. D., BERDEL, W. E., MULLER-TIDOW, C. & SERVE, H. 2007. Activation mechanisms of STAT5 by oncogenic Flt3-ITD. *Blood,* 110**,** 370-4.

CHOUDHARY, C., MULLER-TIDOW, C., BERDEL, W. E. & SERVE, H. 2005a. Signal transduction of oncogenic Flt3. *International Journal of Hematology,* 82**,** 93-9.

CHOUDHARY, C., OLSEN, J. V., BRANDTS, C., COX, J., REDDY, P. N., BOHMER, F. D., GERKE, V., SCHMIDT-ARRAS, D. E., BERDEL, W. E., MULLER-TIDOW, C., MANN, M. & SERVE, H. 2009. Mislocalized activation of oncogenic RTKs switches downstream signaling outcomes. *Molecular Cell,* 36**,** 326-39.

CHOUDHARY, C., SCHWABLE, J., BRANDTS, C., TICKENBROCK, L., SARGIN, B., KINDLER, T., FISCHER, T., BERDEL, W. E., MULLER-TIDOW, C. & SERVE, H. 2005b. AML-associated Flt3 kinase domain mutations show signal transduction differences compared with Flt3 ITD mutations. *Blood,* 106**,** 265-73.

CLERKIN, J. S., NAUGHTON, R., QUINEY, C. & COTTER, T. G. 2008. Mechanisms of ROS modulated cell survival during carcinogenesis. *Cancer letters,* 266**,** 30-36.

COOKE, M. S., EVANS, M. D., DIZDAROGLU, M. & LUNEC, J. 2003. Oxidative DNA damage: mechanisms, mutation, and disease. *FASEB Journal,* 17**,** 1195-214.

CROSS, A. R. & SEGAL, A. W. 2004. The NADPH oxidase of professional phagocytes—prototype of the NOX electron transport chain systems. *Biochimica et Biophysica Acta,* 1657**,** 1-22.

CUCORANU, I., CLEMPUS, R., DIKALOVA, A., PHELAN, P. J., ARIYAN, S., DIKALOV, S. & SORESCU, D. 2005. NAD(P)H Oxidase 4 Mediates Transforming Growth Factor-β1–Induced Differentiation of Cardiac Fibroblasts Into Myofibroblasts. *Circulation research,* 97**,** 900-907.

CUI, X. L., BROCKMAN, D., CAMPOS, B. & MYATT, L. 2006. Expression of NADPH oxidase isoform 1 (Nox1) in human placenta: involvement in preeclampsia. *Placenta,* 27**,** 422-31.

CZECH, M. P., LAWRENCE, J. C. & LYNN, W. S. 1974. Evidence for the involvement of sulfhydryl oxidation in the regulation of fat cell hexose transport by insulin. *Proceedings of the National Academy of Sciences of the United States of America,* 71**,** 4173-7.

D'AUTREAUX, B. & TOLEDANO, M. B. 2007. ROS as signalling molecules: mechanisms that generate specificity in ROS homeostasis. *Nature Reviews Molecular Cell Biology,* 8**,** 813-24.

D'AUTRÉAUX, B. & TOLEDANO, M. B. 2007. ROS as signalling molecules: mechanisms that generate specificity in ROS homeostasis. *Nature reviews. Molecular cell biology,* 8**,** 813-24.

DAY, A. M., BROWN, J. D., TAYLOR, S. R., RAND, J. D., MORGAN, B. A. & VEAL, E. A. 2012. Inactivation of a peroxiredoxin by hydrogen peroxide is critical for thioredoxin-mediated repair of oxidized proteins and cell survival. *Molecular cell,* 45**,** 398-408.

DIAZ, B. & COURTNEIDGE, S. A. 2012. Redox signaling at invasive microdomains in cancer cells. *Free Radical Biology & Medicine,* 52**,** 247-56.

DICKINSON, B. C. & CHANG, C. J. 2010. A targetable fluorescent probe for imaging hydrogen peroxide in the mitochondria of living cells. *Journal of the American Chemical Society,* 130**,** 9638-9639.

DICKINSON, B. C., HUYNH, C. & CHANG, C. J. 2010a. A palette of fluorescent probes with varying emission colors for imaging hydrogen peroxide signaling in living cells. *Journal of the American Chemical Society,* 132**,** 5906-15.

DICKINSON, B. C., LIN, V. S. & CHANG, C. J. 2013. Preparation and use of MitoPY1 for imaging hydrogen peroxide in mitochondria of live cells. *Nature Protocols,* 8**,** 1249-1259.

DICKINSON, B. C., PELTIER, J., STONE, D., SCHAFFER, D. V. & CHANG, C. J. 2011a. Nox2 redox signaling maintains essential cell populations in the brain. *Nature Chemical Biology,* 7**,** 106-12.

DICKINSON, B. C., SRIKUN, D. & CHANG, C. J. 2010b. Mitochondrial-targeted fluorescent probes for reactive oxygen species. *Current Opinion in Chemical Biology,* 14**,** 50-6.

DICKINSON, B. C., TANG, Y., CHANG, Z. & CHANG, C. J. 2011b. A nuclear-localized fluorescent hydrogen peroxide probe for monitoring sirtuin-mediated oxidative stress responses in vivo. *Chem Biol,* 18**,** 943-8.

DINAUER, M. C., PIERCE, E. A., ERICKSON, R. W., MUHLEBACH, T. J., MESSNER, H., ORKIN, S. H., SEGER, R. A. & CURNUTTE, J. T. 1991. Point mutation in the cytoplasmic domain of the neutrophil p22-phox cytochrome b subunit is associated with a nonfunctional NADPH oxidase and chronic granulomatous disease. *Proceedings of the National Academy of Sciences of the United States of America,* 88**,** 11231-5.

DÖHNER, K. & DÖHNER, H. 2008. Molecular characterization of acute myeloid leukemia. *Haematologica,* 93**,** 976-982.

DRUKER, B. J. 2009. Perspectives on the development of imatinib and the future of cancer research. *Natural Medicines,* 15**,** 1149-1152.

EDDERKAOUI, M., NITSCHE, C., ZHENG, L., PANDOL, S. J., GUKOVSKY, I. & GUKOVSKAYA, A. S. 2011. NADPH oxidase activation in pancreatic cancer cells is mediated through Akt-dependent up-regulation of p22phox. *Journal of Biological Chemistry,* 286**,** 7779-87.

EMADI, A. & KARP, J. E. 2014. The state of the union on treatment of acute myeloid leukemia. *Leuk Lymphoma,* 55**,** 2423-5.

ESTEY, E. & DÖHNER, H. 2006. Acute myeloid leukaemia. *The Lancet,* 368**,** 1894-1907.

FAN, J., LI, L., SMALL, D. & RASSOOL, F. 2010. Cells expressing FLT3/ITD mutations exhibit elevated repair errors generated through alternative NHEJ pathways: implications for genomic instability and therapy. *Blood,* 116**,** 5298-305.

FARQUHAR, M. J. & BOWEN, D. T. 2003. Oxidative stress and the myelodysplastic syndromes. *International Journal of Hematology,* 77**,** 342-50.

FENSKI, R., FLESCH, K., SERVE, S., MIZUKI, M., OELMANN, E., KRATZ-ALBERS, K., KIENAST, J., LEO, R., SCHWARTZ, S., BERDEL, W. E. & SERVE, H. 2000. Constitutive activation of FLT3 in acute myeloid leukaemia and its consequences for growth of 32D cells. *British Journal of Haematology,* 108**,** 322-30.

FERLAY, J., SOERJOMATARAM, I., DIKSHIT, R., ESER, S., MATHERS, C., REBELO, M., PARKIN, D. M., FORMAN, D. & BRAY, F. 2015. Cancer incidence and mortality worldwide: Sources, methods and major patterns in GLOBOCAN 2012. *International Journal of Cancer,* 136**,** E359-E386.

FINKEL, T. 1998. Oxygen radicals and signaling. *Current Opinion in Cell Biology,* 10**,** 248-253.

FRAZZIANO, G., AL GHOULEH, I., BAUST, J., SHIVA, S., CHAMPION, H. C. & PAGANO, P. J. 2014. Nox-derived ROS are acutely activated in pressure overload pulmonary hypertension: indications for a seminal role for mitochondrial Nox4. *American Journal of Physiology - Heart and Circulatory Physiology,* 306**,** H197-205.

FRESNO VARA, J. A., CASADO, E., DE CASTRO, J., CEJAS, P., BELDA-INIESTA, C. & GONZALEZ-BARON, M. 2004. PI3K/Akt signalling pathway and cancer. *Cancer Treatment Reviews,* 30**,** 193-204.

FREYHAUS, H., HUNTGEBURTH, M., WINGLER, K., SCHNITKER, J., BÄUMER, A. T., VANTLER, M., BEKHITE, M. M., WARTENBERG, M., SAUER, H. & ROSENKRANZ, S. 2006. Novel Nox inhibitor VAS2870 attenuates PDGF-dependent smooth muscle cell chemotaxis, but not proliferation. *Cardiovascular research,* 71**,** 331-341.

FRIED, L. & ARBISER, J. L. 2008. The reactive oxygen-driven tumor: relevance to melanoma. *Pigment Cell Melanoma Res,* 21**,** 117-22.

FUKUI, T., ISHIZAKA, N., RAJAGOPALAN, S., LAURSEN, J. B., CAPERS, Q., TAYLOR, W. R., HARRISON, D. G., DE LEON, H., WILCOX, J. N. &

GRIENDLING, K. K. 1997. p22phox mRNA Expression and NADPH Oxidase Activity Are Increased in Aortas From Hypertensive Rats. *Circulation research,* 80**,** 45-51.

GARCIA-SANTAMARINA, S., BORONAT S FAU - HIDALGO, E. & HIDALGO, E. 2014. Reversible cysteine oxidation in hydrogen peroxide sensing and signal transduction. *Biochemistry,* 53**,** 2560–2580.

GEISZT, M., KOPP, J. B., VARNAI, P. & LETO, T. L. 2000. Identification of renox, an NAD(P)H oxidase in kidney. *Proceedings of the National Academy of Sciences of the United States of America,* 97**,** 8010-4.

GIANNI, D., TAULET, N., DERMARDIROSSIAN, C. & BOKOCH, G. M. 2010a. c-Src-mediated phosphorylation of NoxA1 and Tks4 induces the reactive oxygen species (ROS)-dependent formation of functional invadopodia in human colon cancer cells. *Molecular Biology of the Cell,* 21**,** 4287-98.

GIANNI, D., TAULET, N., ZHANG, H., DERMARDIROSSIAN, C., KISTER, J., MARTINEZ, L., ROUSH, W. R., BROWN, S. J., BOKOCH, G. M. & ROSEN, H. 2010b. A novel and specific NADPH oxidase-1 (Nox1) small-molecule inhibitor blocks the formation of functional invadopodia in human colon cancer cells. *ACS Chemical Biology,* 5**,** 981-93.

GIANNONI, E., BURICCHI, F., RAUGEI, G., RAMPONI, G. & CHIARUGI, P. 2005. Intracellular reactive oxygen species activate Src tyrosine kinase during cell adhesion and anchorage-dependent cell growth. *Molecular and Cellular Biology,* 25**,** 6391-403.

GILLILAND, D. G. & GRIFFIN, J. D. 2002. Role of FLT3 in leukemia. *Curr Opin Hematol.,* 9**,** 274-81.

GODFREY, R., ARORA, D., BAUER, R., STOPP, S., MULLER, J. P., HEINRICH, T., BOHMER, S. A., DAGNELL, M., SCHNETZKE, U., SCHOLL, S., OSTMAN, A. & BOHMER, F. D. 2012. Cell transformation by FLT3 ITD in acute myeloid leukemia involves oxidative inactivation of the tumor suppressor protein-tyrosine phosphatase DEP-1/ PTPRJ. *Blood,* 119**,** 4499-511.

GORDILLO, G., FANG, H., PARK, H. & ROY, S. 2010. Nox-4–Dependent Nuclear H(2)O(2) Drives DNA Oxidation Resulting in 8-OHdG as Urinary Biomarker and Hemangioendothelioma Formation. *Antioxidants & Redox Signaling,* 12**,** 933-943.

GORIN, Y., RICONO, J. M., KIM, N. H., BHANDARI, B., CHOUDHURY, G. G. & ABBOUD, H. E. 2003. Nox4 mediates angiotensin II-induced activation of Akt/protein kinase B in mesangial cells. *American Journal of Physiology - Renal Physiology,* 285**,** F219-29.

GOUGH, D. R. & COTTER, T. G. 2011. Hydrogen peroxide: a Jekyll and Hyde signalling molecule. *Cell Death and Dis,* 2**,** e213.

GRAFONE, T., PALMISANO, M., NICCI, C. & STORTI, S. 2012. An overview on the role of FLT3-tyrosine kinase receptor in acute myeloid leukemia: biology and treatment. *Oncology Reviews,* 6.

GRIFFITH, J., BLACK, J., FAERMAN, C., SWENSON, L., WYNN, M., LU, F., LIPPKE, J. & SAXENA, K. 2004. The structural basis for autoinhibition of FLT3 by the juxtamembrane domain. *Molecular Cell,* 13**,** 169-78.

GROEMPING, Y., LAPOUGE, K., SMERDON, S. J. & RITTINGER, K. 2003. Molecular basis of phosphorylation-induced activation of the NADPH oxidase. *Cell,* 113**,** 343-55.

GROEMPING, Y. & RITTINGER, K. 2005. Activation and assembly of the NADPH oxidase: a structural perspective. *Biochemical Journal,* 386**,** 401-416.

GROEN, A., LEMEER, S., VAN DER WIJK, T., OVERVOORDE, J., HECK, A. J., OSTMAN, A., BARFORD, D., SLIJPER, M. & DEN HERTOG, J. 2005. Differential oxidation of protein-tyrosine phosphatases. *Journal of Biological Chemistry,* 280**,** 10298-304.

GRUHNE, B., SOMPALLAE, R., MARESCOTTI, D., KAMRANVAR, S. A., GASTALDELLO, S. & MASUCCI, M. G. 2009. The Epstein–Barr virus nuclear antigen-1 promotes genomic instability via induction of reactive oxygen species. *Proceedings of the National Academy of Sciences,* 106**,** 2313-2318.

GRUNWALD, M. R. & LEVIS, M. J. 2013. FLT3 inhibitors for acute myeloid leukemia: a review of their efficacy and mechanisms of resistance. *International Journal of Hematology,* 97**,** 683-94.

GUIDA, M., MARALDI, T., BERETTI, F., FOLLO, M. Y., MANZOLI, L. & DE POL, A. 2014. Nuclear Nox4-derived reactive oxygen species in myelodysplastic syndromes. *Biomed Res Int,* 2014**,** 456937.

HAJAS, G., BACSI, A., AGUILERA-AGUIRRE, L., HEGDE, M. L., TAPAS, K. H., SUR, S., RADAK, Z., BA, X. & BOLDOGH, I. 2013. 8-Oxoguanine DNA glycosylase-1 links DNA repair to cellular signaling via the activation of the small GTPase Rac1. *Free Radical Biology & Medicine,* 61**,** 384-94.

HANAHAN, D. & WEINBERG, R. A. 2000. The hallmarks of cancer. *Cell,* 100**,** 57-70.

HANAHAN, D. & WEINBERG, R. A. 2011. Hallmarks of cancer: the next generation. *Cell,* 144**,** 646-74.

HAWKES, W. C. & ALKAN, Z. 2010. Regulation of redox signaling by selenoproteins. *Biological Trace Element Research,* 134**,** 235-51.

HEIDEL, F., SOLEM, F. K., BREITENBUECHER, F., LIPKA, D. B., KASPER, S., THIEDE, M. H., BRANDTS, C., SERVE, H., ROESEL, J., GILES, F., FELDMAN, E., EHNINGER, G., SCHILLER, G. J., NIMER, S., STONE, R. M., WANG, Y., KINDLER, T., COHEN, P. S., HUBER, C. & FISCHER, T. 2006. Clinical resistance to the kinase inhibitor PKC412 in acute myeloid leukemia by mutation of Asn-676 in the FLT3 tyrosine kinase domain. *Blood,* 107**,** 293-300.

HENDERSON, L. M. & CHAPPEL, J. B. 1996. NADPH oxidase of neutrophils. *Biochimica et Biophysica Acta,* 1273**,** 87-107.

HENDERSON, L. M., CHAPPELL, J. B. & JONES, O. T. 1987. The superoxide-generating NADPH oxidase of human neutrophils is electrogenic and associated with an H+ channel. *Biochemical Journal,* 246**,** 325-9.

HENLE, E. S. & LINN, S. 1997. Formation, Prevention, and Repair of DNA Damage by Iron/Hydrogen Peroxide. *Journal of Biological Chemistry,* 272**,** 19095-19098.

HILENSKI, L. L., CLEMPUS, R. E., QUINN, M. T., LAMBETH, J. D. & GRIENDLING, K. K. 2004. Distinct subcellular localizations of Nox1 and Nox4 in vascular smooth muscle cells. *Arteriosclerosis Thrombosis and Vascular Biology,* 24**,** 677-83.

HIRAGA, R., KATO, M., MIYAGAWA, S. & KAMATA, T. 2013. Nox4-derived ROS Signaling Contributes to TGF-β-induced Epithelial-mesenchymal Transition in Pancreatic Cancer Cells. *Anticancer Research,* 33**,** 4431-4438.

HOLE, P. S., DARLEY, R. L. & TONKS, A. 2011. Do reactive oxygen species play a role in myeloid leukemias ? *Blood,* 117**,** 5816-5826.

HOLE, P. S., ZABKIEWICZ, J., MUNJE, C., NEWTON, Z., PEARN, L., WHITE, P., MARQUEZ, N., HILLS, R. K., BURNETT, A. K., TONKS, A. & DARLEY, R. L. 2013. Overproduction of NOX-derived ROS in AML promotes proliferation and is associated with defective oxidative stress signaling. *Blood,* 122**,** 3322-3330.

HOLE, P. S. D. R. L. T. A. 2011. Do reactive oxygen species play a role in myeloid leukemias? *Blood,* 117**,** 5816-5826.

HOSHI, T. & HEINEMANN, S. 2001. Regulation of cell function by methionine oxidation and reduction. *J Physiol,* 531**,** 1-11.

INOGUCHI, T., SONTA, T., TSUBOUCHI, H., ETOH, T., KAKIMOTO, M., SONODA, N., SATO, N., SEKIGUCHI, N., KOBAYASHI, K., SUMIMOTO, H., UTSUMI, H. & NAWATA, H. 2003. Protein kinase C-dependent increase in reactive oxygen species (ROS) production in vascular tissues of diabetes: role of vascular NAD(P)H oxidase. *Journal of the American Society of Nephrology,* 14**,** S227-32.

IRWIN, M. E., RIVERA-DEL VALLE, N. & CHANDRA, J. 2013. Redox control of leukemia: from molecular mechanisms to therapeutic opportunities. *Antioxidants & Redox Signaling,* 18**,** 1349-83.

ISHIKAWA, K., TAKENAGA, K., AKIMOTO, M., KOSHIKAWA, N., YAMAGUCHI, A., IMANISHI, H., NAKADA, K., HONMA, Y. & HAYASHI, J.-I. 2008. ROS-Generating Mitochondrial DNA Mutations Can Regulate Tumor Cell Metastasis. *Science,* 320**,** 661-664.

JABBOUR, E. & KANTARJIAN, H. 2014. Chronic myeloid leukemia: 2014 update on diagnosis, monitoring, and management. *American Journal of Hematology,* 89**,** 547-56.

JACKSON, A. L. & LOEB, L. A. 2001. The contribution of endogenous sources of DNA damage to the multiple mutations in cancer. *Mutation Research/Fundamental and Molecular Mechanisms of Mutagenesis,* 477**,** 7-21.

JUHASZ, A., GE, Y. U. N., MARKEL, S., CHIU, A., MATSUMOTO, L., VAN BALGOOY, J., ROY, K. & DOROSHOW, J. H. 2009. Expression of NADPH oxidase homologues and accessory genes in human cancer cell

lines, tumours and adjacent normal tissues. *Free radical research,* 43**,** 523-532.

KAO, Y. Y., GIANNI, D., BOHL, B., TAYLOR, R. M. & BOKOCH, G. M. 2008. Identification of a conserved Rac-binding site on NADPH oxidases supports a direct GTPase regulatory mechanism. *Journal of Biological Chemistry,* 283**,** 12736-46.

KARIHTALA, P. & SOINI, Y. 2007. Reactive oxygen species and antioxidant mechanisms in human tissues and their relation to malignancies. *APMIS,* 115**,** 81-103.

KAWAHARA, T., RITSICK, D., CHENG, G. & LAMBETH, J. D. 2005. Point mutations in the proline-rich region of p22phox are dominant inhibitors of Nox1- and Nox2-dependent reactive oxygen generation. *Journal of Biological Chemistry,* 280**,** 31859-69.

KHANNA, K. K. & JACKSON, S. P. 2001. DNA double-strand breaks: signaling, repair and the cancer connection. *Nature Genetics,* 27**,** 247-254.

KIM, E. Y., SEO, J. M., KIM, C., LEE, J. E., LEE, K. M. & KIM, J. H. 2010. BLT2 promotes the invasion and metastasis of aggressive bladder cancer cells through a reactive oxygen species-linked pathway. *Free Radical Biology & Medicine,* 49**,** 1072-81.

KIYOI, H., OHNO, R., UEDA, R., SAITO, H. & NAOE, T. 2002. Mechanism of constitutive activation of FLT3 with internal tandem duplication in the juxtamembrane domain. *Oncogene,* 21**,** 2555-63.

KIYOI, H., TOWATARI, M., YOKOTA, S., HAMAGUCHI, M., OHNO, R., SAITO, H. & NAOE, T. 1998. Internal tandem duplication of the FLT3 gene is a novel modality of elongation mutation which causes constitutive activation of the product. *Leukemia,* 12**,** 1333-7.

KOJIMA, K., KUME, H., ITO, S., OGUMA, T., SHIRAKI, A., KONDO, M., ITO, Y. & SHIMOKATA, K. 2007. Direct effects of hydrogen peroxide on airway smooth muscle tone: Roles of Ca2+ influx and Rho-kinase. *European Journal of Pharmacology,* 556**,** 151-156.

KOPTYRA, M., FALINSKI, R., NOWICKI, M. O., STOKLOSA, T., MAJSTEREK, I., NIEBOROWSKA-SKORSKA, M., BLASIAK, J. & SKORSKI, T. 2006. BCR/ABL kinase induces self-mutagenesis via reactive oxygen species to encode imatinib resistance. *Blood,* 108**,** 319-27.

KOTHE, S., MULLER, J. P., BOHMER, S. A., TSCHONGOV, T., FRICKE, M., KOCH, S., THIEDE, C., REQUARDT, R. P., RUBIO, I. & BOHMER, F. D. 2013. Features of Ras activation by a mislocalized oncogenic tyrosine kinase: FLT3 ITD signals through K-Ras at the plasma membrane of acute myeloid leukemia cells. *Journal of Cell Science,* 126**,** 4746-55.

KUMAR, B., KOUL, S., KHANDRIKA, L., MEACHAM, R. B. & KOUL, H. K. 2008. Oxidative stress is inherent in prostate cancer cells and is required for aggressive phenotype. *Cancer Research,* 68**,** 1777-85.

KURODA, J., NAKAGAWA, K., YAMASAKI, T., NAKAMURA, K., TAKEYA, R., KURIBAYASHI, F., IMAJOH-OHMI, S., IGARASHI, K., SHIBATA, Y., SUEISHI, K. & SUMIMOTO, H. 2005. The superoxide-producing NAD(P)H oxidase Nox4 in the nucleus of human vascular endothelial cells. *Genes to Cells,* 10**,** 1139-51.

KUZMINOV, A. 2001. Single-strand interruptions in replicating chromosomes cause double-strand breaks. *Proceedings of the National Academy of Sciences of the United States of America,* 98**,** 8241-6.

LAMBETH, J. D. 2007. Nox enzymes, ROS, and chronic disease: an example of antagonistic pleiotropy. *Free radical biology & medicine,* 43**,** 332-47.

LAMBETH, J. D. & NEISH, A. S. 2014. Nox enzymes and new thinking on reactive oxygen: a double-edged sword revisited. *Annu Rev Pathol,* 9**,** 119-45.

LANDRISCINA, M., MADDALENA, F., LAUDIERO, G. & ESPOSITO, F. 2009. Adaptation to oxidative stress, chemoresistance, and cell survival. *Antioxidants & Redox Signaling,* 11**,** 2701-16.

LANDRY, W. D., WOOLLEY, J. F. & COTTER, T. G. 2013. Imatinib and Nilotinib inhibit Bcr-Abl-induced ROS through targeted degradation of the NADPH oxidase subunit p22phox. *Leukemia Research,* 37**,** 183-9.

LANE, S. W. & GILLILAND, D. G. 2010. Leukemia stem cells. *Seminars in Cancer Biology,* 20**,** 71-76.

LANE, S. W., SCADDEN, D. T. & GILLILAND, D. G. 2009. The leukemic stem cell niche: current concepts and therapeutic opportunities. *Blood,* 114**,** 1150-1157.

LEE, C. F., QIAO, M., SCHRODER, K., ZHAO, Q. & ASMIS, R. 2010. Nox4 is a novel inducible source of reactive oxygen species in monocytes and

macrophages and mediates oxidized low density lipoprotein-induced macrophage death. *Circulation Research,* 106**,** 1489-97.

LEE, J. W. & HELMANN, J. D. 2006. The PerR transcription factor senses H2O2 by metal-catalysed histidine oxidation. *Nature,* 440**,** 363-7.

LEISCHNER, H., ALBERS, C., GRUNDLER, R., RAZUMOVSKAYA, E., SPIEKERMANN, K., BOHLANDER, S., RONNSTRAND, L., GOTZE, K., PESCHEL, C. & DUYSTER, J. 2012. SRC is a signaling mediator in FLT3-ITD- but not in FLT3-TKD-positive AML. *Blood,* 119**,** 4026-33.

LEVIS, M. 2013. FLT3 mutations in acute myeloid leukemia: what is the best approach in 2013? *Hematology Am Soc Hematol Educ Program,* 2013**,** 220-6.

LEVIS, M. & SMALL, D. 2003. FLT3: ITDoes matter in leukemia. *Leukemia,* 17**,** 1738-52.

LI, Y. & TRUSH, M. A. 1998. Diphenyleneiodonium, an NAD(P)H oxidase inhibitor, also potently inhibits mitochondrial reactive oxygen species production. 253**,** 295-9.

LIPPERT, A. R., VAN DE BITTNER, G. C. & CHANG, C. J. 2011. Boronate oxidation as a bioorthogonal reaction approach for studying the chemistry of hydrogen peroxide in living systems. *Accounts of Chemical Research,* 44**,** 793-804.

LOEB, L. A., LOEB, K. R. & ANDERSON, J. P. 2003. Multiple mutations and cancer. *Proceedings of the National Academy of Sciences of the United States of America,* 100**,** 776-81.

LOU, Y. W., CHEN, Y. Y., HSU, S. F., CHEN, R. K., LEE, C. L., KHOO, K. H., TONKS, N. K. & MENG, T. C. 2008. Redox regulation of the protein tyrosine phosphatase PTP1B in cancer cells. *FEBS Journal,* 275**,** 69-88.

LU, A. L., LI, X., GU, Y., WRIGHT, P. M. & CHANG, D. Y. 2001. Repair of oxidative DNA damage: mechanisms and functions. *Cell Biochemistry and Biophysics,* 35**,** 141-70.

LU, Y., KITAURA, J., OKI, T., KOMENO, Y., OZAKI, K., KIYONO, M., KUMAGAI, H., NAKAJIMA, H., NOSAKA, T., ABURATANI, H. & KITAMURA, T. 2007. Identification of TSC-22 as a potential tumor

suppressor that is upregulated by Flt3-D835V but not Flt3-ITD. *Leukemia,* 21**,** 2246-57.

MACKAREHTSCHIAN, K., HARDIN, J. D., MOORE, K. A., BOAST, S., GOFF, S. P. & LEMISCHKA, I. R. 1995. Targeted disruption of the flk2/flt3 gene leads to deficiencies in primitive hematopoietic progenitors. *Immunity,* 3**,** 147-61.

MAHADEV, K., MOTOSHIMA, H., WU, X., RUDDY, J. M., ARNOLD, R. S., CHENG, G., LAMBETH, J. D. & GOLDSTEIN, B. J. 2004. The NAD(P)H oxidase homolog Nox4 modulates insulin-stimulated generation of H2O2 and plays an integral role in insulin signal transduction. *Molecular and cellular biology,* 24**,** 1844-54.

MAHALINGAIAH, P. K. S. & SINGH, K. P. 2014. Chronic Oxidative Stress Increases Growth and Tumorigenic Potential of MCF-7 Breast Cancer Cells. *PLoS One,* 9**,** e87371.

MALINOUSKI, M., ZHOU, Y., BELOUSOV, V. V., HATFIELD, D. L. & GLADYSHEV, V. N. 2011. Hydrogen peroxide probes directed to different cellular compartments. *PLoS One,* 6**,** e14564.

MARALDI, T., PRATA, C., VIECELI DALLA SEGA, F., CALICETI, C., ZAMBONIN, L., FIORENTINI, D. & HAKIM, G. 2009. NAD(P)H oxidase isoform Nox2 plays a prosurvival role in human leukaemia cells. *Free Radical Research,* 43**,** 1111-21.

MARINHO, H. S., REAL, C., CYRNE, L. S., SOARES, H. & ANTUNES, F. 2014. Hydrogen peroxide sensing, signaling and regulation of transcription factors. *Redox biology,* 2**,** 535-562.

MARTINDALE, J. L. & HOLBROOK, N. J. 2002. Cellular response to oxidative stress: Signaling for suicide and survival. *Journal of Cellular Physiology,* 192**,** 1-15.

MARTYN, K. D., FREDERICK, L. M., VON LOEHNEYSEN, K., DINAUER, M. C. & KNAUS, U. G. 2006. Functional analysis of Nox4 reveals unique characteristics compared to other NADPH oxidases. *Cellular signalling,* 18**,** 69-82.

MASSON, K. & RONNSTRAND, L. 2009. Oncogenic signaling from the hematopoietic growth factor receptors c-Kit and Flt3. *Cellular Signalling,* 21**,** 1717-26.

MATSUSHIMA, S., KURODA, J., AGO, T., ZHAI, P., PARK, J. Y., XIE, L. H., TIAN, B. & SADOSHIMA, J. 2013. Increased oxidative stress in the nucleus caused by Nox4 mediates oxidation of HDAC4 and cardiac hypertrophy. *Circulation Research,* 112**,** 651-63.

MESHINCHI, S., ALONZO, T. A., STIREWALT, D. L., ZWAAN, M., ZIMMERMAN, M., REINHARDT, D., KASPERS, G. J. L., HEEREMA, N. A., GERBING, R., LANGE, B. J. & RADICH, J. P. 2006. Clinical implications of FLT3 mutations in pediatric AML. *Blood,* 108**,** 3654-3661.

MESHINCHI, S. & APPELBAUM, F. R. 2009. Structural and Functional Alterations of FLT3 in Acute Myeloid Leukemia. *Clinical Cancer Research,* 15**,** 4263-4269.

MIKI, H. & FUNATO, Y. 2012. Regulation of intracellular signalling through cysteine oxidation by reactive oxygen species. *Journal of biochemistry,* 151**,** 255-261.

MILLER, E. D., BRYAN C. & CHANG, C. J. 2010. Aquaporin-3 mediates hydrogen peroxide uptake to regulate downstream intracellular signaling. *Proceedings of the National Academy of Sciences,* 107**,** 15681-6.

MILLER, E. W., ALBERS, A. E., PRALLE, A., ISACOFF, E. Y. & CHANG, C. J. 2005. Boronate-Based Fluorescent Probes for Imaging Cellular Hydrogen Peroxide. *Journal of the American Chemical Society,* 127**,** 16652-16659.

MISHINA, N. M., TYURIN-KUZMIN, P. A., MARKVICHEVA, K. N., VOROTNIKOV, A. V., TKACHUK, V. A., LAKETA, V., SCHULTZ, C., LUKYANOV, S. & BELOUSOV, V. V. 2011. Does cellular hydrogen peroxide diffuse or act locally? *Antioxidants & Redox Signaling,* 14**,** 1-7.

MIZUKI, M., FENSKI, R., HALFTER, H., MATSUMURA, I., SCHMIDT, R., MULLER, C., GRUNING, W., KRATZ-ALBERS, K., SERVE, S., STEUR, C., BUCHNER, T., KIENAST, J., KANAKURA, Y., BERDEL, W. E. & SERVE, H. 2000. Flt3 mutations from patients with acute myeloid leukemia induce transformation of 32D cells mediated by the Ras and STAT5 pathways. *Blood,* 96**,** 3907-14.

MOISEEVA, O., BOURDEAU, V., ROUX, A., DESCHENES-SIMARD, X. & FERBEYRE, G. 2009. Mitochondrial dysfunction contributes to oncogene-induced senescence. *Molecular and Cellular Biology,* 29**,** 4495-507.

MONDOL, A. S., TONKS, N. K. & KAMATA, T. 2014. Nox4 redox regulation of PTP1B contributes to the proliferation and migration of glioblastoma cells by

modulating tyrosine phosphorylation of coronin-1C. *Free Radical Biology and Medicine,* 67**,** 285-291.

MOORE, A. S., FAISAL, A., GONZALEZ DE CASTRO, D., BAVETSIAS, V., SUN, C., ATRASH, B., VALENTI, M., DE HAVEN BRANDON, A., AVERY, S., MAIR, D., MIRABELLA, F., SWANSBURY, J., PEARSON, A. D., WORKMAN, P., BLAGG, J., RAYNAUD, F. I., ECCLES, S. A. & LINARDOPOULOS, S. 2012. Selective FLT3 inhibition of FLT3-ITD+ acute myeloid leukaemia resulting in secondary D835Y mutation: a model for emerging clinical resistance patterns. *Leukemia,* 26**,** 1462-70.

MURPHY, M. P., HOLMGREN, A., LARSSON, N.-G., HALLIWELL, B., CHANG, C. J., KALYANARAMAN, B., RHEE, S. G., THORNALLEY, P. J., PARTRIDGE, L., GEMS, D., NYSTRÖM, T., BELOUSOV, V., SCHUMACKER, P. T. & WINTERBOURN, C. C. 2011. Unraveling the biological roles of reactive oxygen species. *Cell Metabolism,* 13**,** 361-6.

NAKASHIMA, I., KATO, M., AKHAND, A. A., SUZUKI, H., TAKEDA, K., HOSSAIN, K. & KAWAMOTO, Y. 2002. Redox-linked signal transduction pathways for protein tyrosine kinase activation. *Antioxidants & Redox Signaling,* 4**,** 517-31.

NAUGHTON, R., QUINEY, C., TURNER, S. D. & COTTER, T. G. 2009. Bcr-Abl-mediated redox regulation of the PI3K/AKT pathway. *Leukemia,* 23**,** 1432-40.

NIEBOROWSKA-SKORSKA, M., KOPINSKI, P. K., RAY, R., HOSER, G., NGABA, D., FLIS, S., CRAMER, K., REDDY, M. M., KOPTYRA, M., PENSERGA, T., GLODKOWSKA-MROWKA, E., BOLTON, E., HOLYOAKE, T. L., EAVES, C. J., CERNY-REITERER, S., VALENT, P., HOCHHAUS, A., HUGHES, T. P., VAN DER KUIP, H., SATTLER, M., WIKTOR-JEDRZEJCZAK, W., RICHARDSON, C., DORRANCE, A., STOKLOSA, T., WILLIAMS, D. A. & SKORSKI, T. 2012. Rac2-MRC-cIII–generated ROS cause genomic instability in chronic myeloid leukemia stem cells and primitive progenitors. *Blood,* 119**,** 4253-4263.

NISIMOTO, Y., DIEBOLD, B. A., CONSTENTINO-GOMES, D. & LAMBETH, J. D. 2014. Nox4: a hydrogen peroxide-generating oxygen sensor. *Biochemistry,* 53**,** 5111-20.

NOWICKI, M. O., FALINSKI, R., KOPTYRA, M., SLUPIANEK, A., STOKLOSA, T., GLOC, E., NIEBOROWSKA-SKORSKA, M., BLASIAK, J. & SKORSKI, T. 2004. BCR/ABL oncogenic kinase promotes unfaithful repair

of the reactive oxygen species-dependent DNA double-strand breaks. *Blood,* 104**,** 3746-53.

O'DONNELL, B. V., TEW, D. G., JONES, O. T. & ENGLAND, P. J. 1993. Studies on the inhibitory mechanism of iodonium compounds with special reference to neutrophil NADPH oxidase. *Biochemical Journal,* 290**,** 41-49.

OHYE, H. & SUGAWARA, M. 2010. Dual oxidase, hydrogen peroxide and thyroid diseases. *Experimental Biology and Medicine (Maywood),* 235**,** 424-33.

OSTMAN, A., FRIJHOFF, J., SANDIN, A. & BOHMER, F. D. 2011. Regulation of protein tyrosine phosphatases by reversible oxidation. *J Biochem,* 150**,** 345-56.

OSTRONOFF, F. & ESTEY, E. 2013. The role of quizartinib in the treatment of acute myeloid leukemia. *Expert Opin Investig Drugs,* 22**,** 1659-69.

PALAZZOLO-BALLANCE, A. M., SUQUET, C. & HURST, J. K. 2007. Pathways for intracellular generation of oxidants and tyrosine nitration by a macrophage cell line. *Biochem.,* 46**,** 7536-48.

PAZHANISAMY, S. K., LI, H., WANG, Y., BATINIC-HABERLE, I. & ZHOU, D. 2011. NADPH oxidase inhibition attenuates total body irradiation-induced haematopoietic genomic instability. *Mutagenesis,* 26**,** 431-5.

PEDDIE, C. M., WOLF CR FAU - MCLELLAN, L. I., MCLELLAN LI FAU - COLLINS, A. R., COLLINS AR FAU - BOWEN, D. T. & BOWEN, D. T. 1997. Oxidative DNA damage in CD34+ myelodysplastic cells is associated with intracellular redox changes and elevated plasma tumour necrosis factor-alpha concentration. *British Journal of Haematology,* 99**,** 625-31.

PELICANO, H., CARNEY, D. & HUANG, P. 2004. ROS stress in cancer cells and therapeutic implications. *Drug Resist Updat,* 7**,** 97-110.

PELOQUIN, G. L., CHEN, Y. B. & FATHI, A. T. 2013. The evolving landscape in the therapy of acute myeloid leukemia. *Protein Cell,* 4**,** 735-46.

PETROS, J. A., BAUMANN, A. K., RUIZ-PESINI, E., AMIN, M. B., SUN, C. Q., HALL, J., LIM, S., ISSA, M. M., FLANDERS, W. D., HOSSEINI, S. H., MARSHALL, F. F. & WALLACE, D. C. 2005. mtDNA mutations increase tumorigenicity in prostate cancer. *Proceedings of the National Academy of Sciences of the United States of America,* 102**,** 719-724.

PETRY, A., DJORDJEVIC, T., WEITNAUER, M., KIETZMANN, T., HESS, J. & GORLACH, A. 2006. NOX2 and NOX4 mediate proliferative response in endothelial cells. *Antioxidants & Redox Signaling,* 8**,** 1473-84.

PILOTO, O., WRIGHT, M., BROWN, P., KIM, K.-T., LEVIS, M. & SMALL, D. 2007. Prolonged exposure to FLT3 inhibitors leads to resistance via activation of parallel signaling pathways. *Blood,* 109**,** 1643-52.

POPP, H. D. & BOHLANDER, S. K. 2010. Genetic instability in inherited and sporadic leukemias. *Genes Chromosomes & Cancer,* 49**,** 1071-81.

PRABHAKAR, N. R. 2000. Oxygen sensing by the carotid body chemoreceptors. *J Appl Physiol (1985),* 88**,** 2287-95.

PRATA, C., MARALDI, T., FIORENTINI, D., ZAMBONIN, L., HAKIM, G. & LANDI, L. 2008. Nox-generated ROS modulate glucose uptake in a leukaemic cell line. *Free Radical Research,* 42**,** 405-14.

PUCA, R., NARDINOCCHI, L., STARACE, G., RECHAVI, G., SACCHI, A., GIVOL, D. & D'ORAZI, G. 2010. Nox1 is involved in p53 deacetylation and suppression of its transcriptional activity and apoptosis. *Free Radical Biology & Medicine,* 48**,** 1338-46.

RASSOOL, F. V., GAYMES, T. J., OMIDVAR, N., BRADY, N., BEURLET, S., PLA, M., REBOUL, M., LEA, N., CHOMIENNE, C., THOMAS, N. S. B., MUFTI, G. J. & PADUA, R. A. 2007. Reactive Oxygen Species, DNA Damage, and Error-Prone Repair: A Model for Genomic Instability with Progression in Myeloid Leukemia? *Cancer research,* 67**,** 8762-8771.

REDDY, M. M., FERNANDES, M. S., SALGIA, R., LEVINE, R. L., GRIFFIN, J. D. & SATTLER, M. 2011. NADPH oxidases regulate cell growth and migration in myeloid cells transformed by oncogenic tyrosine kinases. *Leukemia : official journal of the Leukemia Society of America, Leukemia Research Fund, U.K,* 25**,** 281-9.

RHEE, S. G., BAE, Y. S., LEE, S. R. & KWON, J. 2000. Hydrogen peroxide: a key messenger that modulates protein phosphorylation through cysteine oxidation. *Sci STKE,* 2000**,** pe1.

ROBINSON, K. M., JANES, M. S. & BECKMAN, J. S. 2008. The selective detection of mitochondrial superoxide by live cell imaging. *Nature Protocols,* 3**,** 941-7.

ROBINSON, K. M., JANES, M. S., PEHAR, M., MONETTE, J. S., ROSS, M. F., HAGEN, T. M., MURPHY, M. P. & BECKMAN, J. S. 2006. Selective fluorescent imaging of superoxide in vivo using ethidium-based probes. *Proceedings of the National Academy of Sciences of the United States of America,* 103**,** 15038-43.

ROBOZ, G. J. 2012. Current treatment of acute myeloid leukemia. *Current Opinion in Oncology,* 24**,** 711-9.

ROSNET, O. & BIRNBAUM, D. 1993. Hematopoietic receptors of class III receptor-type tyrosine kinases. *Critical Reviews in Oncogenesis,* 4**,** 595-613.

ROSNET, O., BUHRING, H. J., MARCHETTO, S., RAPPOLD, I., LAVAGNA, C., SAINTY, D., ARNOULET, C., CHABANNON, C., KANZ, L., HANNUM, C. & BIRNBAUM, D. 1996. Human FLT3/FLK2 receptor tyrosine kinase is expressed at the surface of normal and malignant hematopoietic cells. *Leukemia,* 10**,** 238-48.

SABHARWAL, S. S. & SCHUMACKER, P. T. 2014. Mitochondrial ROS in cancer: initiators, amplifiers or an Achilles' heel? *Nature Reviews Cancer,* 14**,** 709-721.

SALLMYR, A., FAN, J., DATTA, K., KIM, K.-T., GROSU, D., SHAPIRO, P., SMALL, D. & RASSOOL, F. 2008a. Internal tandem duplication of FLT3 (FLT3/ITD) induces increased ROS production, DNA damage, and misrepair: implications for poor prognosis in AML. *Blood,* 111**,** 3173-82.

SALLMYR, A., FAN, J. & RASSOOL, F. V. 2008b. Genomic instability in myeloid malignancies: increased reactive oxygen species (ROS), DNA double strand breaks (DSBs) and error-prone repair. *Cancer Letters,* 270**,** 1-9.

SANCHEZ-SANCHEZ, B., GUTIERREZ-HERRERO, S., LOPEZ-RUANO, G., PRIETO-BERMEJO, R., ROMO-GONZALEZ, M., LLANILLO, M., PANDIELLA, A., GUERRERO, C., MIGUEL, J. F., SANCHEZ-GUIJO, F., DEL CANIZO, C. & HERNANDEZ-HERNANDEZ, A. 2014. NADPH oxidases as therapeutic targets in chronic myelogenous leukemia. *Clin Cancer Res,* 20**,** 4014-25.

SANCHO, P. & FABREGAT, I. 2011. The NADPH oxidase inhibitor VAS2870 impairs cell growth and enhances TGF-β-induced apoptosis of liver tumor cells. *Biochemical Pharmacology,* 81**,** 917-924.

SATO, T., YANG, X., KNAPPER, S., WHITE, P., SMITH, B. D., GALKIN, S., SMALL, D., BURNETT, A. & LEVIS, M. 2011. FLT3 ligand impedes the efficacy of FLT3 inhibitors in vitro and in vivo. *Blood,* 117**,** 3286-93.

SCHIEBER, M. & CHANDEL, N. S. 2014. ROS function in redox signaling and oxidative stress. *Current Biology,* 24**,** R453-62.

SCHMIDT-ARRAS, D.-E., BÖHMER, A., MARKOVA, B., CHOUDHARY, C., SERVE, H. & BÖHMER, F.-D. 2005. Tyrosine Phosphorylation Regulates Maturation of Receptor Tyrosine Kinases. *Molecular and cellular biology,* 25**,** 3690-3703.

SCHMIDT-ARRAS, D., BOHMER, S. A., KOCH, S., MULLER, J. P., BLEI, L., CORNILS, H., BAUER, R., KORASIKHA, S., THIEDE, C. & BOHMER, F. D. 2009. Anchoring of FLT3 in the endoplasmic reticulum alters signaling quality. *Blood,* 113**,** 3568-76.

SCHUMACKER, P. T. 2006. Reactive oxygen species in cancer cells: Live by the sword, die by the sword. *Cancer Cell,* 10**,** 175-176.

SEEDHOUSE, C. H., HUNTER, H. M., LLOYD-LEWIS, B., MASSIP, A.-M., PALLIS, M., CARTER, G. I., GRUNDY, M., SHANG, S. & RUSSELL, N. H. 2006. DNA repair contributes to the drug-resistant phenotype of primary acute myeloid leukaemia cells with FLT3 internal tandem duplications and is reversed by the FLT3 inhibitor PKC412. *Leukemia,* 20**,** 2130-6.

SERRANDER, L., CARTIER, L., BEDARD, K., BANFI, B., LARDY, B., PLASTRE, O., SIENKIEWICZ, A., FÓRRÓ, L., SCHLEGEL, W. & KRAUSE, K.-H. 2007. NOX4 activity is determined by mRNA levels and reveals a unique pattern of ROS generation. *Biochemical Journal,* 406**,** 105-114.

SHOWEL, M. M. & LEVIS, M. 2014. Advances in treating acute myeloid leukemia. *F1000Prime Rep,* 6**,** 96.

SIEBER, O. M., HEINIMANN, K. & TOMLINSON, I. P. M. 2003. Genomic instability--the engine of tumorigenesis? *Nature Reviews: Cancer,* 3**,** 701-8.

SMITH, C. C., WANG, Q., CHIN, C.-S., SALERNO, S., DAMON, L. E., LEVIS, M. J., PERL, A. E., TRAVERS, K. J., WANG, S., HUNT, J. P., ZARRINKAR, P. P., SCHADT, E. E., KASARSKIS, A., KURIYAN, J. & SHAH, N. P. 2012. Validation of ITD mutations in FLT3 as a therapeutic target in human acute myeloid leukaemia. *Nature,* 485**,** 260-263.

SONGYANG, Z., BALTIMORE, D., CANTLEY, L. C., KAPLAN, D. R. & FRANKE, T. F. 1997. Interleukin 3-dependent survival by the Akt protein kinase. *Proceedings of the National Academy of Sciences of the United States of America,* 94**,** 11345-50.

SPENCER, N. Y., YAN, Z., BOUDREAU, R. L., ZHANG, Y., LUO, M., LI, Q., TIAN, X., SHAH, A. M., DAVISSON, R. L., DAVIDSON, B., BANFI, B. & ENGELHARDT, J. F. 2011. Control of hepatic nuclear superoxide production by glucose 6-phosphate dehydrogenase and NADPH oxidase-4. *Journal of Biological Chemistry,* 286**,** 8977-87.

SPIEKERMANN, K., BAGRINTSEVA, K., SCHWAB, R., SCHMIEJA, K. & HIDDEMANN, W. 2003. Overexpression and Constitutive Activation of FLT3 Induces STAT5 Activation in Primary Acute Myeloid Leukemia Blast Cells. *Clinical Cancer Research,* 9**,** 2140-2150.

STIELOW, C., CATAR, R. A., MULLER, G., WINGLER, K., SCHEURER, P., SCHMIDT, H. H. H. W. & MORAWIETZ, H. 2006. Novel Nox inhibitor of oxLDL-induced reactive oxygen species formation in human endothelial cells. *Biochemical and biophysical research communications,* 344**,** 200-205.

STIREWALT, D. L. & RADICH, J. P. 2003. The role of FLT3 in haematopoietic malignancies. *Nature Reviews Cancer,* 3**,** 650-65.

STONE, R. M., DEANGELO, D. J., KLIMEK, V., GALINSKY, I., ESTEY, E., NIMER, S. D., GRANDIN, W., LEBWOHL, D., WANG, Y., COHEN, P., FOX, E. A., NEUBERG, D., CLARK, J., GILLILAND, D. G. & GRIFFIN, J. D. 2005. Patients with acute myeloid leukemia and an activating mutation in FLT3 respond to a small-molecule FLT3 tyrosine kinase inhibitor, PKC412. *Blood,* 105**,** 54-60.

STUIBLE, M. & TREMBLAY, M. L. 2010. In control at the ER: PTP1B and the down-regulation of RTKs by dephosphorylation and endocytosis. *Trends in Cell Biology,* 20**,** 672-679.

SUMIMOTO, H. 2008. Structure, regulation and evolution of Nox-family NADPH oxidases that produce reactive oxygen species. *FEBS Journal,* 275**,** 3249-3277.

SUMIMOTO, H., HATA, K., MIZUKI, K., ITO, T., KAGE, Y., SAKAKI, Y., FUKUMAKI, Y., NAKAMURA, M. & TAKESHIGE, K. 1996. Assembly and activation of the phagocyte NADPH oxidase. Specific interaction of the N-terminal Src homology 3 domain of p47phox with p22phox is required for

activation of the NADPH oxidase. *Journal of Biological Chemistry,* 271**,** 22152-8.

SUNDARESAN, M., YU, Z.-X., FERRANS, V. J., IRANI, K. & FINKEL, T. 1995. Requirement for Generation of H2O2 for Platelet-Derived Growth Factor Signal Transduction. *Science,* 270**,** 296-299.

SZATROWSKI, T. P. & NATHAN, C. F. 1991. Production of large amounts of hydrogen peroxide by human tumor cells. *Cancer research,* 51**,** 794-798.

TAKAC, I., SCHRODER, K., ZHANG, L., LARDY, B., ANILKUMAR, N., LAMBETH, J. D., SHAH, A. M., MOREL, F. & BRANDES, R. P. 2011. The E-loop is involved in hydrogen peroxide formation by the NADPH oxidase Nox4. *Journal of Biological Chemistry,* 286**,** 13304-13.

TAKAHASHI, S. 2011. Downstream molecular pathways of FLT3 in the pathogenesis of acute myeloid leukemia: biology and therapeutic implications. *Journal of Hematology & Oncology,* 4**,** 13.

THANNICKAL, V. J. & FANBURG, B. L. 2000. Reactive oxygen species in cell signaling. *American Journal of Physiology - Lung Cellular and Molecular Physiology,* 279**,** L1005-L1028.

TRACHOOTHAM, D., ALEXANDRE, J. & HUANG, P. 2009. Targeting cancer cells by ROS-mediated mechanisms: a radical therapeutic approach? *Nat Rev Drug Discov,* 8**,** 579-591.

TRACHOOTHAM, D., LU, W., OGASAWARA, M. A., NILSA, R. D. & HUANG, P. 2008. Redox regulation of cell survival. *Antioxidants & Redox Signaling,* 10**,** 1343-74.

TURNER, A. M., LIN, N. L., ISSARACHAI, S., LYMAN, S. D. & BROUDY, V. C. 1996. FLT3 receptor expression on the surface of normal and malignant human hematopoietic cells. *Blood,* 88**,** 3383-3390.

UENO, N., TAKEYA, R., MIYANO, K., KIKUCHI, H. & SUMIMOTO, H. 2005. The NADPH oxidase Nox3 constitutively produces superoxide in a p22phox-dependent manner: its regulation by oxidase organizers and activators. *Journal of Biological Chemistry,* 280**,** 23328-39.

USHIO-FUKAI, M. 2009. Compartmentalization of Redox Signaling Through NADPH Oxidase–Derived ROS. *Antioxidants & Redox Signaling,* 11**,** 1289-99.

VAFA, O., WADE, M., KERN, S., BEECHE, M., PANDITA, T. K., HAMPTON, G. M. & WAHL, G. M. 2002. c-Myc Can Induce DNA Damage, Increase Reactive Oxygen Species, and Mitigate p53 Function: A Mechanism for Oncogene-Induced Genetic Instability. *Molecular cell,* 9**,** 1031-1044.

VALAVANIDIS, A., VLACHOGIANNI, T. & FIOTAKIS, C. 2009. 8-hydroxy-2' -deoxyguanosine (8-OHdG): A critical biomarker of oxidative stress and carcinogenesis. *J Environ Sci Health C Environ Carcinog Ecotoxicol Rev,* 27**,** 120-39.

VALDIGLESIAS, V., GIUNTA, S., FENECH, M., NERI, M. & BONASSI, S. 2013. gammaH2AX as a marker of DNA double strand breaks and genomic instability in human population studies. *Mutation Research,* 753**,** 24-40.

VALKO, M., IZAKOVIC, M., MAZUR, M., RHODES, C. J. & TELSER, J. 2004. Role of oxygen radicals in DNA damage and cancer incidence. *Molecular and Cellular Biochemistry,* 266**,** 37-56.

VON LÖHNEYSEN, K., NOACK, D., HAYES, P., FRIEDMAN, J. S. & KNAUS, U. G. 2012. Constitutive NADPH Oxidase 4 Activity Resides in the Composition of the B-loop and the Penultimate C Terminus. *Journal of Biological Chemistry,* 287**,** 8737-8745.

WALLACE, D. C. 2005. A mitochondrial paradigm of metabolic and degenerative diseases, aging, and cancer: a dawn for evolutionary medicine. *Annual Review of Genetics,* 39**,** 359-407.

WANDER, S. A., LEVIS, M. J. & FATHI, A. T. 2014. The evolving role of FLT3 inhibitors in acute myeloid leukemia: quizartinib and beyond. *Ther Adv Hematol,* 5**,** 65-77.

WANG, Y., LIU, L., PAZHANISAMY, S. K., LI, H., MENG, A. & ZHOU, D. 2010. Total body irradiation causes residual bone marrow injury by induction of persistent oxidative stress in murine hematopoietic stem cells. *Free radical biology & medicine,* 48**,** 348-56.

WANG, Y., YANG, J. & YI, J. 2012. Redox sensing by proteins: oxidative modifications on cysteines and the consequent events. *Antioxidants & Redox Signaling,* 16**,** 649-57.

WARIS, G. & AHSAN, H. 2006. Reactive oxygen species: role in the development of cancer and various chronic conditions. *J Carcinog,* 5**,** 14.

WEYEMI, U. & DUPUY, C. 2012. The emerging role of ROS-generating NADPH oxidase NOX4 in DNA-damage responses. *Mutation research,* 751**,** 77-81.

WEYEMI, U., LAGENTE-CHEVALLIER, O., BOUFRAQECH, M., PRENOIS, F., COURTIN, F., CAILLOU, B., TALBOT, M., DARDALHON, M., AL GHUZLAN, A., BIDART, J.-M., SCHLUMBERGER, M. & DUPUY, C. 2012. ROS-generating NADPH oxidase NOX4 is a critical mediator in oncogenic H-Ras-induced DNA damage and subsequent senescence. *Oncogene,* 31**,** 1117-29.

WEYEMI, U., REDON, C. E., PAREKH, P. R., DUPUY, C. & BONNER, W. M. 2013. NADPH Oxidases NOXs and DUOXs as putative targets for cancer therapy. *Anticancer Agents Med Chem,* 13**,** 502-14.

WHITMAN, S. P., ARCHER, K. J., FENG, L., BALDUS, C., BECKNELL, B., CARLSON, B. D., CARROLL, A. J., MROZEK, K., VARDIMAN, J. W., GEORGE, S. L., KOLITZ, J. E., LARSON, R. A., BLOOMFIELD, C. D. & CALIGIURI, M. A. 2001. Absence of the wild-type allele predicts poor prognosis in adult de novo acute myeloid leukemia with normal cytogenetics and the internal tandem duplication of FLT3: a cancer and leukemia group B study. *Cancer Research,* 61**,** 7233-9.

WIND, S., BEUERLEIN, K., EUCKER, T., MULLER, H., SCHEURER, P., ARMITAGE, M. E., HO, H., SCHMIDT, H. H. & WINGLER, K. 2010. Comparative pharmacology of chemically distinct NADPH oxidase inhibitors. *British Journal of Pharmacology,* 161**,** 885-98.

WINTERBOURN, C. C. 2008. Reconciling the chemistry and biology of reactive oxygen species. *Nature Chemical Biology,* 4**,** 278-86.

WOOLLEY, J. F., CORCORAN, A., GROEGER, G., LANDRY, W. D. & COTTER, T. G. 2013a. Redox-regulated growth factor survival signaling. *Antioxid Redox Signal,* 19**,** 1815-27.

WOOLLEY, J. F., NAUGHTON, R., STANICKA, J., GOUGH, D. R., BHATT, L., DICKINSON, B. C., CHANG, C. J. & COTTER, T. G. 2012. H(2)O(2) Production Downstream of FLT3 Is Mediated by p22phox in the Endoplasmic Reticulum and Is Required for STAT5 Signalling. *PLoS One,* 7**,** e34050.

WOOLLEY, J. F., STANICKA, J. & COTTER, T. G. 2013b. Recent advances in reactive oxygen species measurement in biological systems. *Trends in Biochemical Sciences,* 38**,** 556-65.

WRIGHT, V. P., REISER, P. J. & CLANTON, T. L. 2009. Redox modulation of global phosphatase activity and protein phosphorylation in intact skeletal muscle. *J Physiol,* 587**,** 5767-81.

WU, L. L., CHIOU, C. C., CHANG, P. Y. & WU, J. T. 2004. Urinary 8-OHdG: a marker of oxidative stress to DNA and a risk factor for cancer, atherosclerosis and diabetics. *Clin Chim Acta,* 339**,** 1-9.

WU, R. F. & TERADA, L. S. 2009. Ras and Nox: linked signaling networks? *Free radical biology & medicine,* 47**,** 1276-1281.

WU, W. S. 2006. The signaling mechanism of ROS in tumor progression. *Cancer and Metastasis Reviews,* 25**,** 695-705.

YAMAMOTO, Y., KIYOI, H., NAKANO, Y., SUZUKI, R., KODERA, Y., MIYAWAKI, S., ASOU, N., KURIYAMA, K., YAGASAKI, F., SHIMAZAKI, C., AKIYAMA, H., SAITO, K., NISHIMURA, M., MOTOJI, T., SHINAGAWA, K., TAKESHITA, A., SAITO, H., UEDA, R., OHNO, R. & NAOE, T. 2001. Activating mutation of D835 within the activation loop of FLT3 in human hematologic malignancies. *Blood,* 97**,** 2434-2439.

ZARRINKAR, P. P., GUNAWARDANE, R. N., CRAMER, M. D., GARDNER, M. F., BRIGHAM, D., BELLI, B., KARAMAN, M. W., PRATZ, K. W., PALLARES, G., CHAO, Q., SPRANKLE, K. G., PATEL, H. K., LEVIS, M., ARMSTRONG, R. C., JAMES, J. & BHAGWAT, S. S. 2009. AC220 is a uniquely potent and selective inhibitor of FLT3 for the treatment of acute myeloid leukemia (AML). *Blood,* 114**,** 2984-92.

ZHENG, R., BAILEY, E., NGUYEN, B., YANG, X., PILOTO, O., LEVIS, M. & SMALL, D. 2011. Further Activation of FLT3 Mutants by FLT3 Ligand. *Oncogene,* 30**,** 4004-4014.

ZHOU, F. L., ZHANG, W. G., WEI, Y. C., MENG, S., BAI, G. G., WANG, B. Y., YANG, H. Y., TIAN, W., MENG, X., ZHANG, H. & CHEN, S. P. 2010. Involvement of oxidative stress in the relapse of acute myeloid leukemia. *Journal of Biological Chemistry,* 285**,** 15010-5.

ZHOU, Y., HILEMAN, E. O., PLUNKETT, W., KEATING, M. J. & HUANG, P. 2003. Free radical stress in chronic lymphocytic leukemia cells and its role in cellular sensitivity to ROS-generating anticancer agents. *Blood,* 101**,** 4098-4104.

ZIELONKA, J. & KALYANARAMAN, B. 2010. Hydroethidine- and MitoSOX-derived red fluorescence is not a reliable indicator of intracellular superoxide

formation: another inconvenient truth. *Free Radical Biology & Medicine,* 48**,** 983-1001.

Appendices

Published papers:

WOOLLEY, J. F., NAUGHTON, R., STANICKA, J., GOUGH, D. R., BHATT, L., DICKINSON, B. C., CHANG, C. J. & COTTER, T. G. 2012. H(2)O(2) Production Downstream of FLT3 Is Mediated by p22phox in the Endoplasmic Reticulum and Is Required for STAT5 Signalling. *PloS one,* 7**,** e34050.

WOOLLEY, J. F., STANICKA, J. & COTTER, T. G. 2013b. Recent advances in reactive oxygen species measurement in biological systems. *Trends Biochem Sci,* 38**,** 556-65.

RUSSELL, E. G., O'SULLIVAN, E. C., MILLER, C. M., STANICKA, J., MCCARTHY, F. O. & COTTER, T. G. 2014. Ellipticine derivative induces potent cytostatic effect in acute myeloid leukaemia cells. *Invest New Drugs,* 32**,** 1113-22.

STANICKA, J., RUSSELL, E. G., WOOLLEY, J. F. & COTTER, T. G. 2015. NADPH oxidase-generated hydrogen peroxide induces DNA damage in mutant FLT3-expressing leukemia cells. *J Biol Chem*. (currently under review).